

Multi-scale Computational Mechanics

industrial applications



Stéphane P.A. Bordas

Main contributors

Pierre Kerfriden	Associate Prof. Cardiff
Lars Beex	Research Associate
Jack Hale	Research Associates
Elena Atroshchenko	Assistant Professor, Chile

Ahmad Akbari	Ph.D. graduate 2014	
Olivier Goury	Ph.D. graduate 2014	
Haojie Lian	Ph.D. graduate 2014	
Sundararajan Natarajan	Ph.D. graduate 2011	now assistant Professor IIT Madras
Alexander Menk	Ph.D. graduate 2011	now at Bosch GmbH
Hadrien Courtecuisse	Post-doc graduate 2013	now CNRS Permanent Researcher

Motivation understand and optimise material durability

Multi-scale **Methods** - two approaches compared

Industrial and Clinical Applications

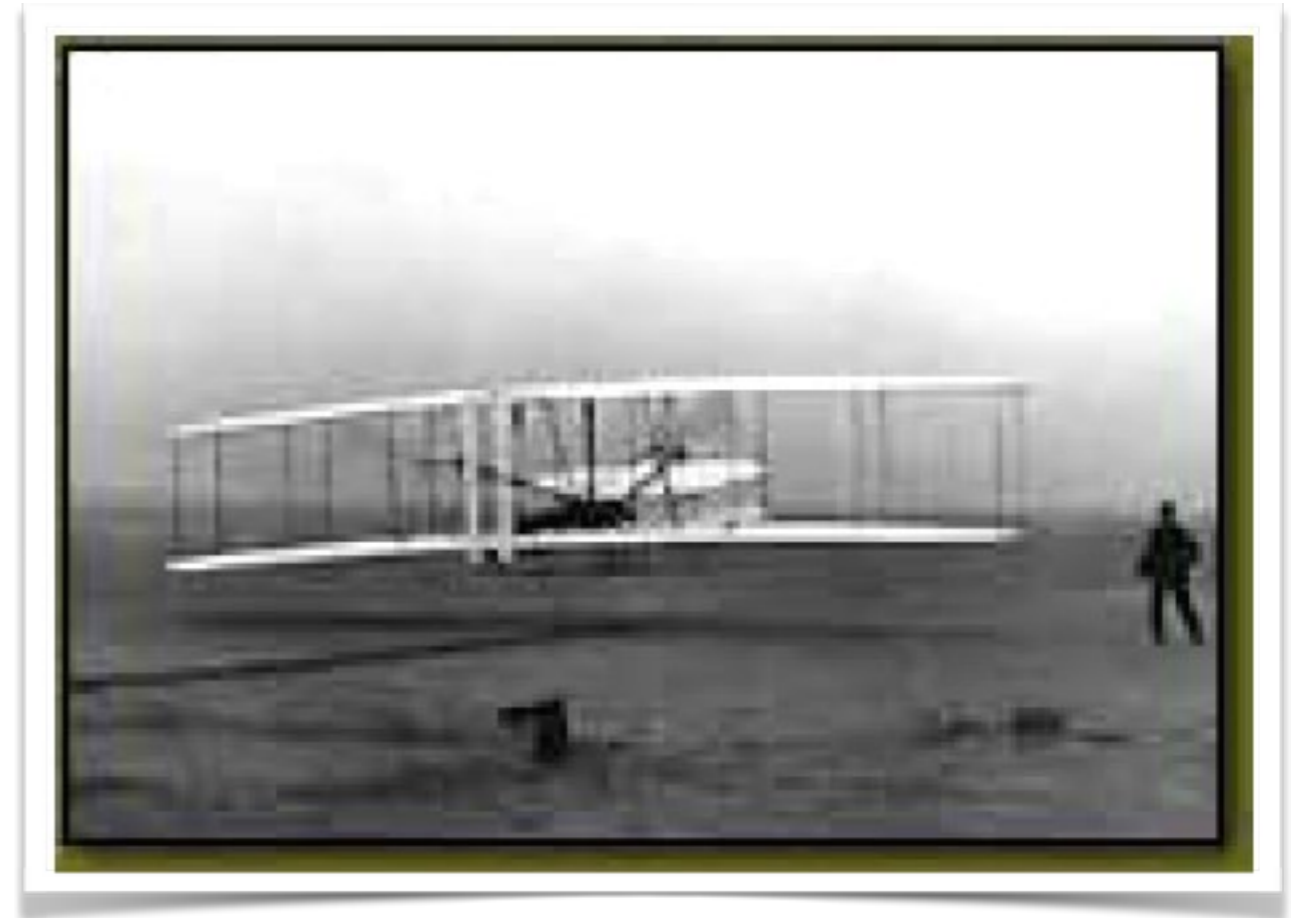
Outlook

Challenges

Wilbur and Orville Wright, 1903

Wright Flyer

10:35am Dec 17, 1903

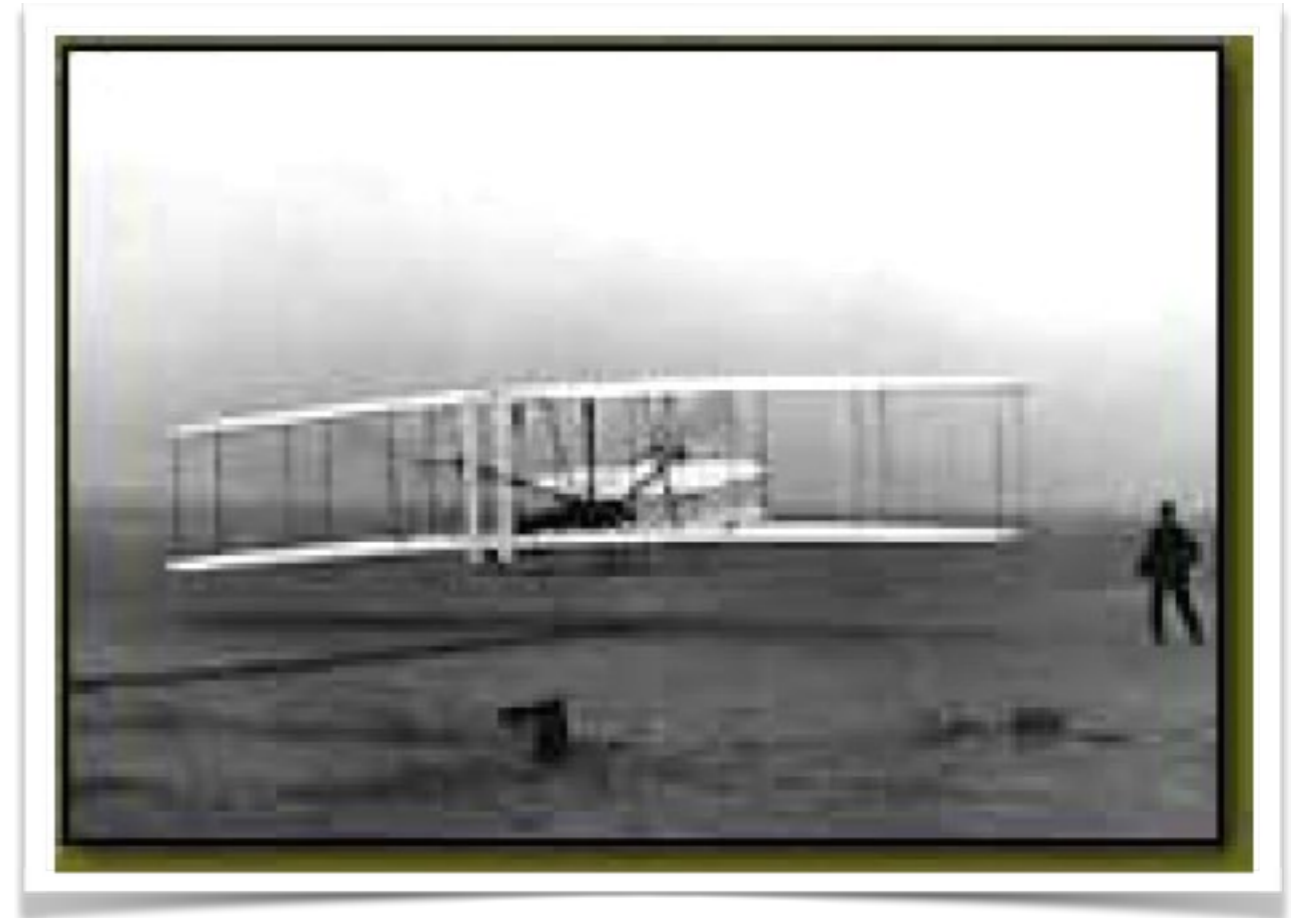


Wilbur and Orville Wright, 1903

On Dec 14 Wilbur won the coin toss, made the first attempt and stalled

Orville made the first flight on Dec. 17

12 seconds & 120 ft



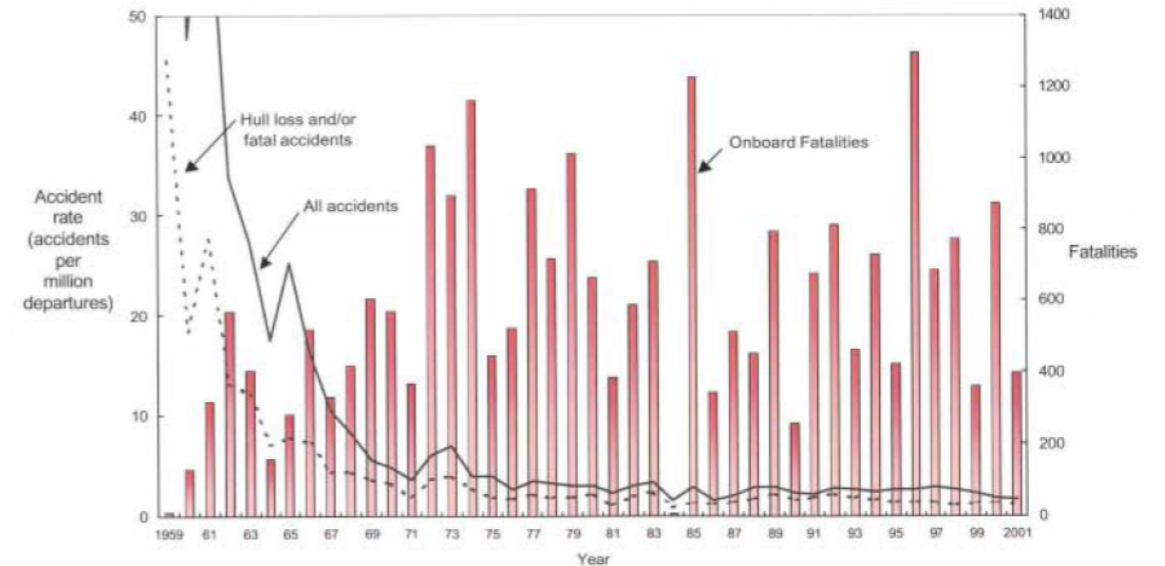
Aircraft safety

20,000 years



Worldwide statistics

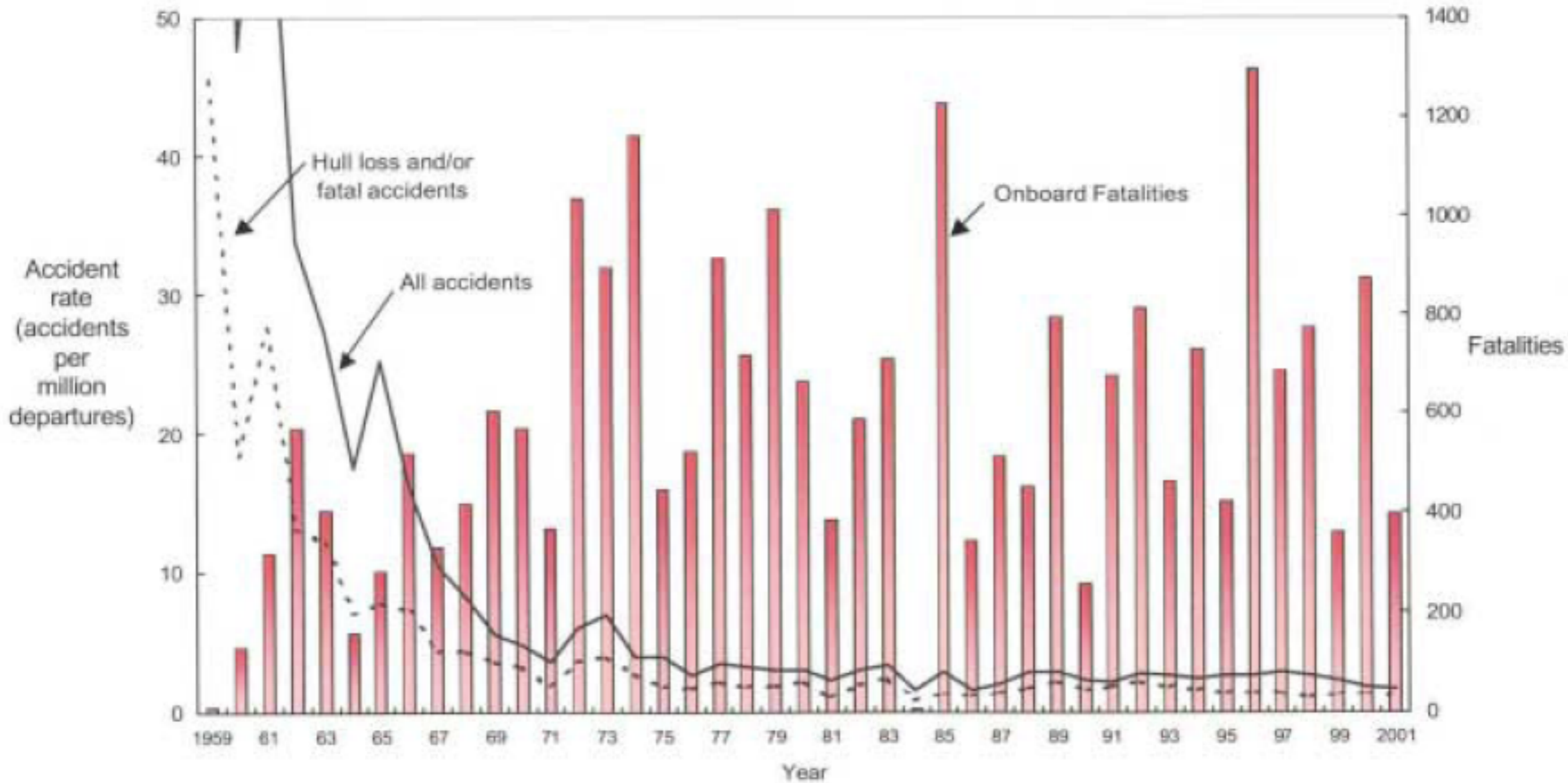
[1959-2001] 1,307
commercial jet aircraft
losses



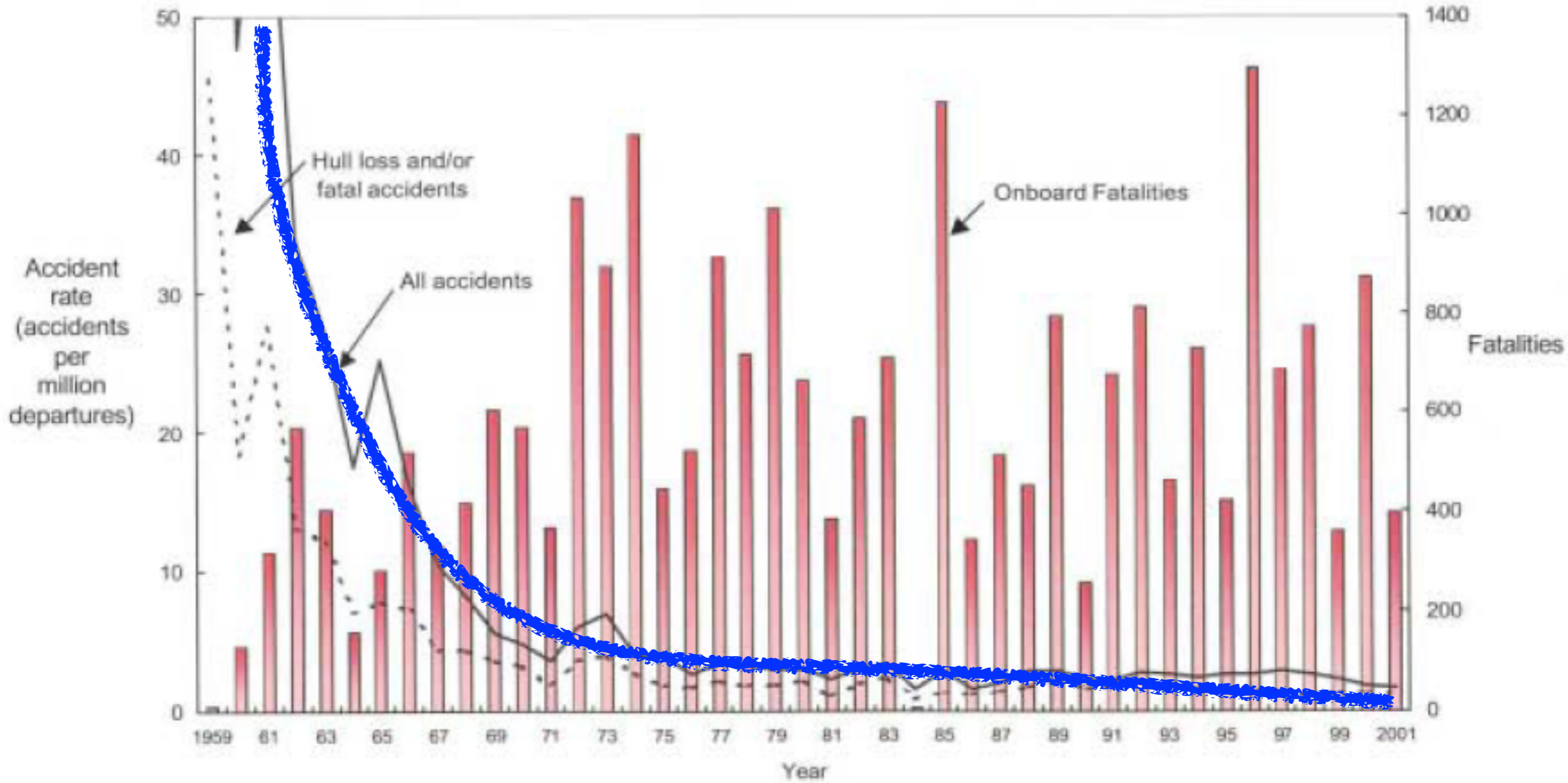
Today:

1 accident per
1,000,000
departures

Accident rates and fatalities/year

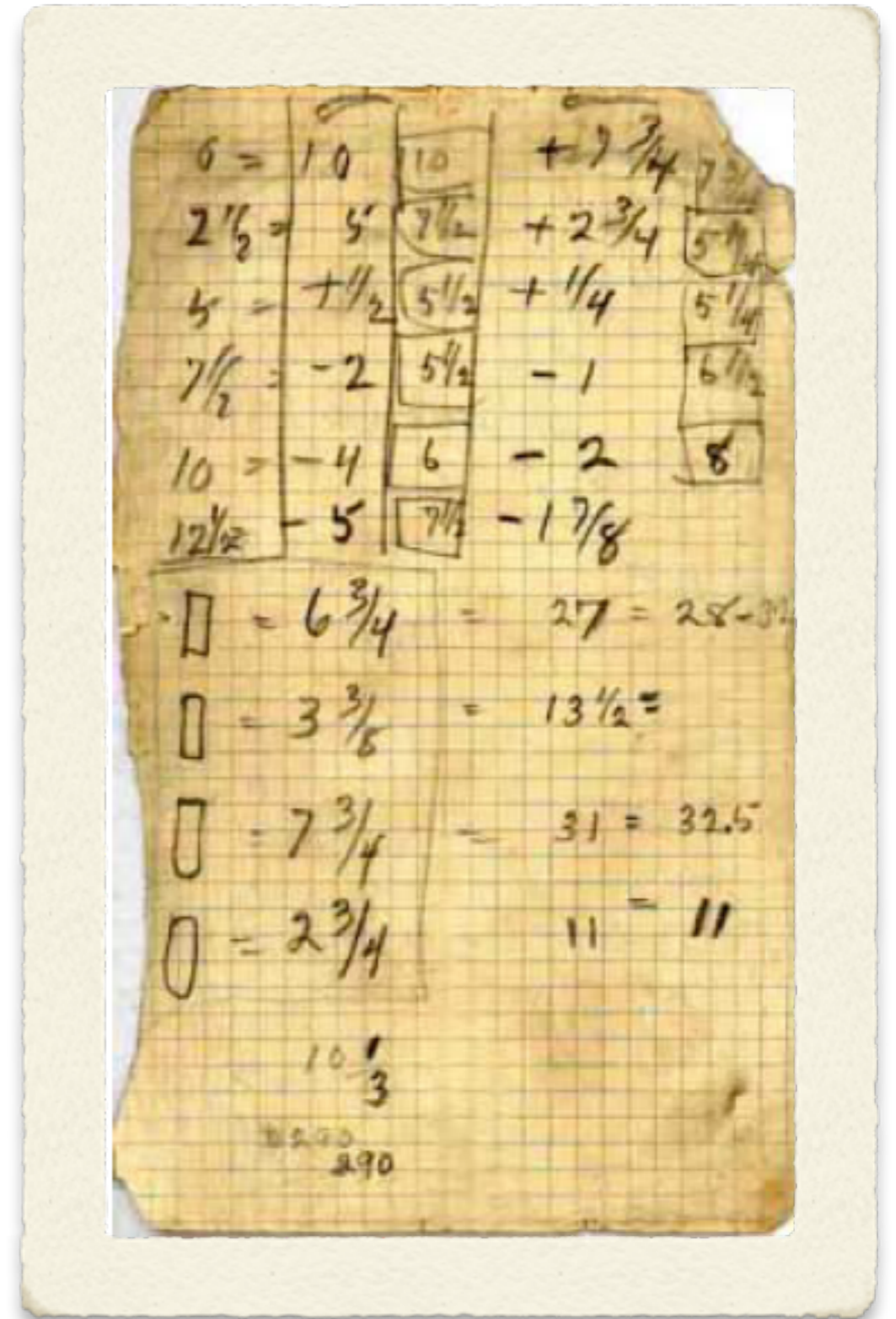
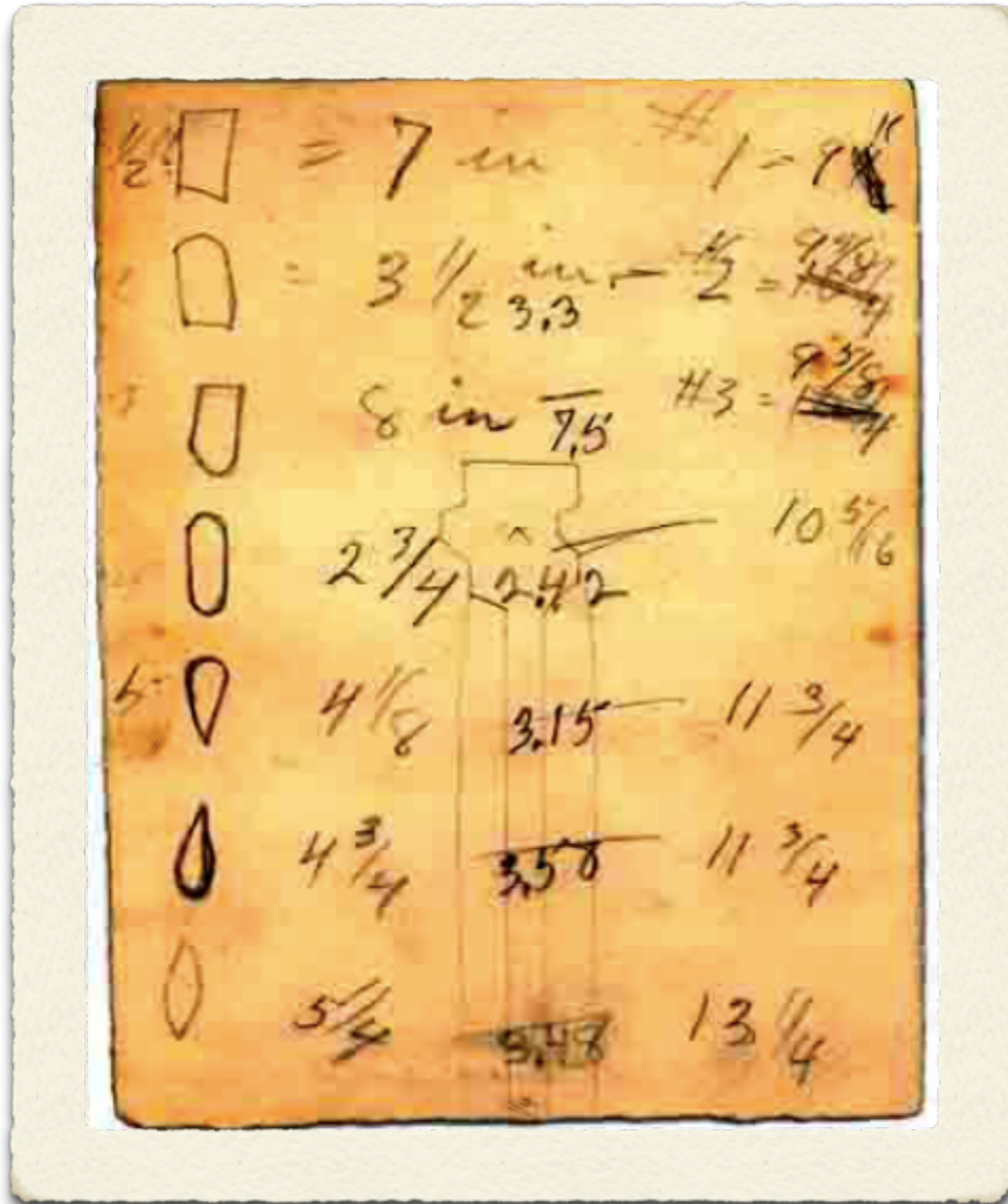


Accident rates and fatalities/year



Source: Flight Safety Foundation/Boeing Commercial Airplane Group

Learning from intuition & theory



Franklin Institute Science Museum. Wilbur Wright's handwriting

teach?...

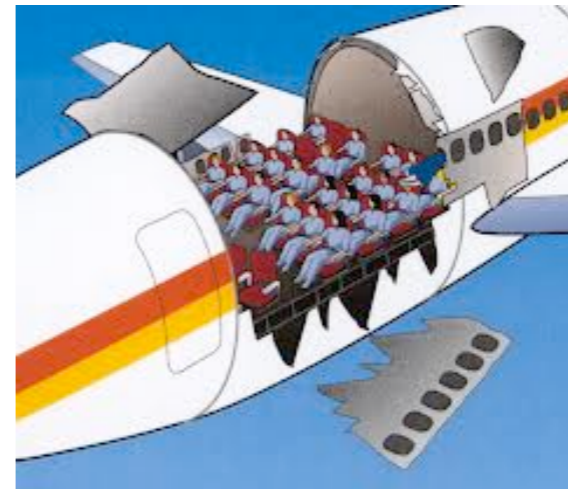


Learning from experience

Increased practical understanding of mechanics — in particular fracture and fatigue



Bird strikes



Aloha airlines accident - fatigue cracks at corners

Novel convertible aircraft

Learning from experiments

World's largest wind tunnel (2014)



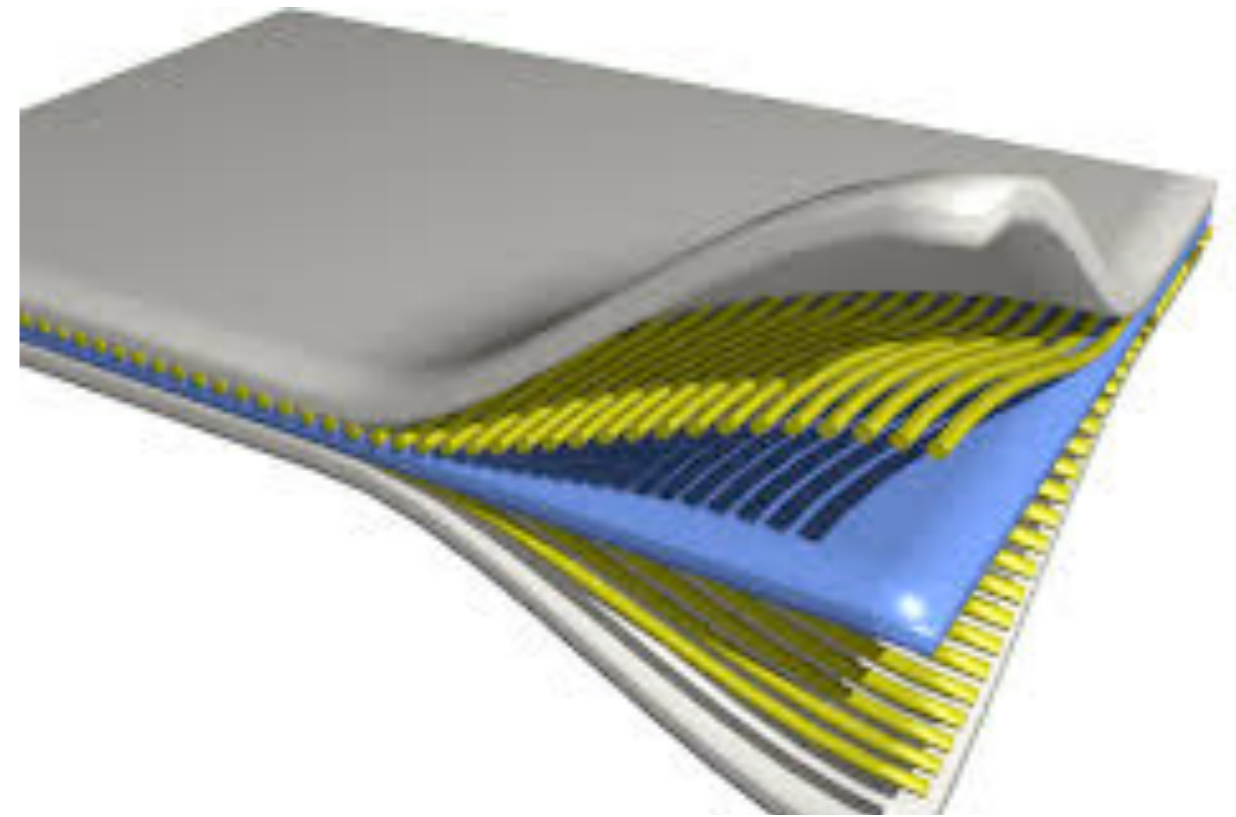
© AFP/Getty Images



Replica of the 1901 Wright Wind Tunnel
(constructed with assistance from Orville
Wright)

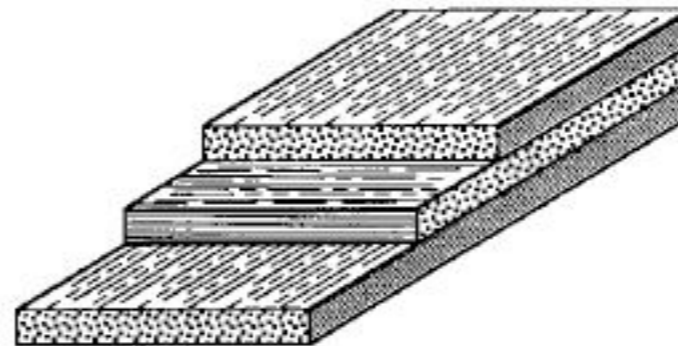
New materials for more payload

Introduction of composite materials have reduced the weight of structures by 20%

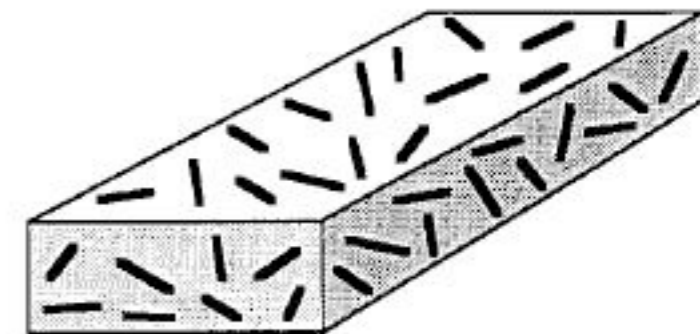


Over 1,000km saving of 8,660kg of fuel [A340-300]

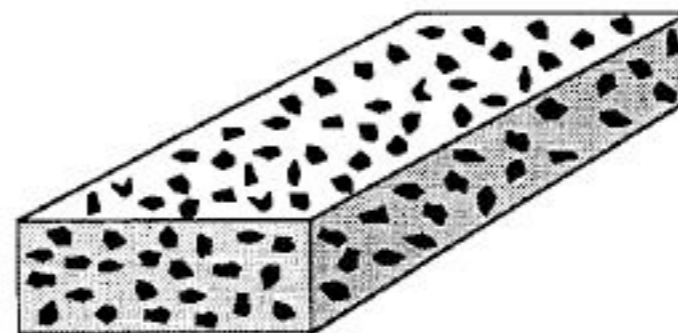
Continuous Fibers



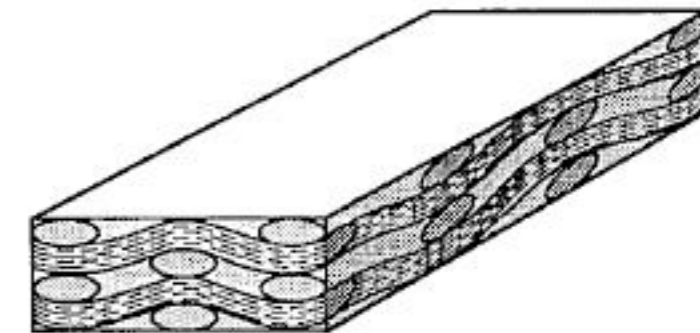
Discontinuous Fibers, Whiskers



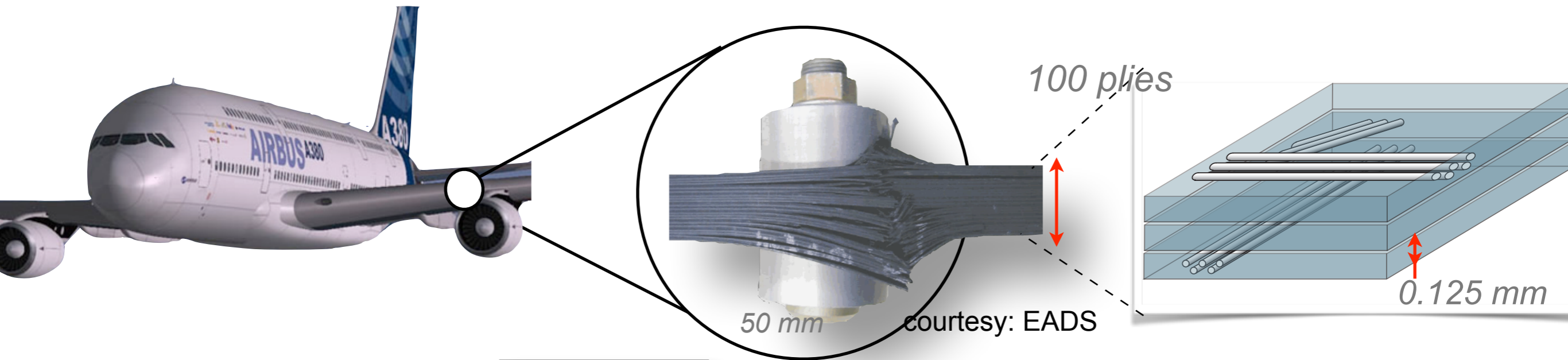
Particles



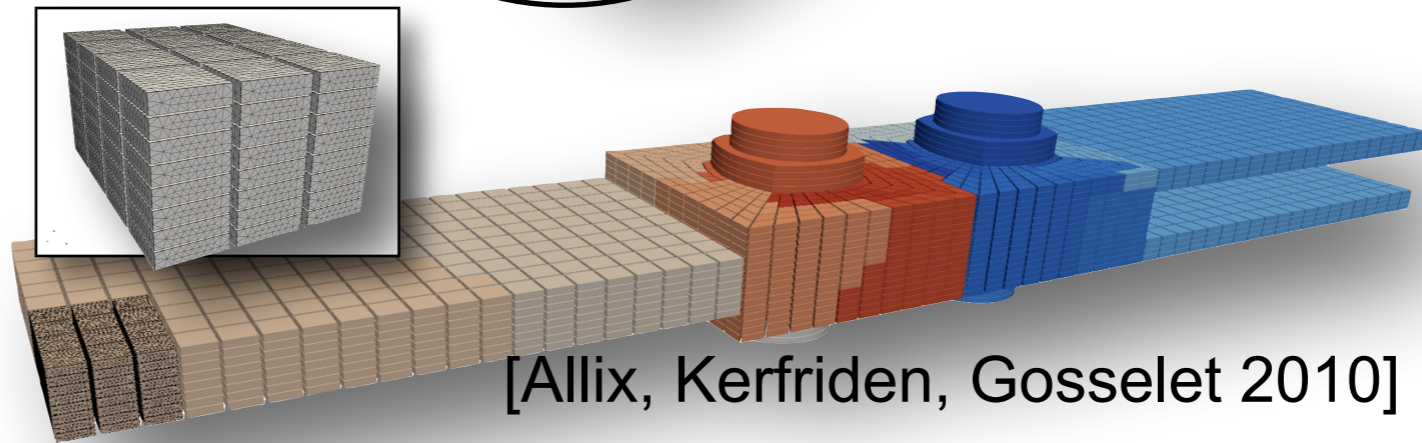
Fabric, Braid, Etc.



New kinds of experiments for new kinds of models

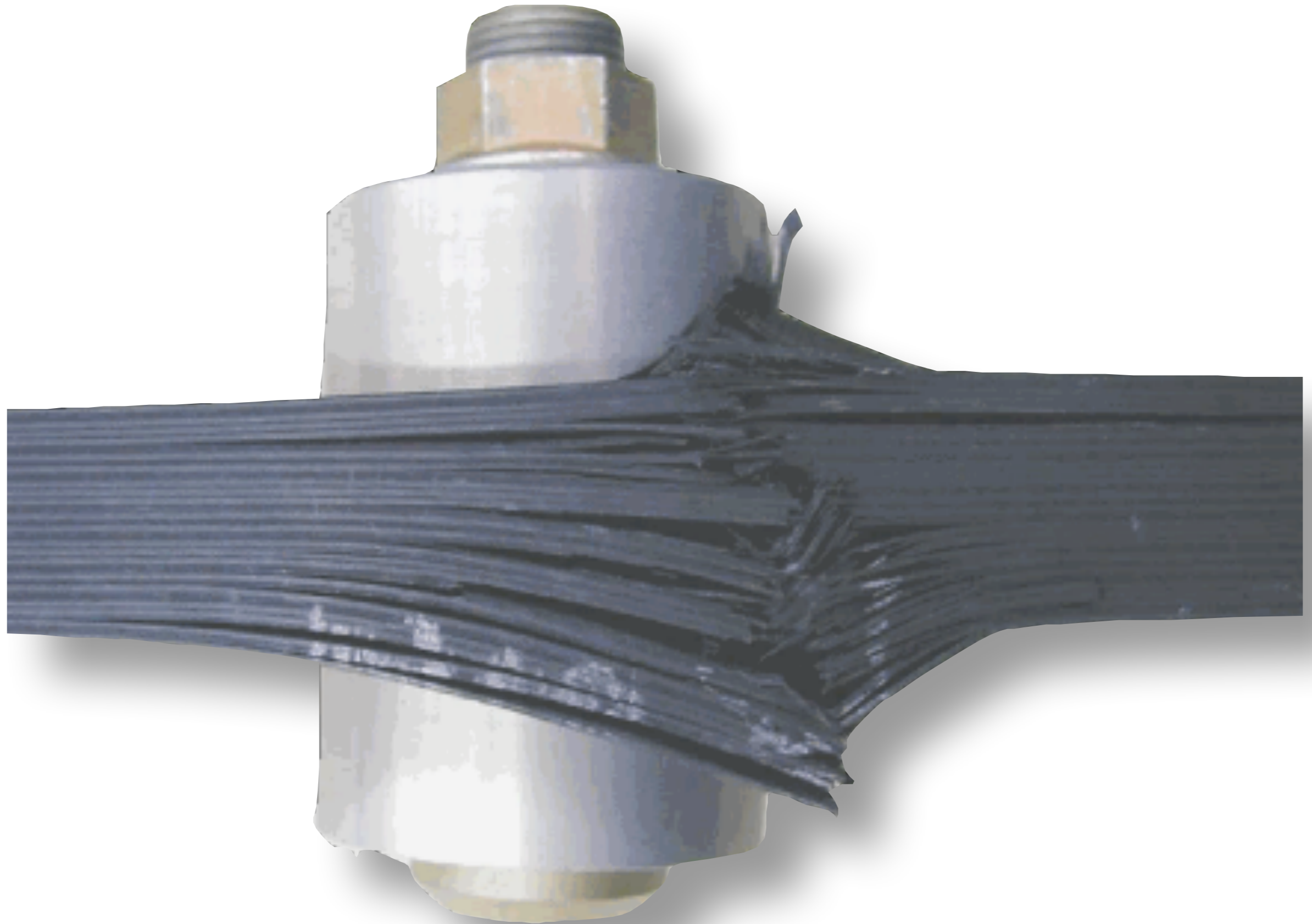


Discretise

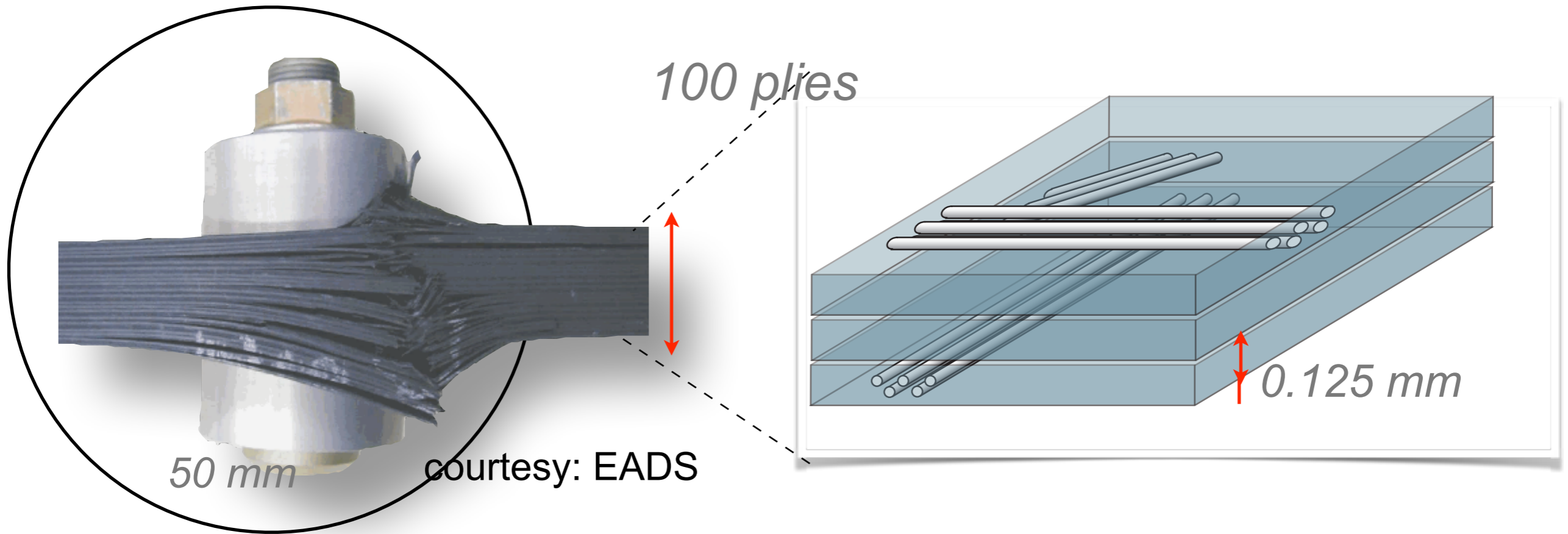


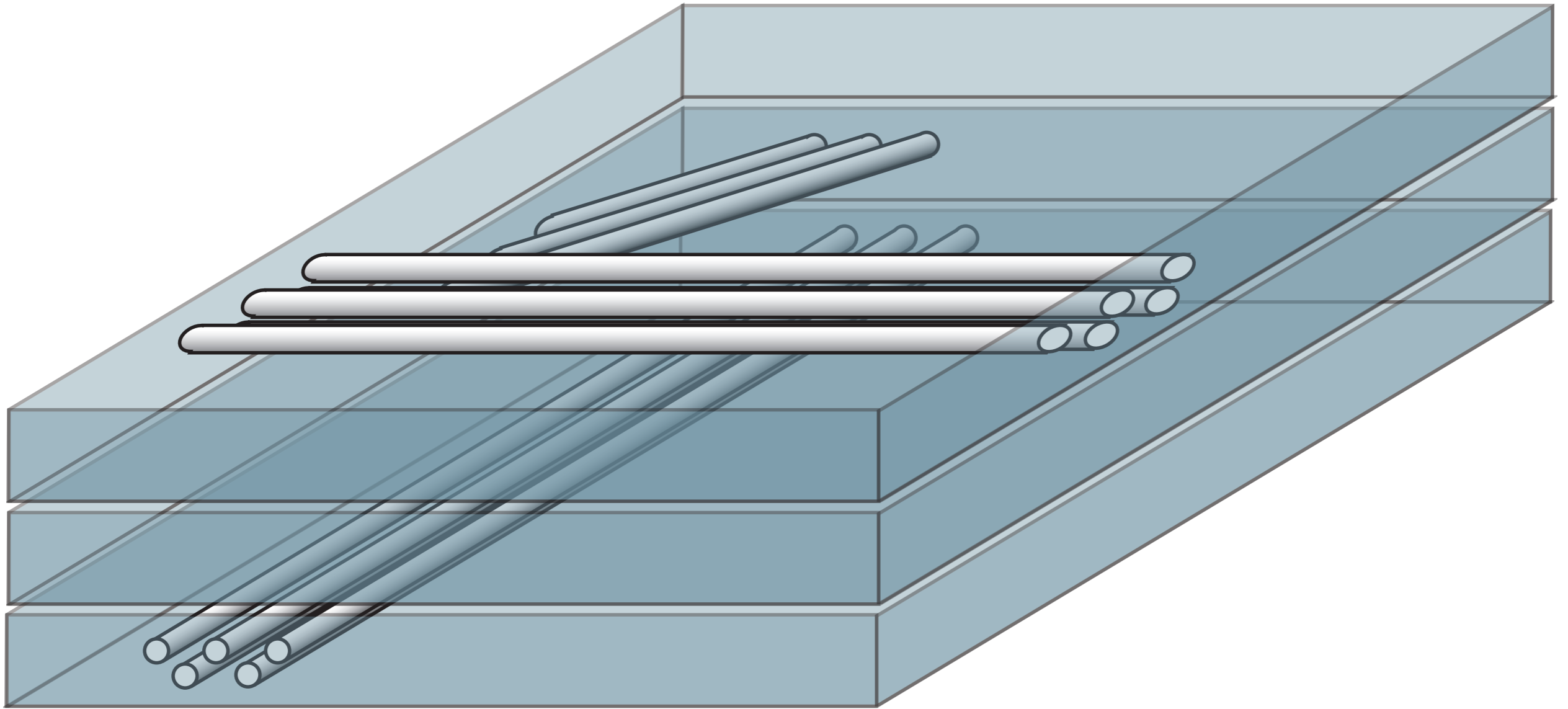
[Allix, Kerfriden, Gosselet 2010]

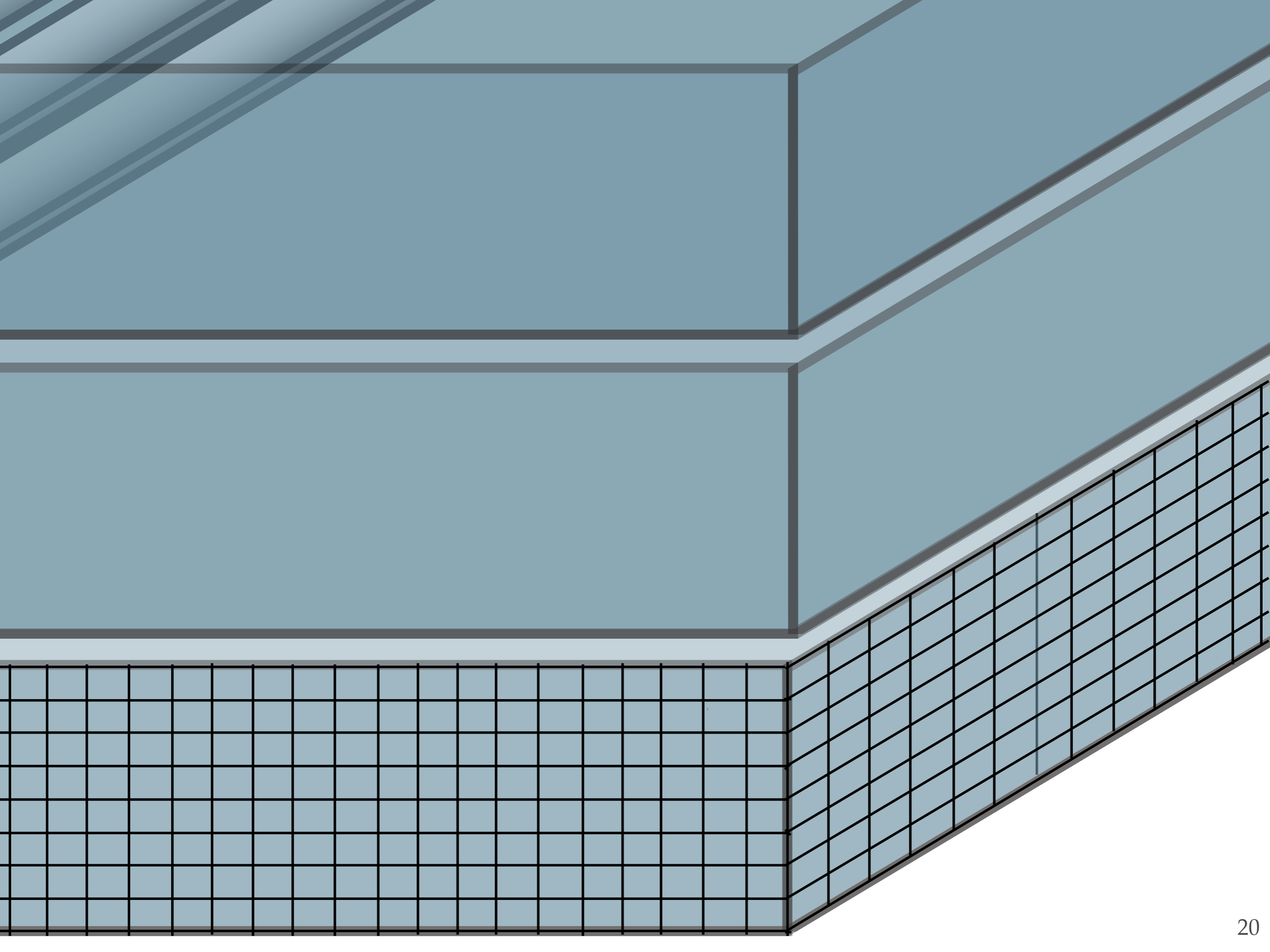
A bolted joint



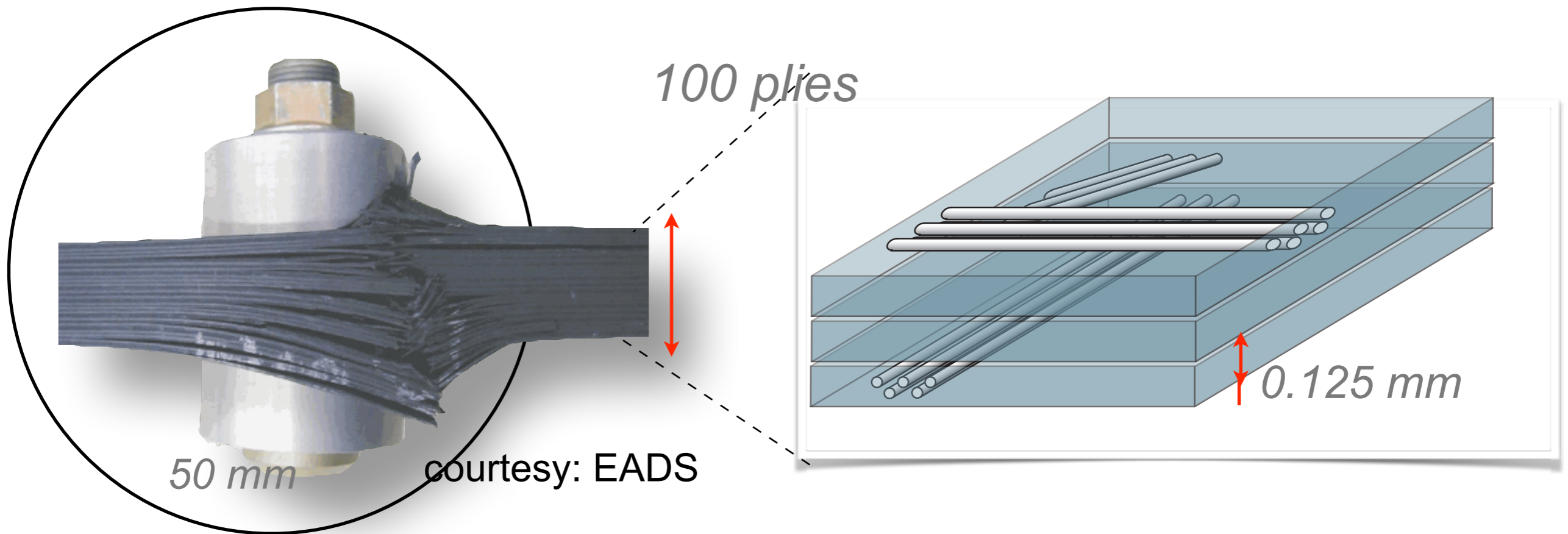
A bolted joint



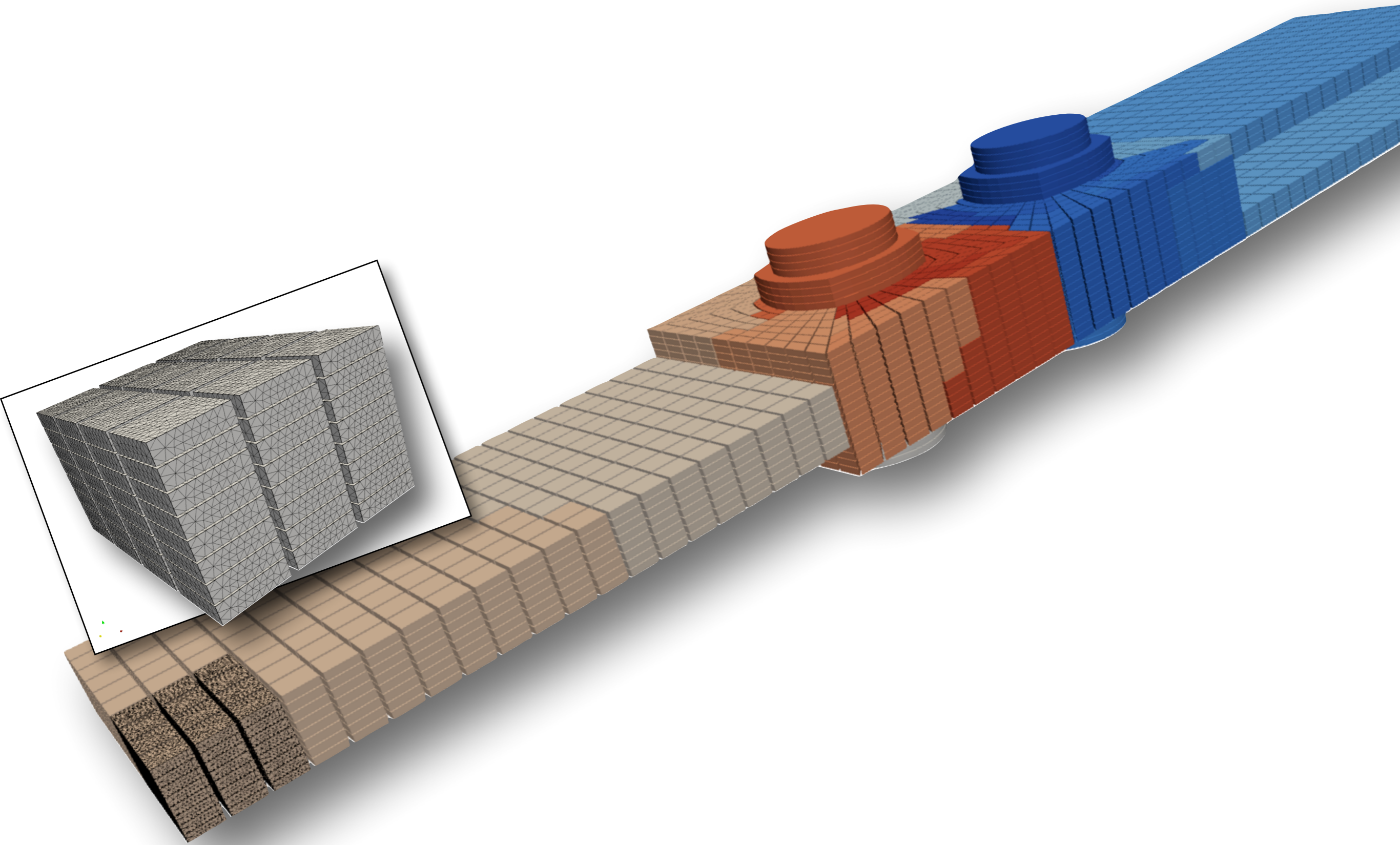


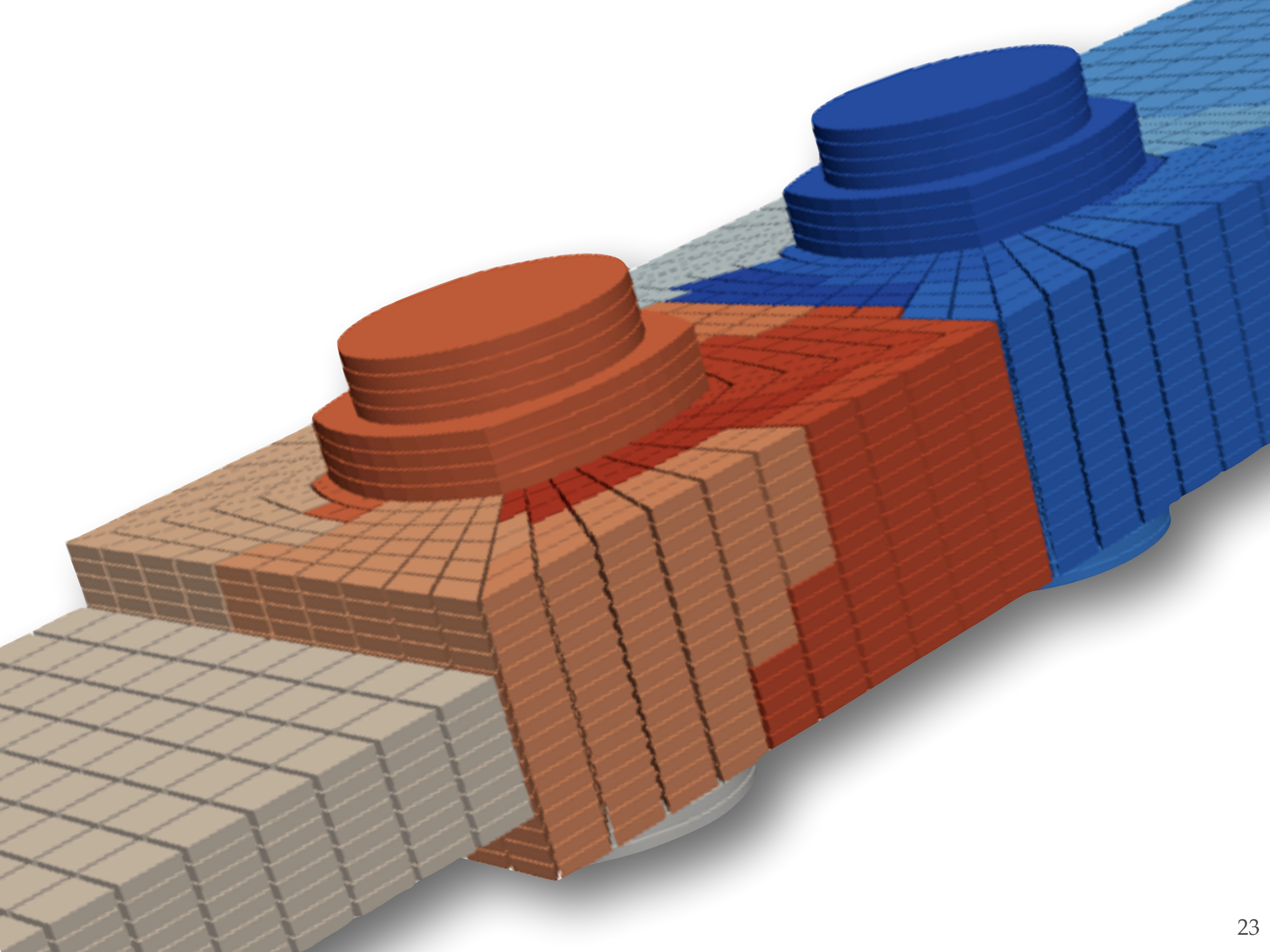


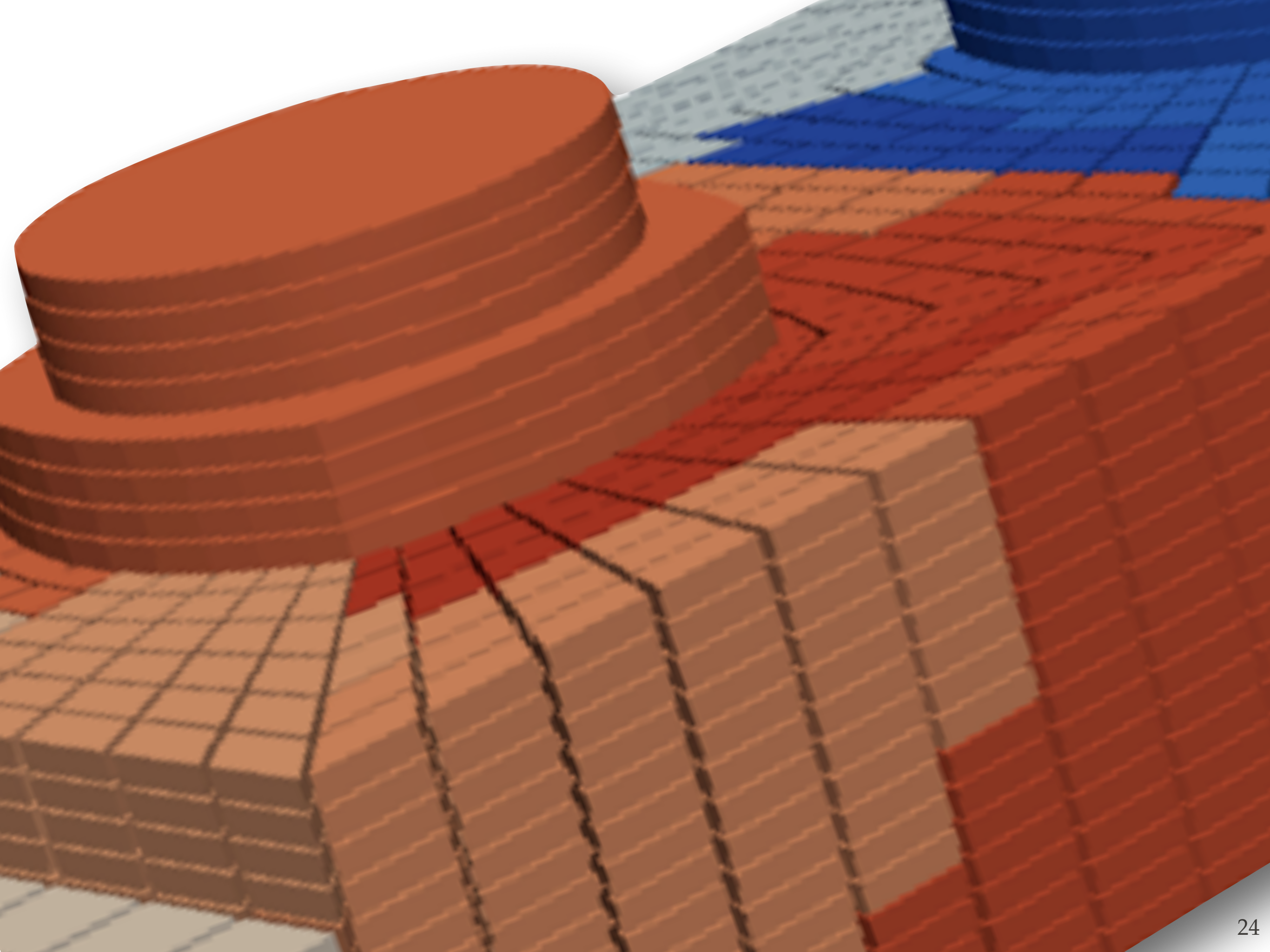
A bolted joint



- 5 elements through the thickness of a ply => 0.025mm/element
 - 50mm bolted joint area => 2,000 elements
 - 50mm x 50mm x 100 plies => 2,000 x 2,000 x (100 x 5)
- => 2 billion elements**







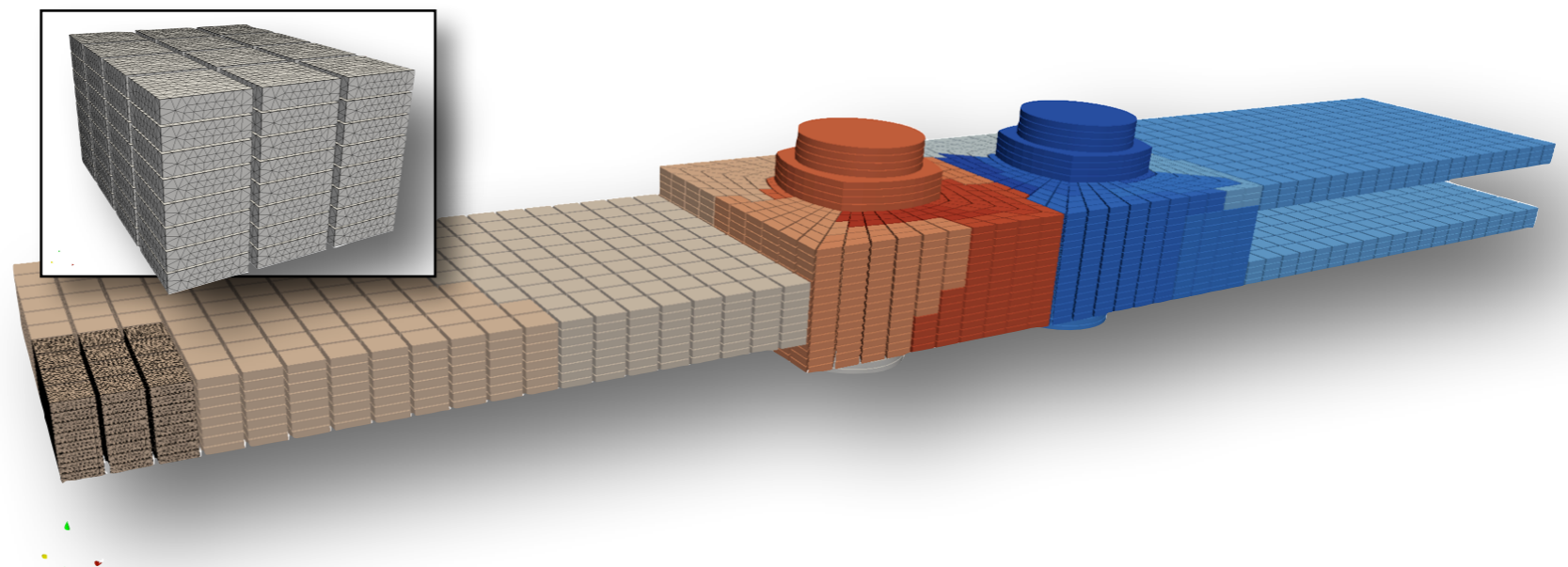
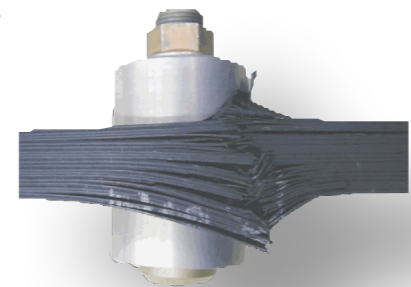
A380 giant



Large structures

whose behaviour is governed by
small-scale effects

=> **intractable problem size**



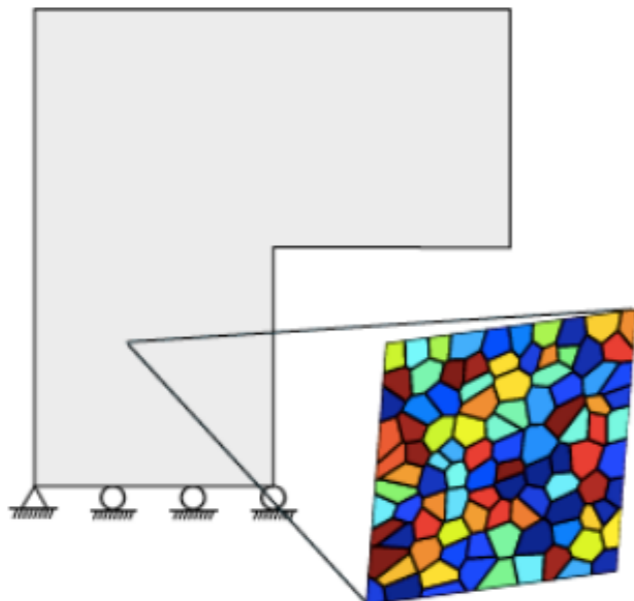
How can the problem size
be reduced but the
accuracy controlled?

Challenge

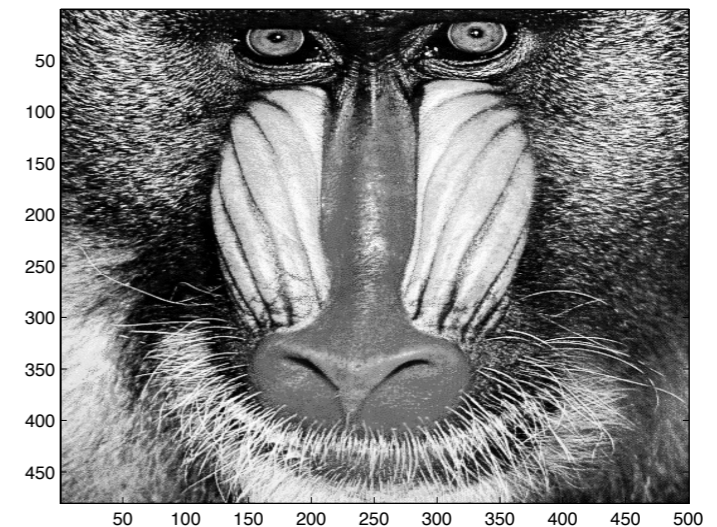
- Reduce the problem size
- Preserve essential features

Reduce computational
expense
Control the error

Physics based model
reduction a.k.a. **Multiscale
Methods**



Algebraic based model
reduction a.k.a. **Machine
Learning**

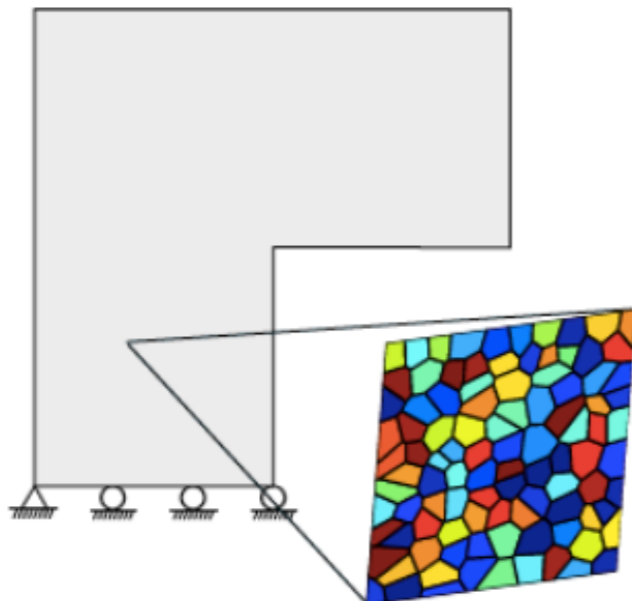


Challenge

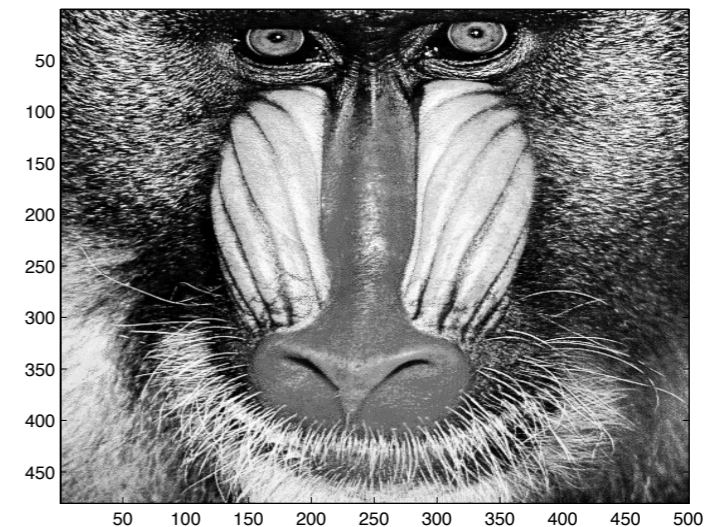
- Reduce the problem size
- Preserve essential features

Reduce computational
expense
Control the error

Physics based model
reduction a.k.a. Multiscale
Methods



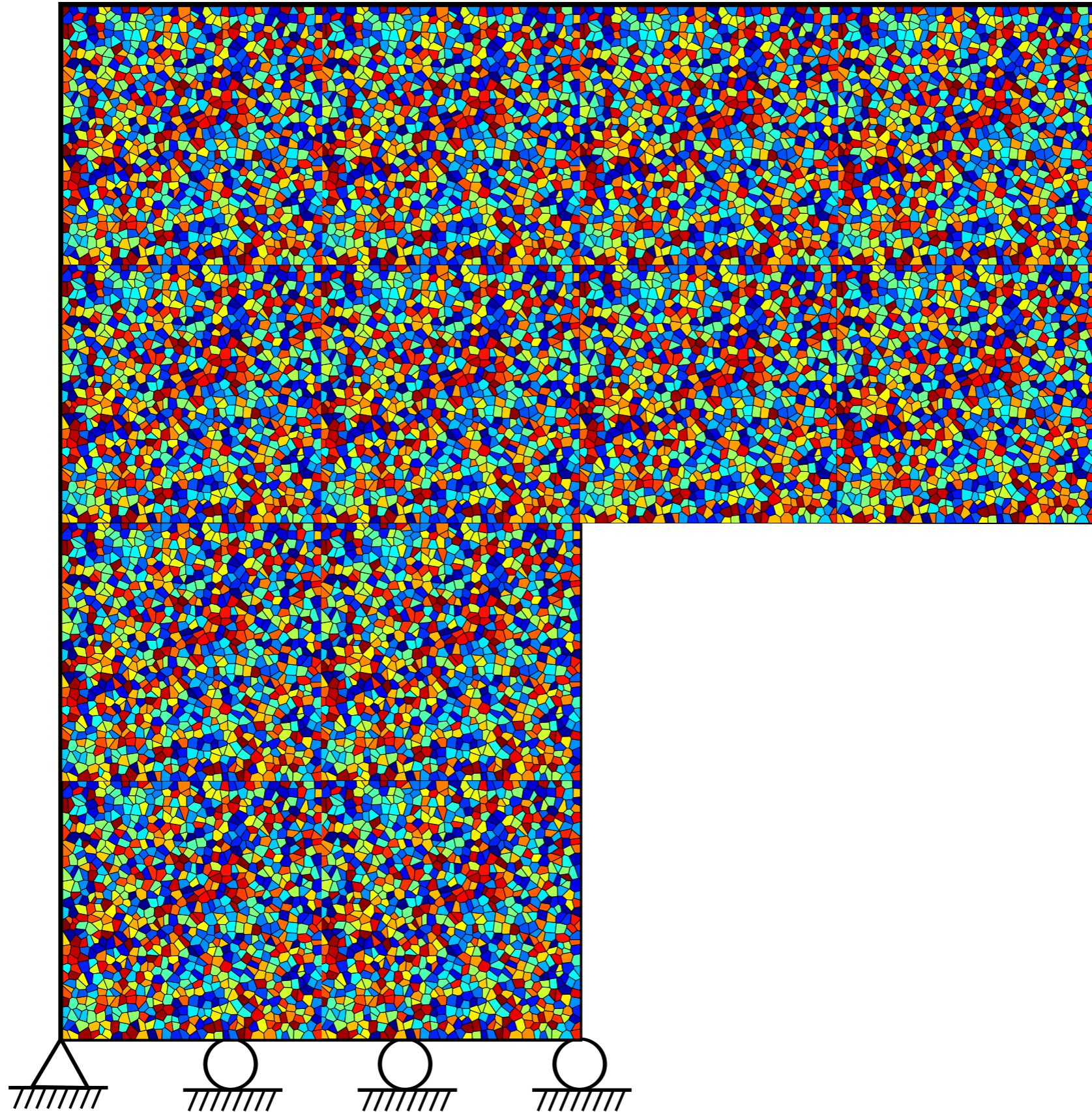
Algebraic based model
reduction a.k.a. Machine
Learning

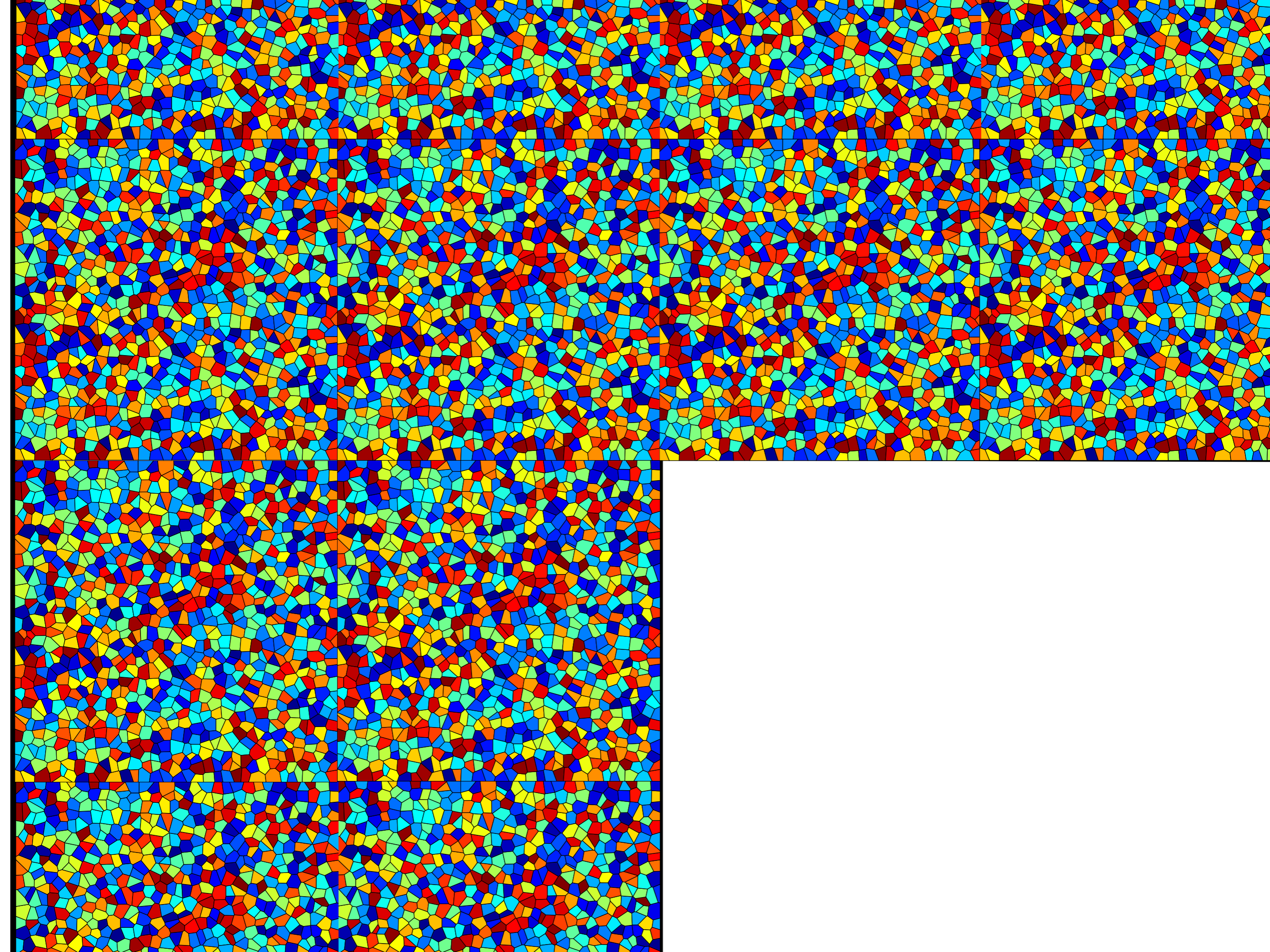


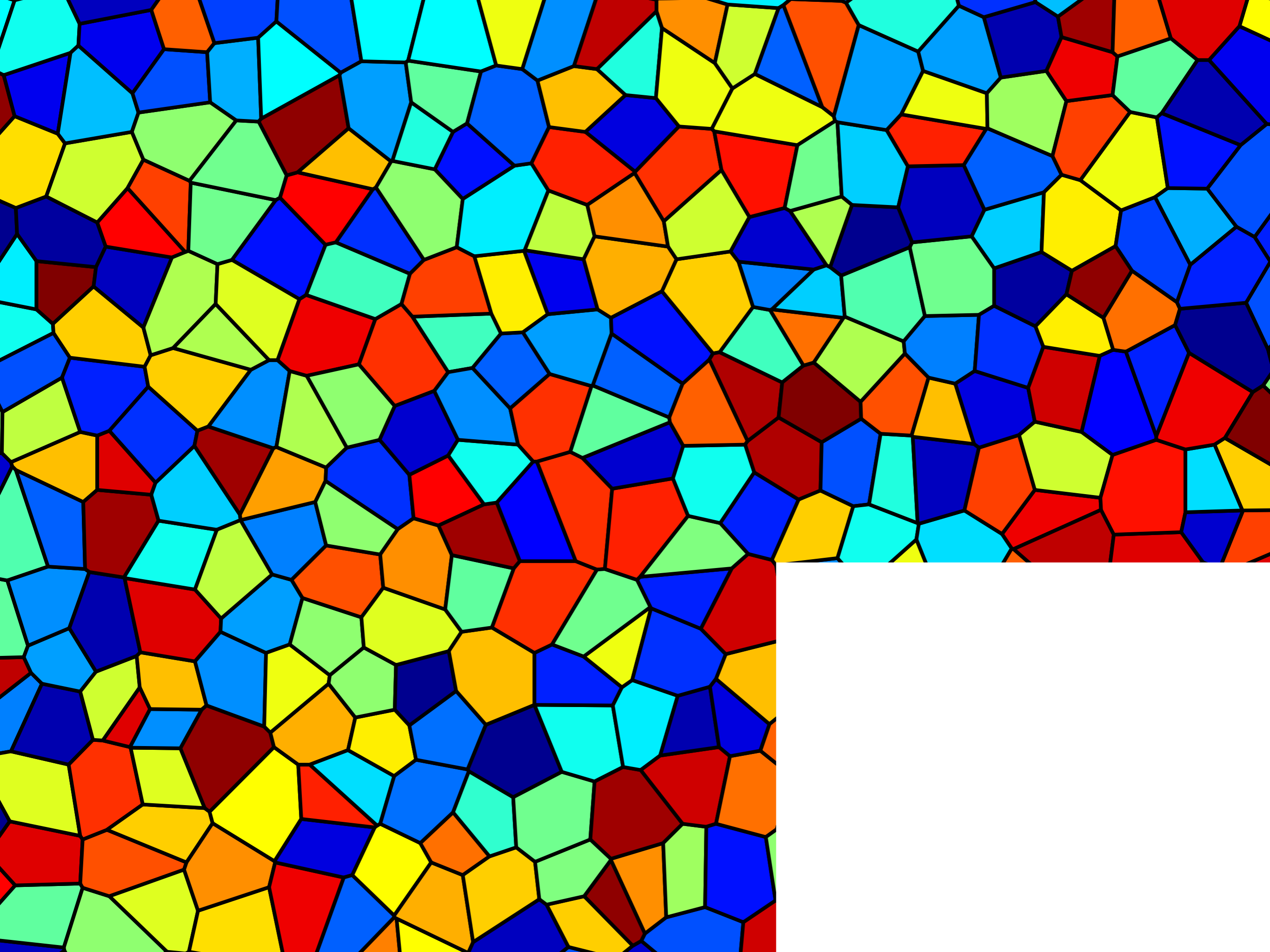
Physics-based
model reduction methods

multi-scale methods

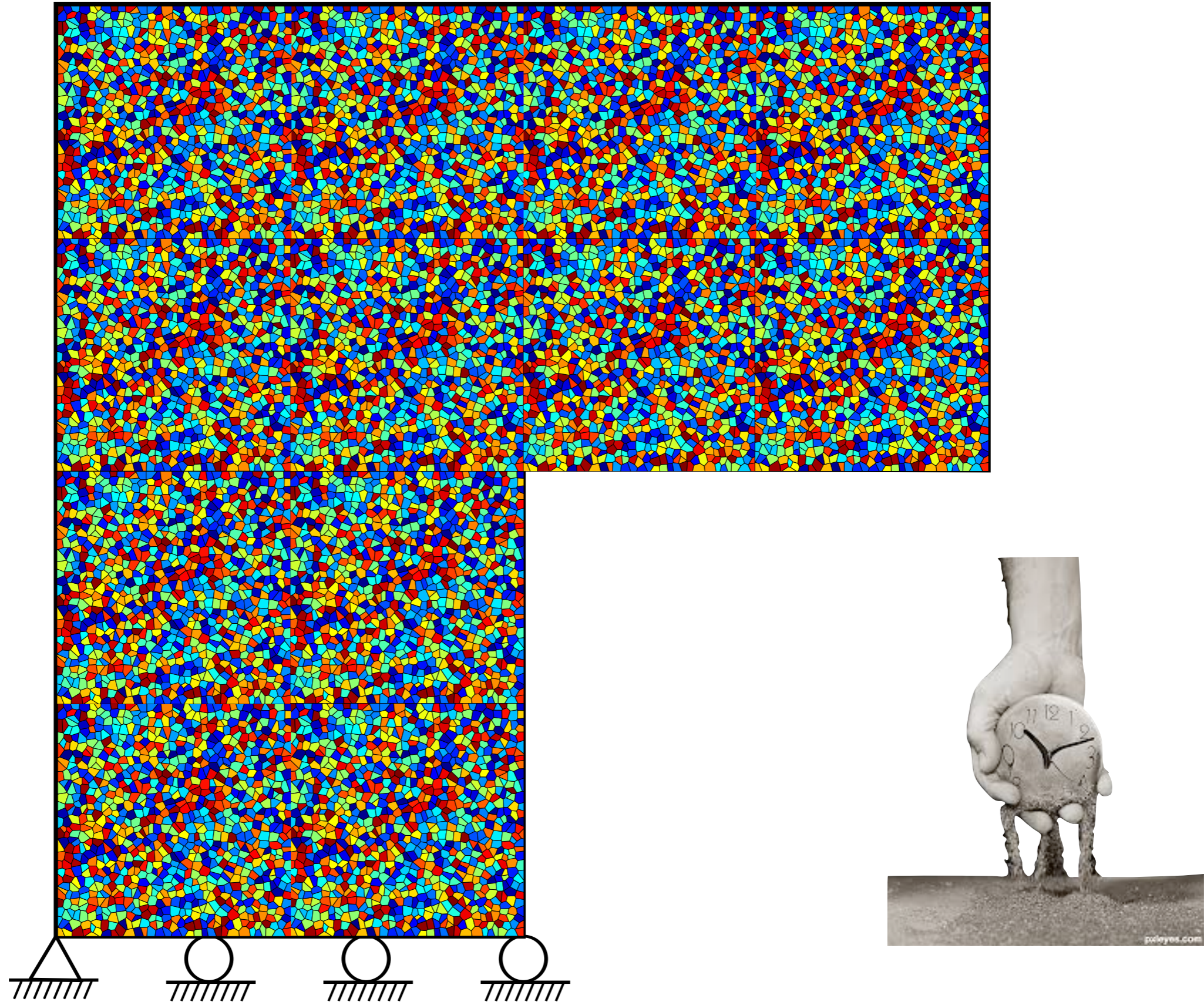
Full-scale





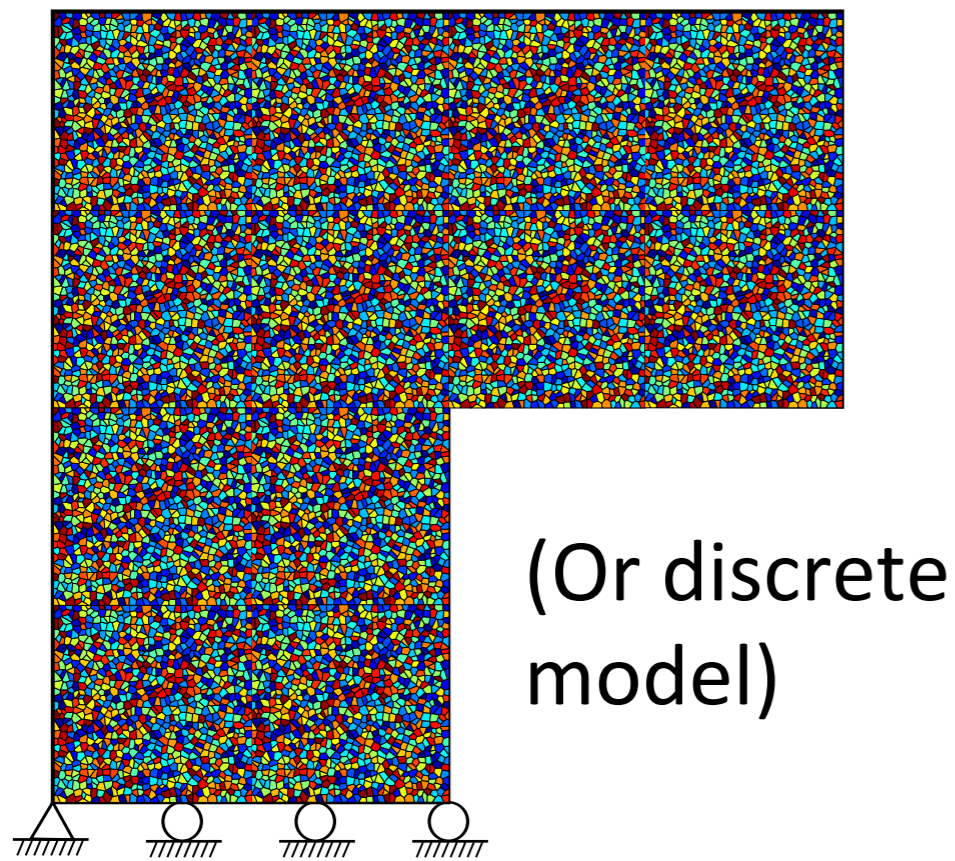


Full-scale

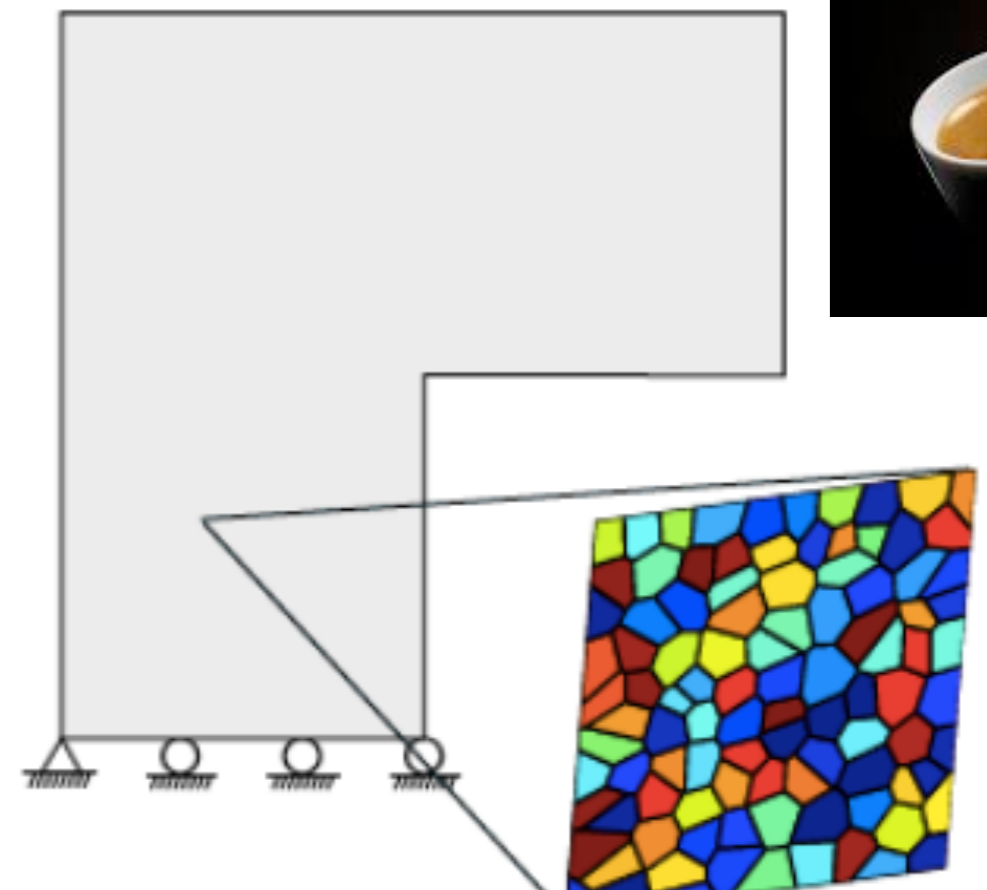
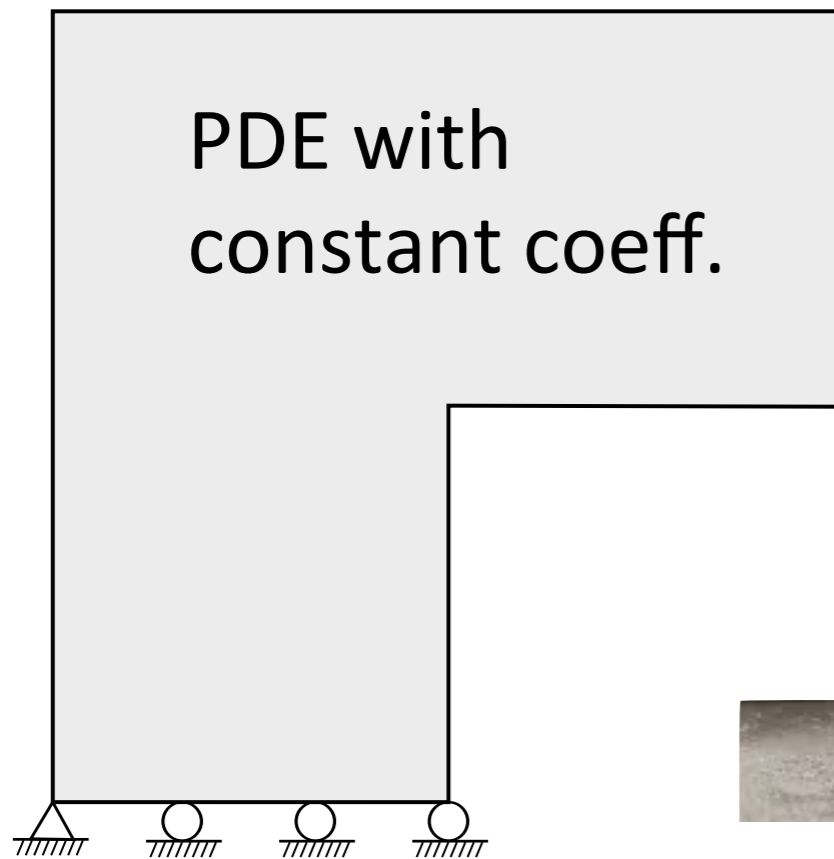


Multi-scale methods

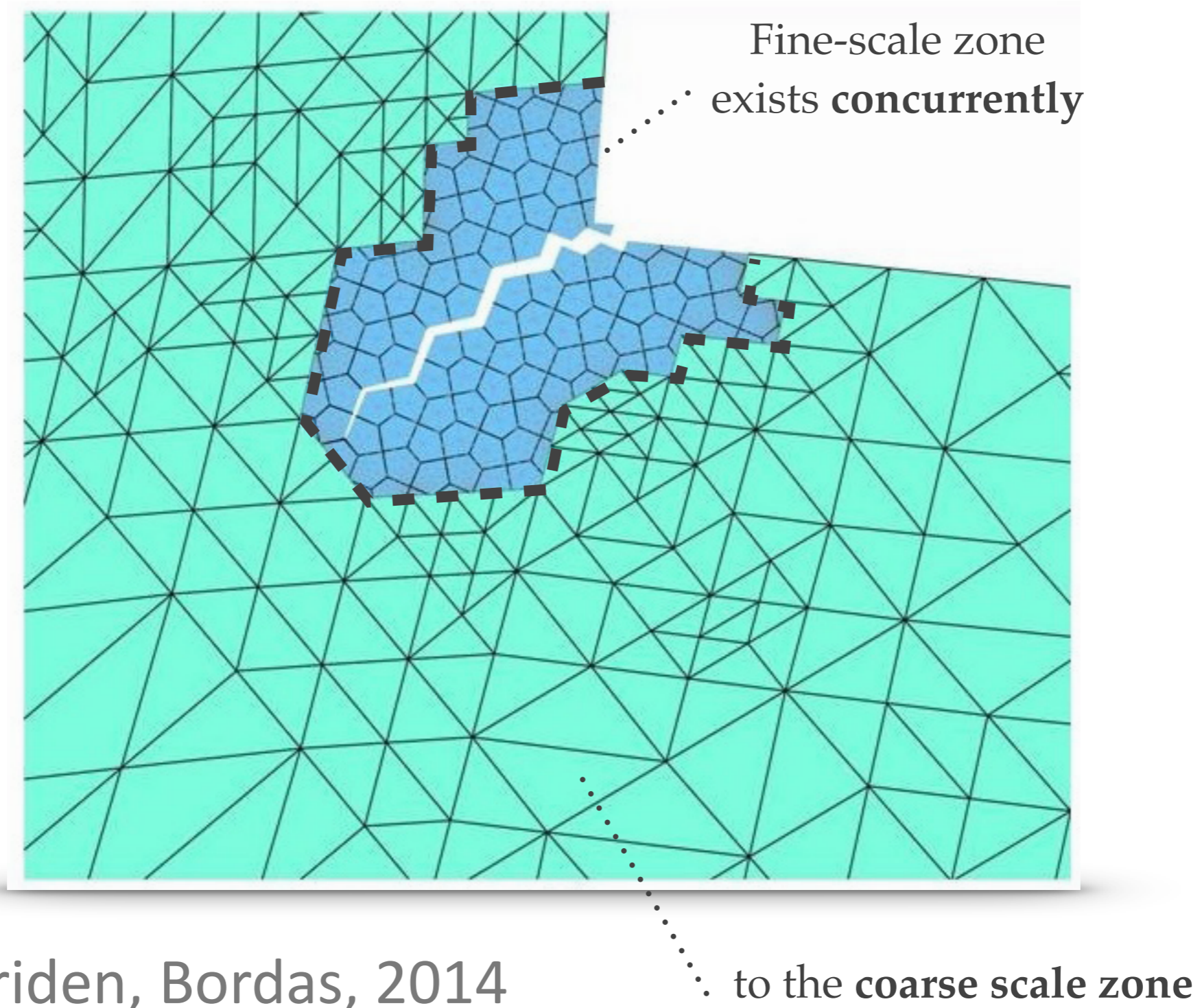
Replace the heterogeneous fine-scale model by an equivalent smoother model at the scale where the predictions are required



↓ Homogenisation

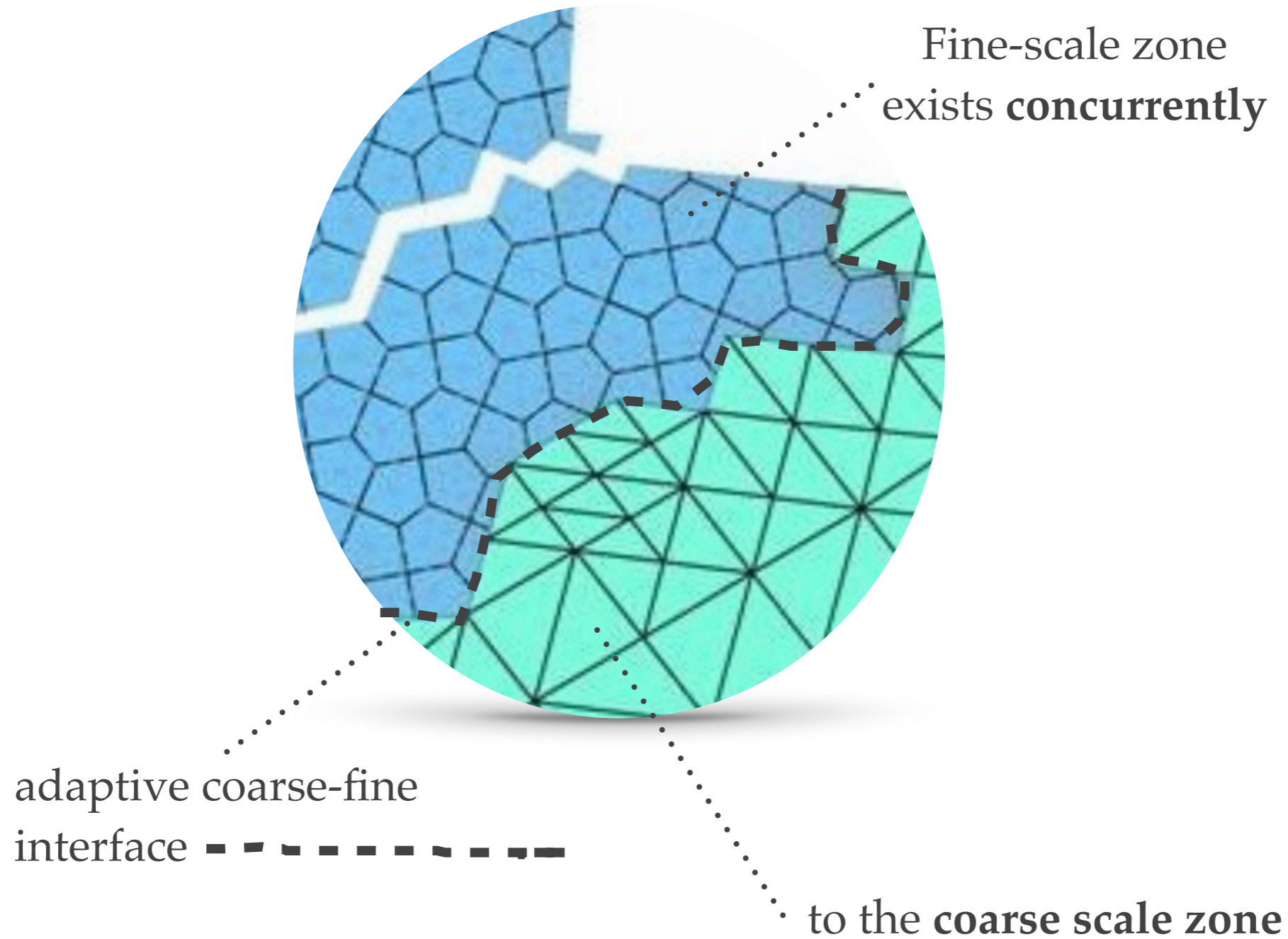


Concurrent methods

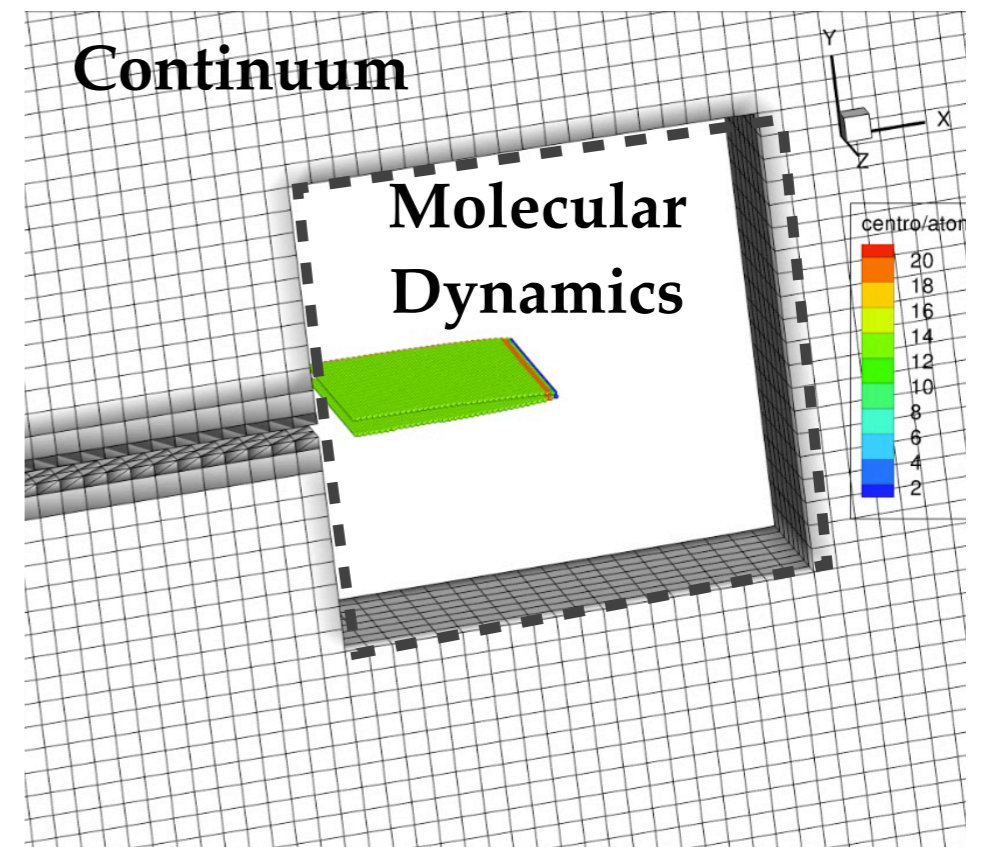
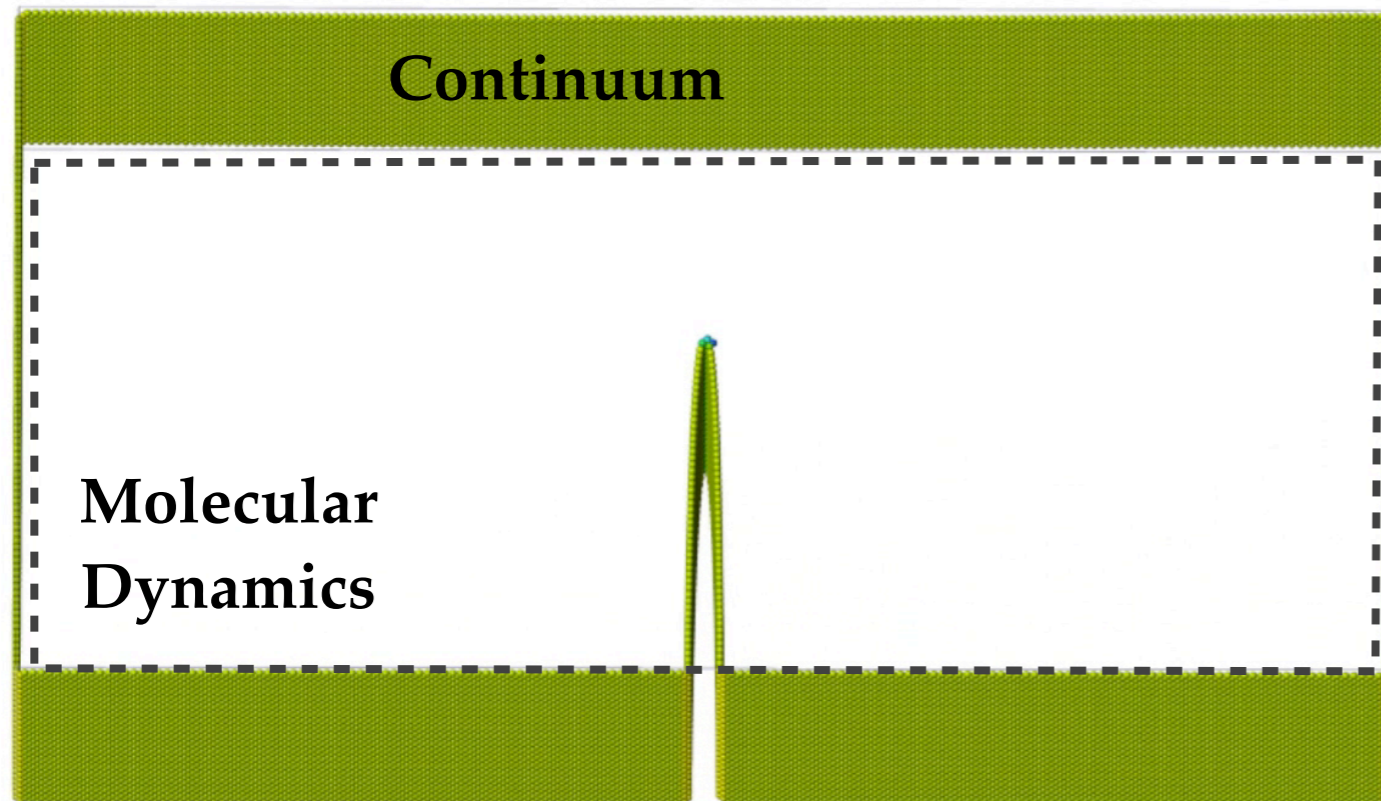
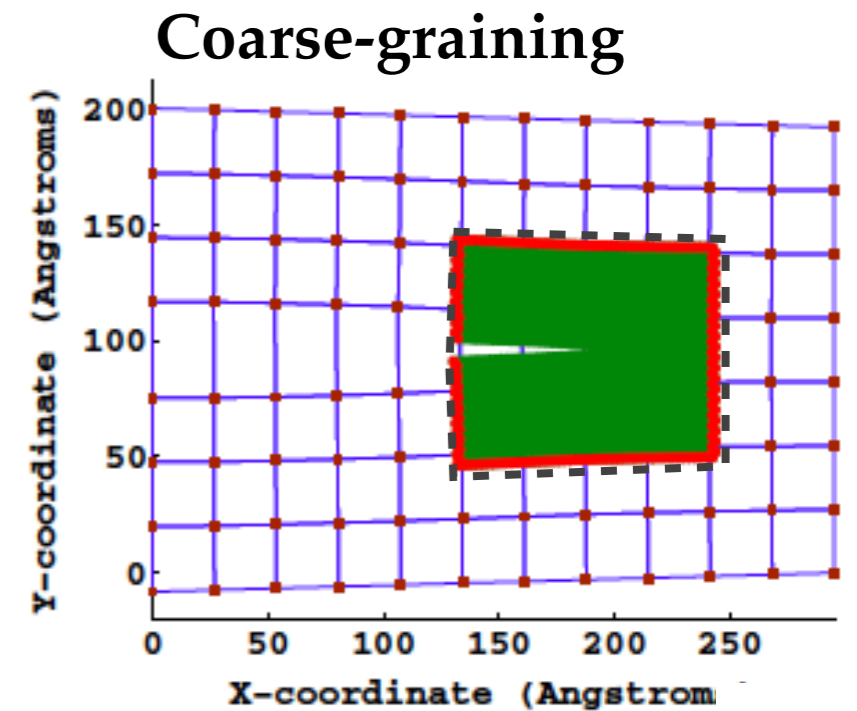
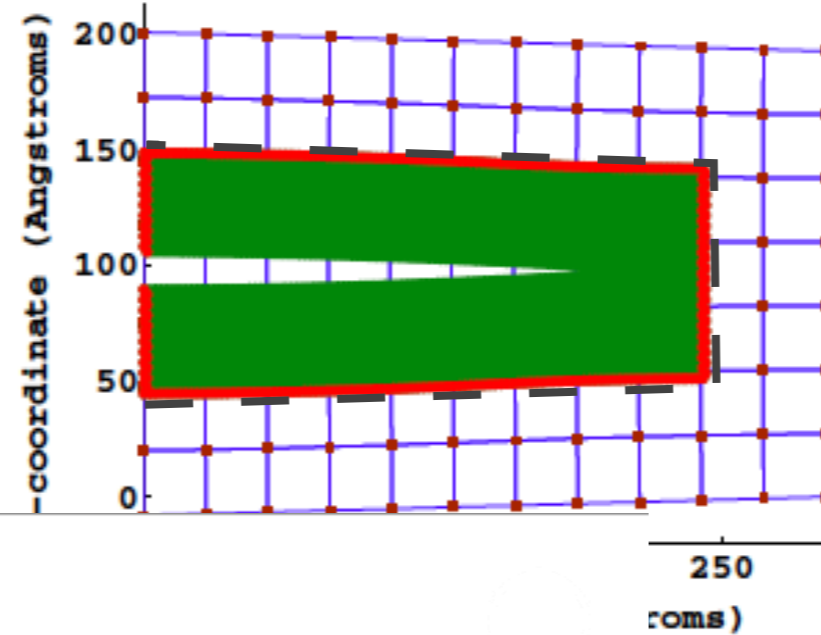
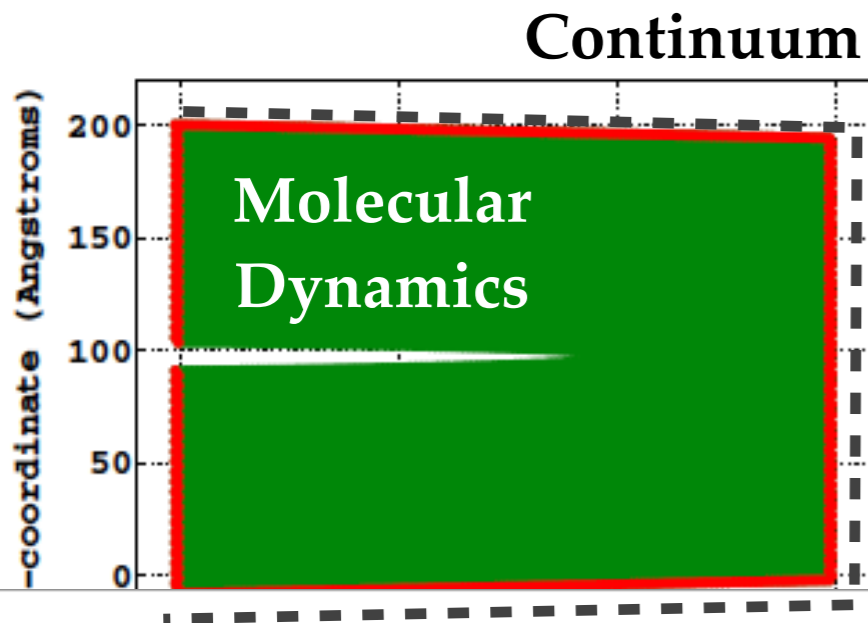


Akbari, Kerfriden, Bordas, 2014

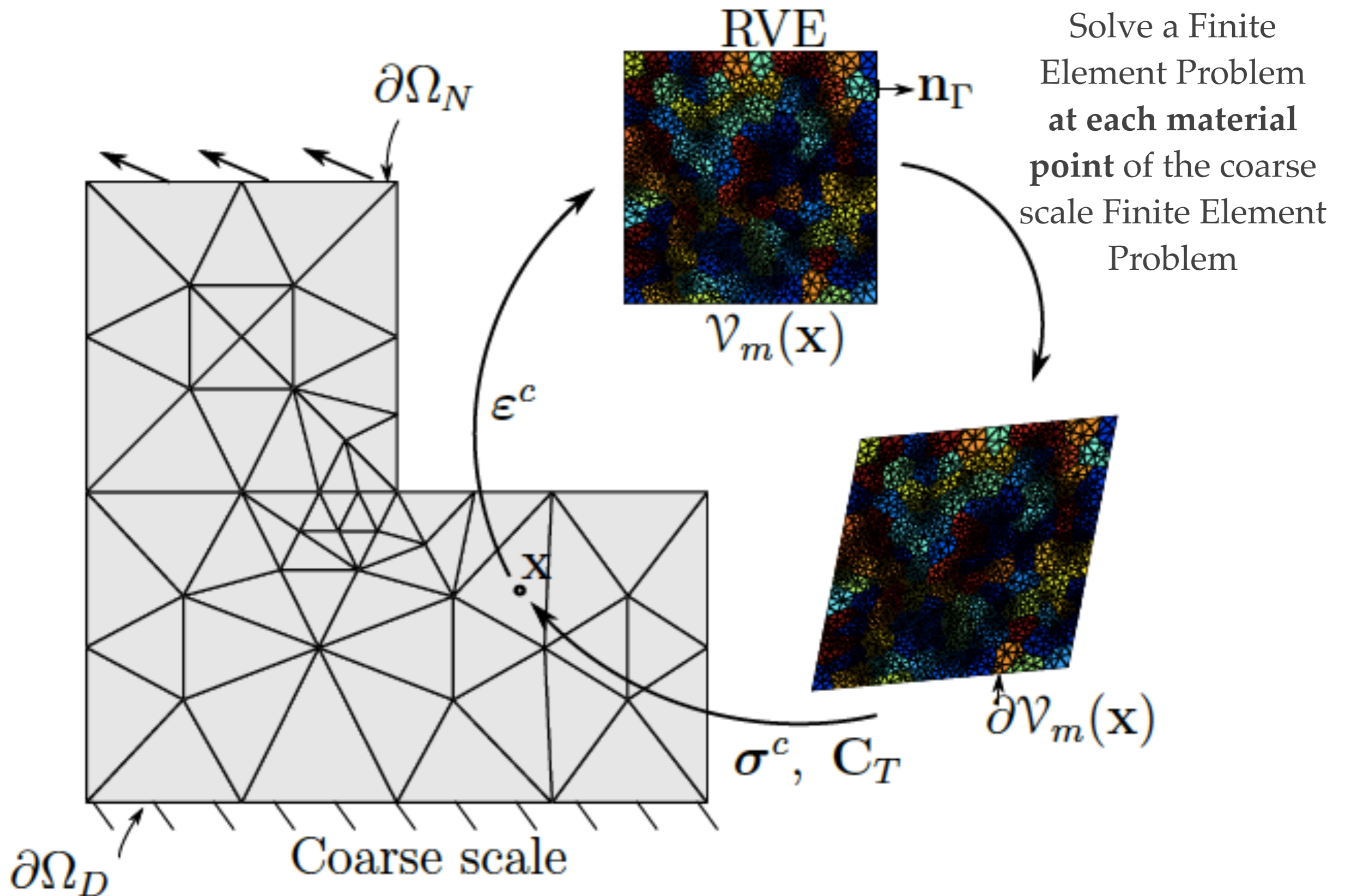
Concurrent methods



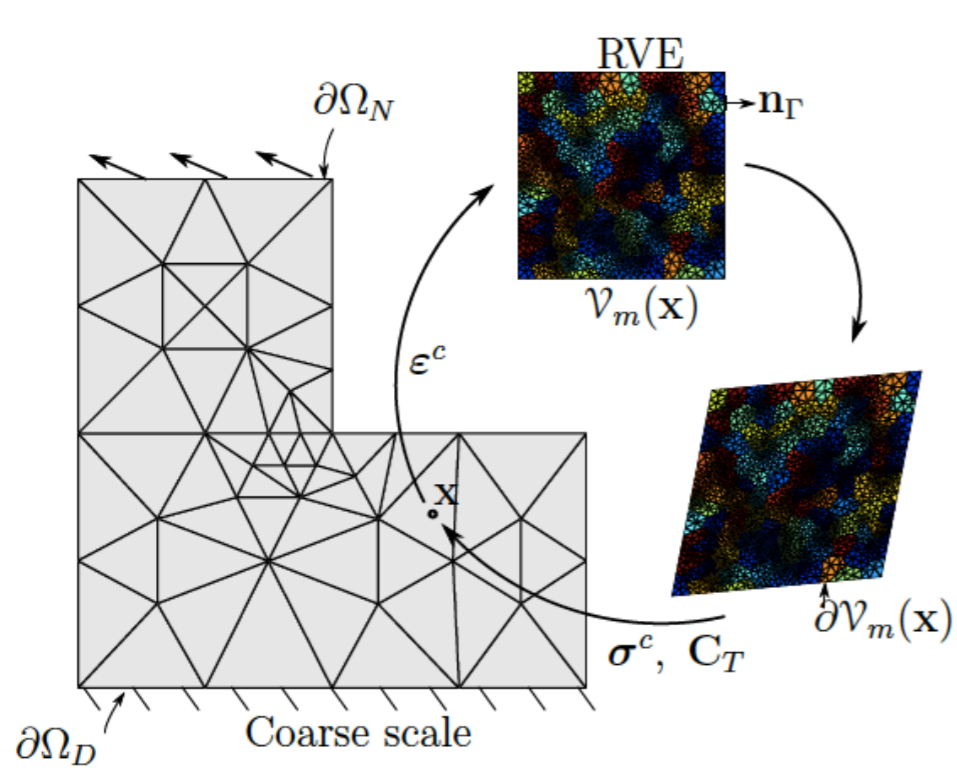
Concurrent methods



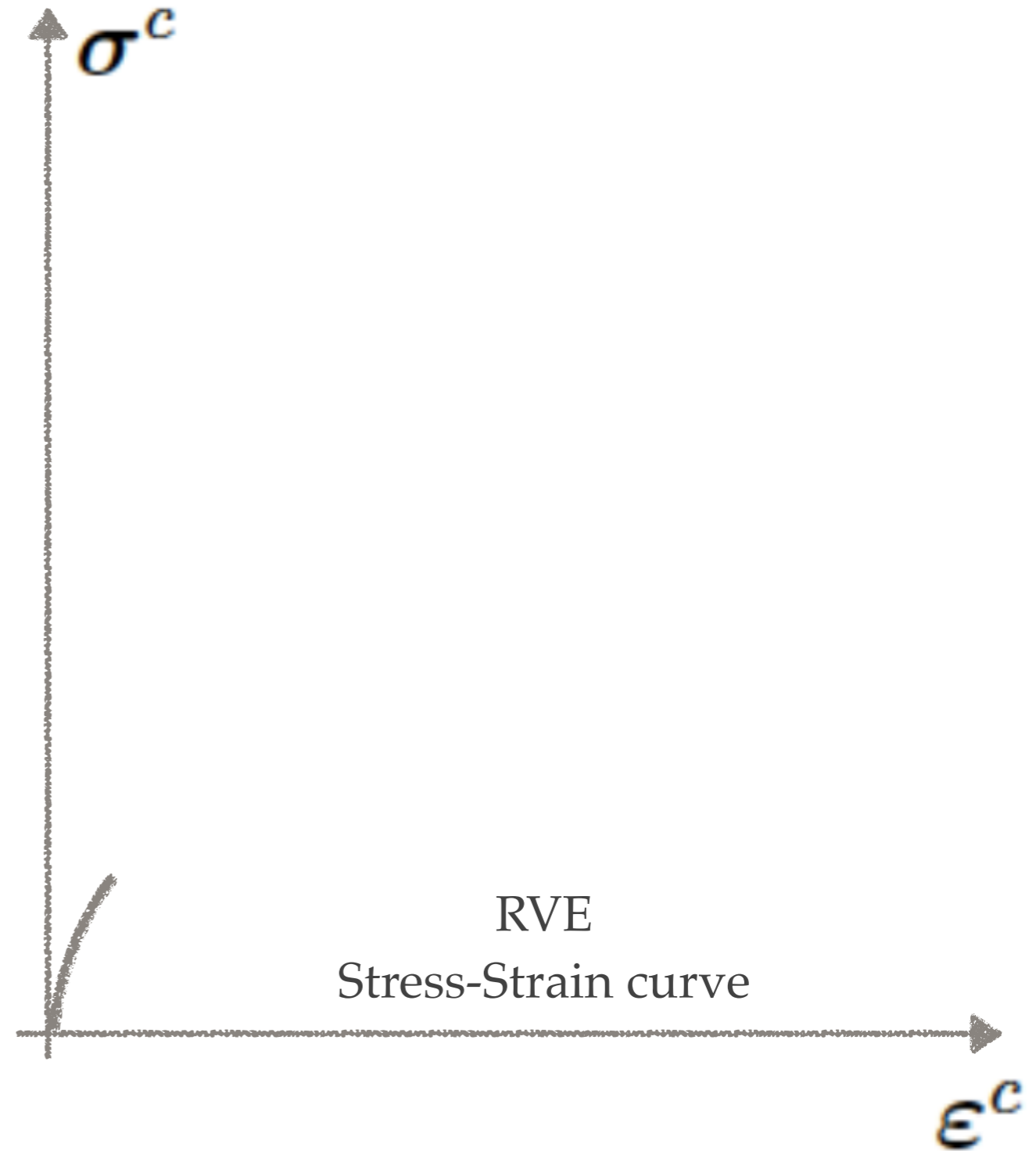
Hierarchical methods FE²



Hierarchical methods FE²

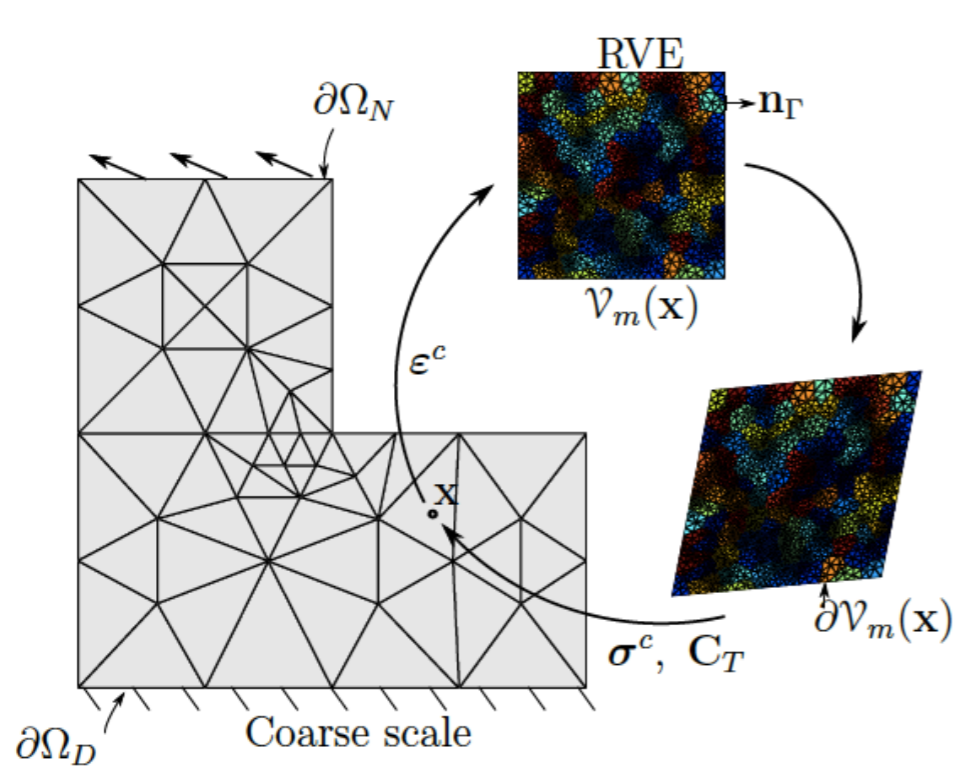


Loading

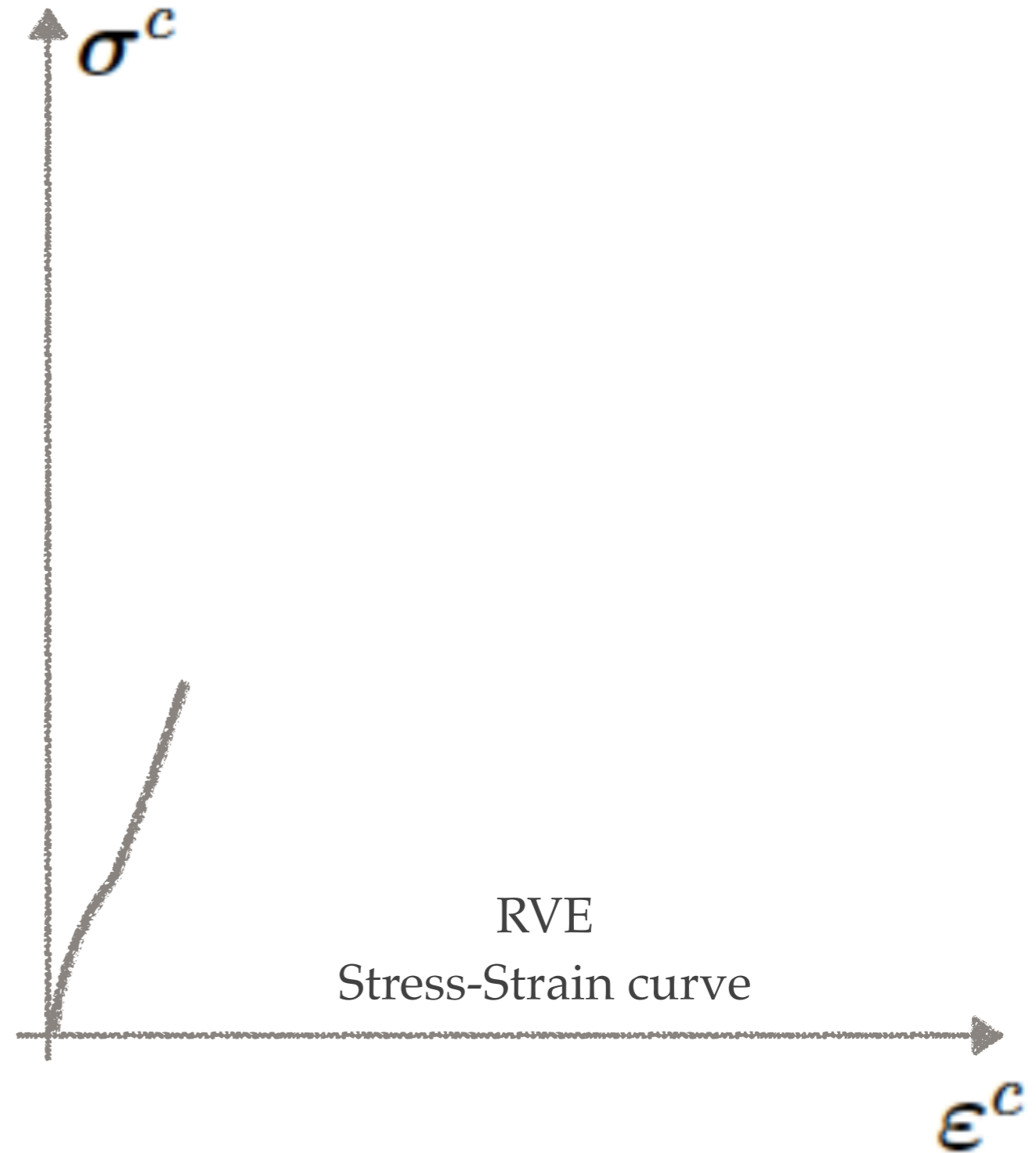


Feyel, Chaboche, 2000 - Akbari, Kerfriden, Bordas, 2014

Hierarchical methods FE²

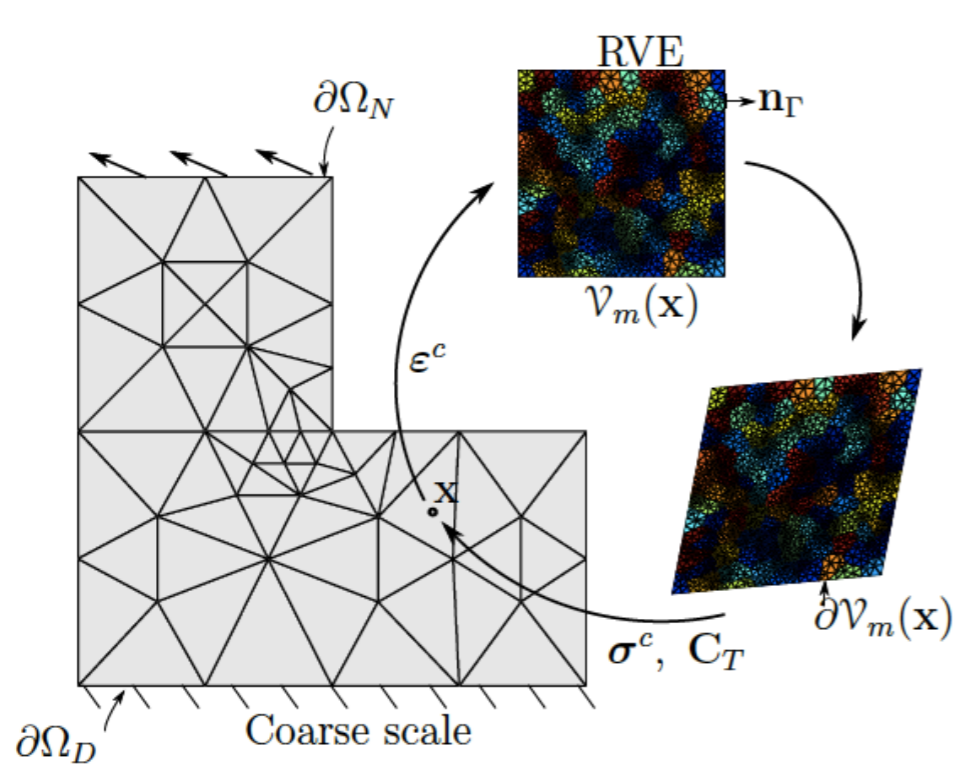


Loading

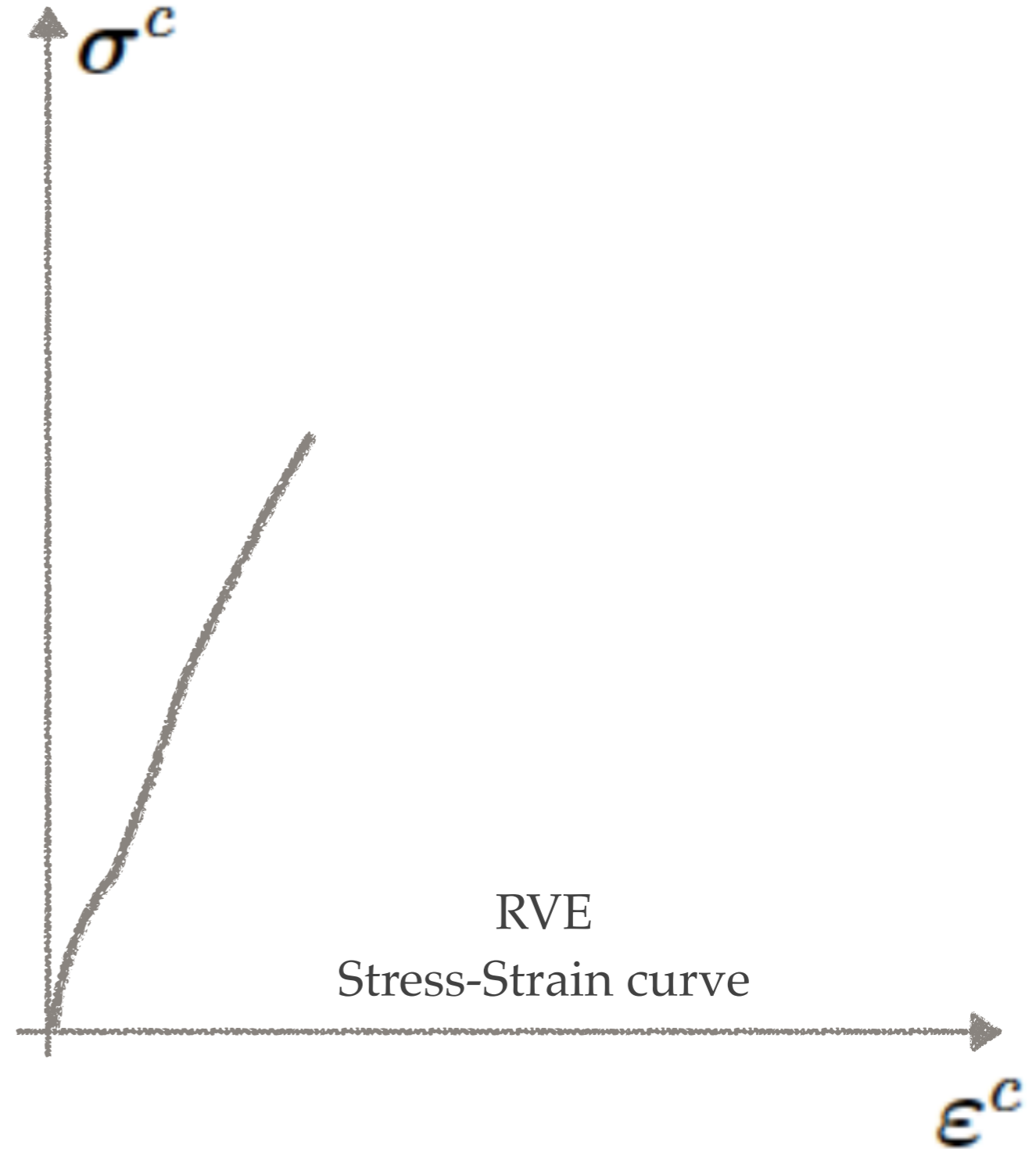


Feyel, Chaboche, 2000 - Akbari, Kerfriden, Bordas, 2014

Hierarchical methods FE²

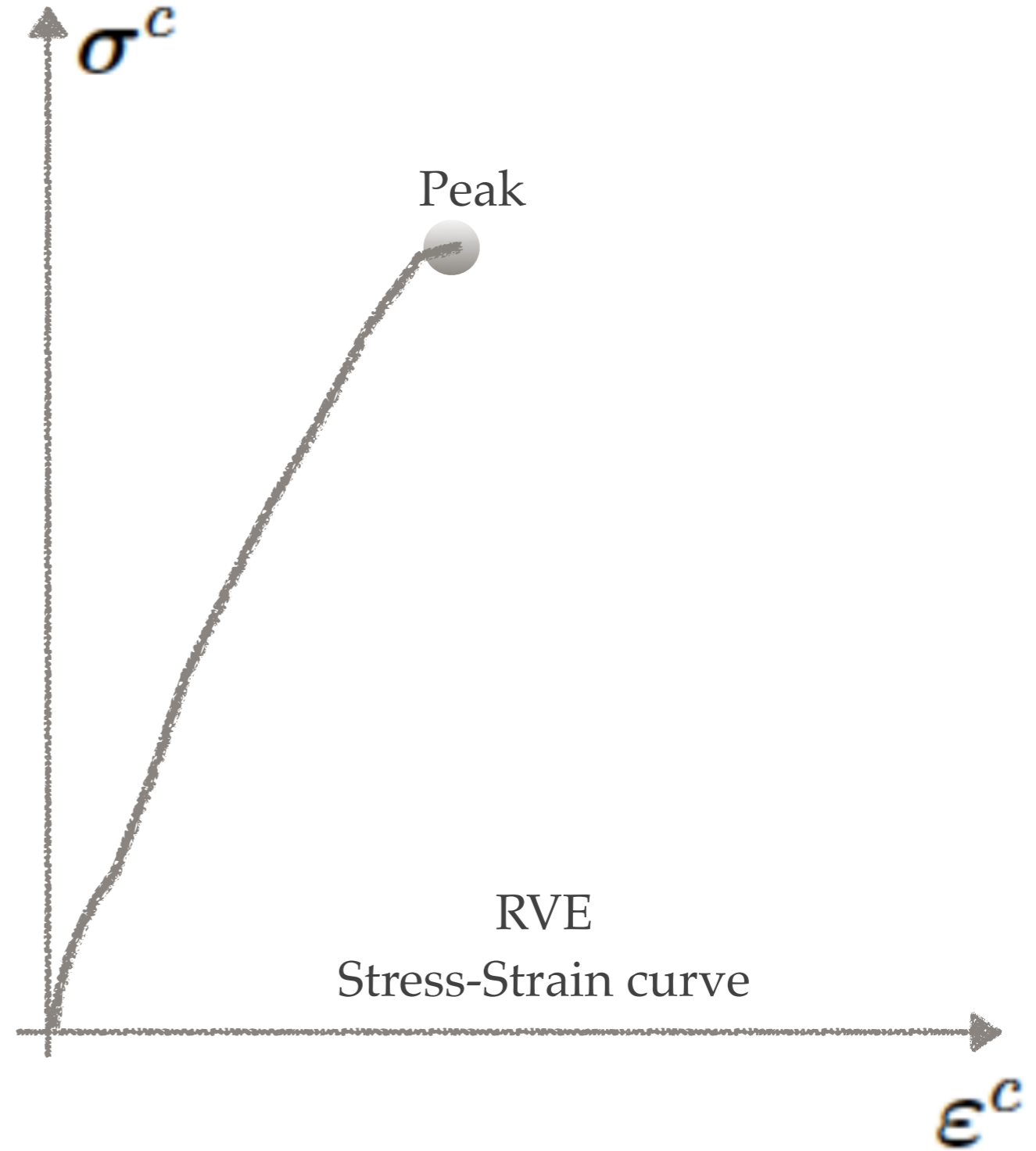
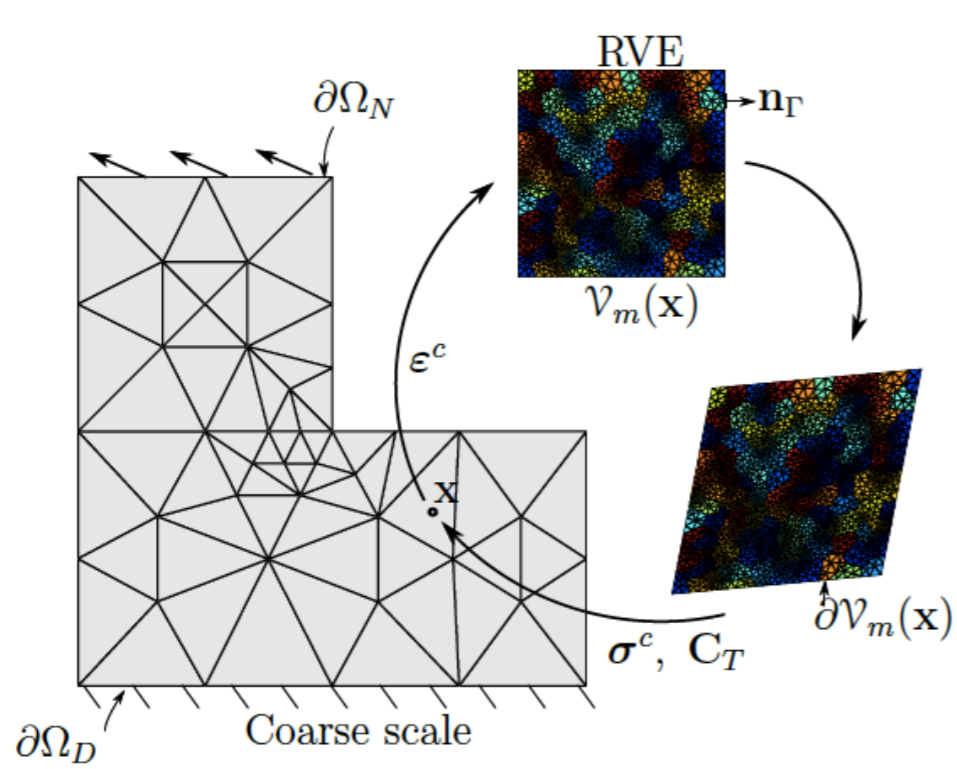


Loading



Feyel, Chaboche, 2000 - Akbari, Kerfriden, Bordas, 2014

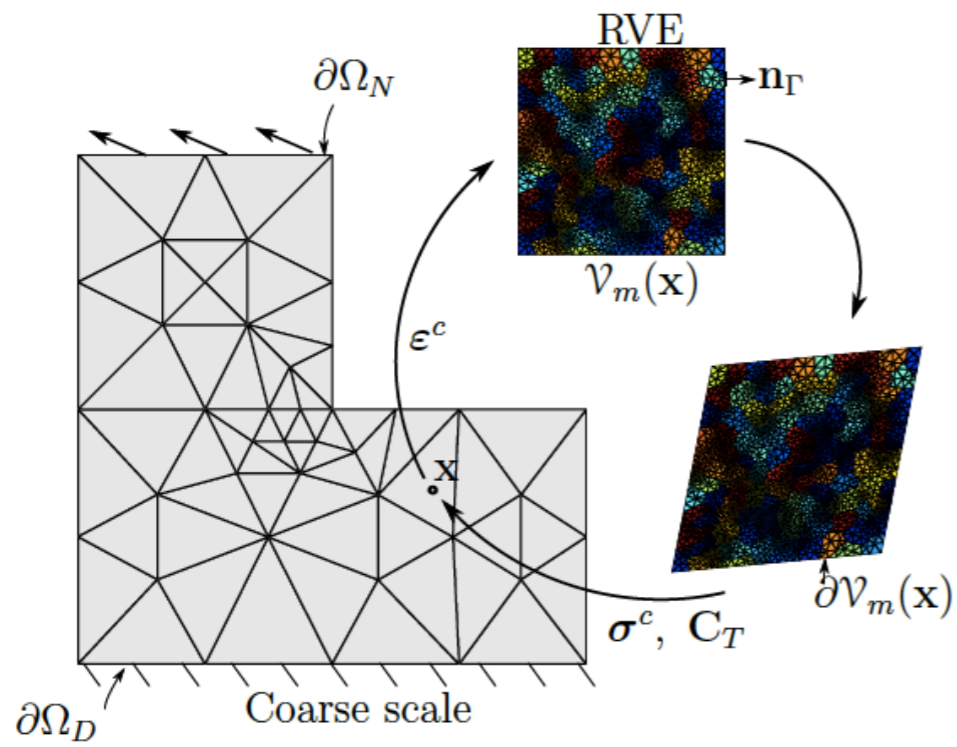
Hierarchical methods FE²



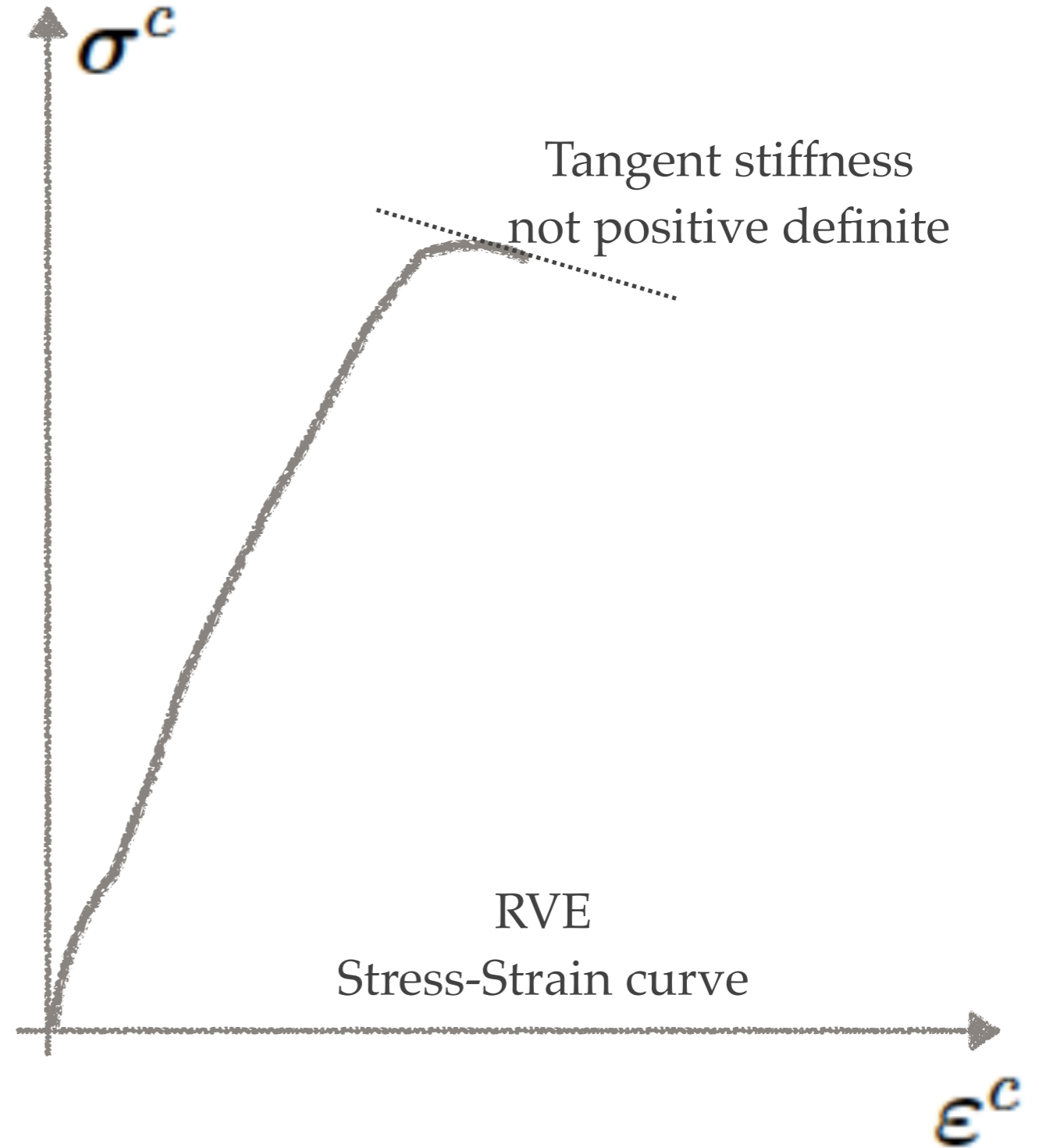
Peak

Feyel, Chaboche, 2000 - Akbari, Kerfriden, Bordas, 2014

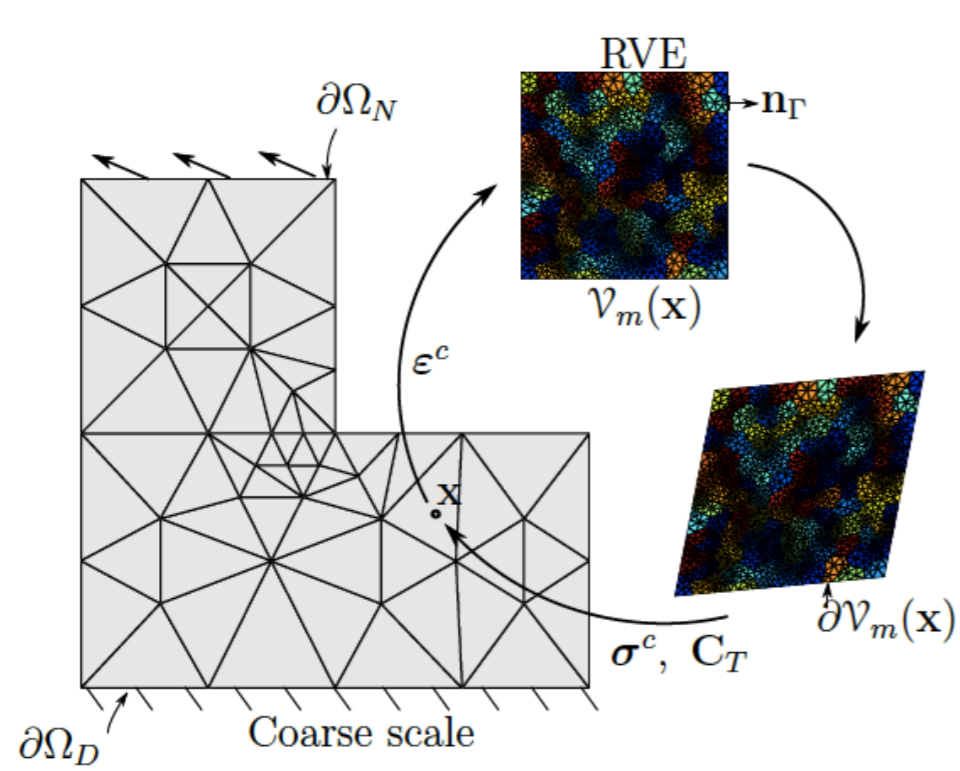
Hierarchical methods FE²



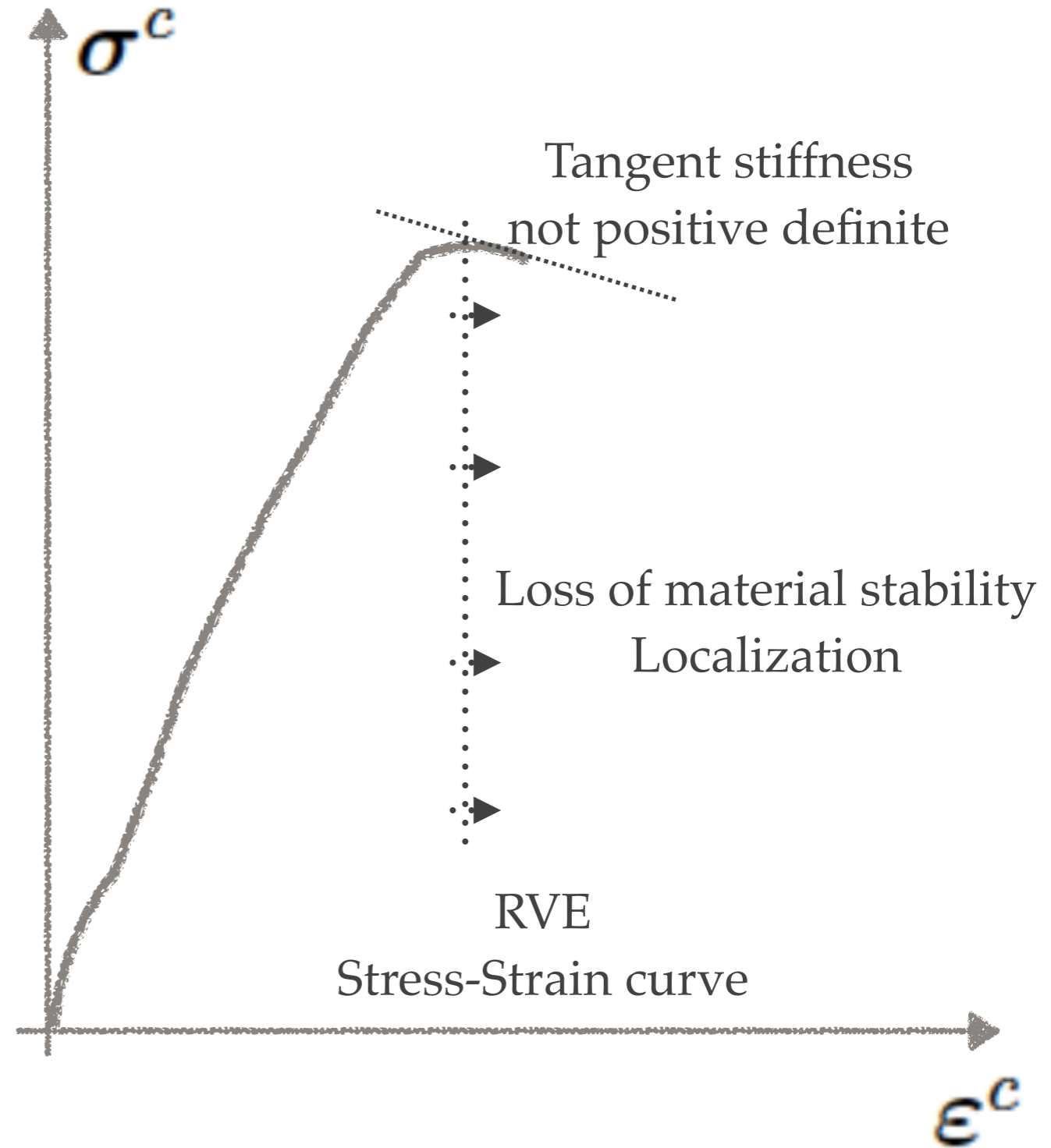
Unloading



Hierarchical methods FE²

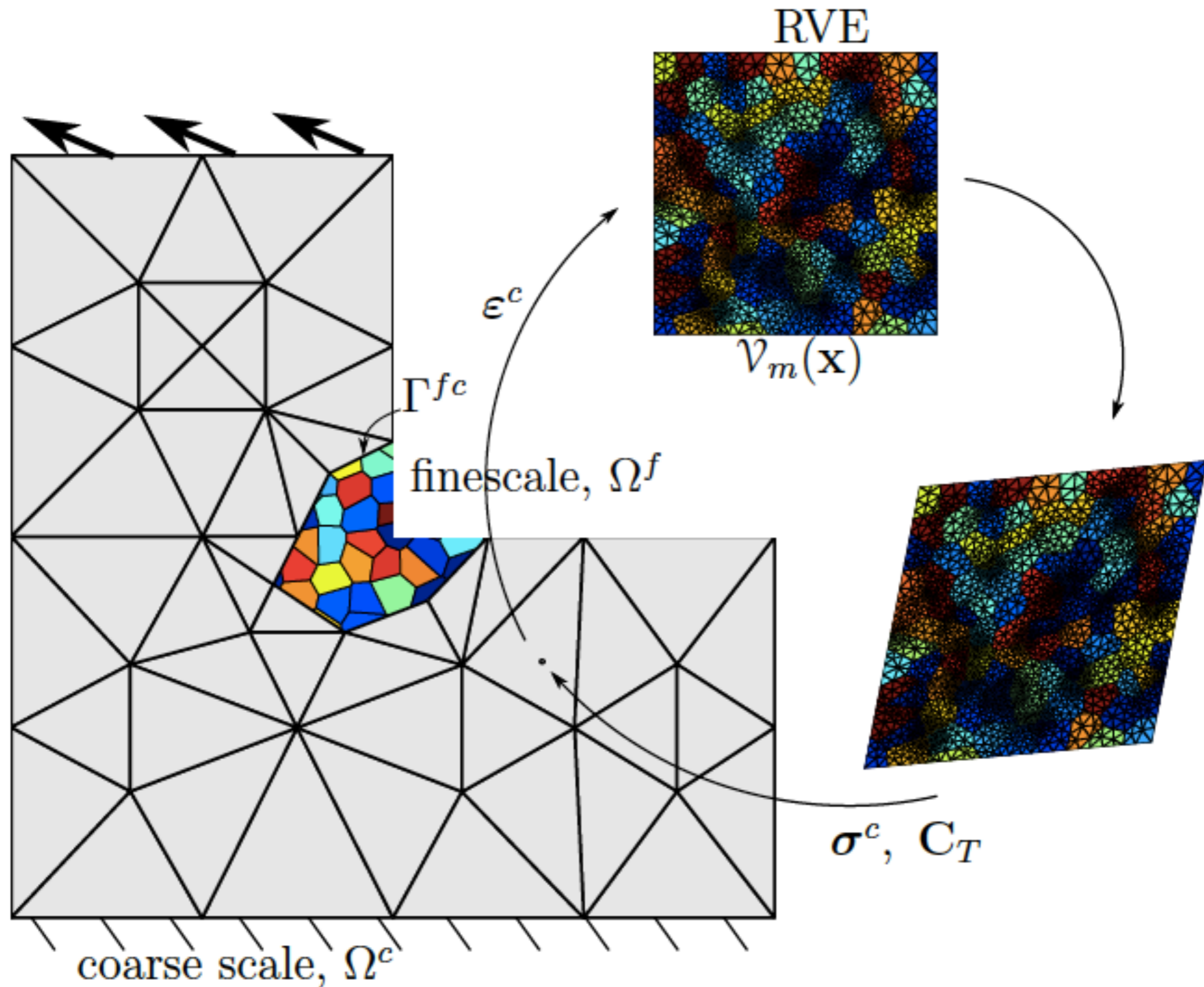


Unloading
RVE does not exist



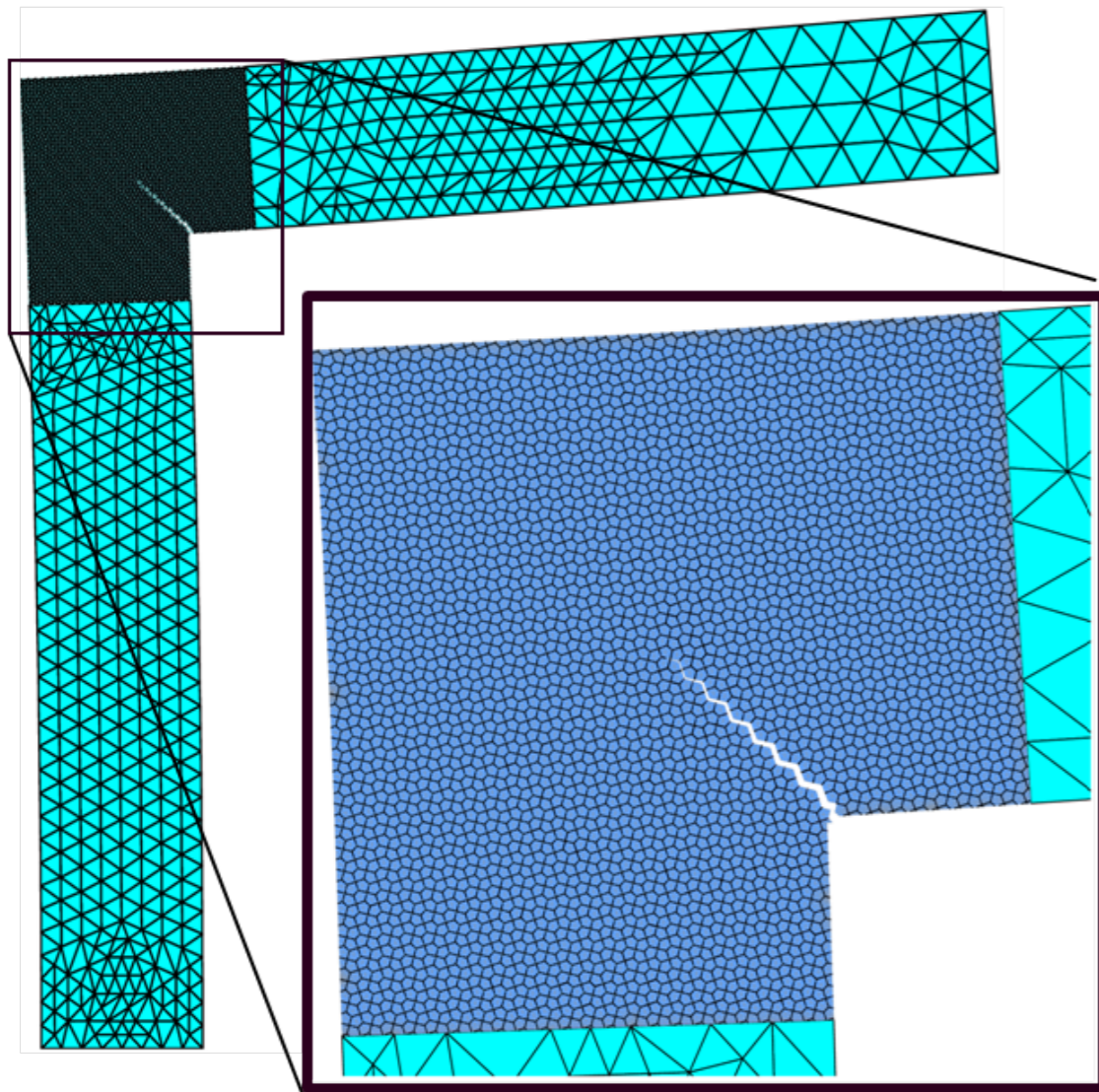
Feyel, Chaboche, 2000 - Akbari, Kerfriden, Bordas, 2014

Hybrid methods

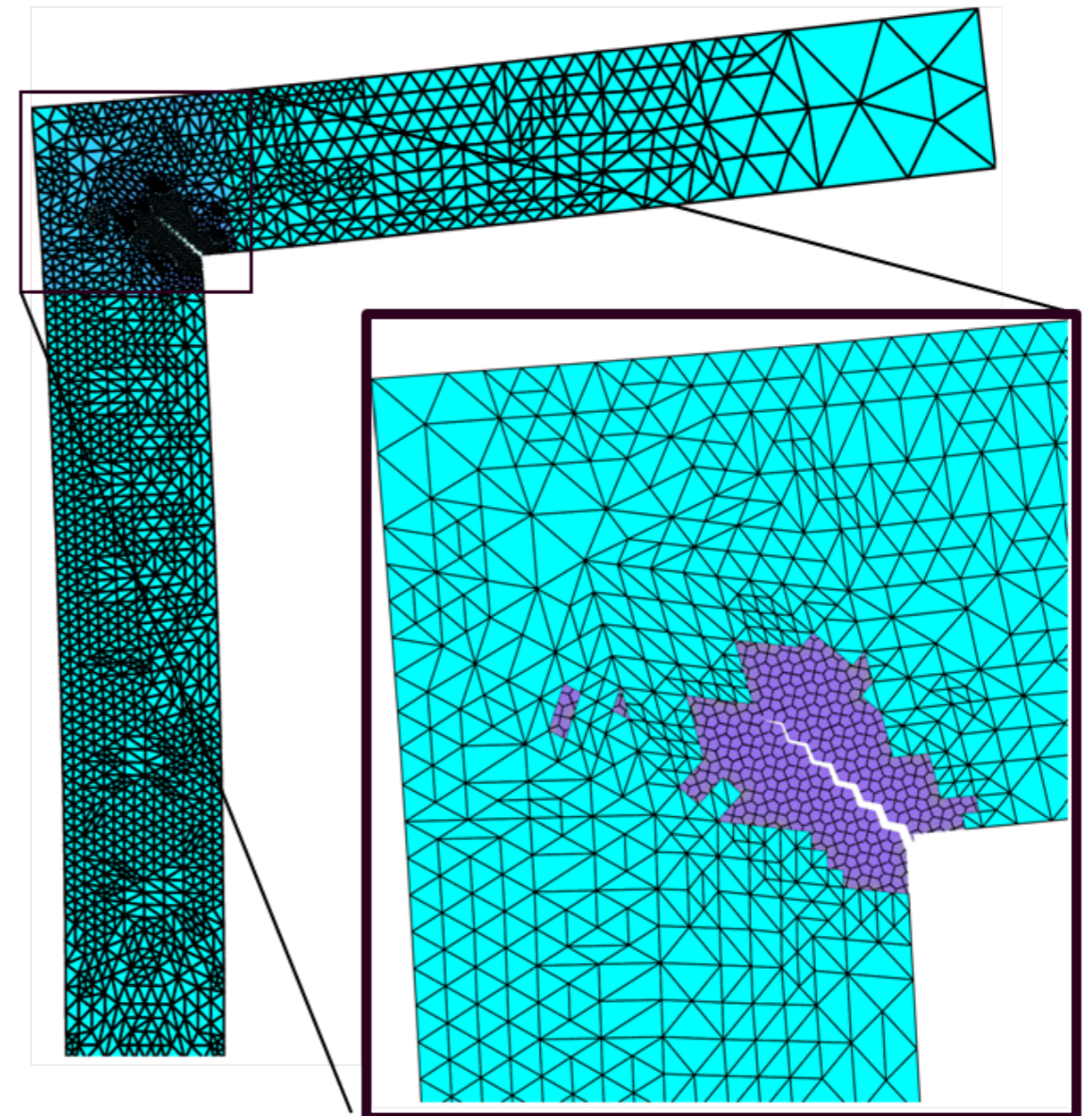


Example

Direct Numerical Solution



Adaptive Multiscale method



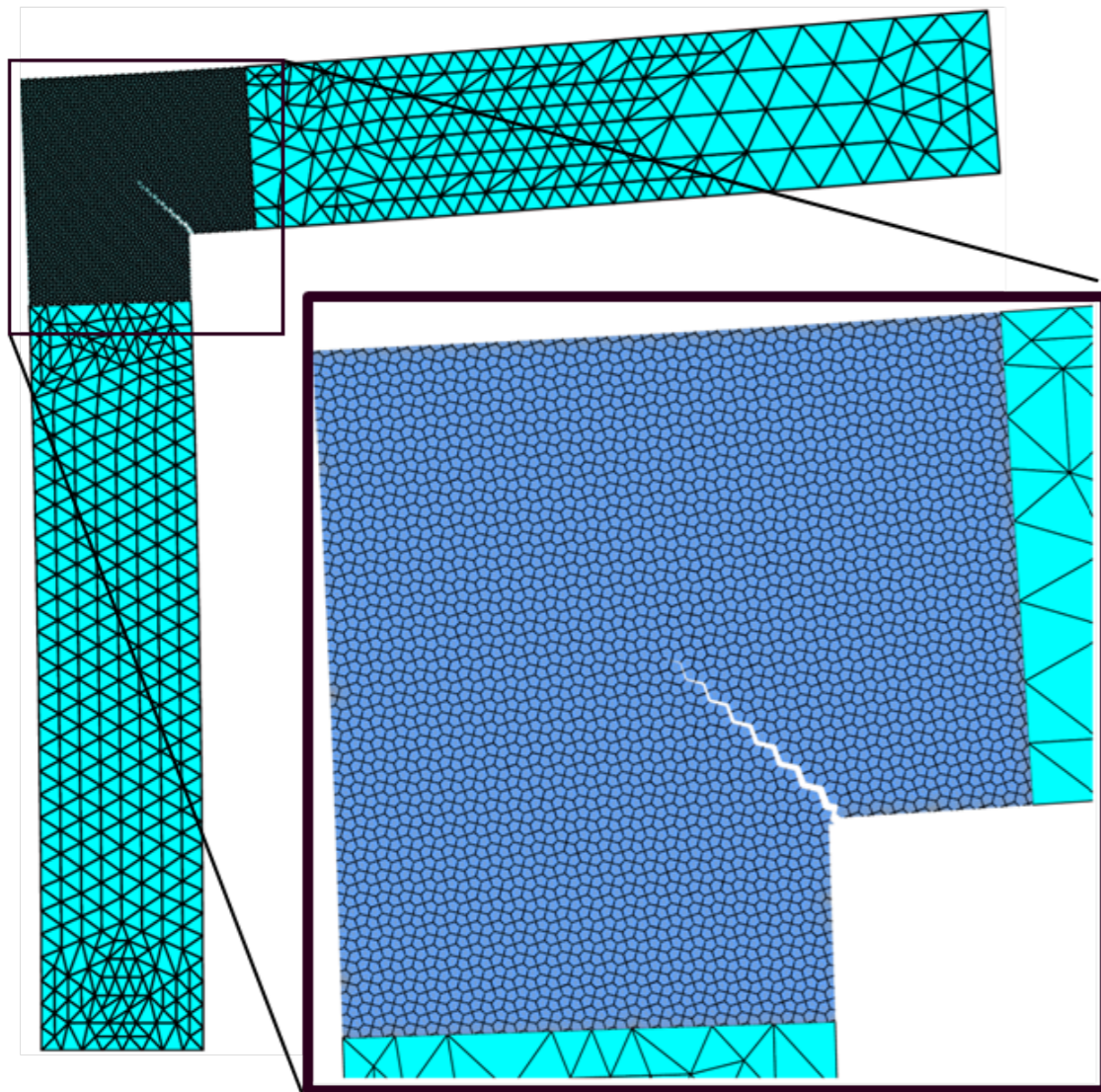
Example



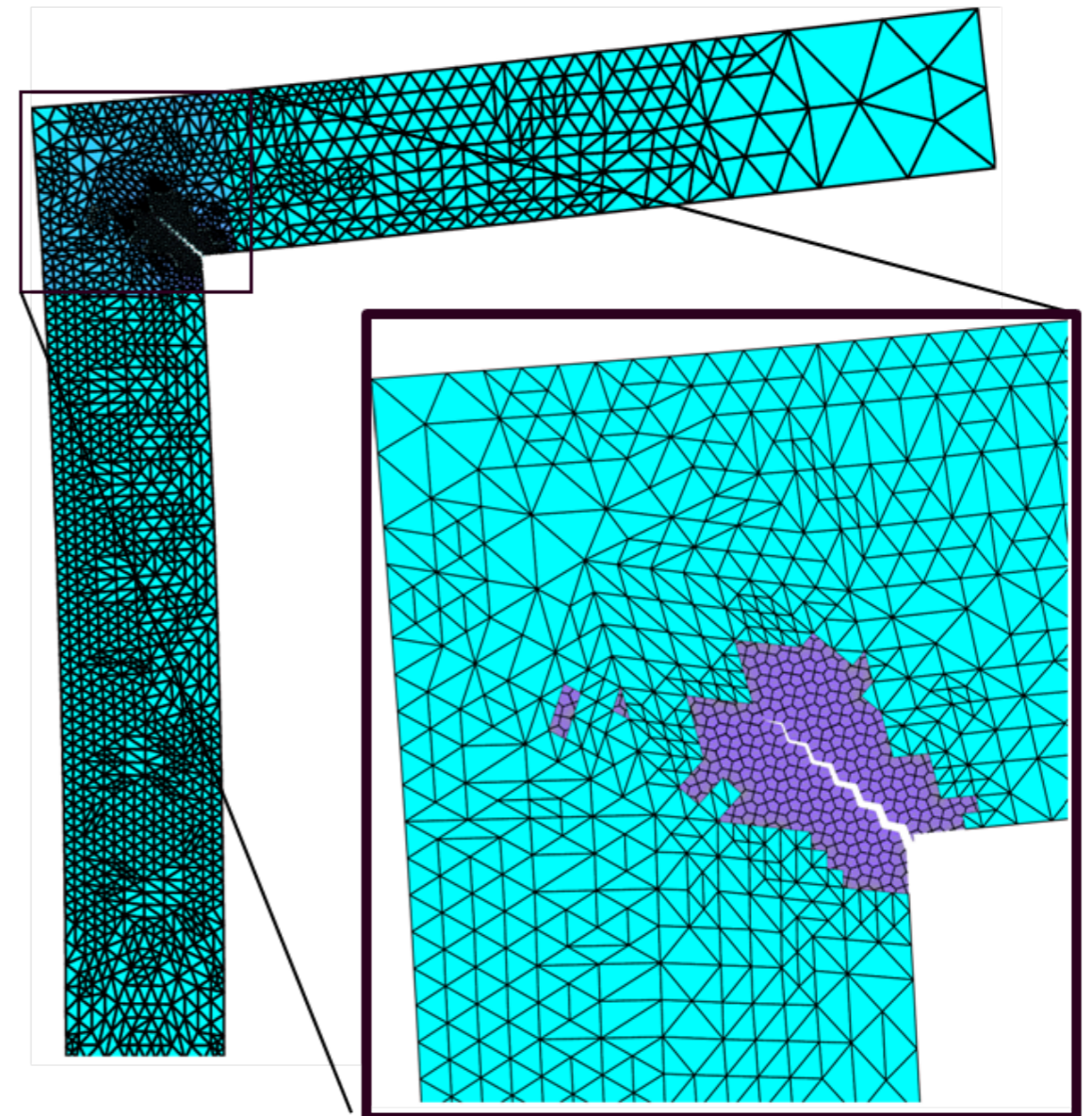
20-100 times fewer unknowns in 2D ~ 1000 times fewer in 3D



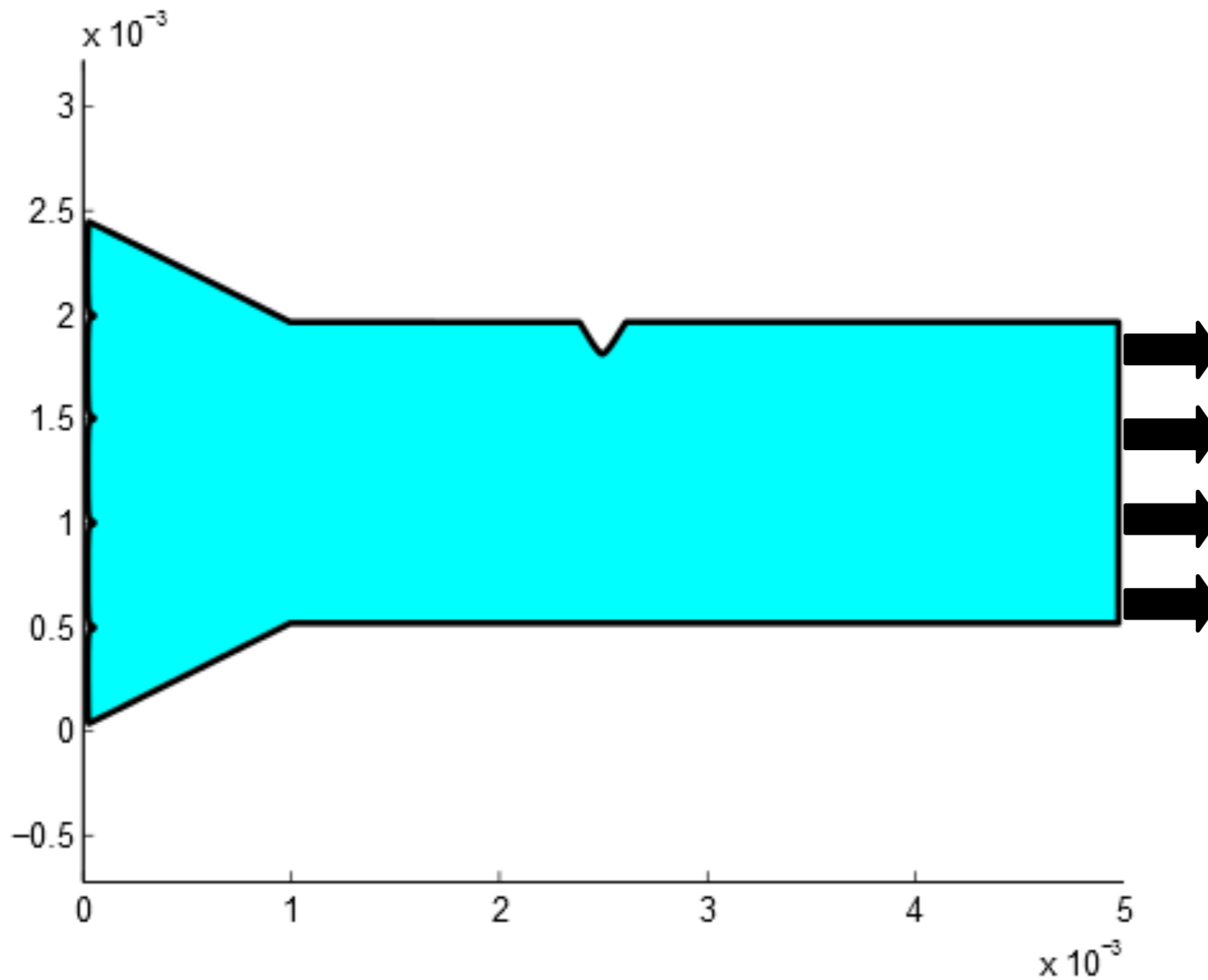
Direct Numerical Solution



Adaptive Multiscale method



Results: uni-axial tension

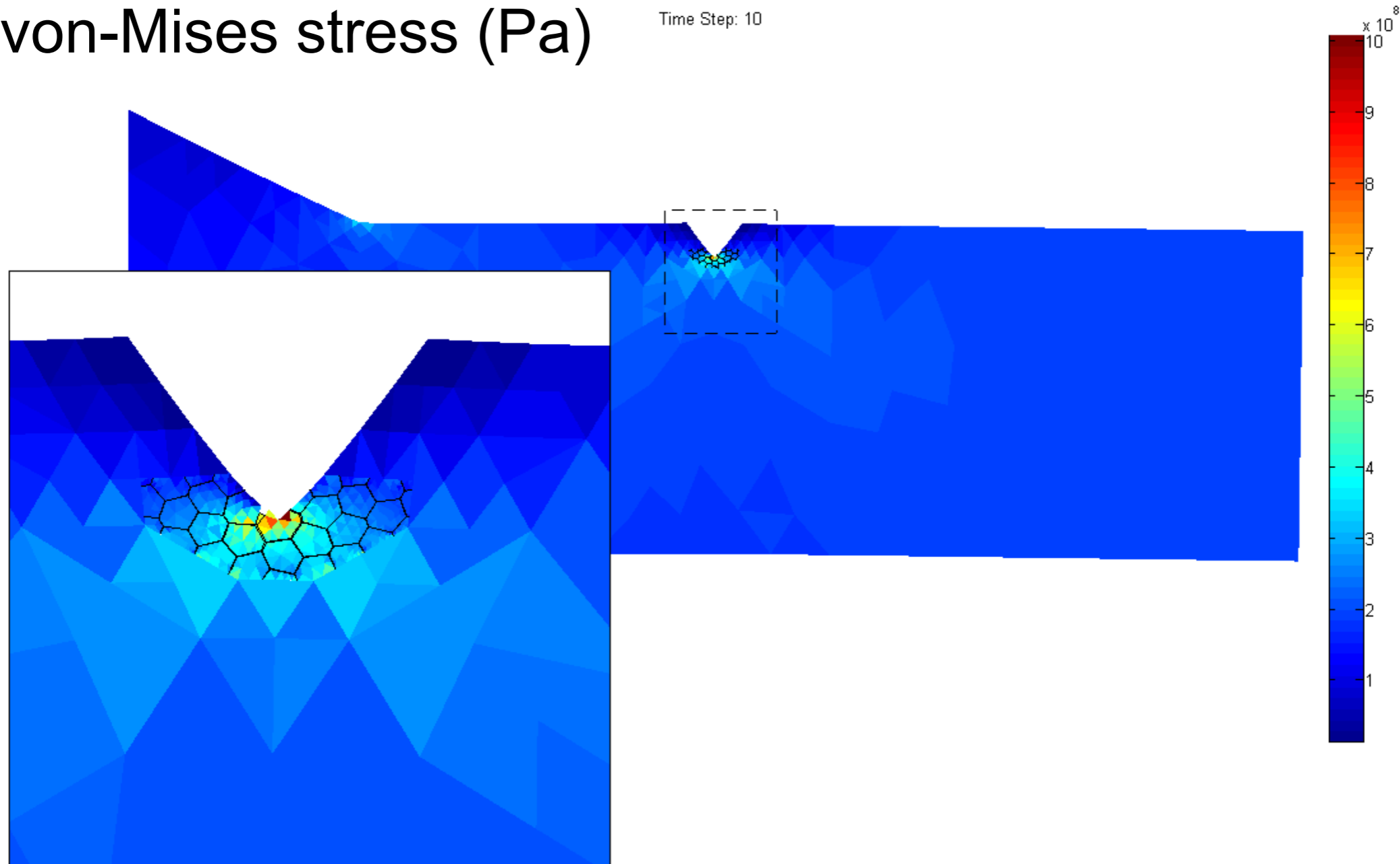


❖ Sizes are in mm

Results: uni-axial tension

von-Mises stress (Pa)

Time Step: 10

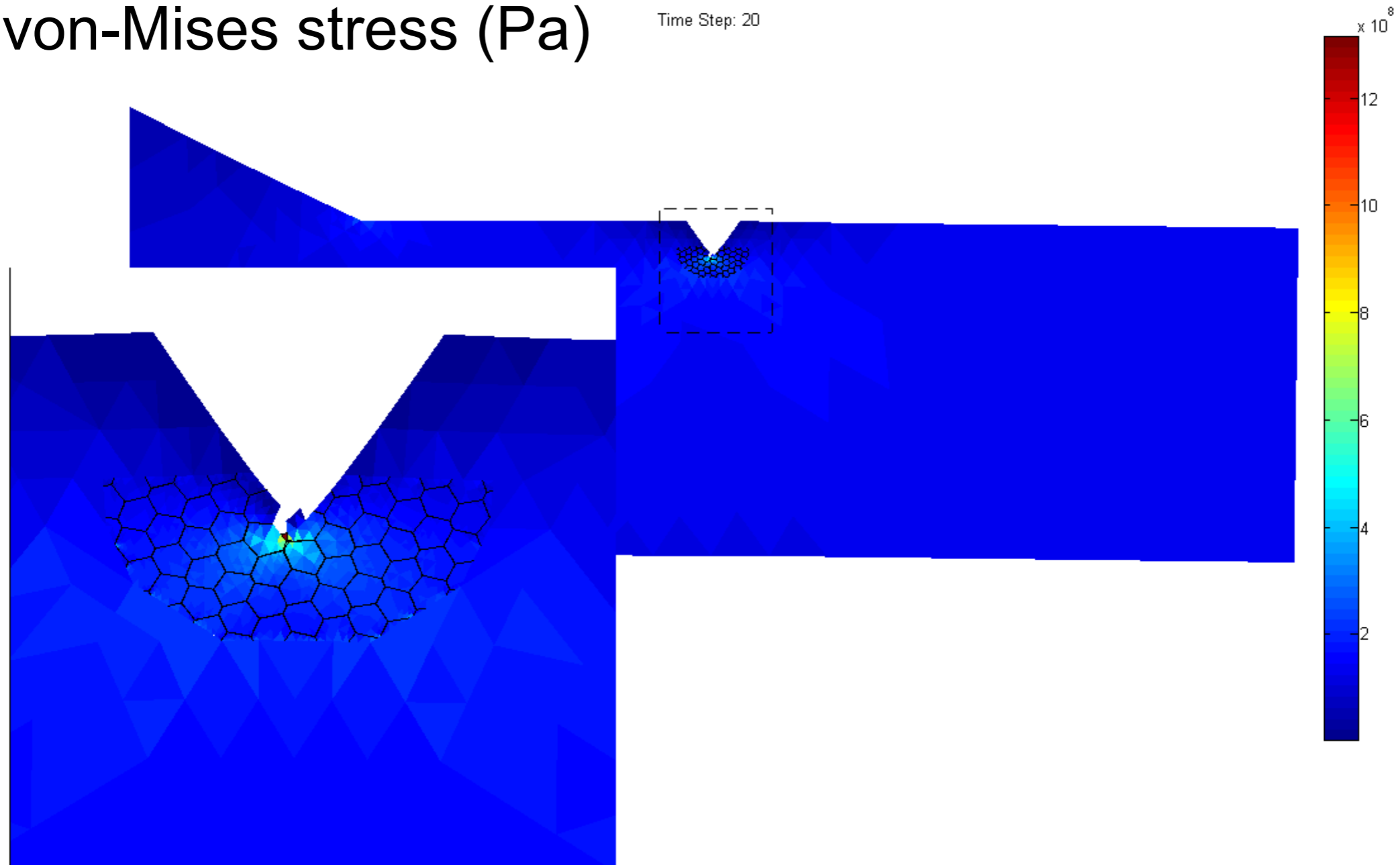


❖ 100X (magnification of displacement)

Results: uni-axial tension

von-Mises stress (Pa)

Time Step: 20

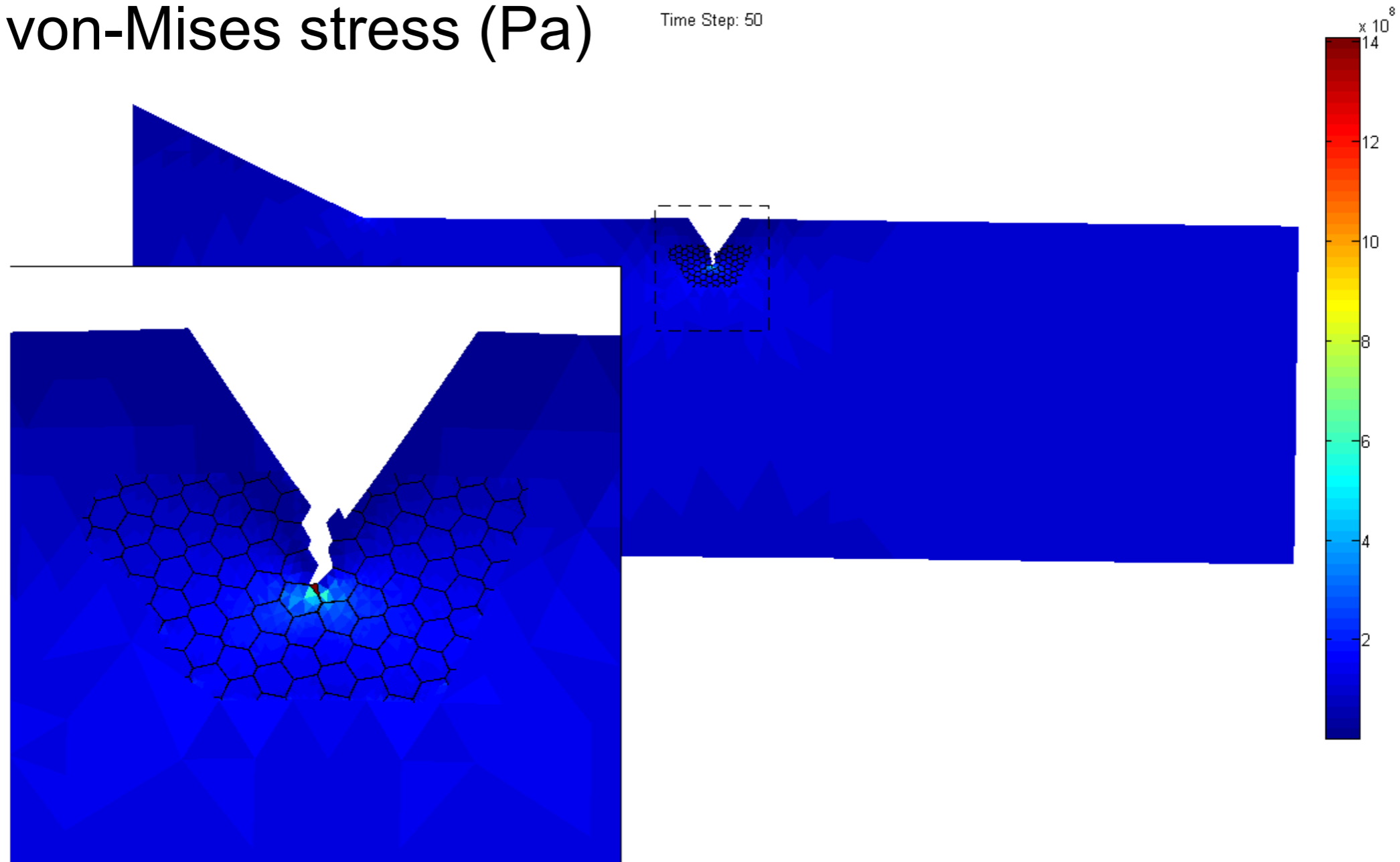


❖ 100X (magnification of displacement)

Results: uni-axial tension

von-Mises stress (Pa)

Time Step: 50

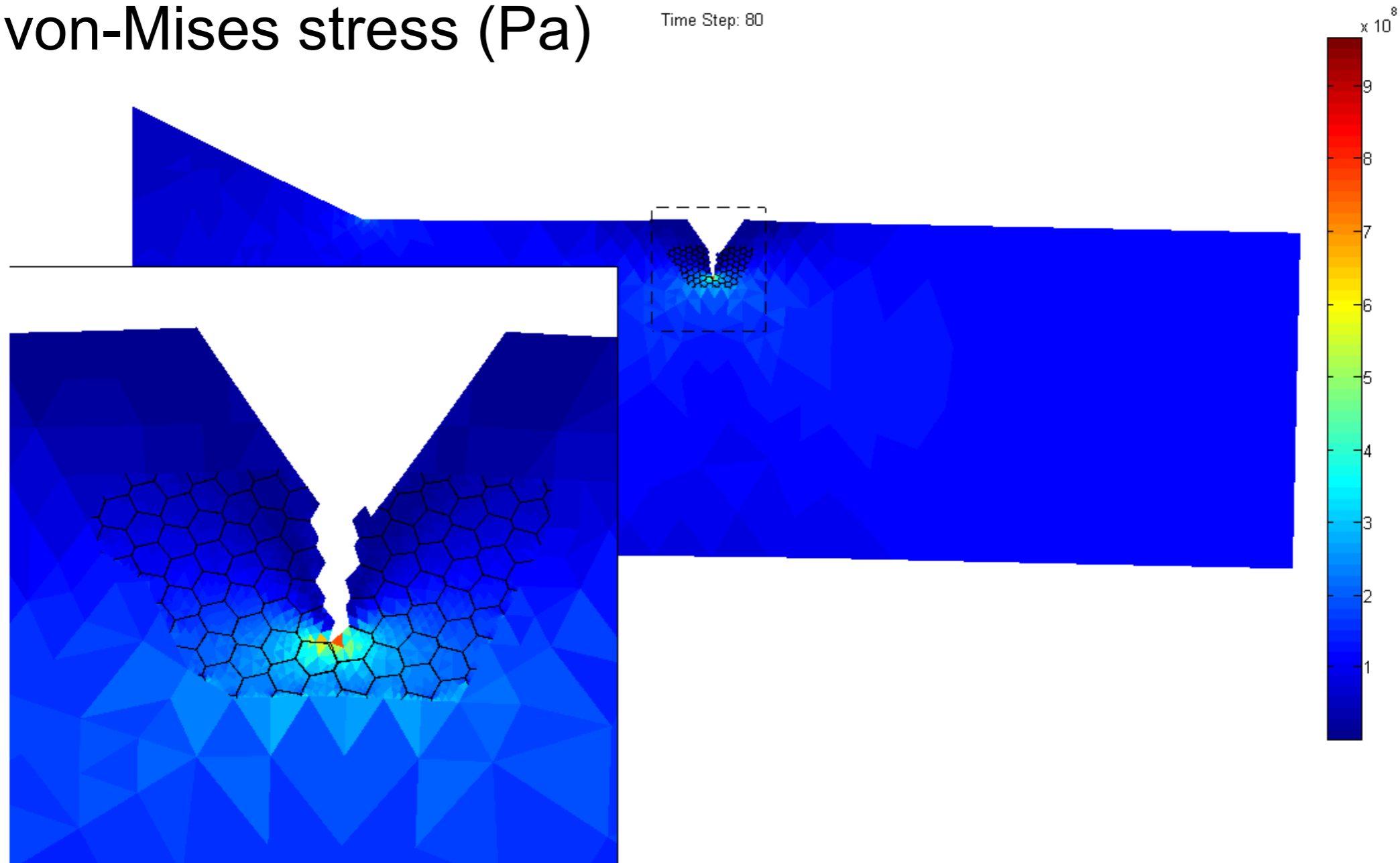


❖ 100X (magnification of displacement)

Results: uni-axial tension

von-Mises stress (Pa)

Time Step: 80

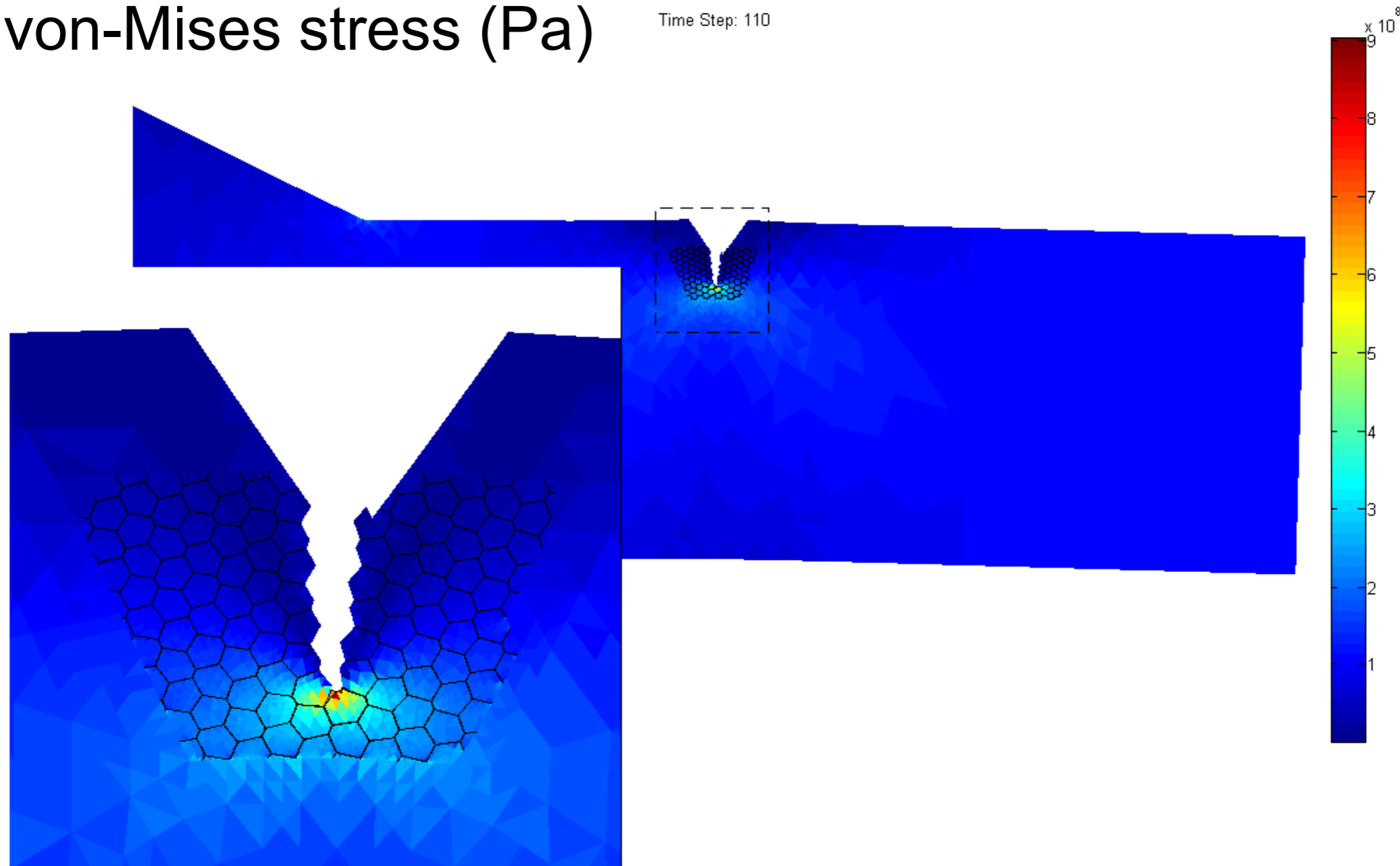


❖ 100X (magnification of displacement)

Results: uni-axial tension

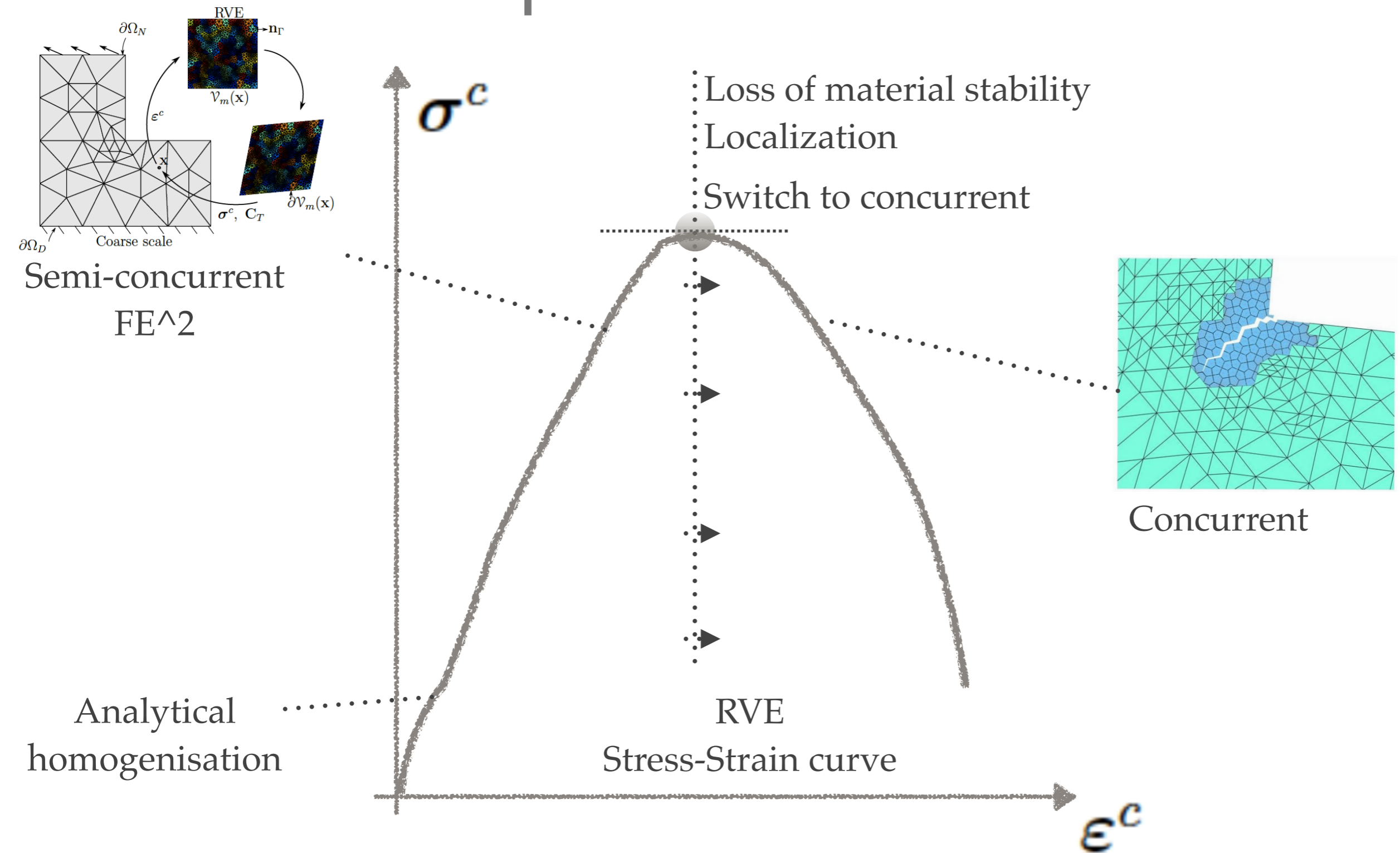
von-Mises stress (Pa)

Time Step: 110



❖ 100X (magnification of displacement)

Adaptive multi-scale



Open problem

- model selection and error control

Possible approach

- machine learning and statistical inference, e.g. Bayesian statistics

Open problem

- statistical variability at the fine scale (geometry, material parameter)

Possible approach

- identification through small-scale experiments (costly, difficult to characterize interfaces)
- Monte Carlo

Open problem

- material parameter identification at small scales

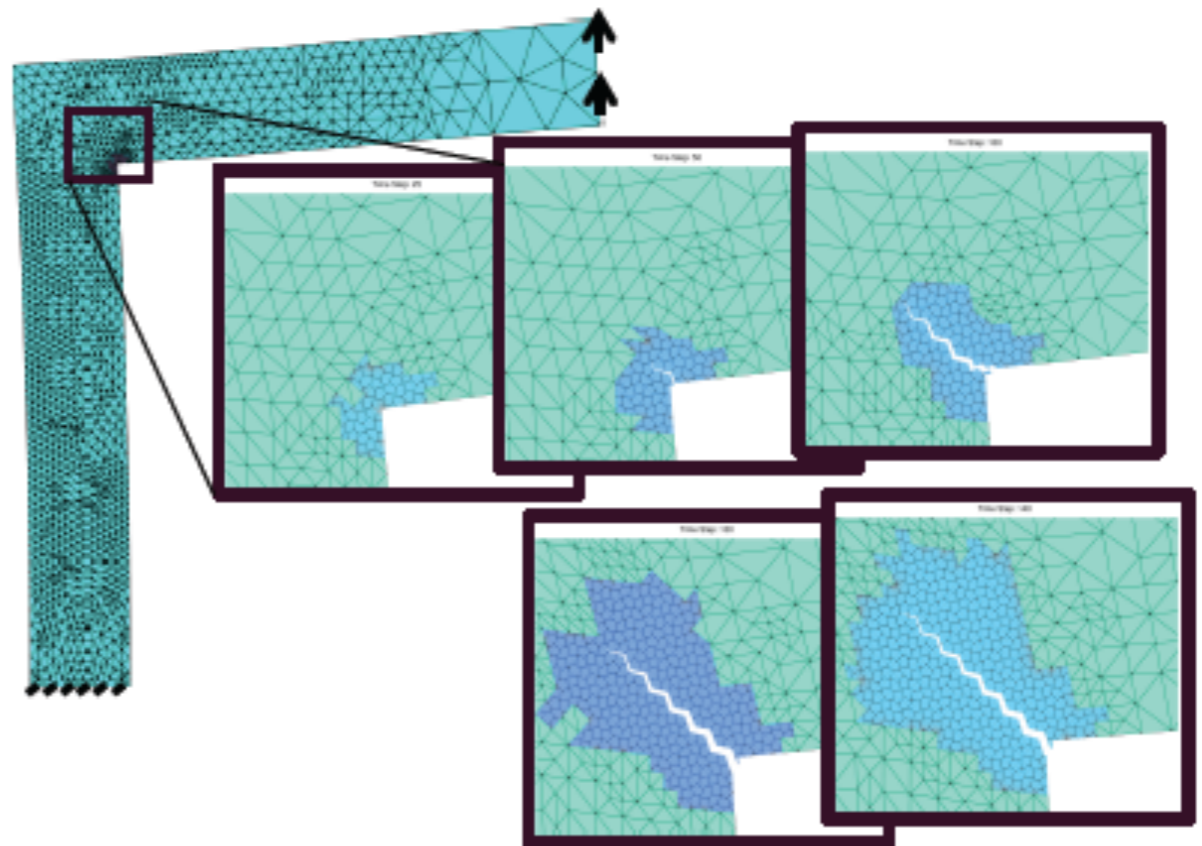
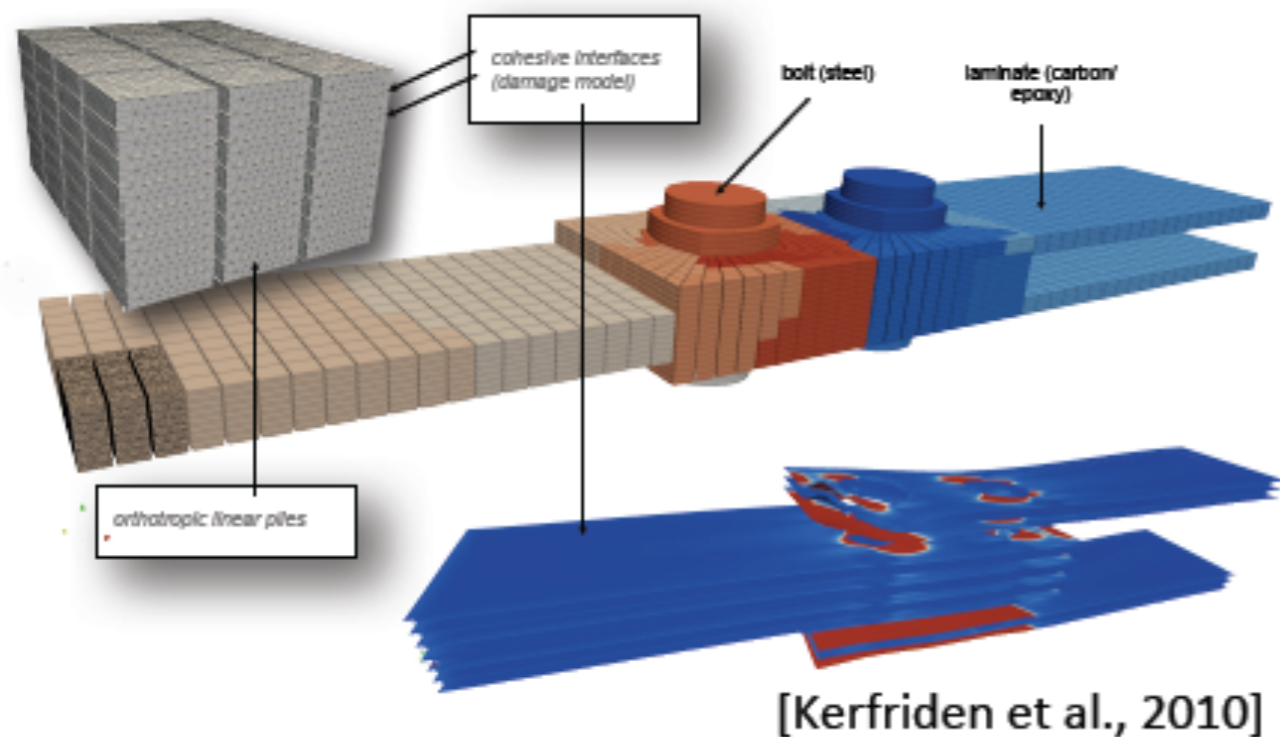
Possible approach

- small-scale experiments - costly

Model reduction - physics-based (1)

- Multilevel methods to reduce CPU time by orders of magnitude and devise robust, efficient code/model coupling

- HPC Adaptive multiscale models/solvers with controlled accuracy



[Akbari et al., 2013]

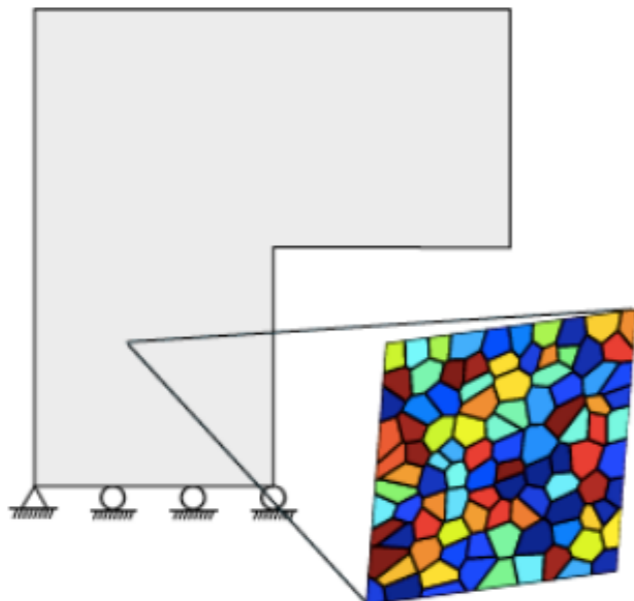
Open problem: adaptive error controlled algorithms for model and discretization error. Use the right model at the right place/time.

Challenge

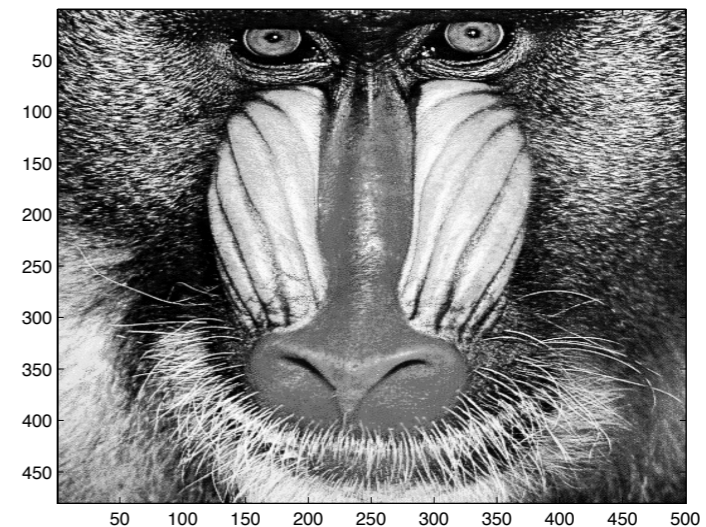
- Reduce the problem size
- Preserve essential features

Reduce computational
expense
Control the error

Physics based model
reduction a.k.a. **Multiscale
Methods**



Algebraic based model
reduction a.k.a. **Machine
Learning**



Algebraic model reduction methods

Use precomputed solutions to accelerate online simulations

Example - parametric problems

Method of separated representation

Proper orthogonal decomposition (POD)

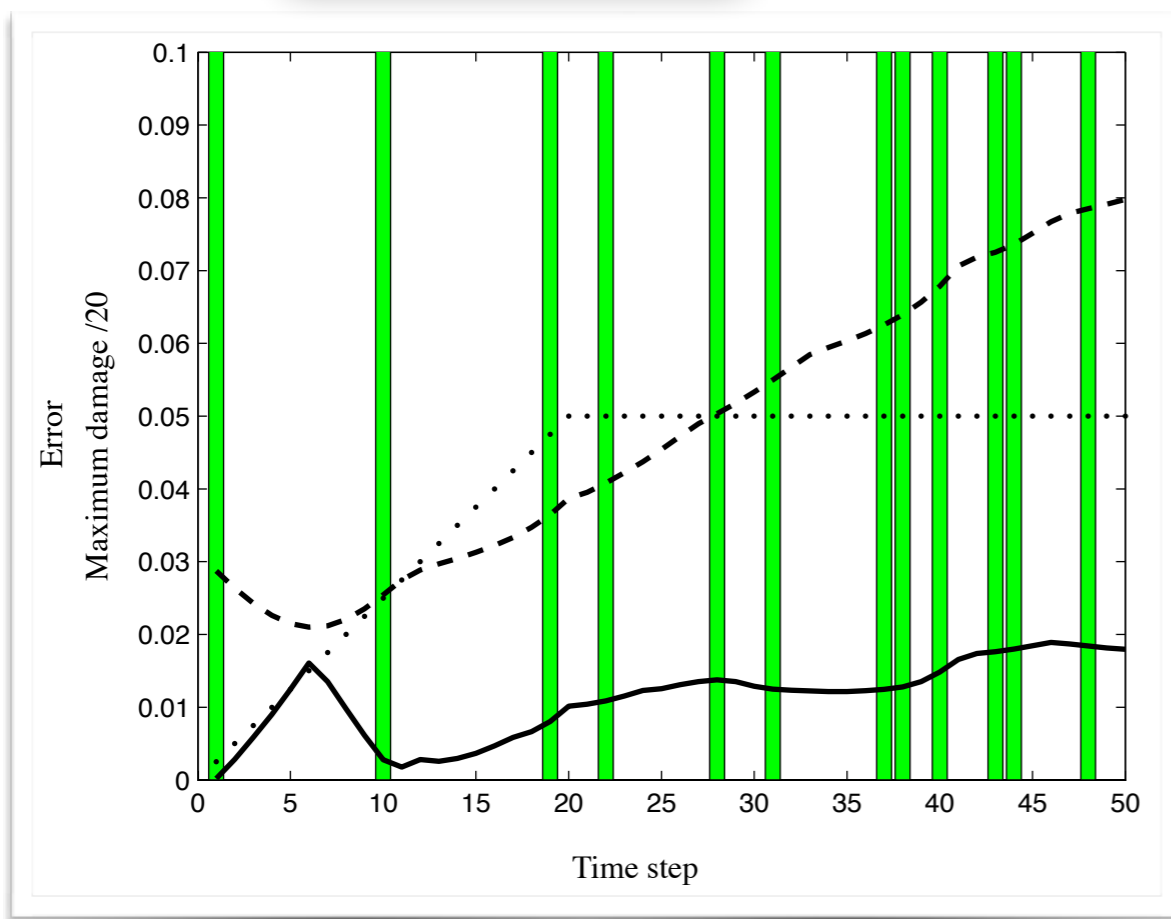
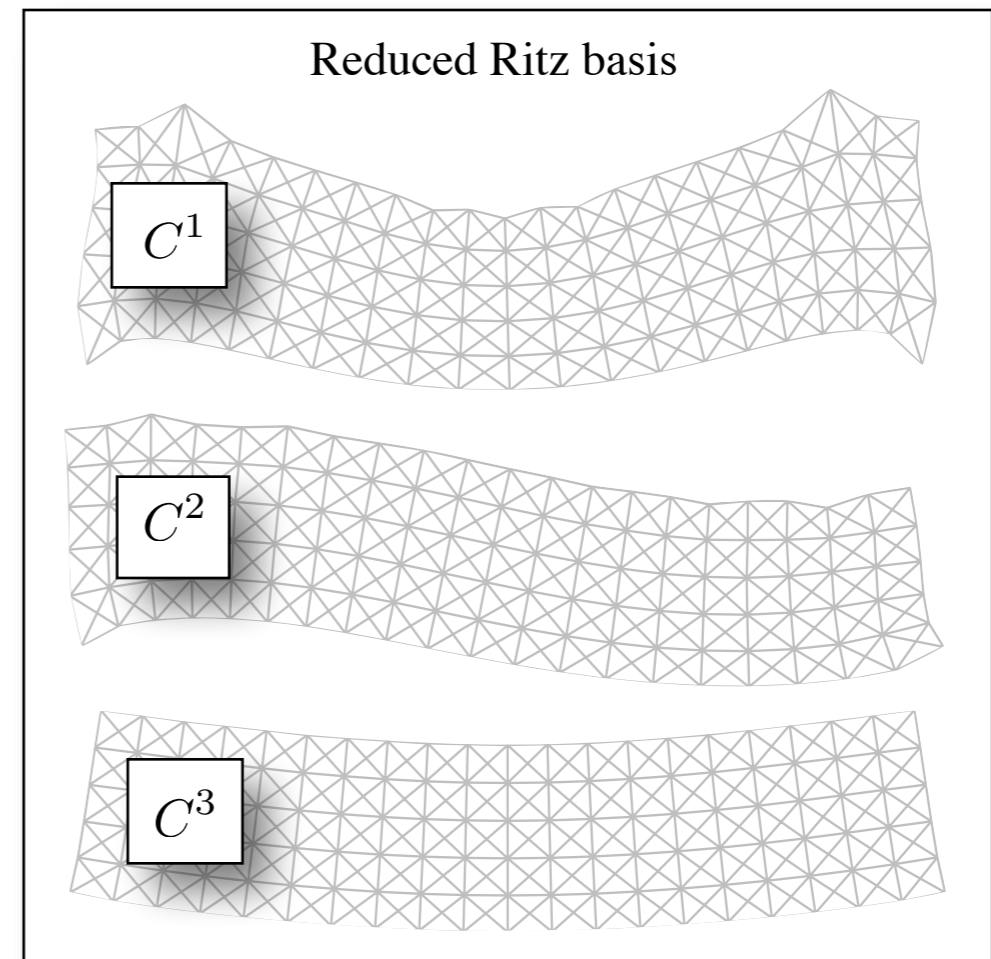
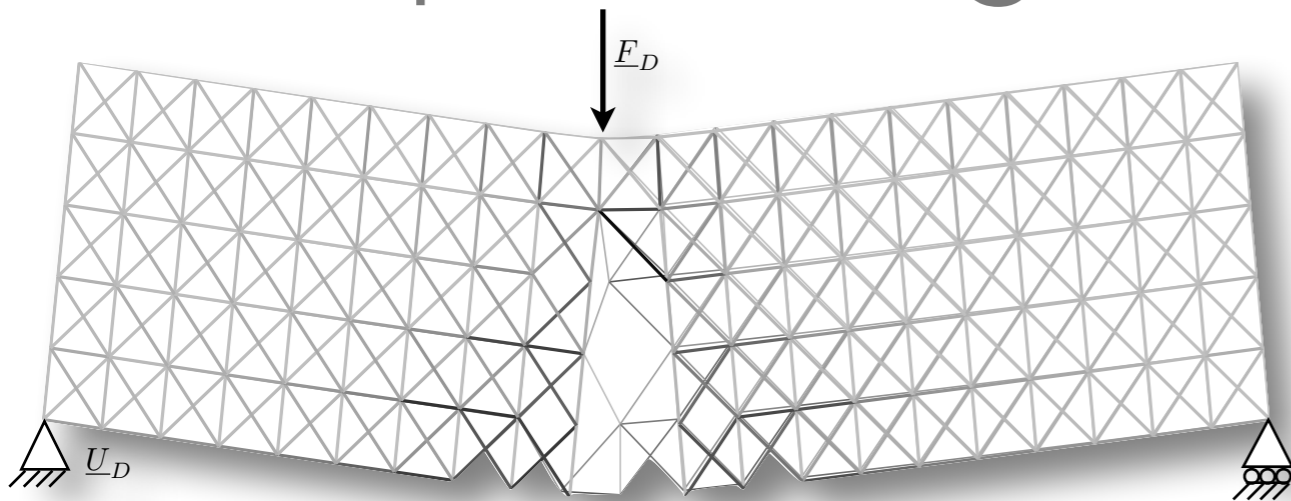


Illustration of the method of separated representation

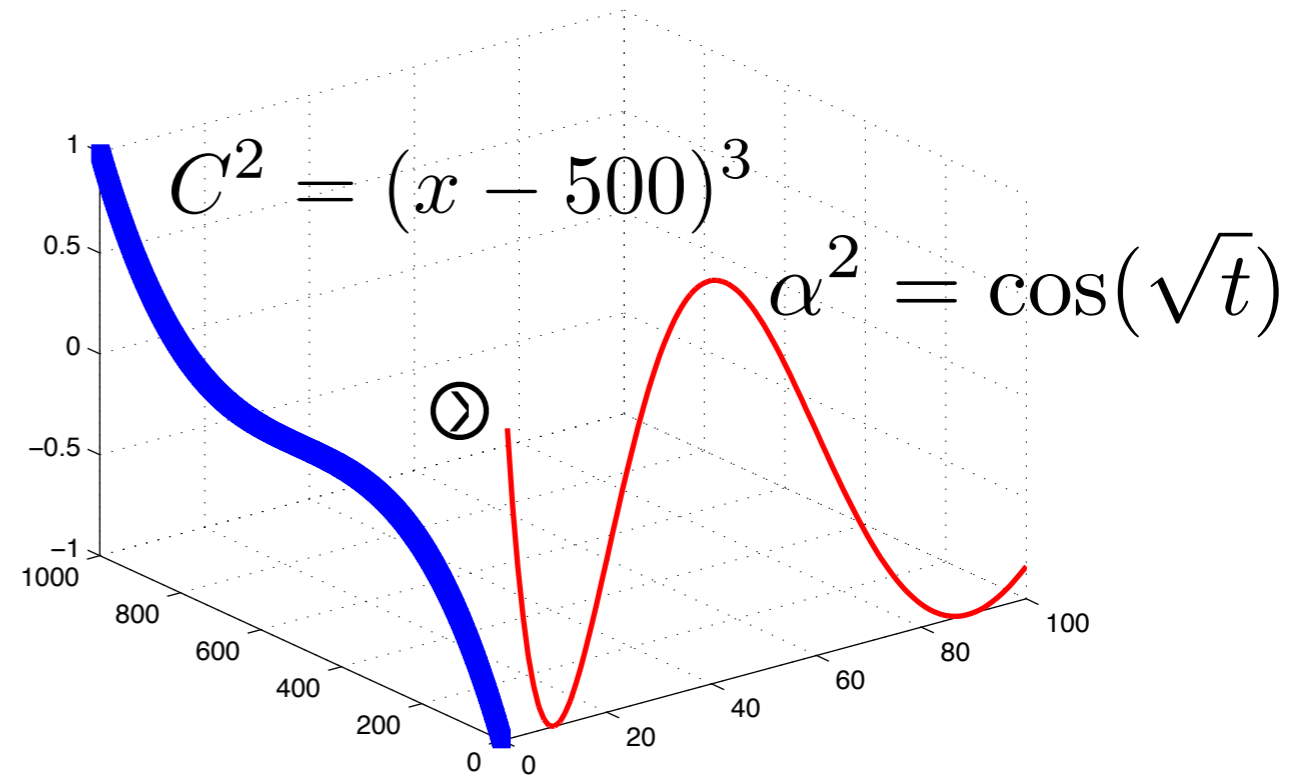
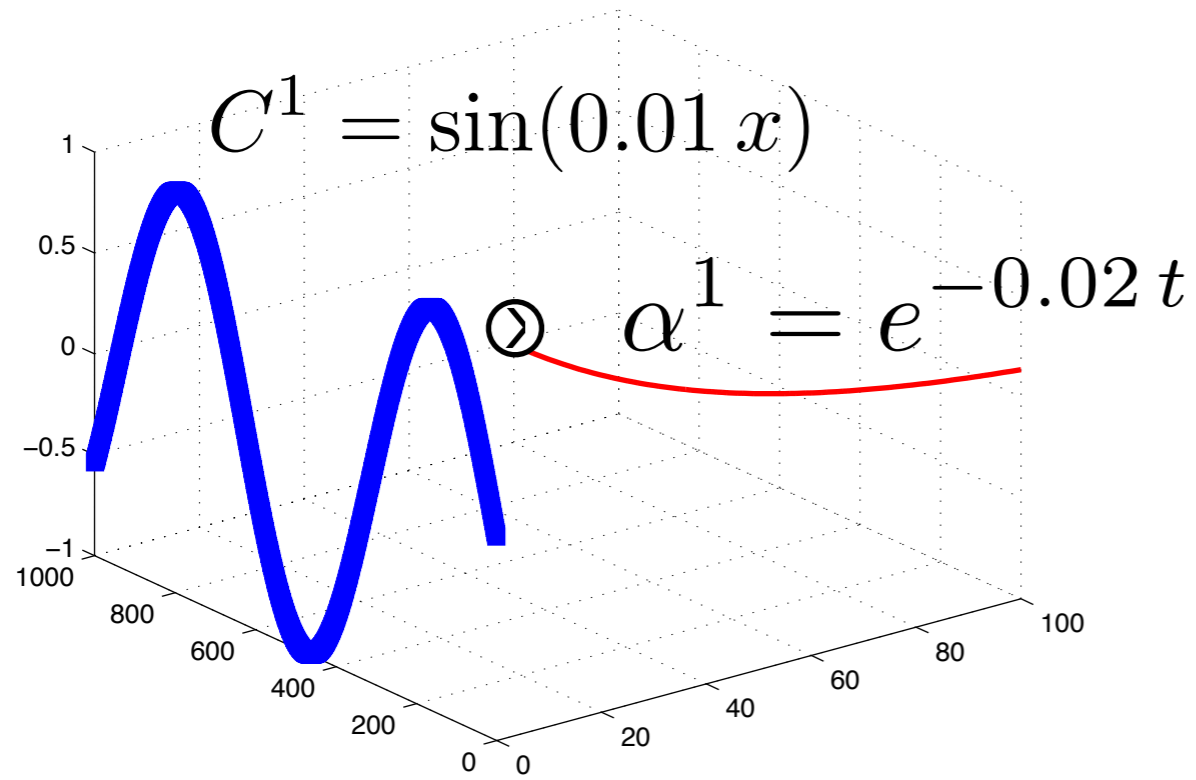


Illustration of the method of separated representation

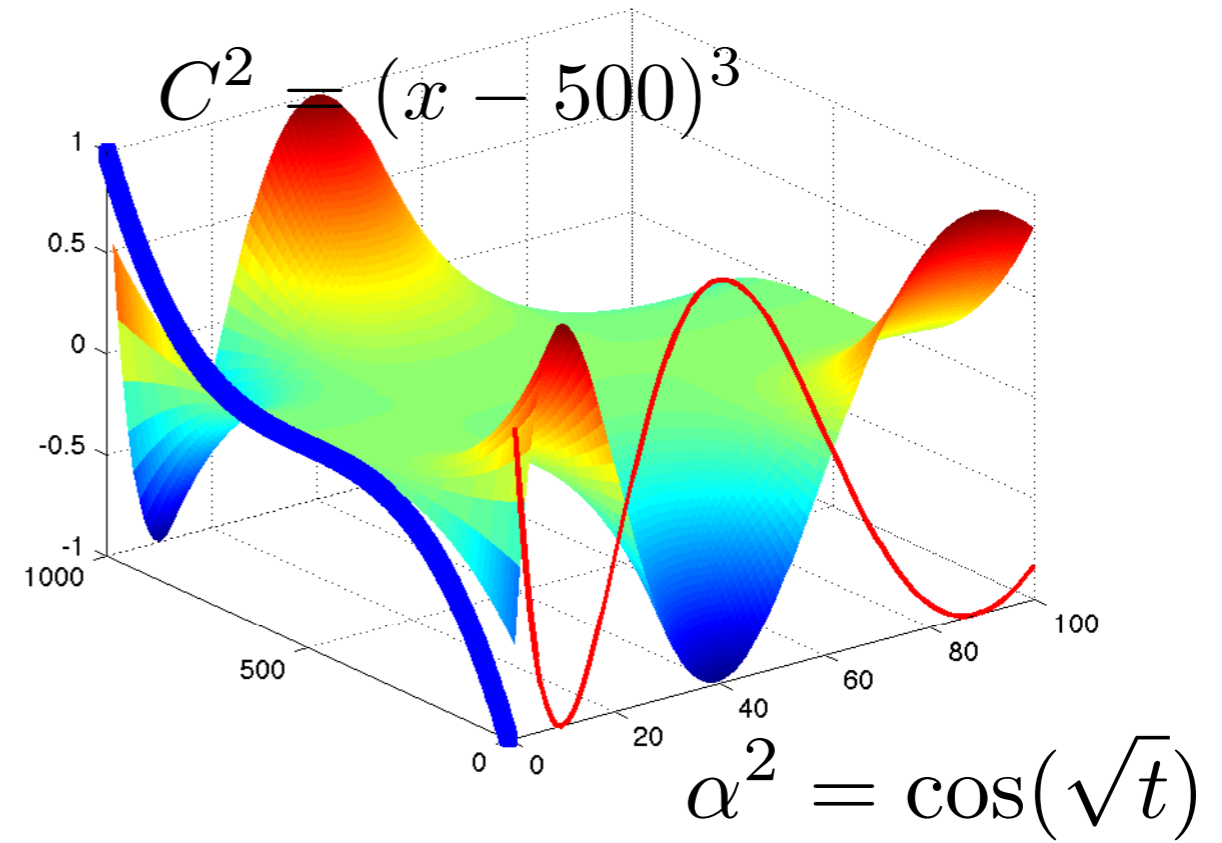
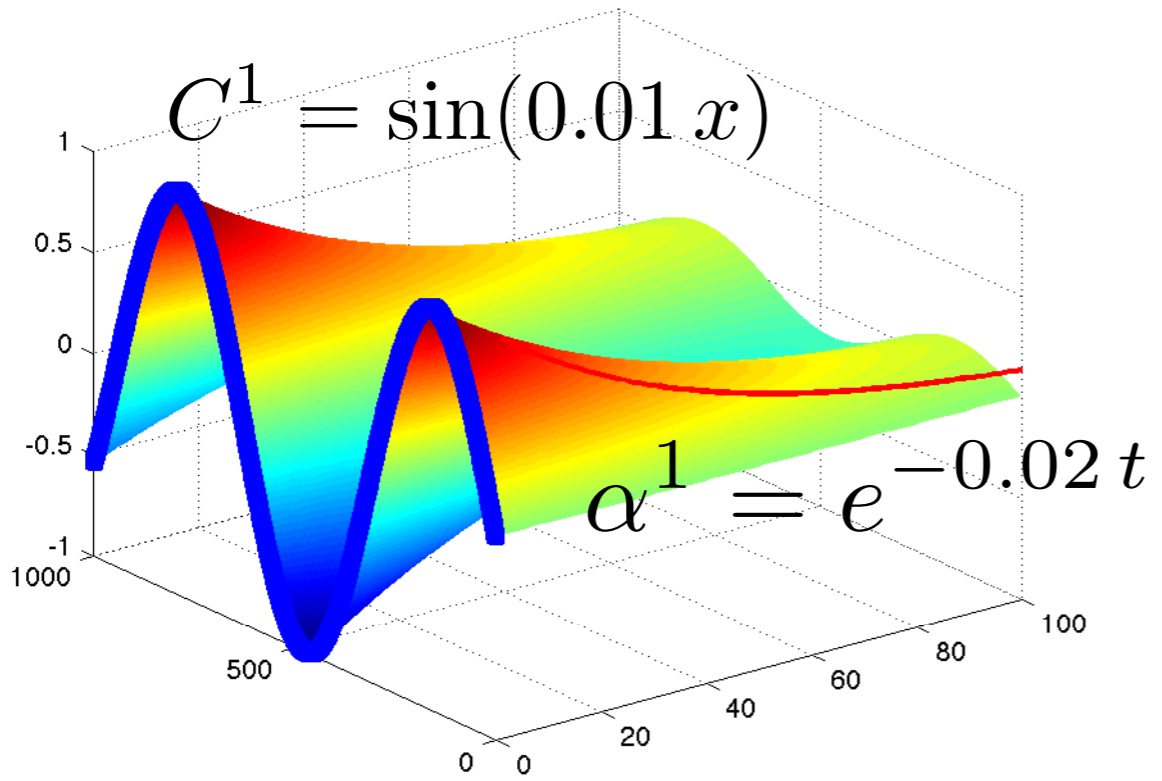
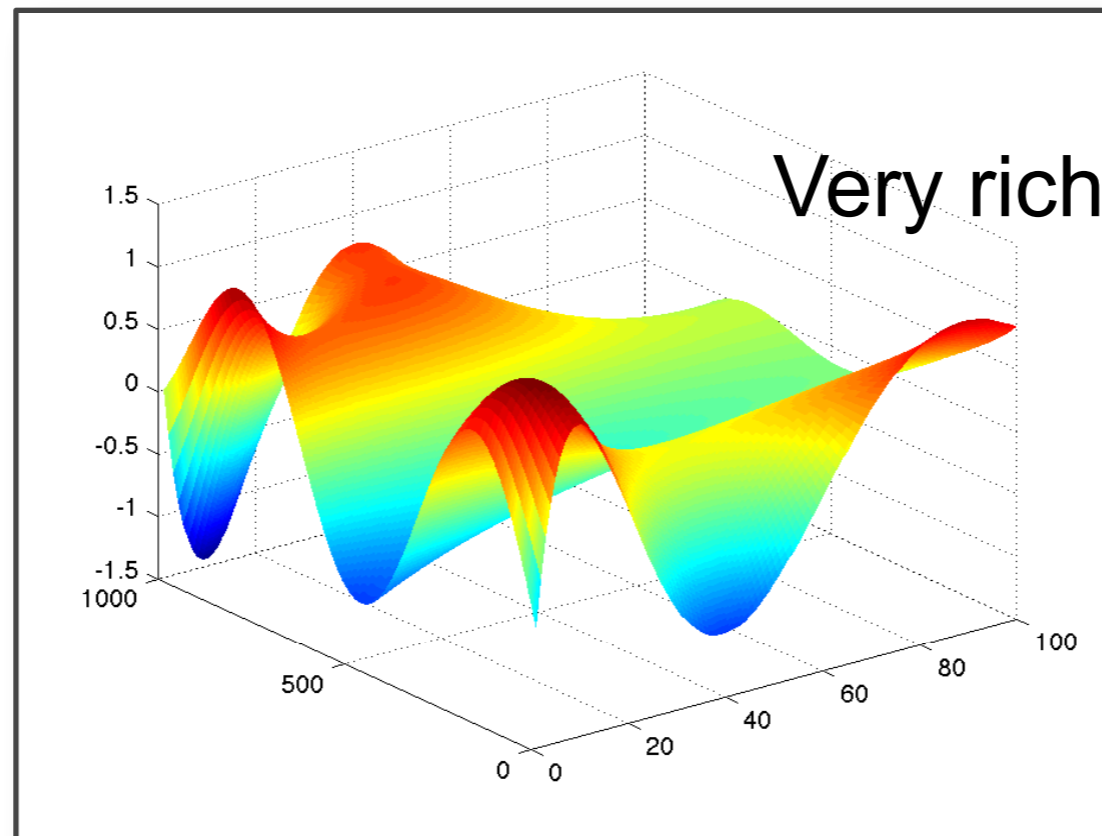
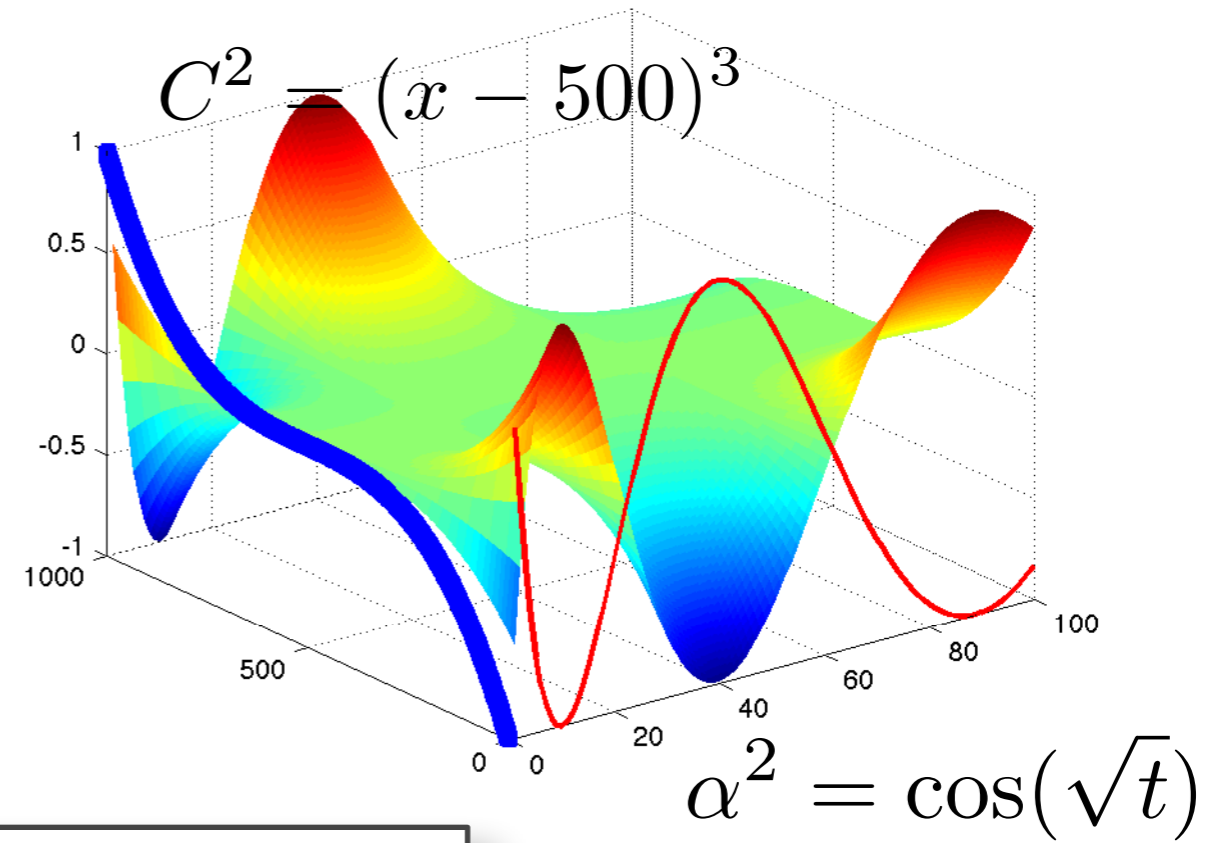
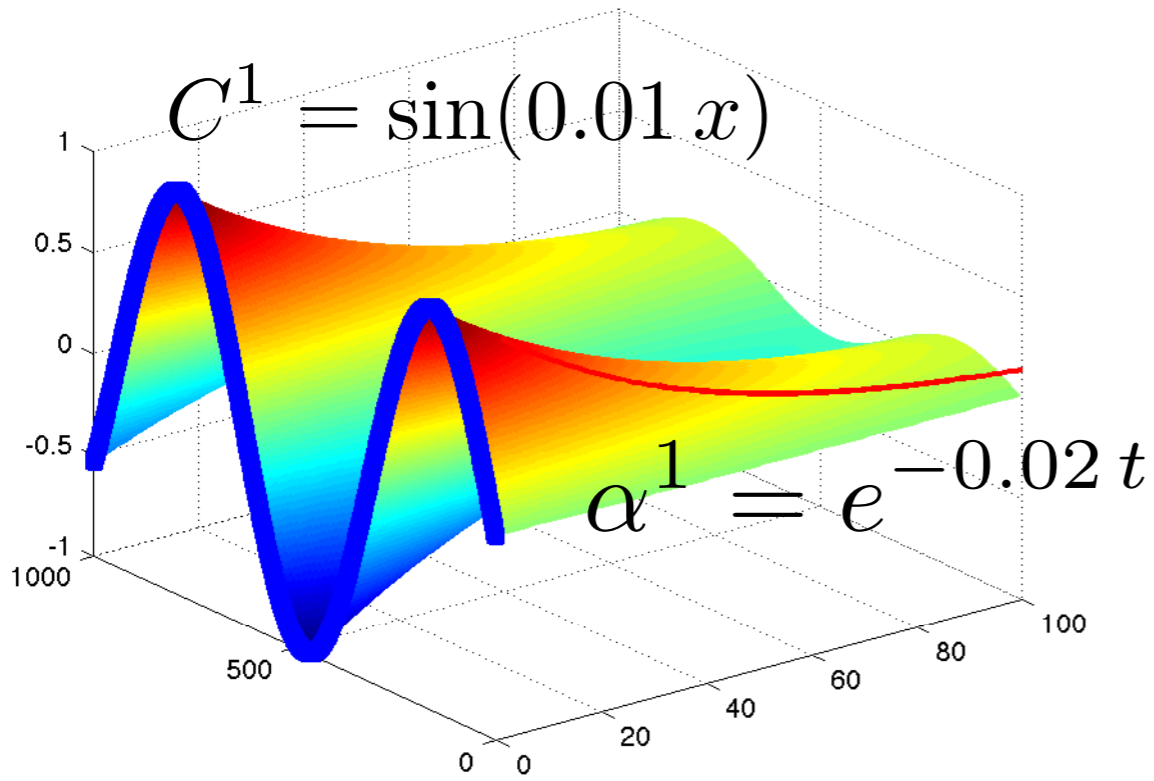
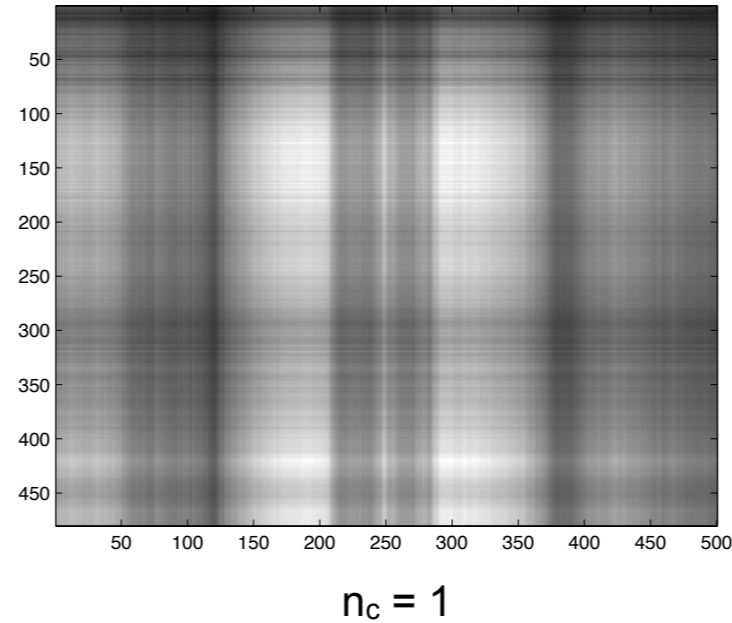
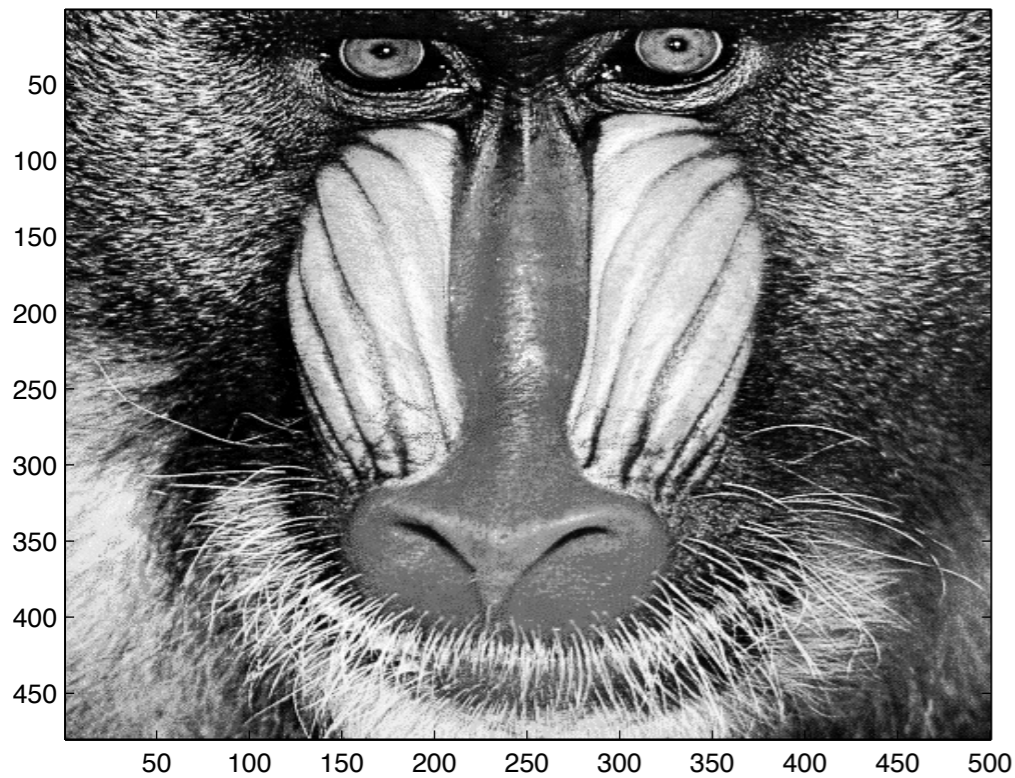


Illustration of the method of separated representation



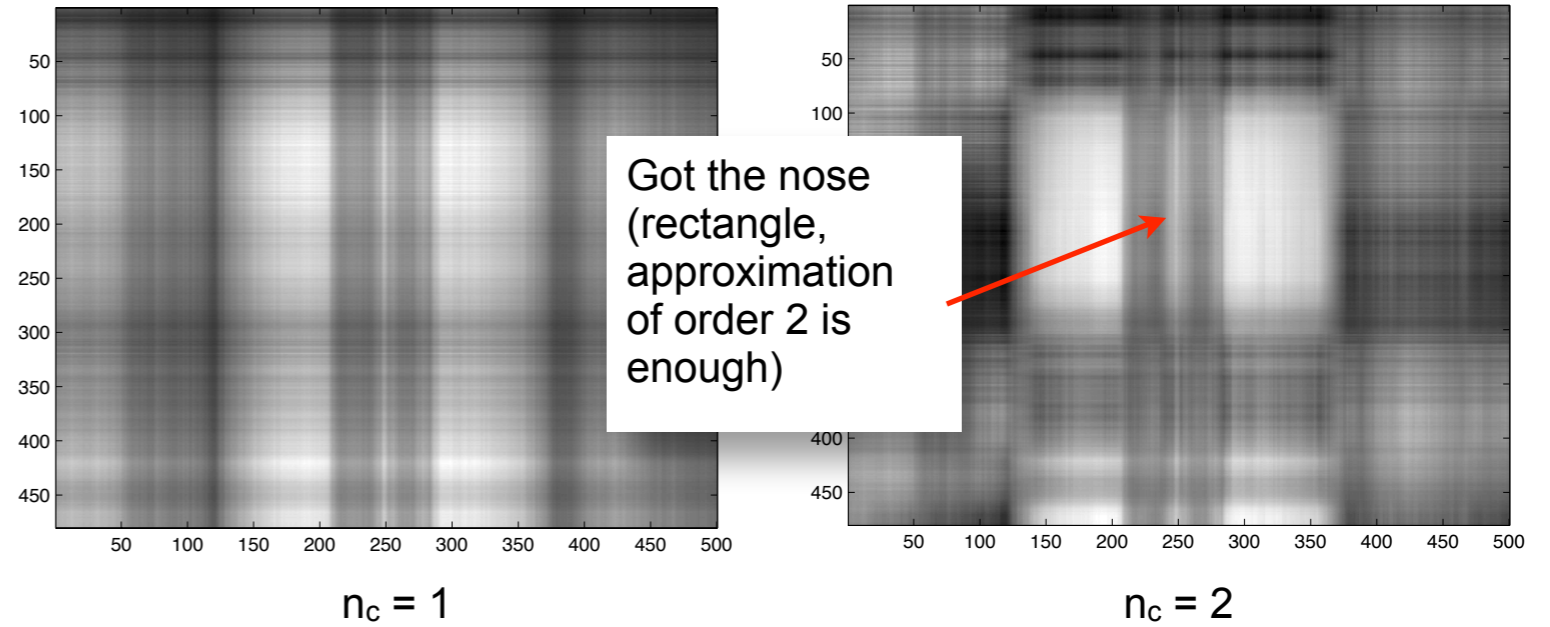
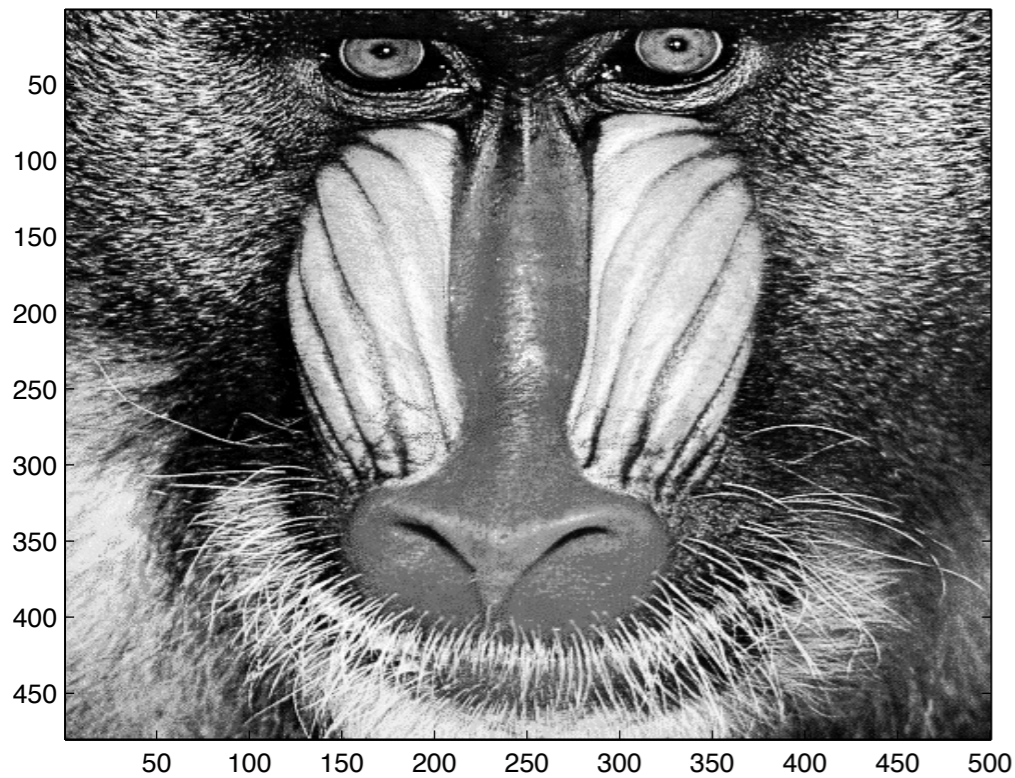
Data compression: get the nose with the POD!



$$\bar{u}(x_i, y_j) = \sum_{i=1}^{n_c} \underline{C}_x^i(x_i) \underline{C}_y^i(y_j)$$

$$(\underline{C}_x^i, \underline{C}_y^i)_{i \in [1, n_c]} = \operatorname{argmin} \sum_{x_i} \sum_{y_j} (u(x_i, y_j) - \bar{u}(x_i, y_j))^2$$

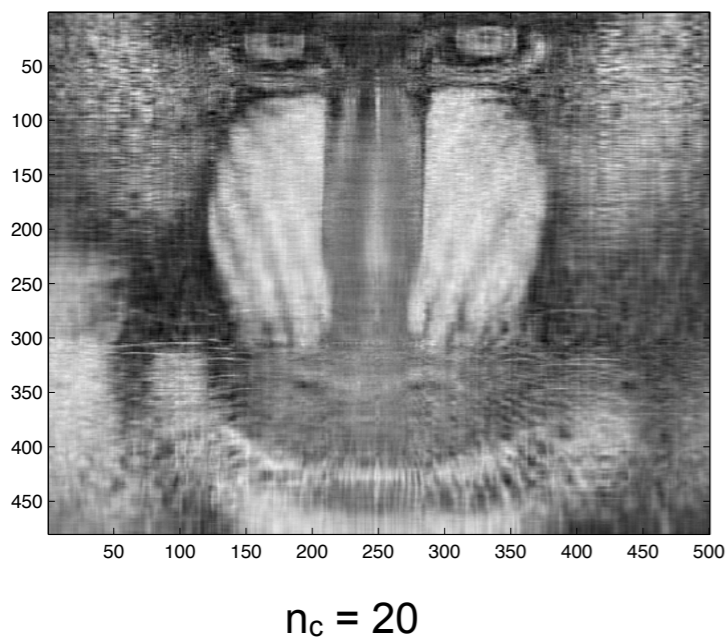
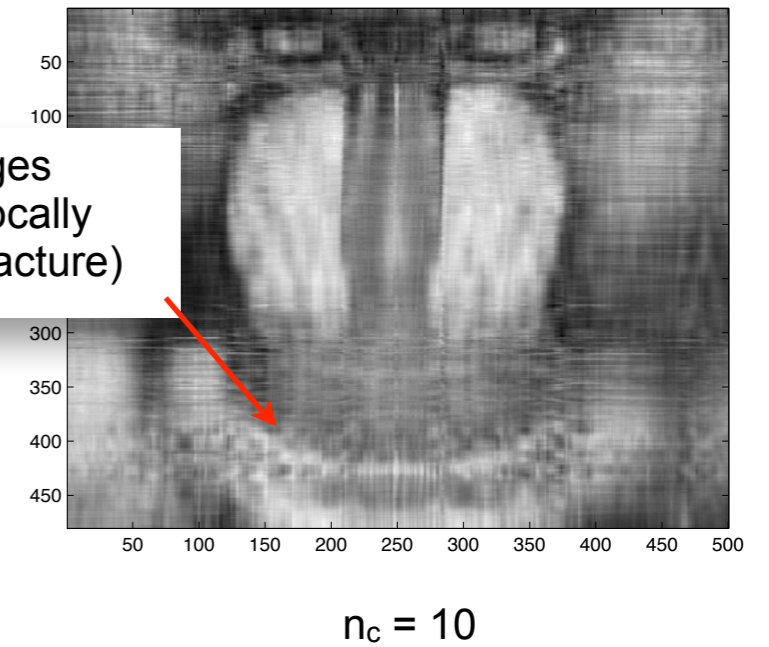
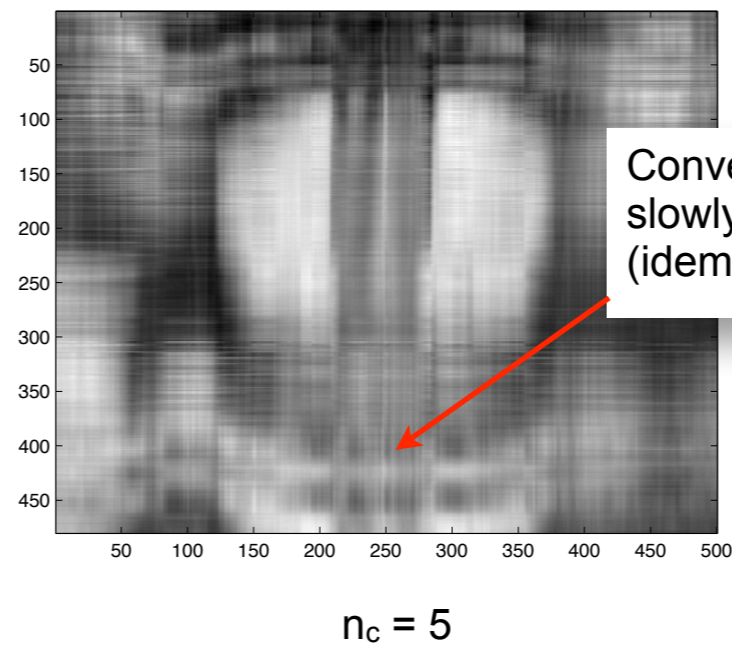
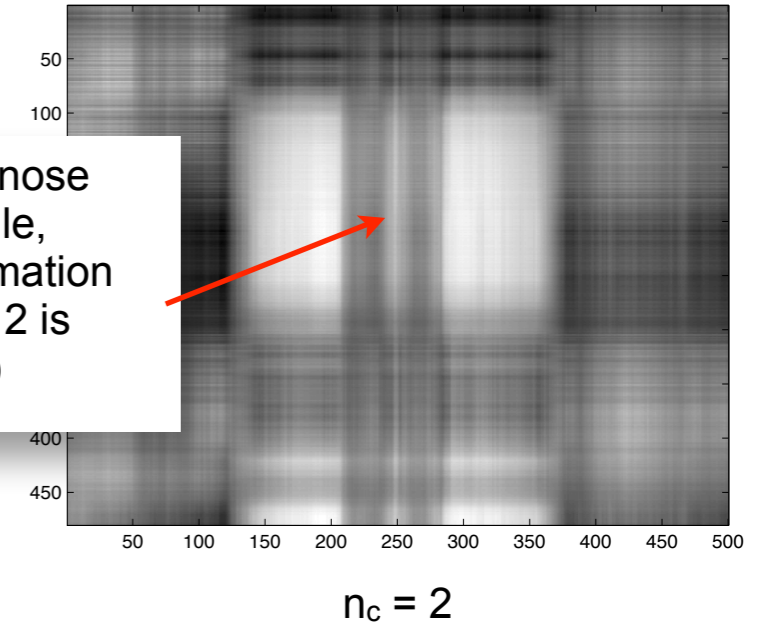
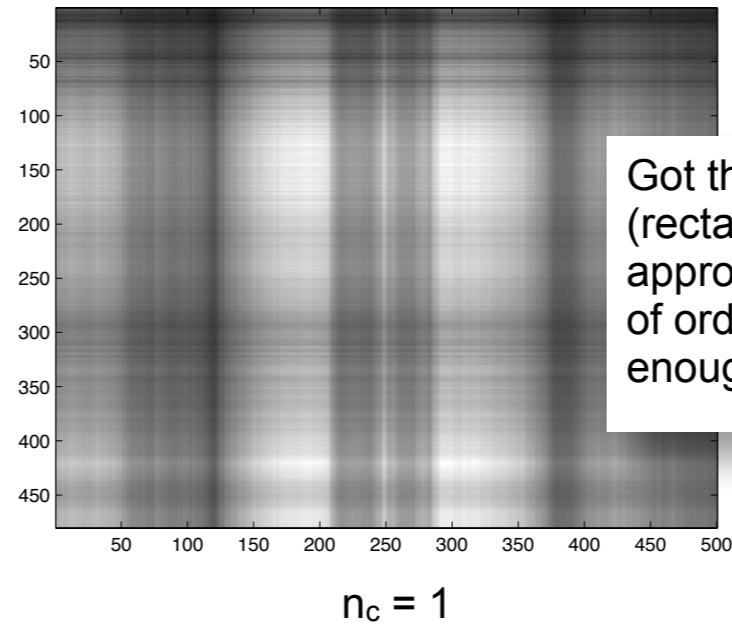
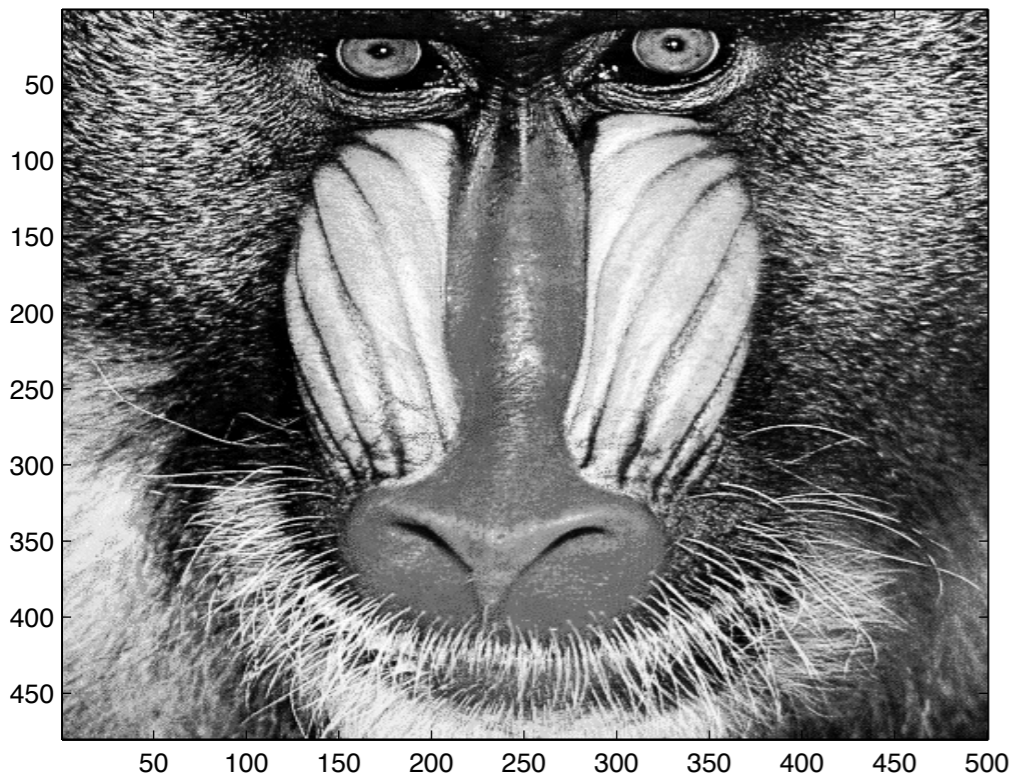
Data compression: get the nose with the POD!



$$\bar{u}(x_i, y_i) = \sum_{i=1}^{n_c} \underline{C}_x^i(x_i) \underline{C}_y^i(y_i)$$

$$(\underline{C}_x^i, \underline{C}_y^i)_{i \in [1, n_c]} = \operatorname{argmin} \sum_{x_i} \sum_{y_j} (u(x_i, y_j) - \bar{u}(x_i, y_j))^2$$

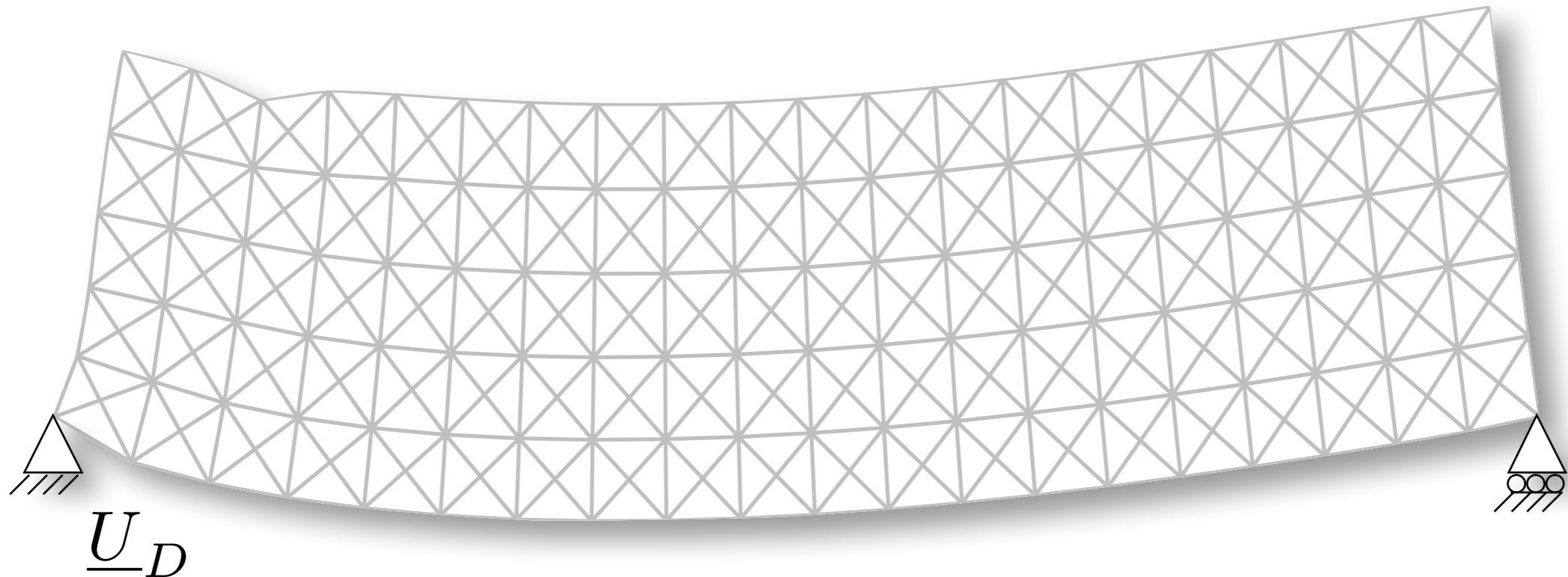
Data compression: get the nose with the POD!



$$\bar{u}(x_i, y_i) = \sum_{i=1}^{n_c} \underline{C}_x^i(x_i) \underline{C}_y^i(y_i)$$

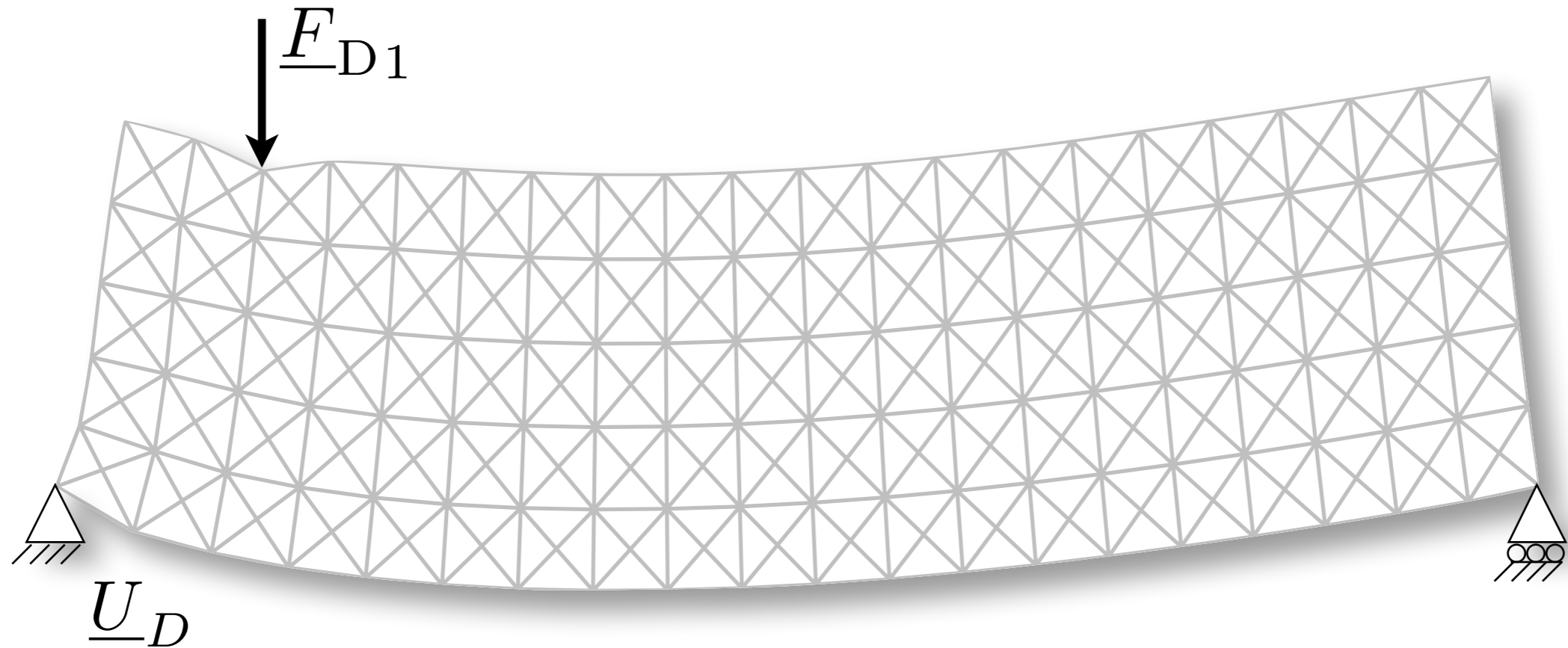
$$(\underline{C}_x^i, \underline{C}_y^i)_{i \in [1, n_c]} = \operatorname{argmin} \sum_{x_i} \sum_{y_j} (u(x_i, y_j) - \bar{u}(x_i, y_j))^2$$

Lattice beam problem



Aim: accelerate the simulation using pre-computations

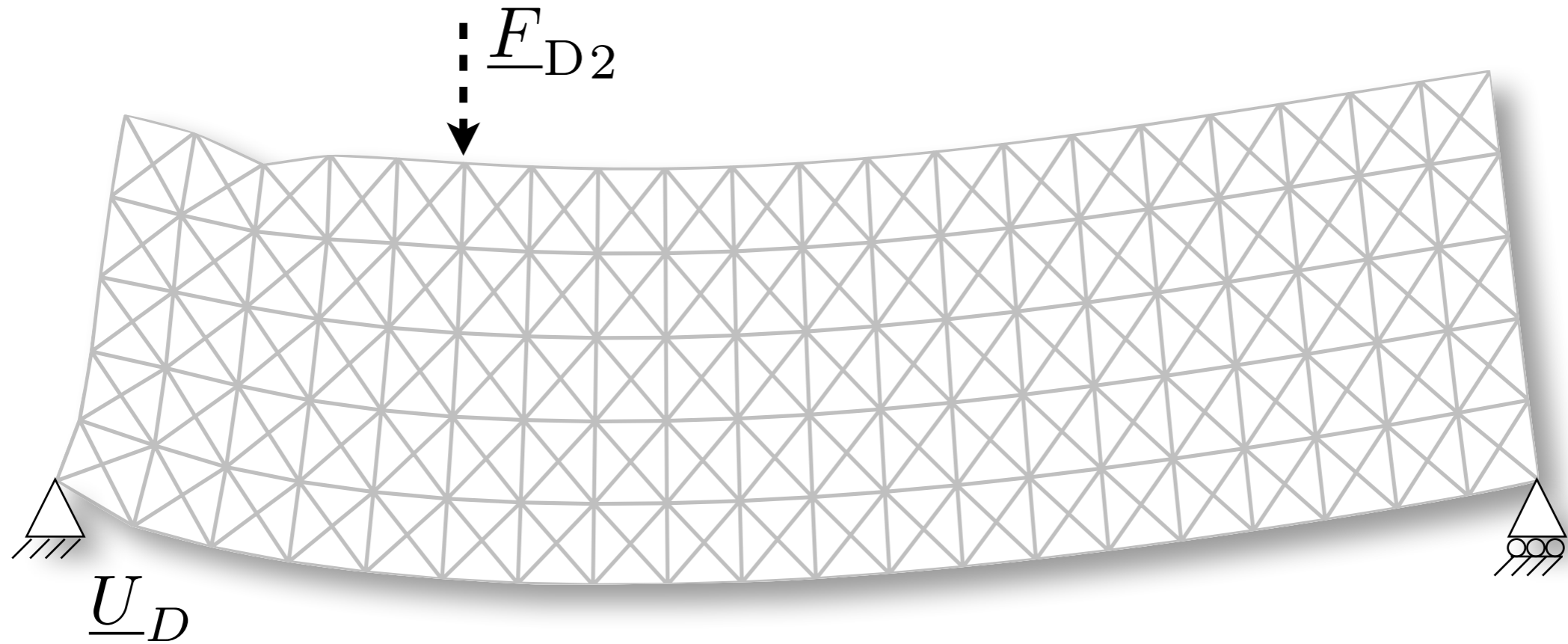
Lattice beam problem



$$\underline{\underline{\mathbf{S}}} = \left(\underline{\underline{\mathbf{S}}^1} \right)$$

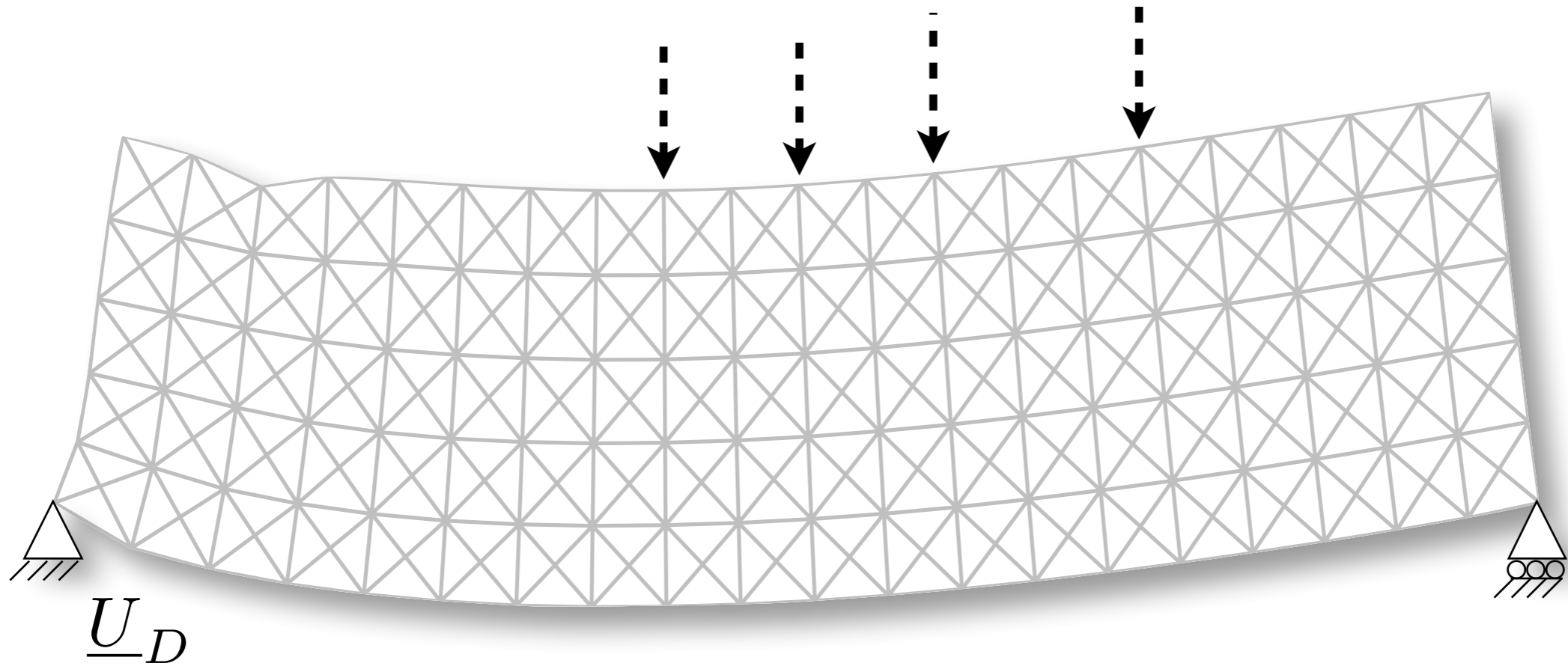
Compute solutions for several loading conditions

Lattice beam problem



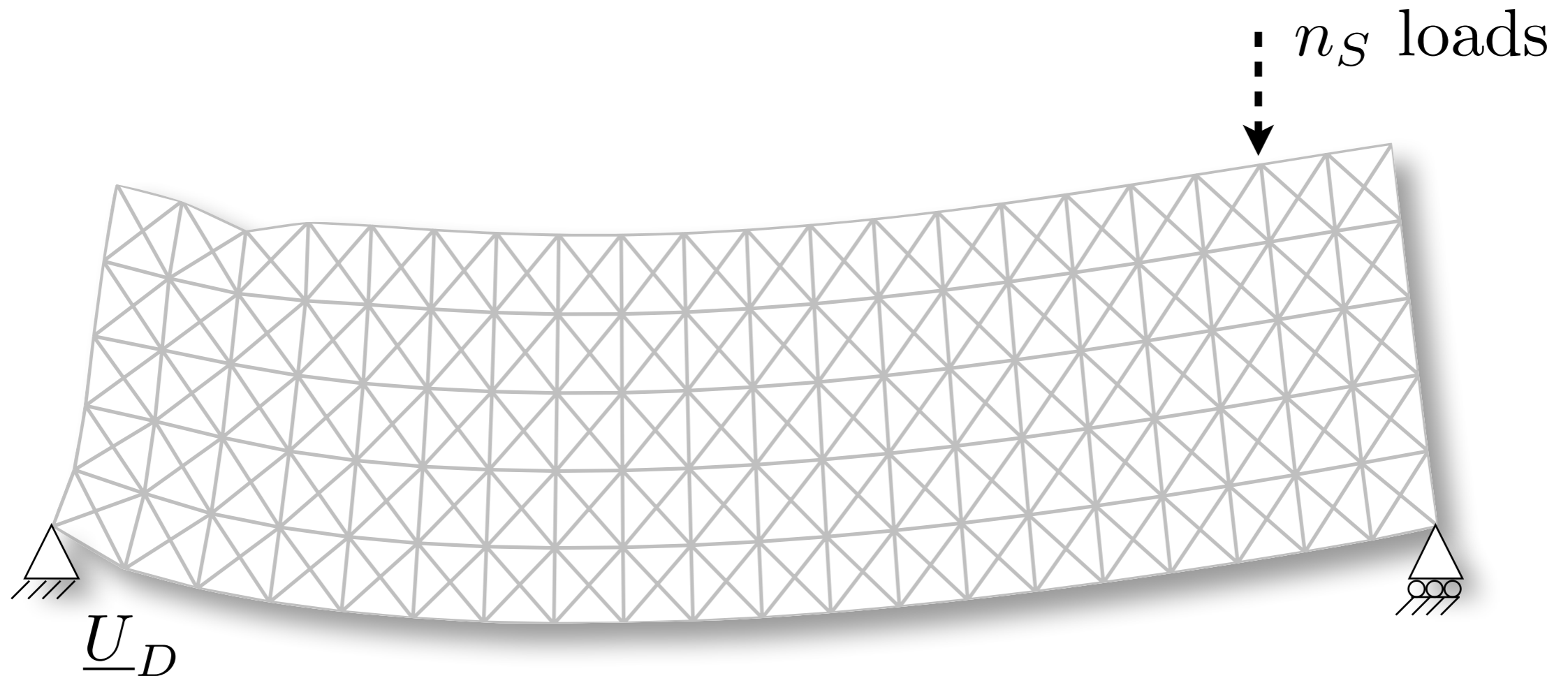
$$\underline{\underline{\mathbf{S}}} = \left(\underline{\underline{\mathbf{S}}^1} \quad \underline{\underline{\mathbf{S}}^2} \right)$$

Lattice beam problem



$$\underline{\underline{\mathbf{S}}} = \left(\underline{\underline{\mathbf{S}}^1} \quad \underline{\underline{\mathbf{S}}^2} \quad \dots \right)$$

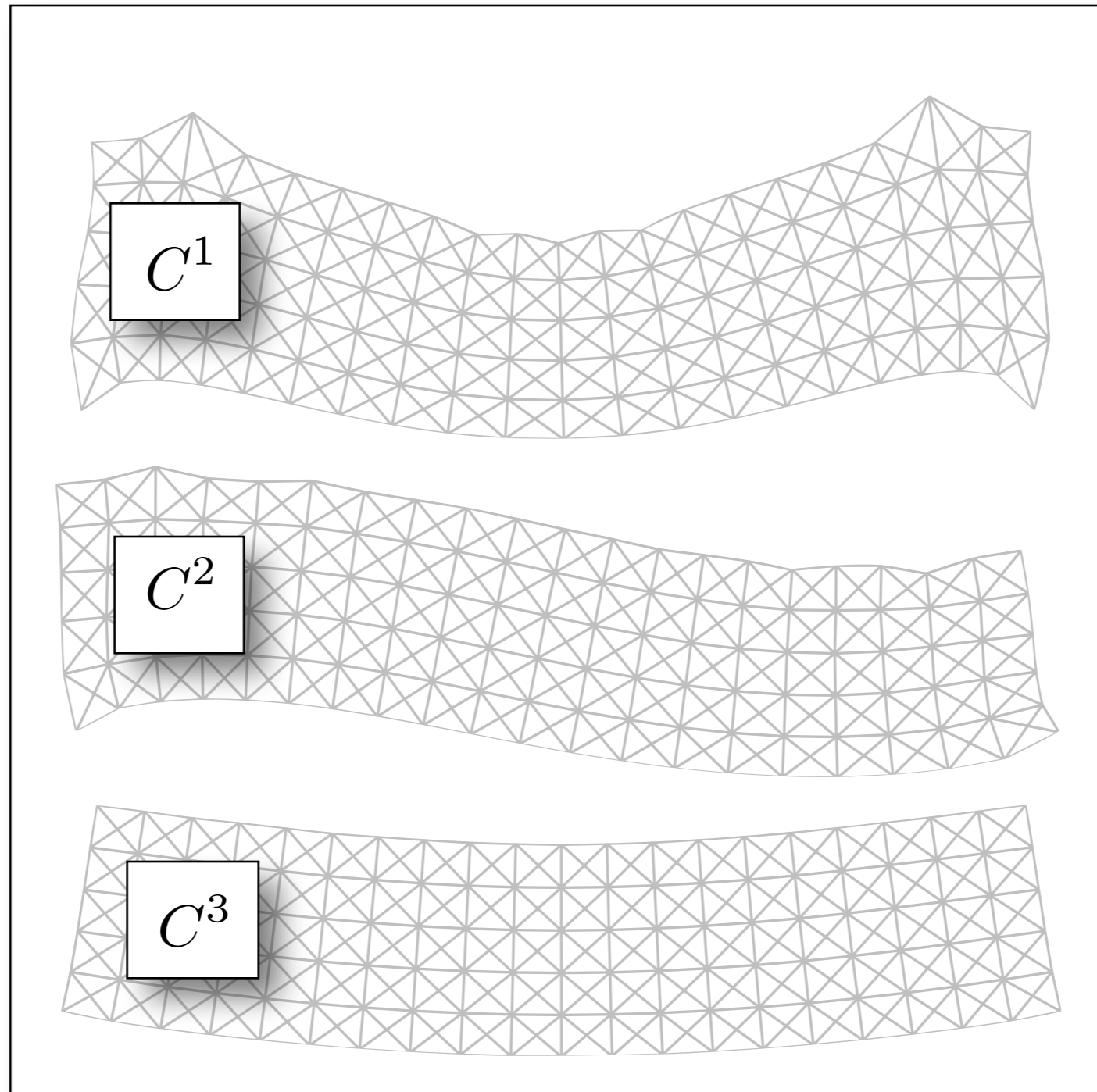
Lattice beam problem



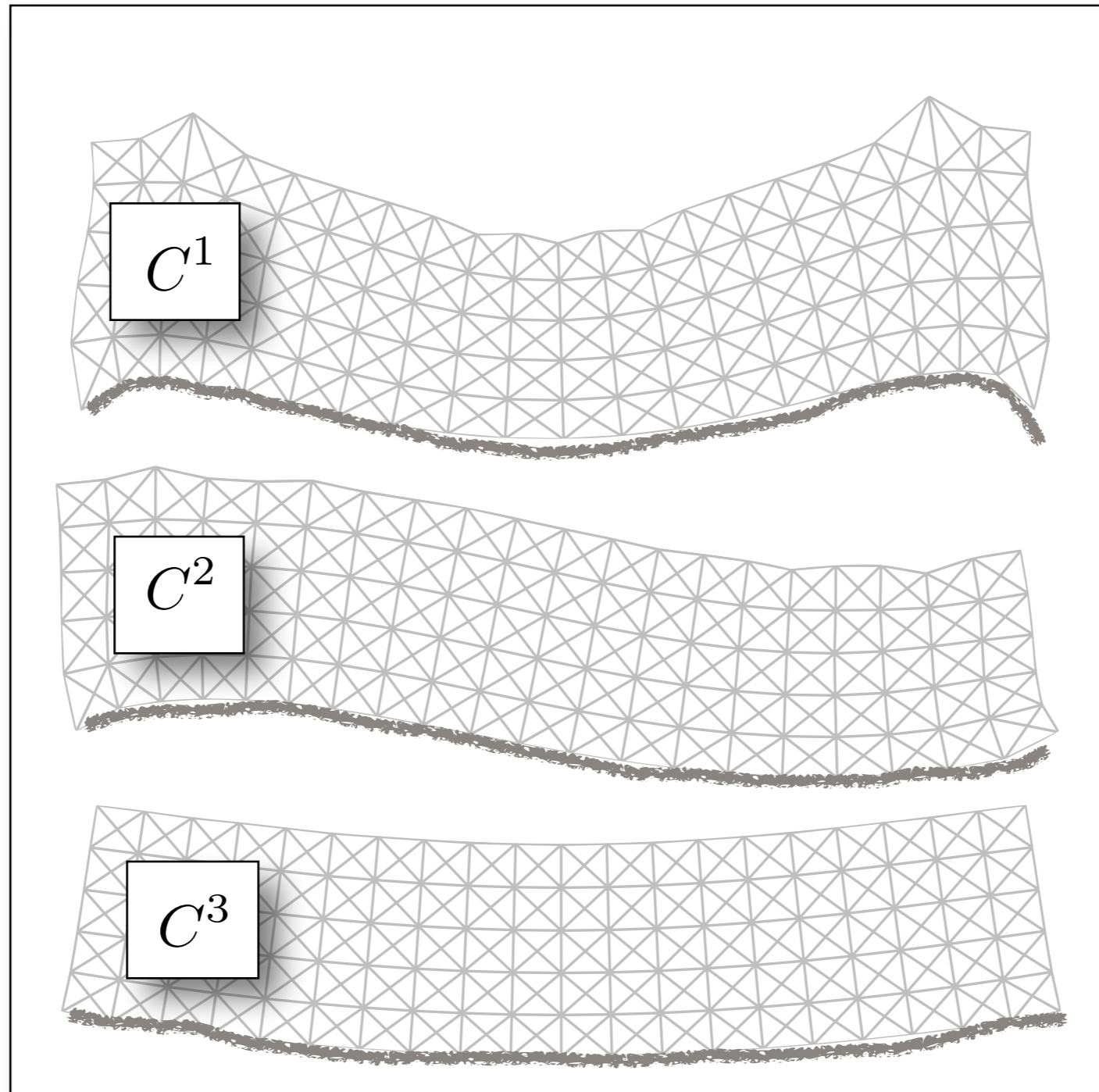
$$\underline{\underline{\mathbf{S}}} = \left(\underline{\underline{\mathbf{S}}^1} \quad \underline{\underline{\mathbf{S}}^2} \quad \dots \quad \underline{\underline{\mathbf{S}}^{n_S}} \right)$$

Perform singular value decomposition - POD
to obtain “most energetic modes”

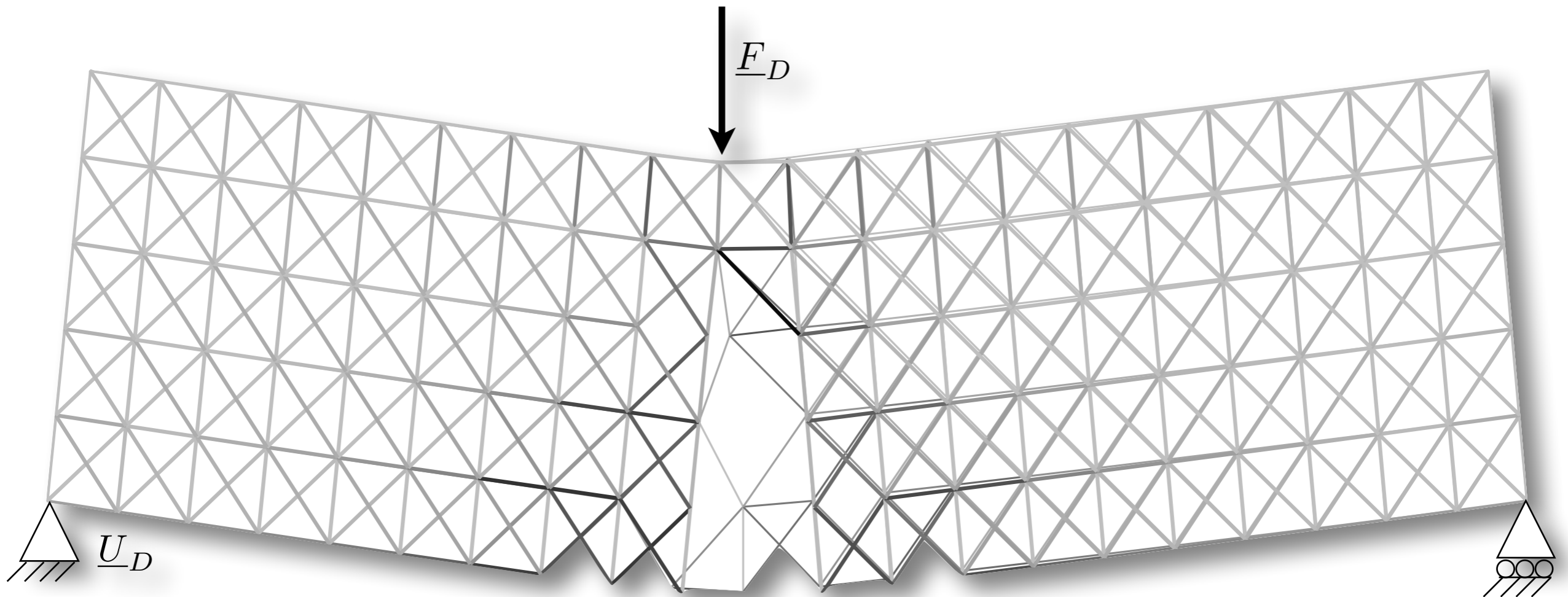
Reduced basis



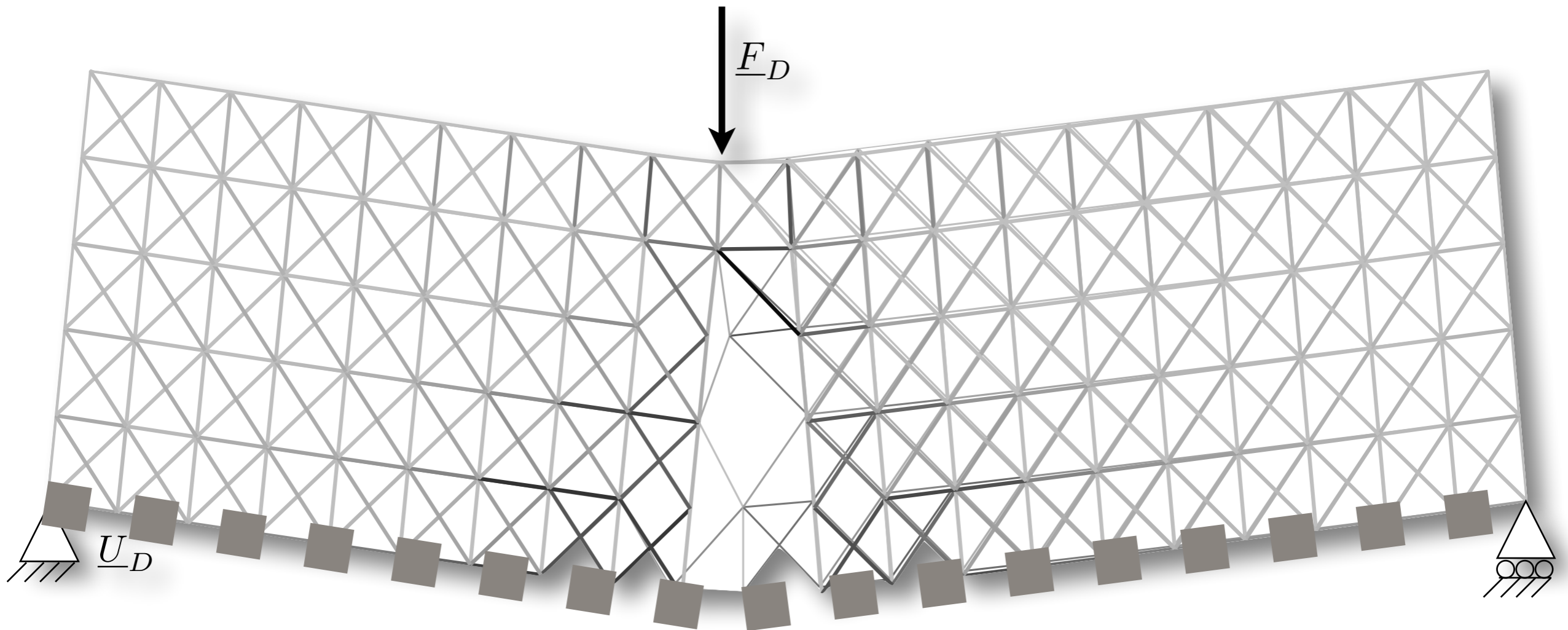
Reduced basis

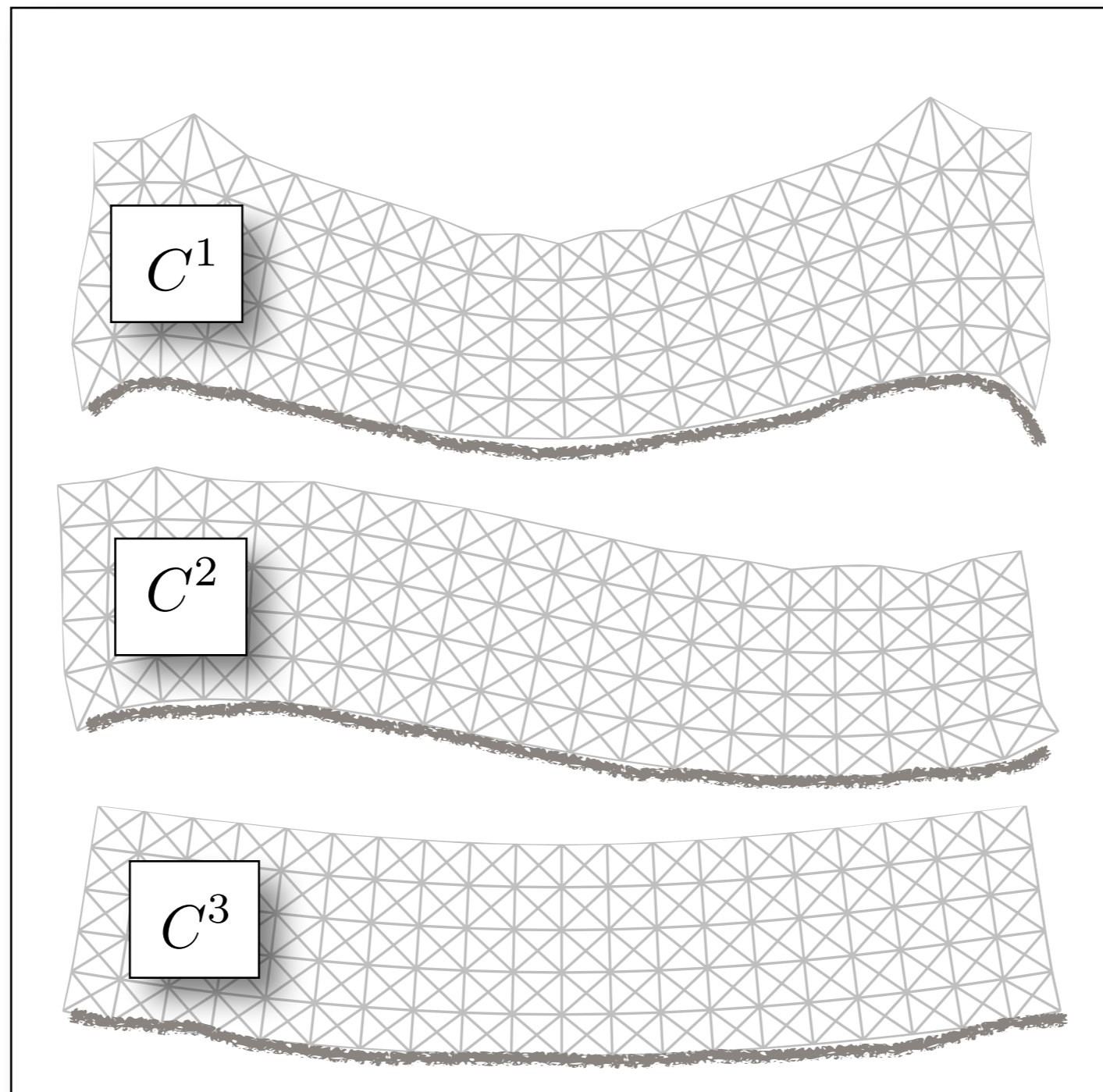


Beyond the elastic limit

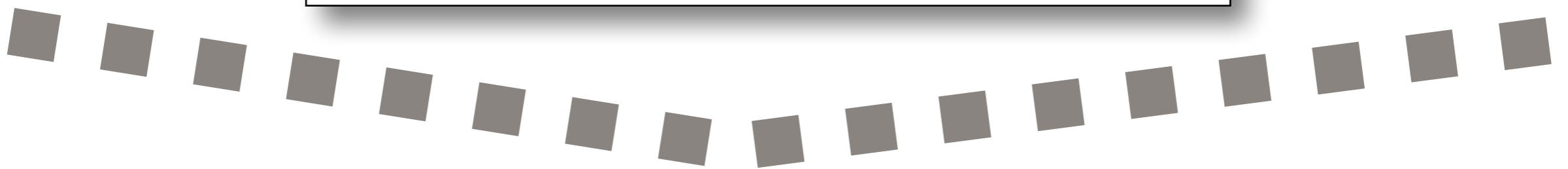


Beyond the elastic limit

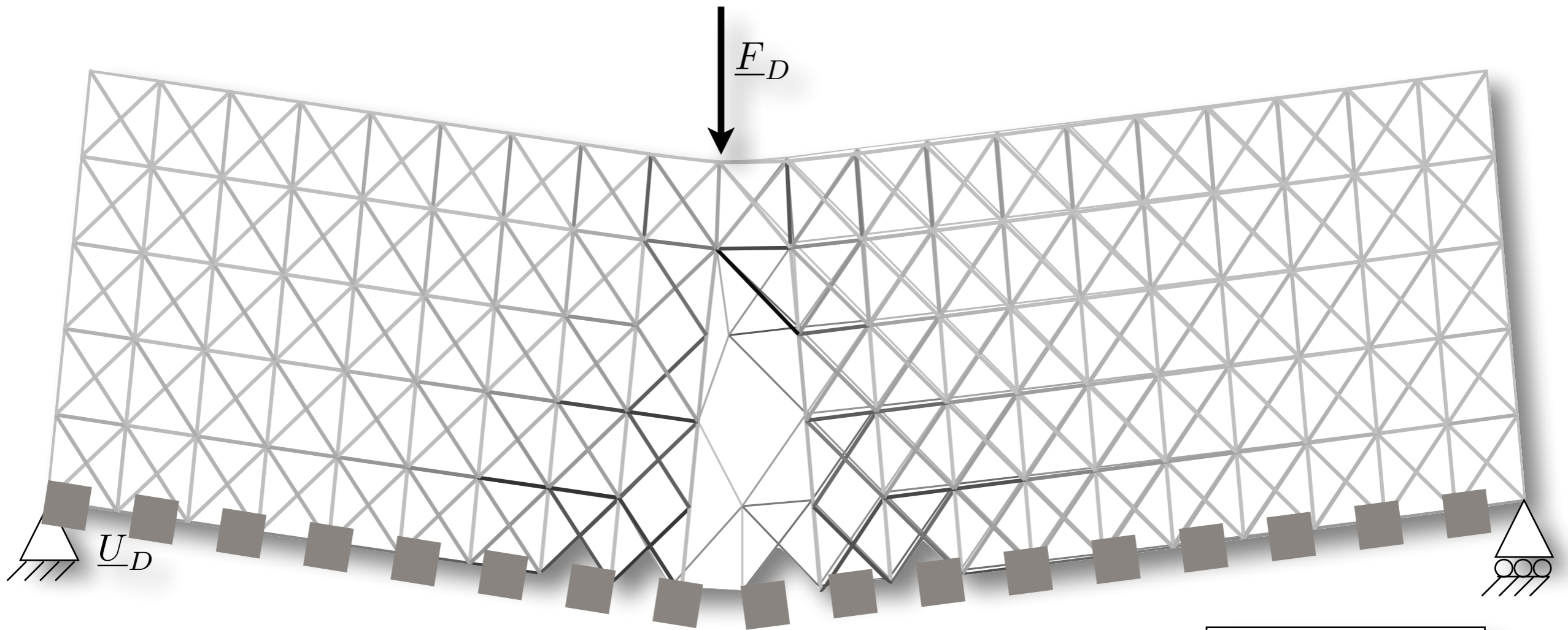




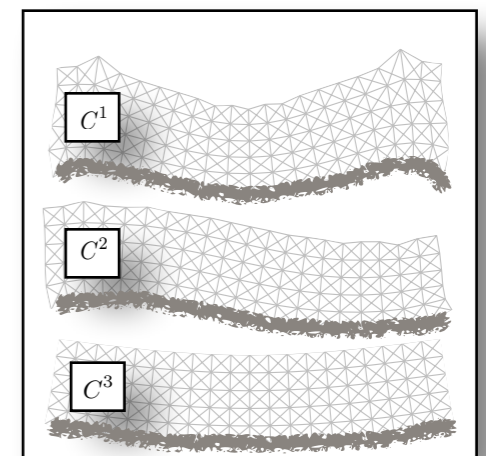
Smooth



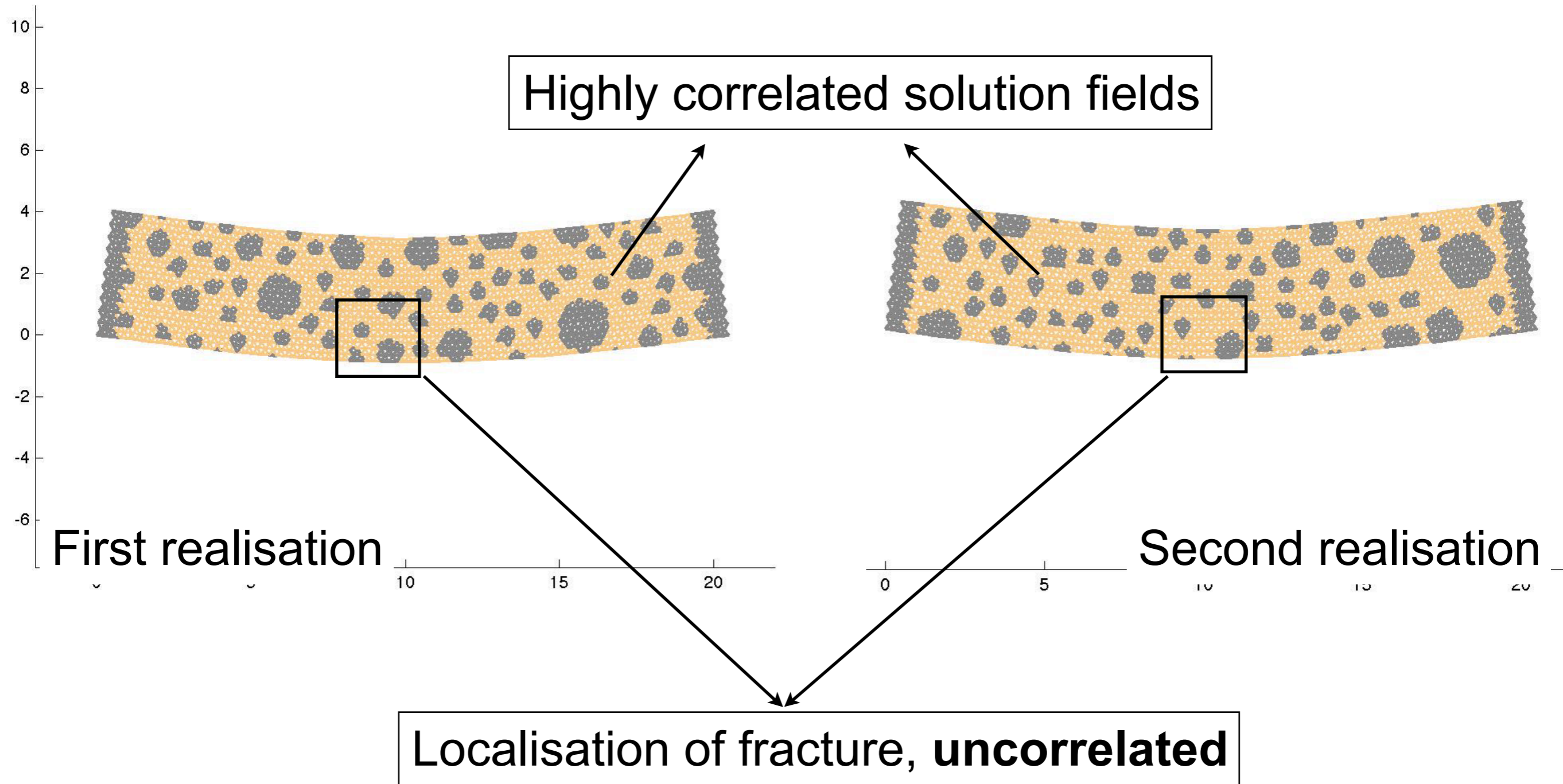
Kink



This solution is not in the snapshot !



Parametric / stochastic multiscale fracture mechanics



- Search for the solution in space / time / parameter in a product space:

$$\underline{\bar{U}} : \mathcal{U}_{\text{sep}} = \mathbb{R}^n \times \mathcal{T} \times \mathcal{P} \rightarrow \mathbb{R}^n$$

$$\underline{\bar{U}}(t, \mu) = \sum_{i=1}^{n_C} \underline{\mathbf{C}}_i \beta_i(t) \gamma_i(\mu),$$

$$\underline{\mathbf{C}}^i \in \mathbb{R}^n$$

$$\beta^i : \mathcal{T} \rightarrow \mathbb{R}, \quad \forall i \in \llbracket 1, n_C \rrbracket,$$

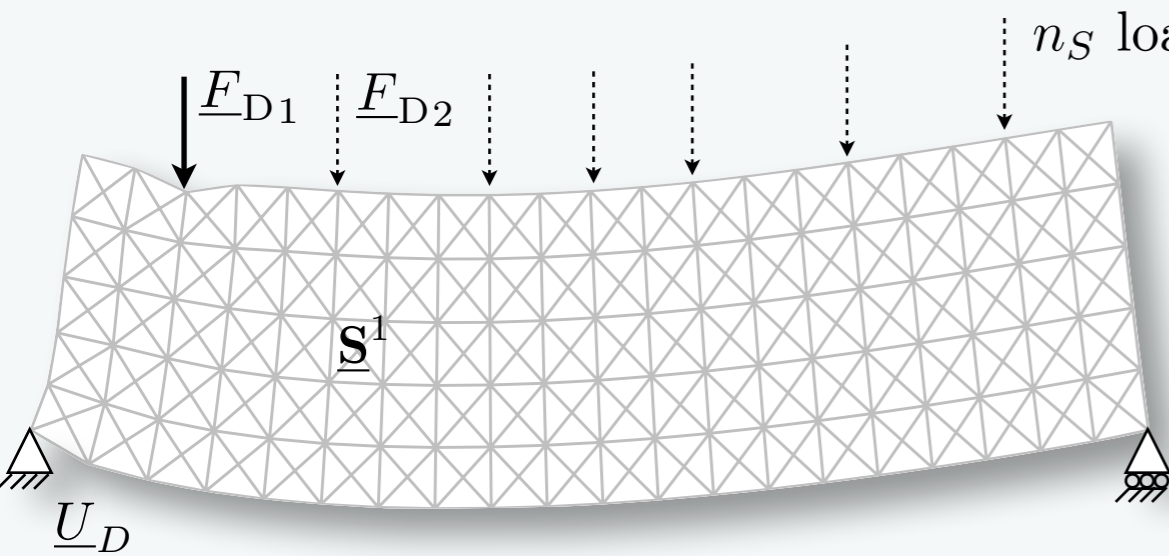
$$\gamma^i : \mathcal{P} \rightarrow \mathbb{R}, \quad \forall i \in \llbracket 1, n_C \rrbracket,$$

- Optimality of an expansion of order n_C with respect to a particular metric defined on \mathcal{U}_{sep}

➡ different metrics lead to different methods, which have their pro/cons

➡ Choice strongly dependent on the context

- ▶ Data compression: **POD** (Proper Orthogonal Decomposition) is a classical choice in dimension 2
- ▶ Data compression in many dimensions: **multilinear POD**
- ▶ Solver in many dimensions without *a priori* knowledge of the solution: **PGD**
- ▶ Model order reduction: **Snapshot POD, Snapshot PGD**
- ▶ Initialiser, preconditioners: **low-order POD, low-order PGD, Snapshot POD**



(1) Solve FINE for n_S parameters (EXPENSIVE!)

$$\underline{\underline{S}} = (\underline{s}^1 \quad \underline{s}^2 \quad \dots \quad \underline{s}^{n_S})$$

(2) Singular value decomposition

$$\underline{\underline{S}} = \underline{\underline{U}} \underline{\underline{\Sigma}} \underline{\underline{V}}^T = \sum_{k=1}^{n_S} \Sigma^k \underline{U}^k \underline{V}^{kT}$$

n_S solutions, sorted by relevance

where $(\Sigma^k)_{k \in \llbracket 1 \ n_S \rrbracket}$ in decreasing order

(3) Truncation

Initial set of equations

$$\underline{\underline{F}}_{\text{Int}} (\underline{\underline{U}}) + \underline{\underline{F}}_{\text{Ext}} = 0$$

(4) Galerkin orthogonality

$$\underline{\underline{C}}^T \underline{\underline{F}}_{\text{int}} (\underline{\underline{C}} \underline{\alpha}) + \underline{\underline{C}}^T \underline{\underline{F}}_{\text{ext}} = 0$$

Approximation of the solution in a space of small dimension (n_c)

Family of representative solutions

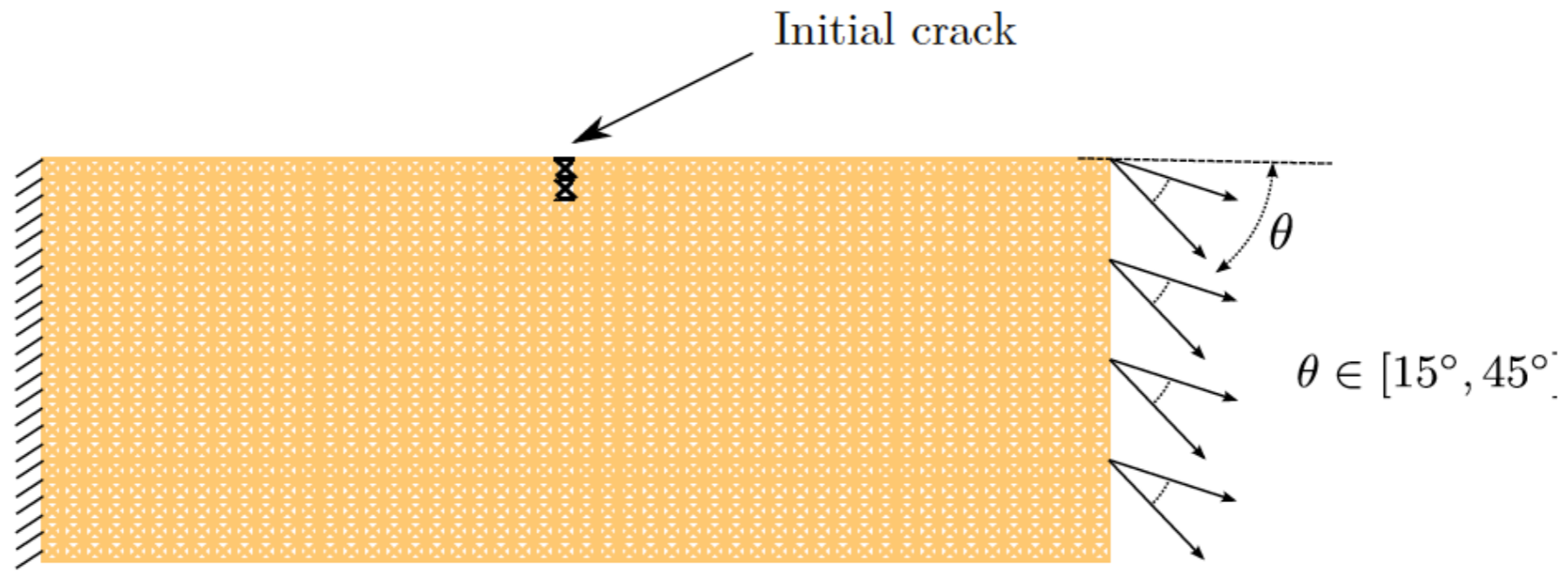
$$\underline{\underline{U}} = \underline{\underline{C}} \underline{\alpha}$$

Solution Coefficients

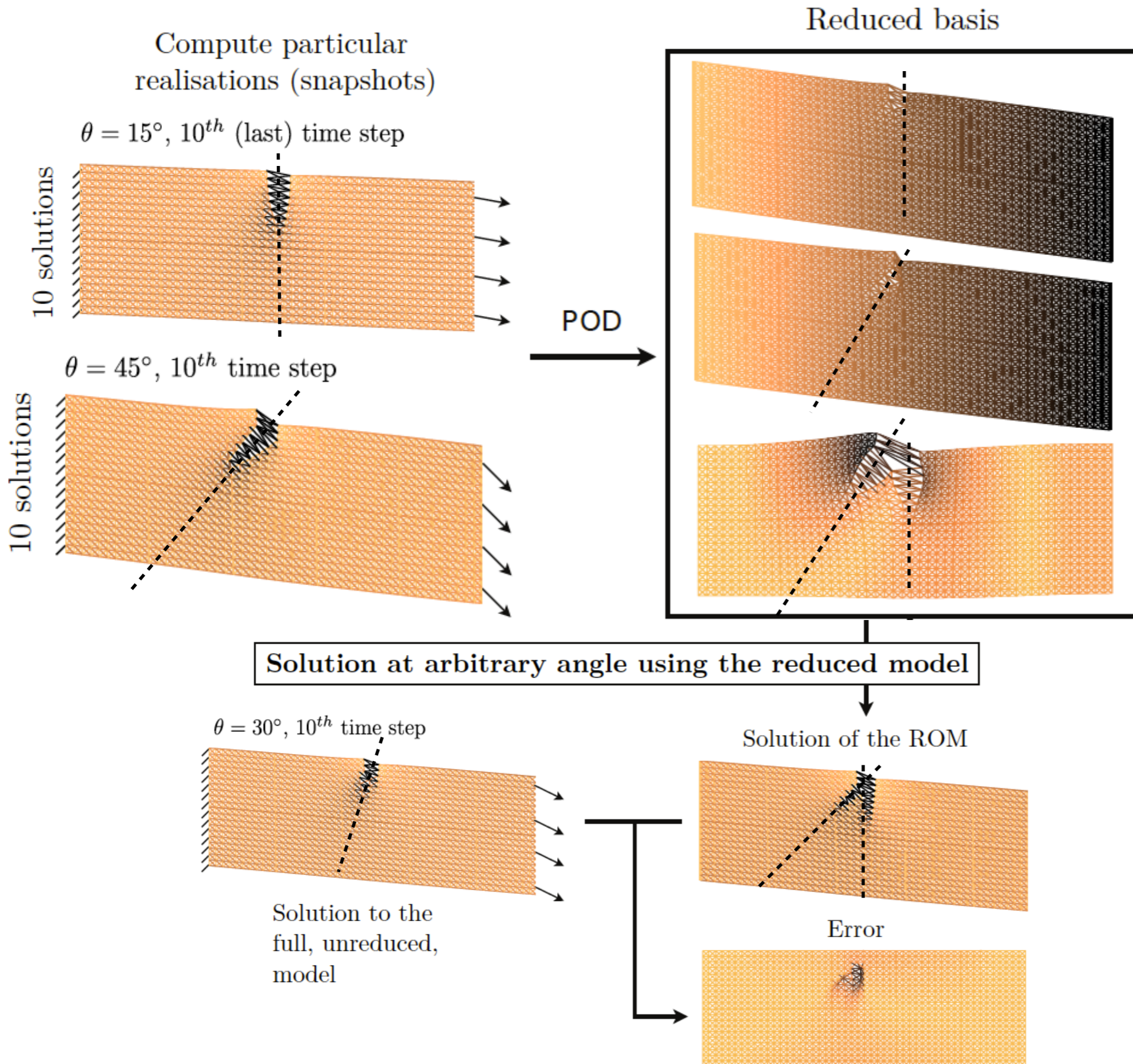
Reduced basis: family of representative solutions

$\underline{\underline{C}} = (\underline{U}^1 \quad \underline{U}^2 \quad \dots \quad \underline{U}^{n_c})$

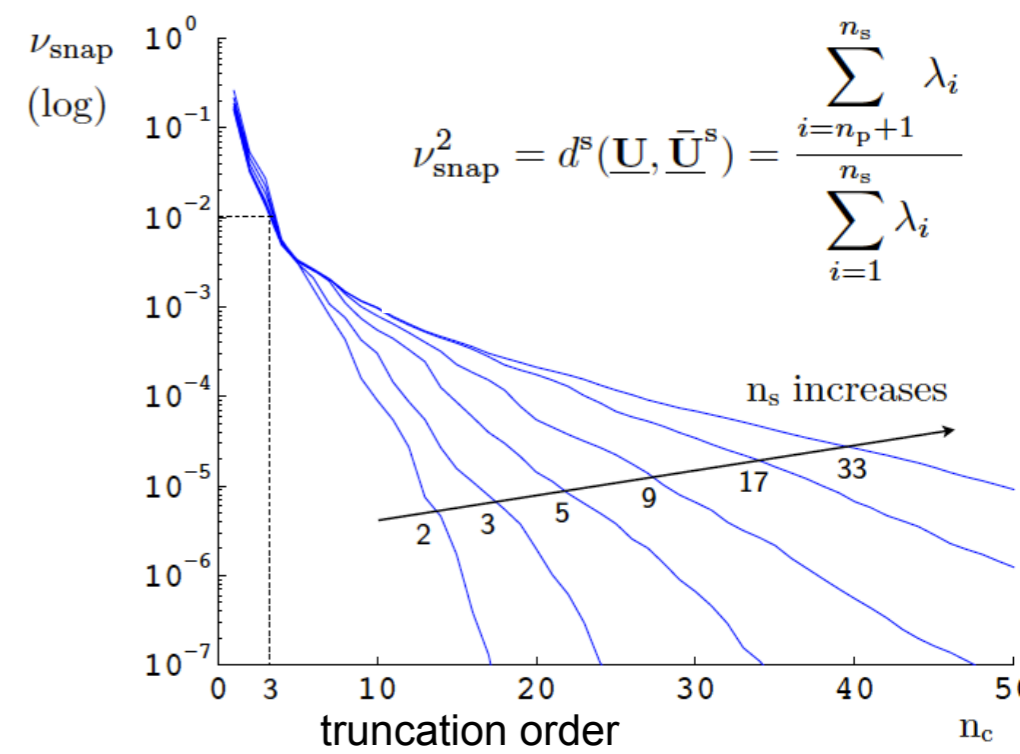
Application to a parametric fracture problem



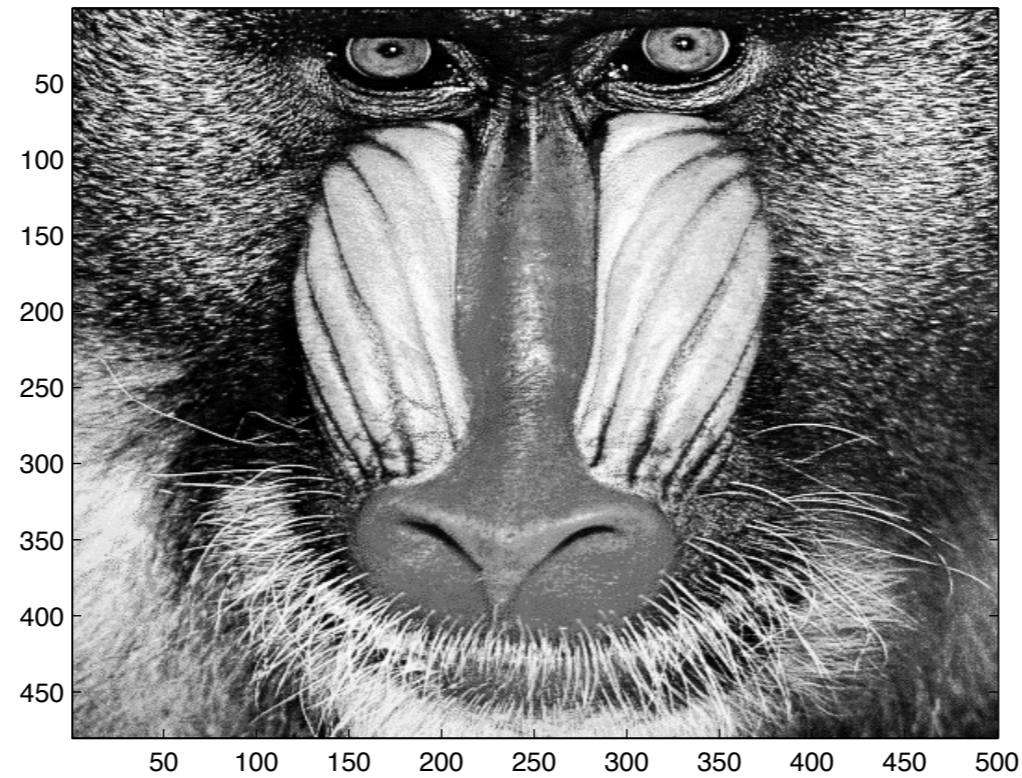
Application to a parametric fracture problem



- ▶ The POD solution is not able to reproduce the solution in the cracked area
- ▶ Due to lack of correlation introduced by crack growth
- ▶ Leads to a local projection error



Return of the monkey



- What can we do to address this lack of separation of scales/
reducibility?

Model reduction in mechanics (non exhaustive)

- Model order reduction in a domain decomposition context
 - Craig-Bampton [Craig and Bampton '68, Rixen et al. '04]
 - LaTIn method / PGD [Ladevèze et al. '03, Ladevèze et al. '10]
 - Partitioned Component Mode Synthesis [Park and Park '04, Markovic and Ibrahimbegovic '09]
 - Partitioned POD [Kerfriden et al. '11]
- Model order reduction of substructures not requiring a fine analysis *a priori*
 - Modal truncation [Barbone et al. '03, Rickelt and Reese '04]
 - POD [Rickelt and Reese '06]
- Patches
 - Finite element enrichment of PGD models by VMM [Ammar et al. '11]
 - XFEM discontinuities in soft tissues [Niroomandi et al. '11]
- Model order reduction for heterogeneous/nonlinear materials fracture
 - *A priori* Hyperreduction for plasticity [Ryckelynck et al. '08] and damage [Kerfriden et al. '10]
 - Adaptive POD and morphing in the XFEM context [Galland et al. '09]
 - Reduced model multiscale method [Yvonnet et al. '07]
 - LaTIn method [Ladevèze et al. '03]

How we got to this point...

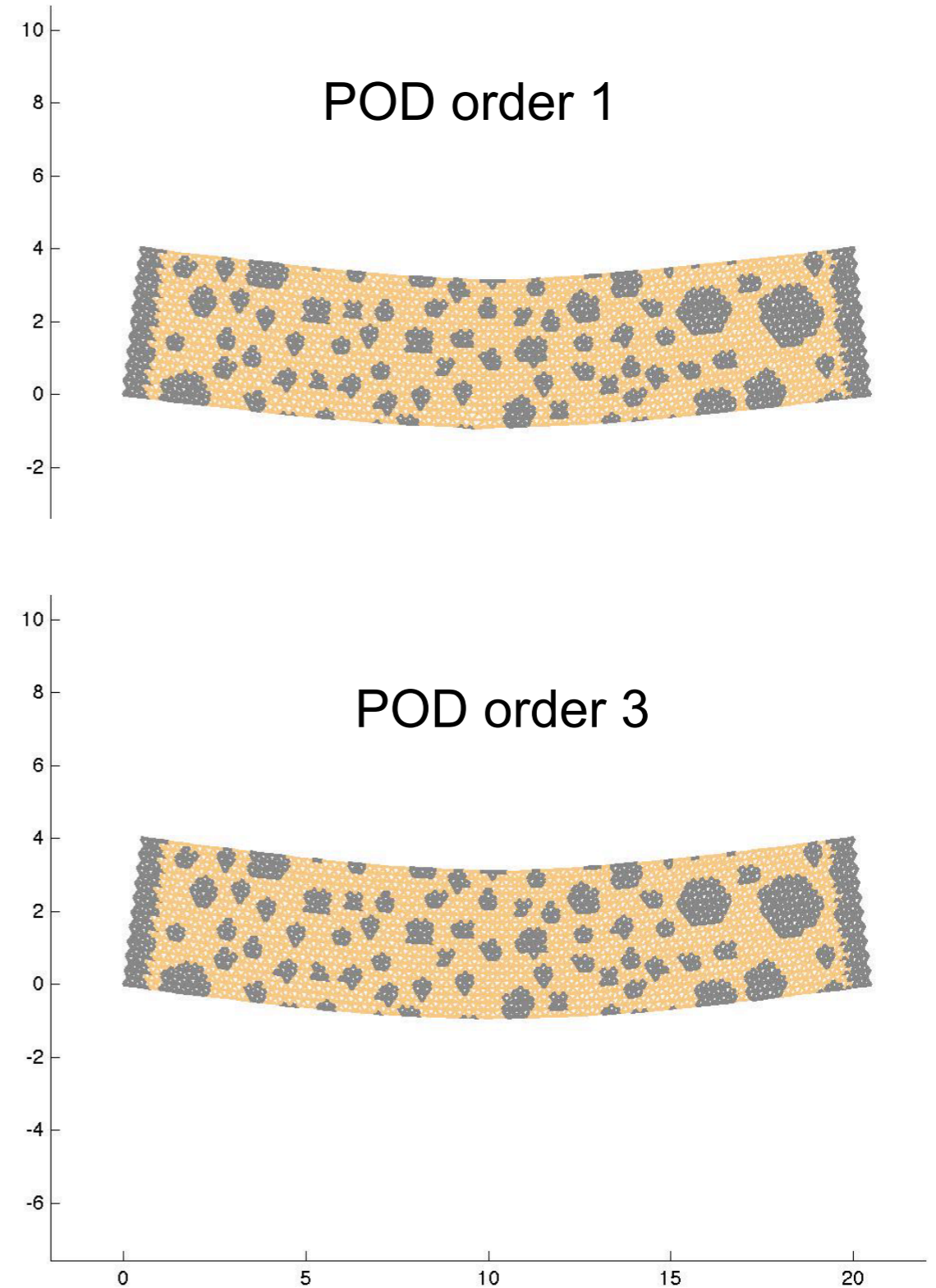
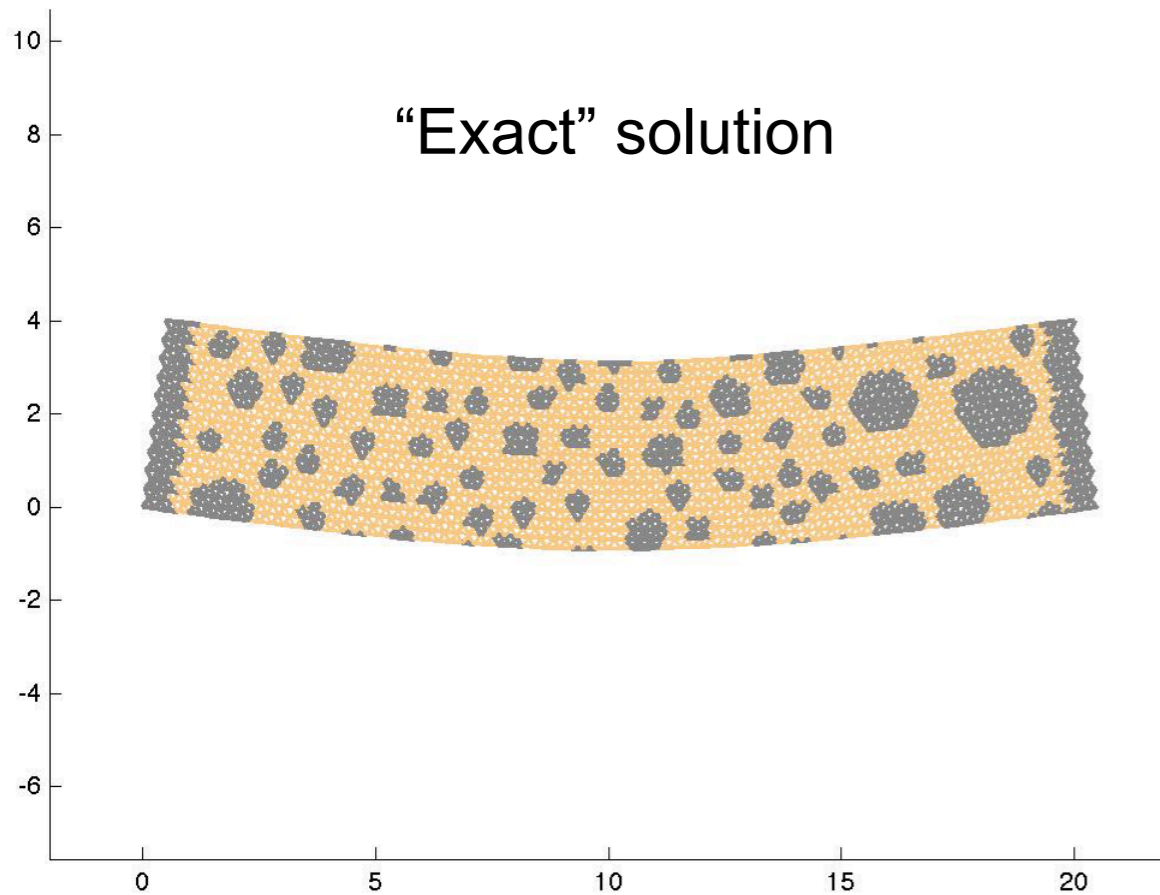
P. Kerfriden, P. Gosselet, S. Adhikari, and S. Bordas. Bridging proper orthogonal decomposition methods and augmented Newton-Krylov algorithms: an adaptive model order reduction for highly nonlinear mechanical problems. *Computer Methods in Applied Mechanics and Engineering*, 200(5-8):850–866, 2011.

P. Kerfriden, J.C. Passieux, and S. Bordas. Local/global model order reduction strategy for the simulation of quasi-brittle fracture. *International Journal for Numerical Methods in Engineering*, 89(2):154–179, 2011.

P. Kerfriden, K.M. Schmidt, T. Rabczuk, and Bordas S.P.A. Statistical extraction of process zones and representative subspaces in fracture of random composites. *Accepted for publication in International Journal for Multiscale Computational Engineering*, *arXiv:1203.2487v2*, 2012.

Data compression: fracture

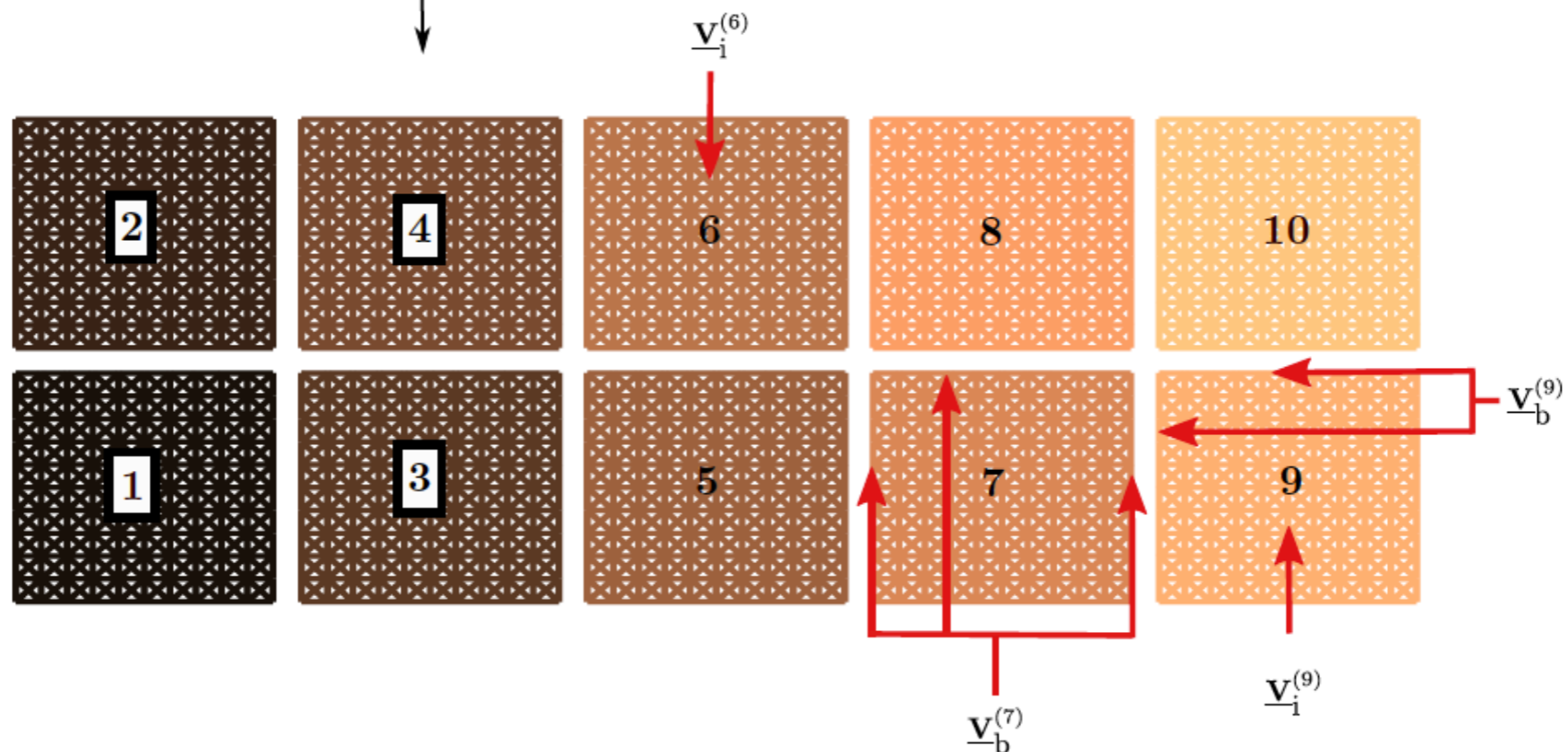
Snapshot POD (snapshot space is spanned by the ensemble of solutions at all time steps)



Partitioned POD/DDDM



Domain Decomposition Method

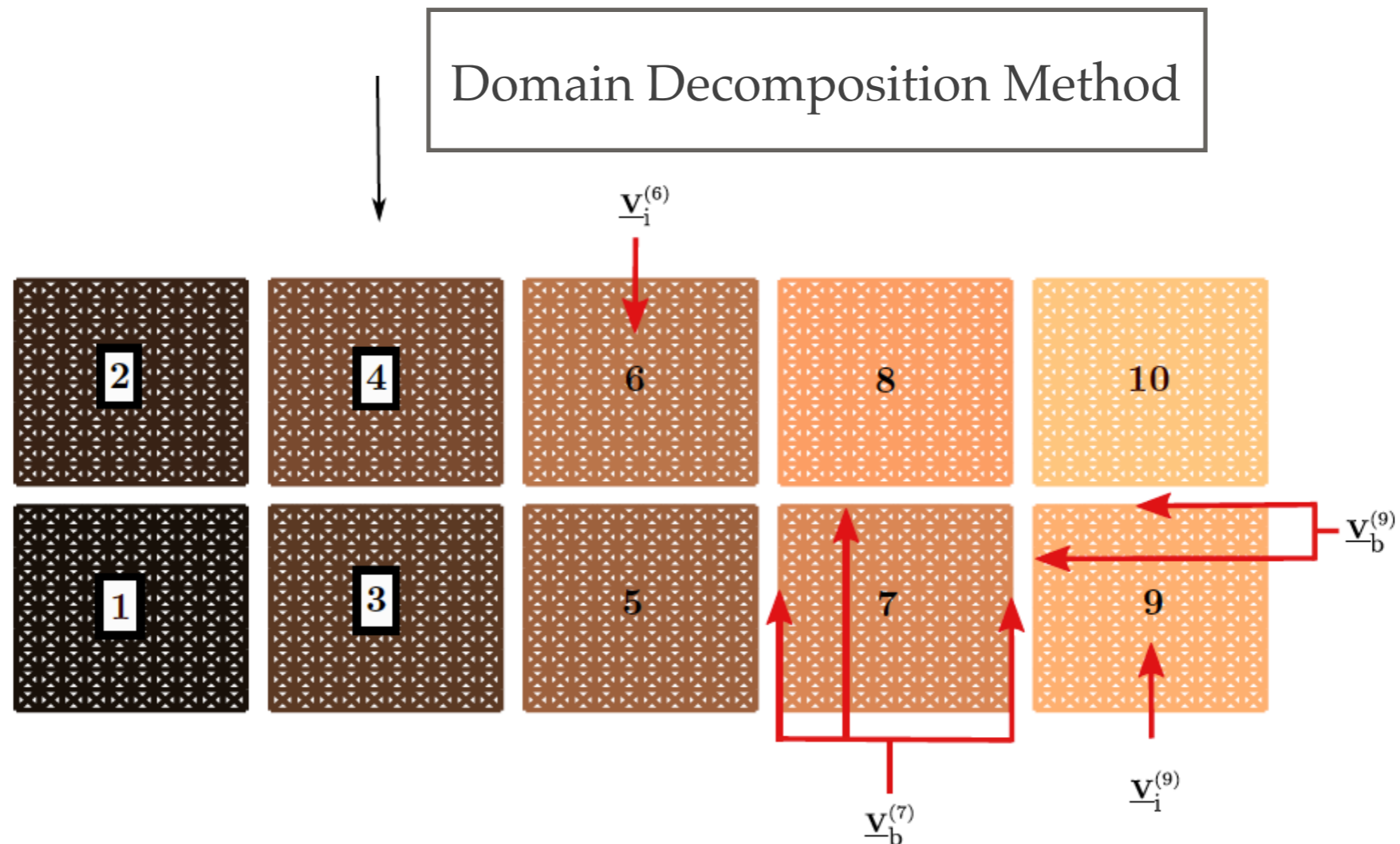


Partitioned POD/DDDM



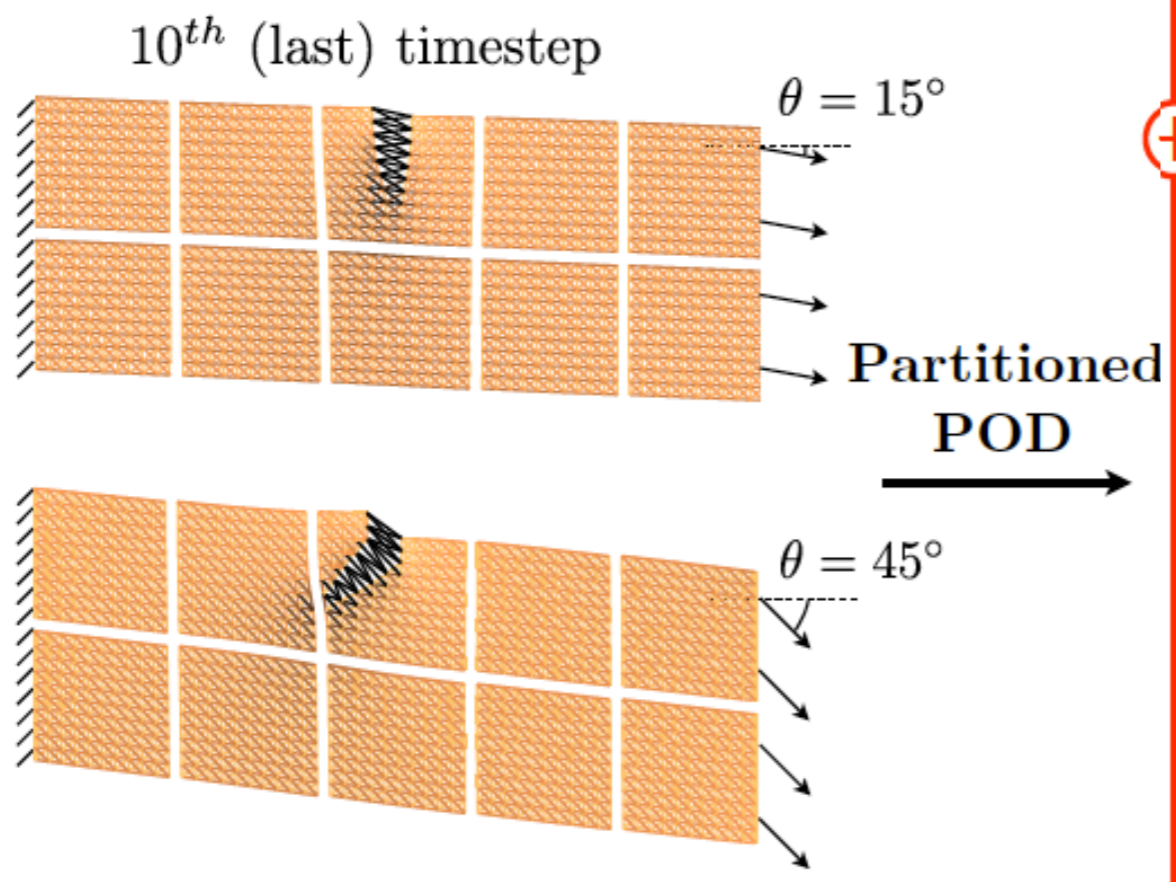
Domain Decomposition Method

Partitioned POD/DDM

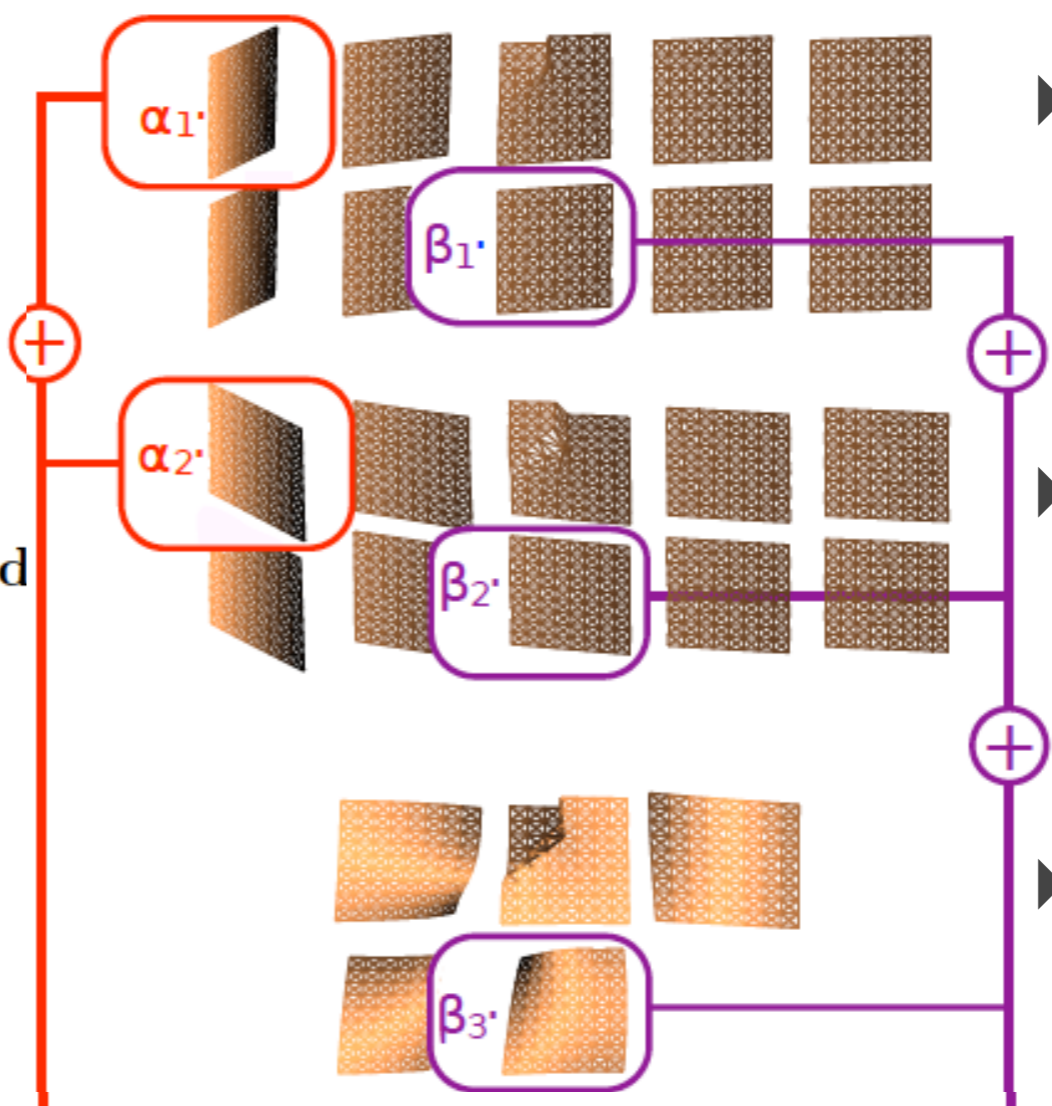


Compute particular realisations

(cost intensive) using domain decomposition (snapshots)

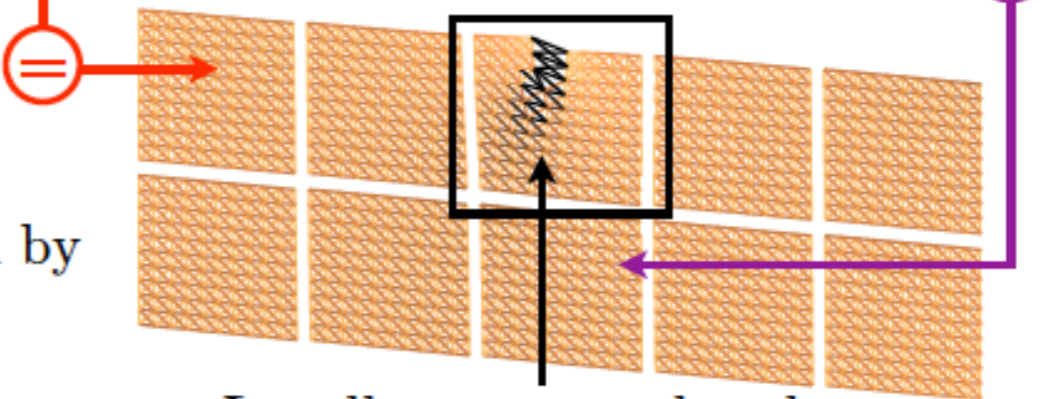
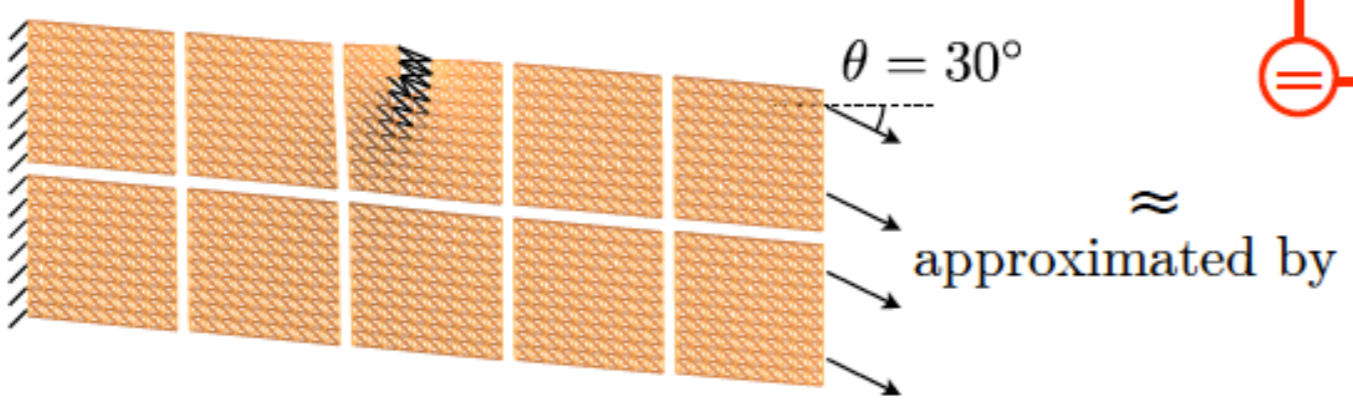


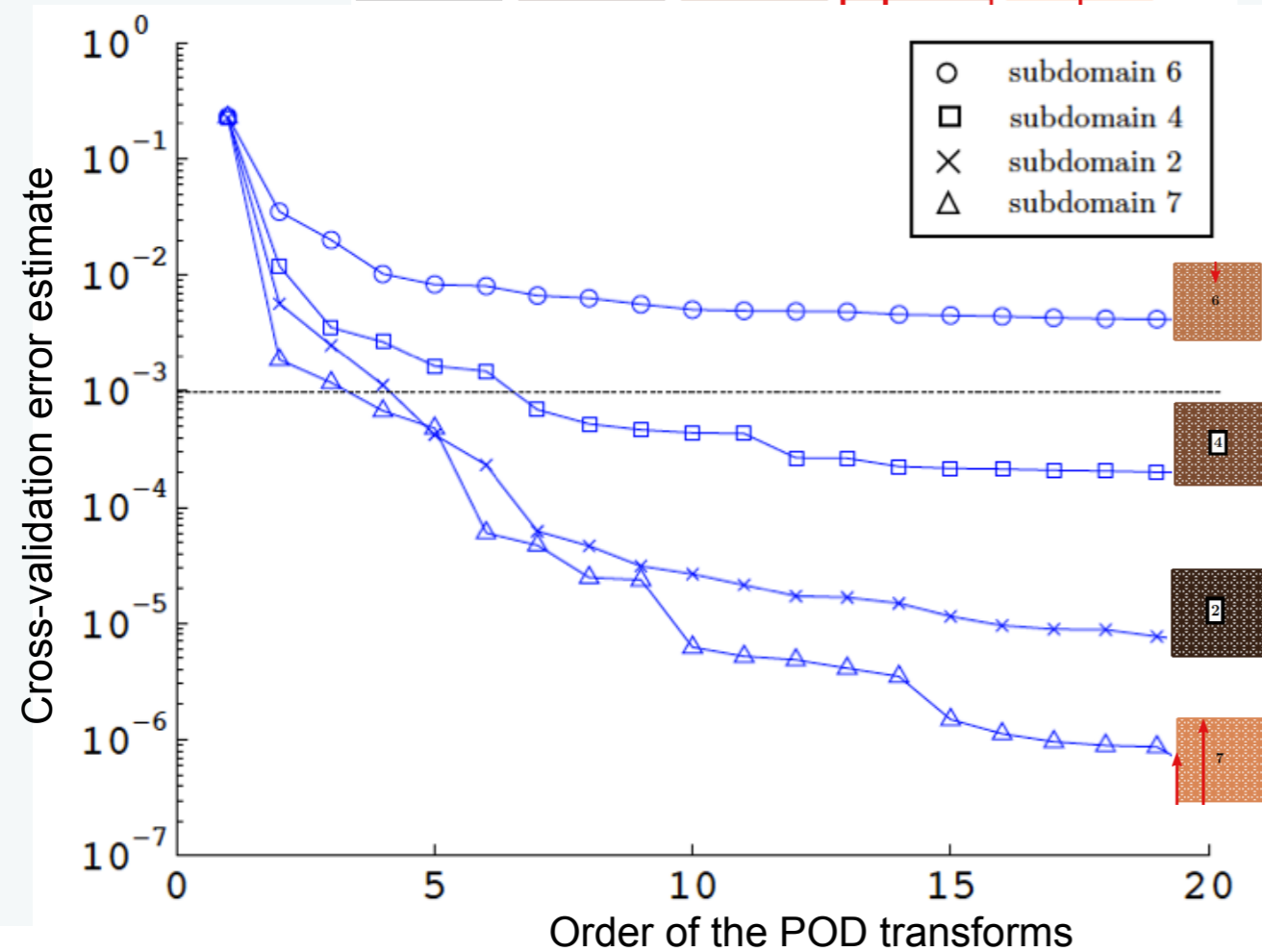
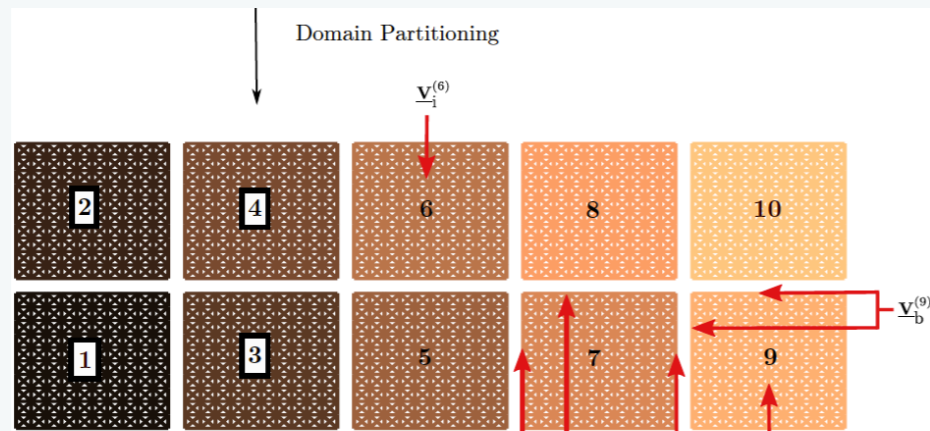
Partitioned reduced basis



- ▶ Decompose the structure into subdomains
- ▶ Perform a reduction in the highly correlated region
- ▶ Couple the reduced to the non-reduced region by a primal Schur complement

Solution for arbitrary parameter using reduced model





$$\left(\tilde{\nu}_{\text{snap}}^{(e)}\right)^2 = \frac{\sum_{\mu \in \mathcal{P}^s} \sum_{t_n \in \mathcal{T}^h} \left\| \underline{\mathbf{U}}_i(t_n, \mu) - \sum_{j=1}^{n_c^{(e)}} \left(\tilde{\mathbf{C}}_{i,j}^{(e),(\mu)T} \underline{\mathbf{U}}_i(t_n, \mu) \right) \tilde{\mathbf{C}}_{i,j}^{(e),(\mu)} \right\|_2^2}{\sum_{t_n \in \mathcal{T}^h} \sum_{\mu \in \mathcal{P}^s} \|\underline{\mathbf{U}}_i(t_n, \mu)\|_2^2}$$

- Reduced subspaces are independent and we assume a snapshot is *a priori* available
 - ▶ (1) Dimension of the local space for each subdomain?
 - ▶ (2) Is a given subdomain is reducible?
- (1) and (2) will be treated by cross-validation (e.g. W. J. Krzanowski. Cross-validation in principal component analysis. Biometrics, 43(3):575-584, 1987.)
 - ▶ **Training set:** snapshot
 - ▶ **Validation set:** set of additional finescale solutions
 - ▶ Independent training/validation avoids overfitting
 - ▶ Cross validation **emulates independence**. Error calculated using the local reduced basis obtained by a snapshot POD transform of all the available snapshot solutions except the one corresponding to the value of the summation variable.
- **NOTE:** If the snapshot is not assumed *a priori* then
 - ▶ Assess whether the snapshot contains sufficient information, and generate additional, suitable, data if required
 - ▶ Most analysis (mostly by statisticians) assume the snapshot is known *a priori*. Recent review: Hervé Abdi and Lynne J. Williams. Principal component analysis. Wiley Interdisciplinary Reviews: Computational Statistics, 2(4):433{459, 2010.

System approximation

$$\underline{\underline{\mathbf{C}}}^T \underline{\underline{\mathbf{F}}}_{\text{int}}(\underline{\underline{\mathbf{C}}}\underline{\underline{\alpha}}) + \underline{\underline{\mathbf{C}}}^T \underline{\underline{\mathbf{F}}}_{\text{ext}} = 0$$

EXPENSIVE! REQUIRES
INTEGRATION OVER THE WHOLE
DOMAIN

- Governing equations
- Linearisation (or higher order Taylor) of the non-linear terms in the set of equations
 - Reduced linear operators computed “offline” once and for all
 - Reused “online” in the Newton solver
 - Usability of such techniques is “local” along the trajectory of the reduced state variables

$$\underline{\underline{\mathbf{F}}}_{\text{int}}(\underline{\underline{\mathbf{C}}}\underline{\underline{\alpha}}(t_n, \mu)) = \sum_{i=1}^{n_d} \underline{\underline{\mathbf{D}}}_i \beta_i(t_n, \mu) = \underline{\underline{\mathbf{D}}}\underline{\underline{\beta}}(t_n, \mu) \quad \underline{\underline{\beta}}(t_n, \mu) = \underset{\underline{\underline{\beta}}^*}{\operatorname{argmin}} \|\underline{\underline{\mathbf{D}}}\underline{\underline{\beta}}^*(t_n, \mu) - \underline{\underline{\mathbf{F}}}_{\text{int}}(\underline{\underline{\mathbf{C}}}\underline{\underline{\alpha}}(t_n, \mu))\|_{\underline{\underline{\mathbf{P}}}}$$

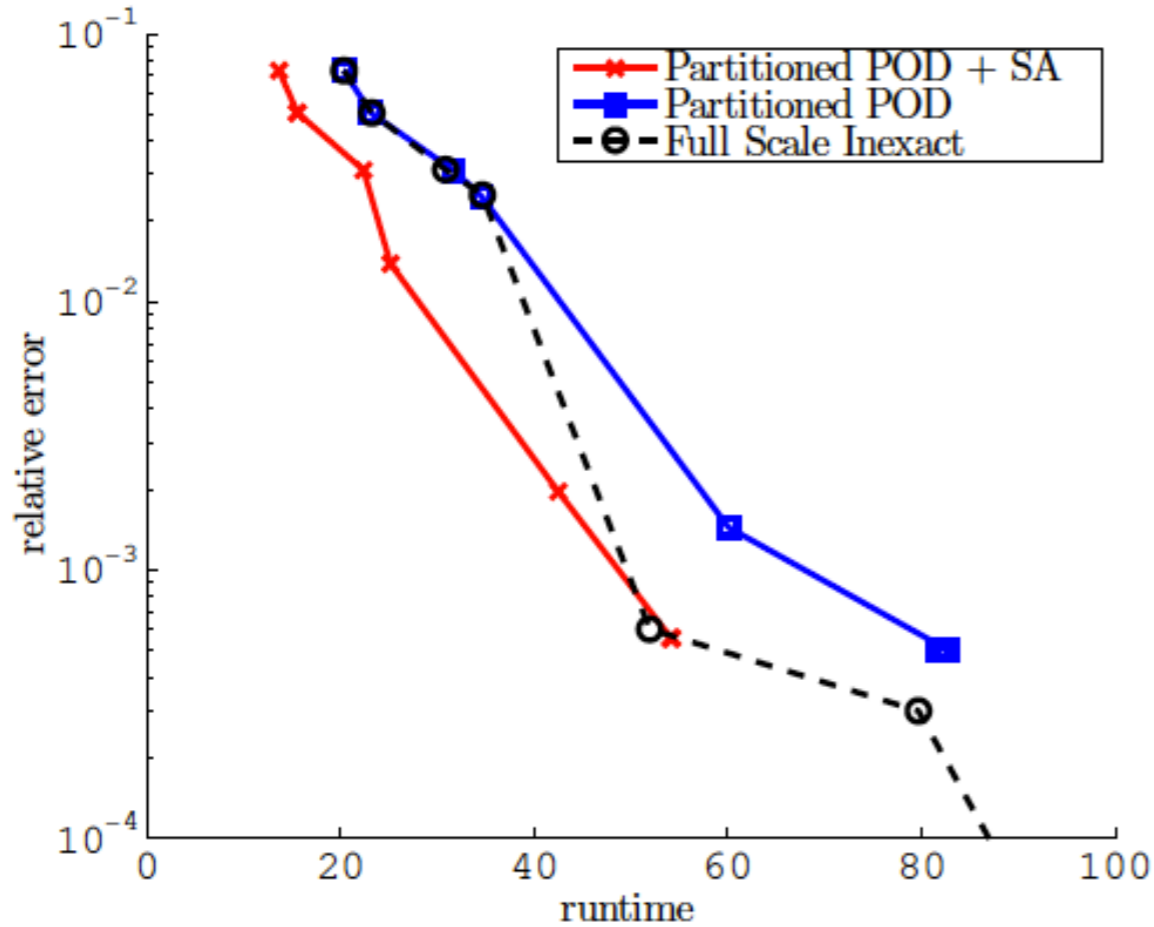
$$\underline{\underline{\mathbf{D}}} \left(\underline{\underline{\mathbf{D}}}^T \underline{\underline{\mathbf{P}}} \underline{\underline{\mathbf{D}}} \right)^{-1} \underline{\underline{\mathbf{D}}}^T \underline{\underline{\mathbf{P}}} \underline{\underline{\mathbf{F}}}_{\text{int}}(\underline{\underline{\mathbf{C}}}\underline{\underline{\alpha}}) + \underline{\underline{\mathbf{F}}}_{\text{ext}} = \underline{\underline{\mathbf{R}}}(\underline{\underline{\alpha}})$$

- “Collocation” methods look for a solution which is optimal with respect to a few equations of the system (least squares or Galerkin frameworks can be used).

Performance: load angle 40 | 27 - 121 nodes

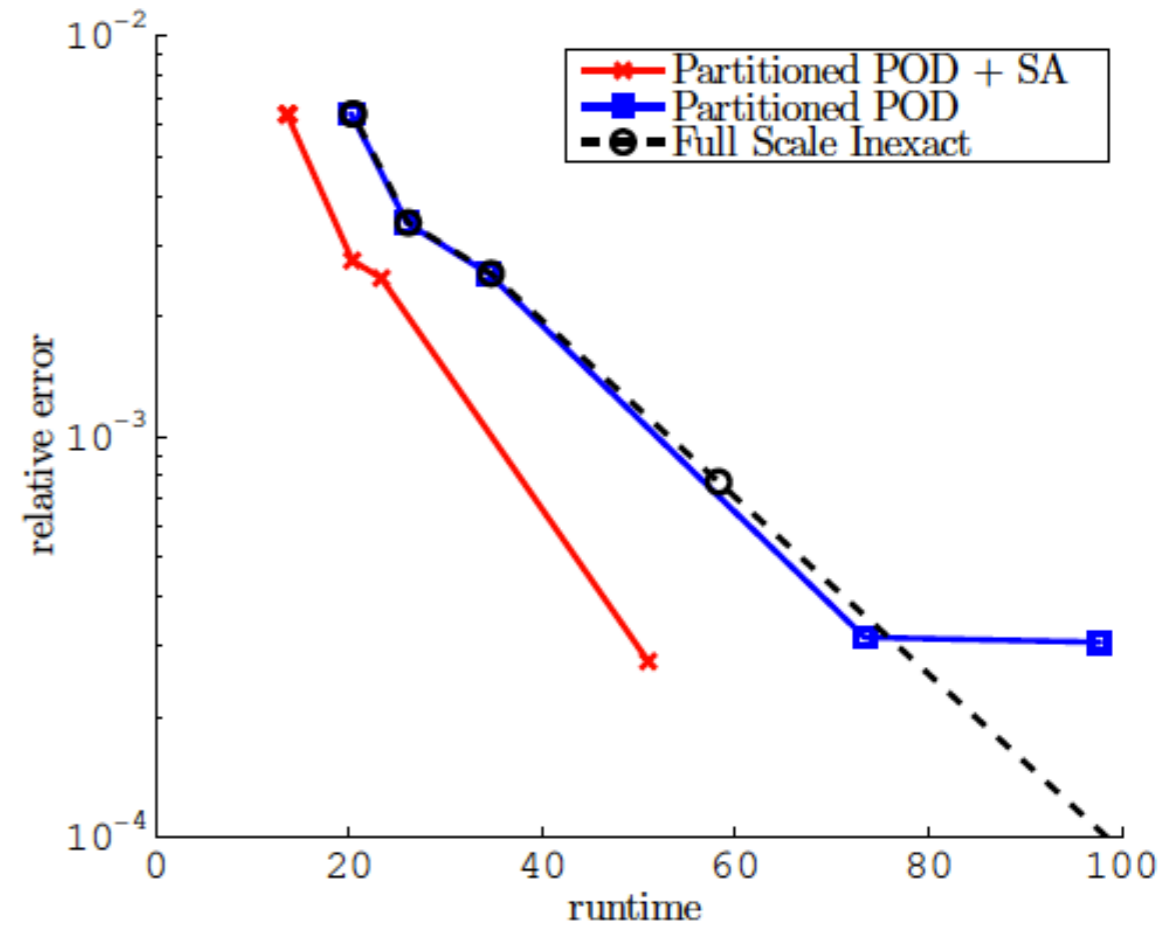
$$\nu^{\text{app},(\mu)}(\underline{\mathbf{U}}^{\text{app}})^2 = \frac{\sum_{t_n \in \mathcal{T}^h} \|\underline{\mathbf{U}}^{\text{app}}(t_n, \mu) - \underline{\mathbf{U}}^{\text{ex}}(t_n, \mu)\|_2^2}{\sum_{t_n \in \mathcal{T}^h} \|\underline{\mathbf{U}}^{\text{ex}}(t_n, \mu)\|_2^2}$$

40°



(a) Relative error for the different models using 121 nodes per subdomain

27°

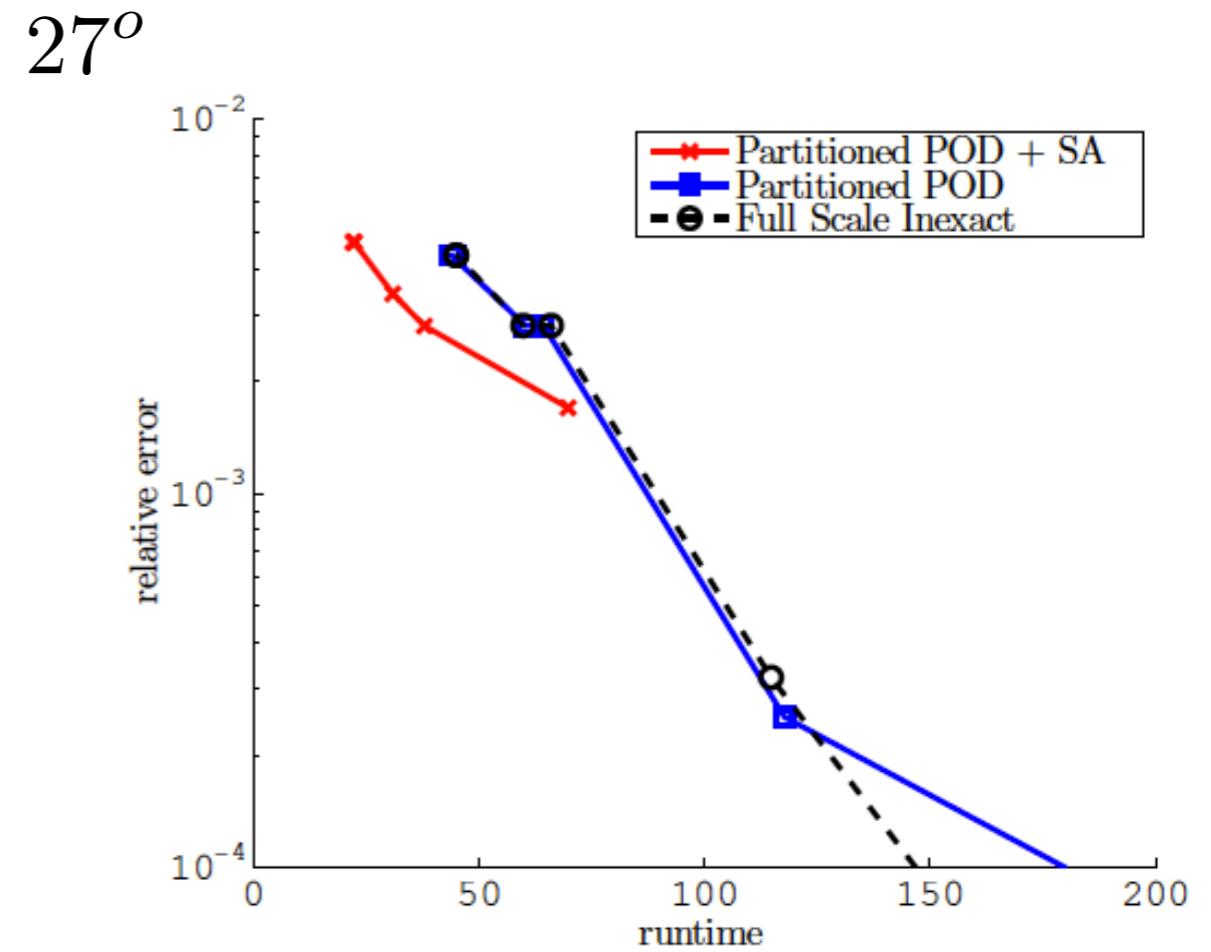
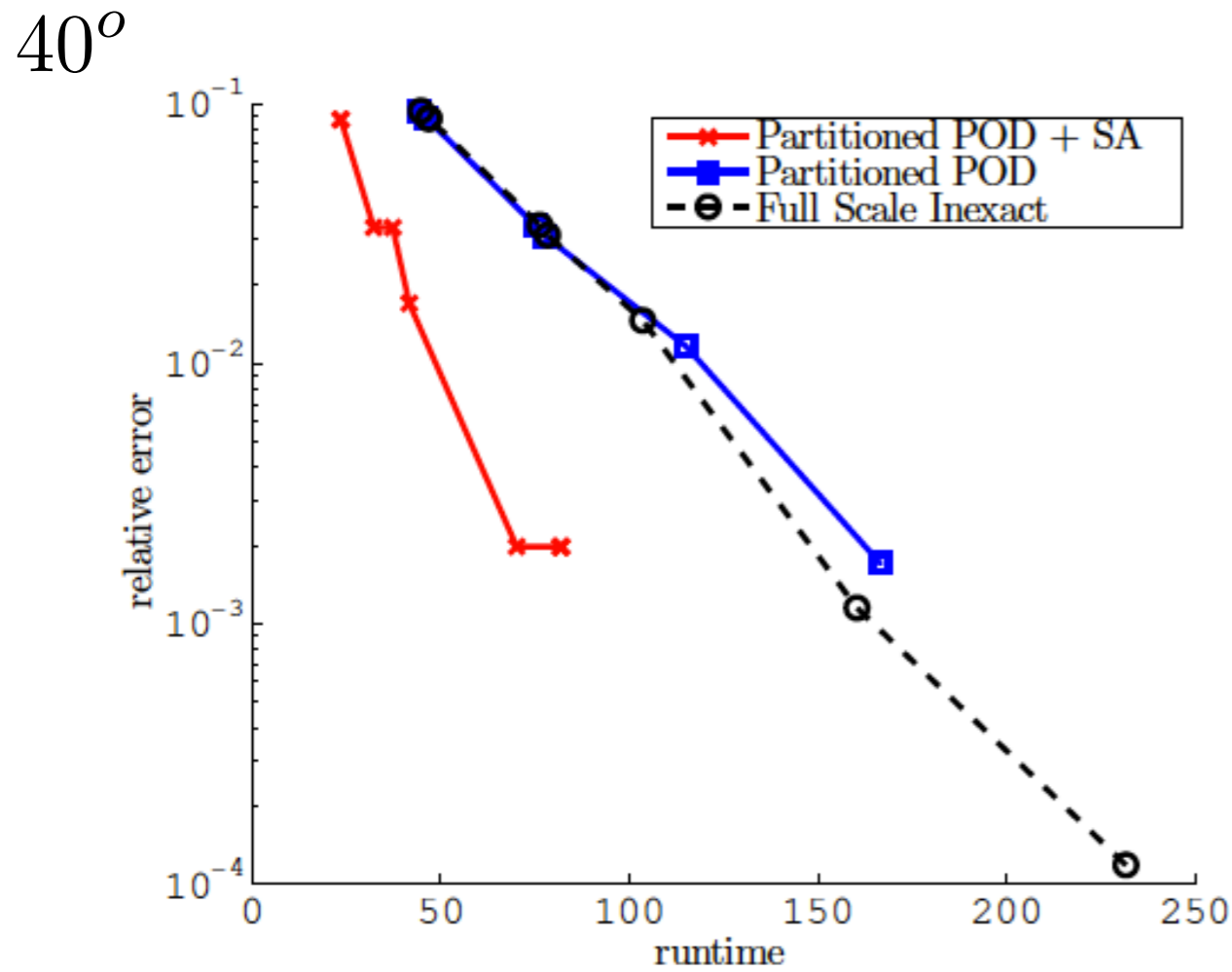


(a) Relative error for the different models using 121 nodes per subdomain

Performance: load angle 40 | 27 - 256 nodes

- Relative error

$$\nu^{\text{app},(\mu)}(\underline{\mathbf{U}}^{\text{app}})^2 = \frac{\sum_{t_n \in \mathcal{T}^h} \|\underline{\mathbf{U}}^{\text{app}}(t_n, \mu) - \underline{\mathbf{U}}^{\text{ex}}(t_n, \mu)\|_2^2}{\sum_{t_n \in \mathcal{T}^h} \|\underline{\mathbf{U}}^{\text{ex}}(t_n, \mu)\|_2^2}$$



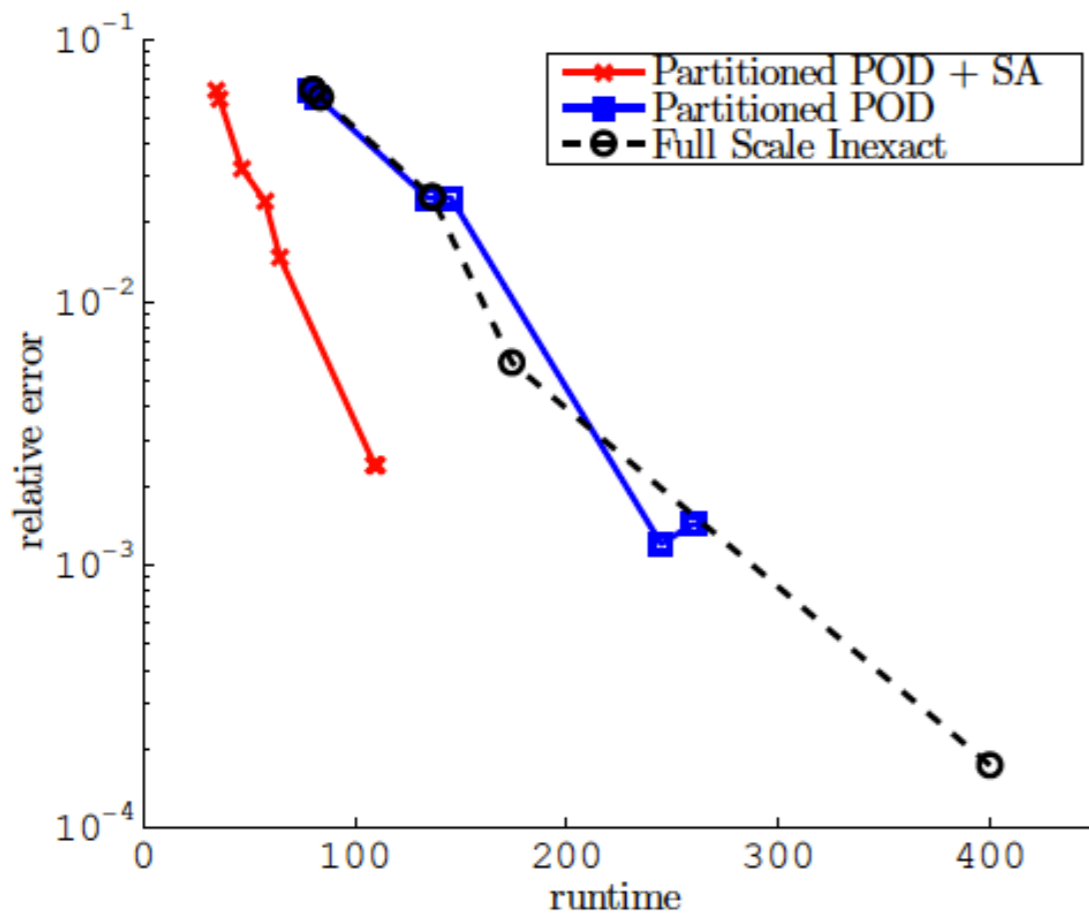
(b) Relative error for the different models using 256 nodes per subdomain

(b) Relative error for the different models using 256 nodes per subdomain

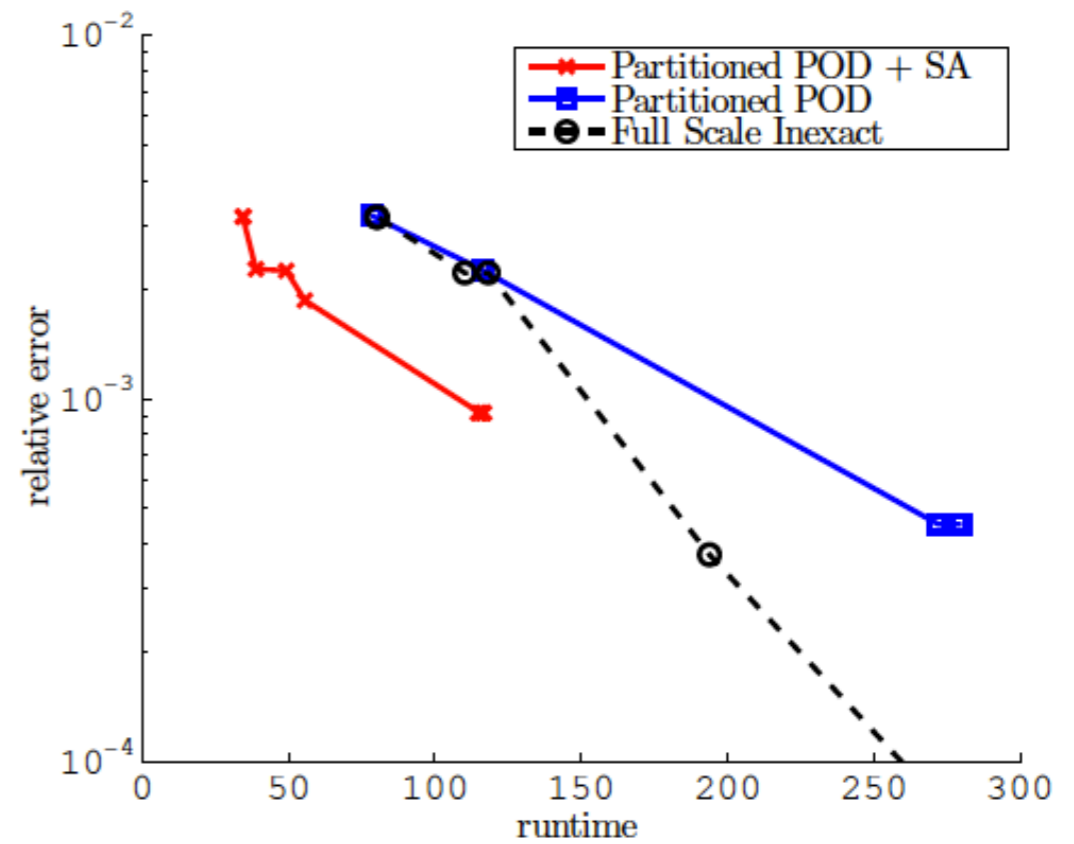
Performance: load angle 40 | 27 - 441 nodes

$$\nu^{\text{app},(\mu)}(\underline{\mathbf{U}}^{\text{app}})^2 = \frac{\sum_{t_n \in \mathcal{T}^h} \|\underline{\mathbf{U}}^{\text{app}}(t_n, \mu) - \underline{\mathbf{U}}^{\text{ex}}(t_n, \mu)\|_2^2}{\sum_{t_n \in \mathcal{T}^h} \|\underline{\mathbf{U}}^{\text{ex}}(t_n, \mu)\|_2^2}$$

40°



27°



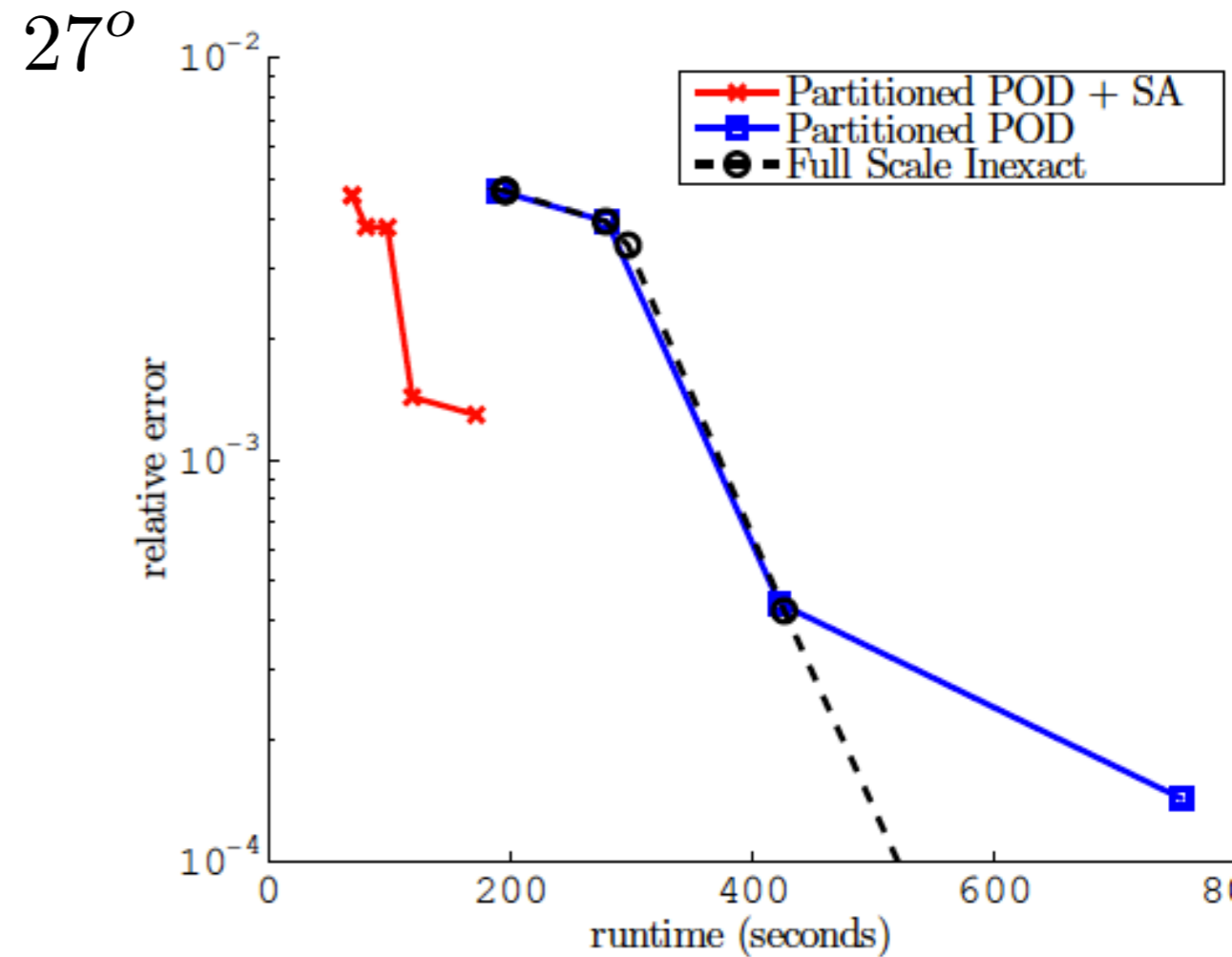
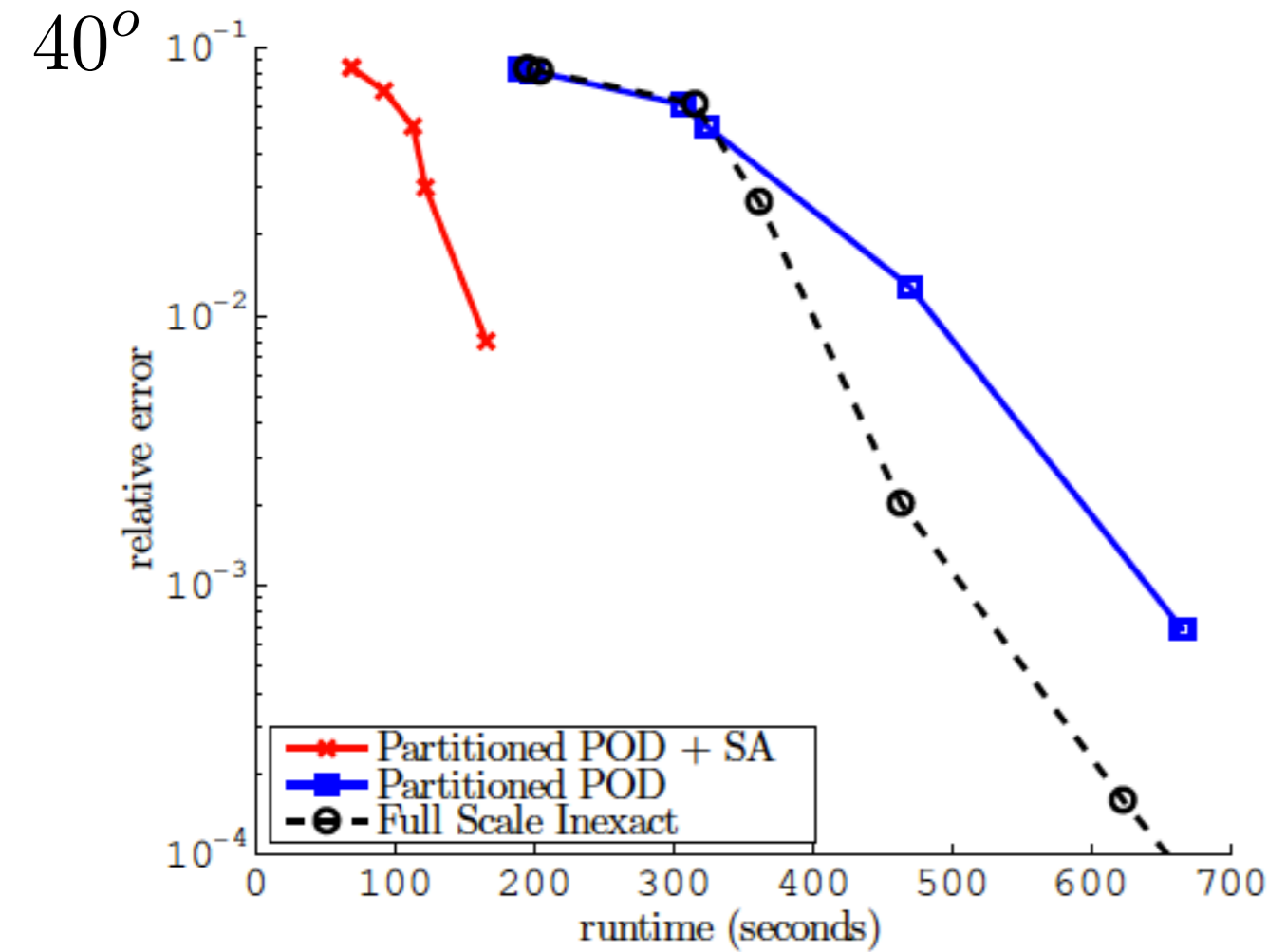
(c) Relative error for the different models using 441 nodes per subdomain

(c) Relative error for the different models using 441 nodes per subdomain

Performance: load angle 40 | 27 - 961 nodes

- Relative error

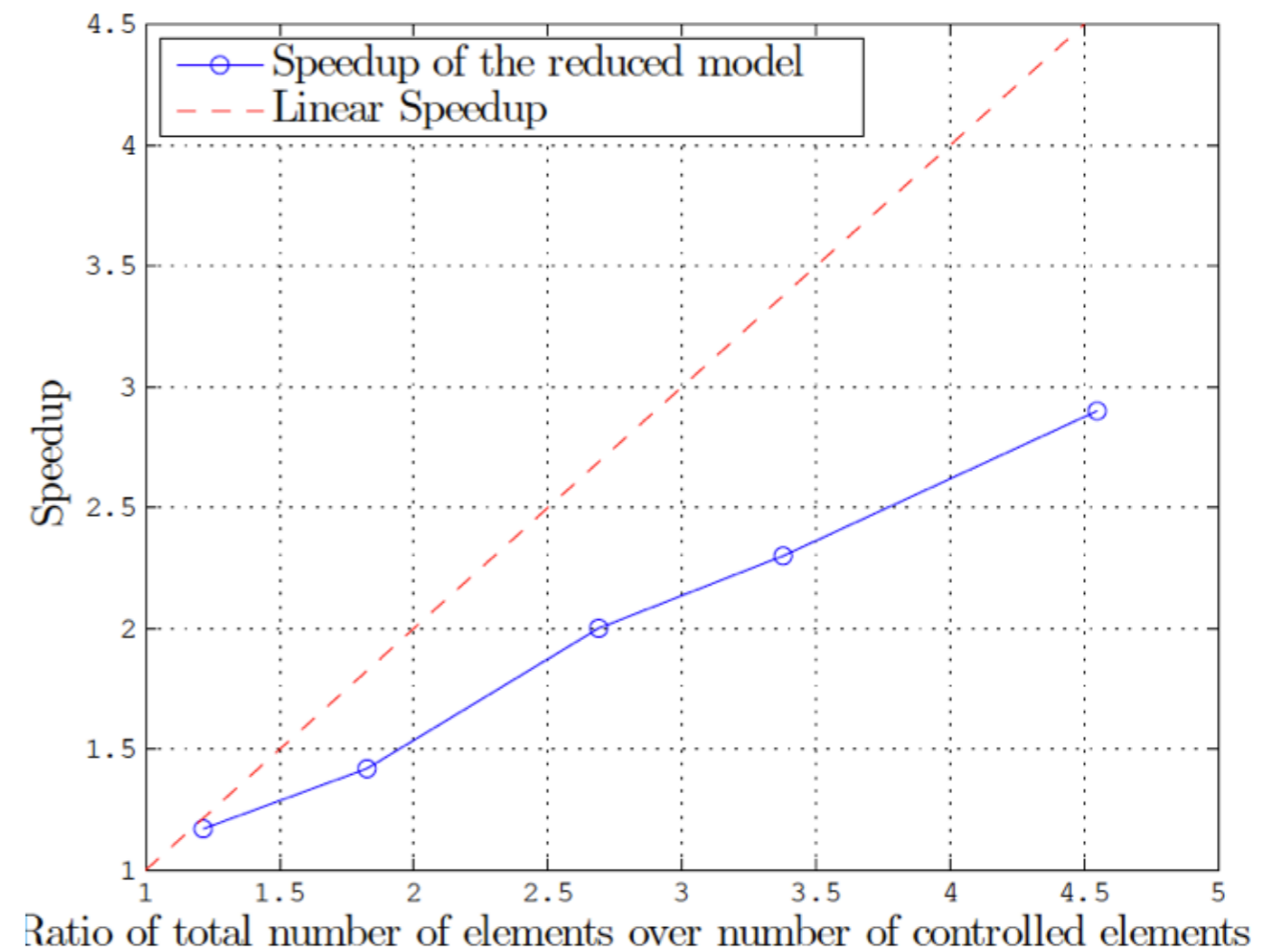
$$\nu^{\text{app},(\mu)}(\underline{\mathbf{U}}^{\text{app}})^2 = \frac{\sum_{t_n \in \mathcal{T}^h} \|\underline{\mathbf{U}}^{\text{app}}(t_n, \mu) - \underline{\mathbf{U}}^{\text{ex}}(t_n, \mu)\|_2^2}{\sum_{t_n \in \mathcal{T}^h} \|\underline{\mathbf{U}}^{\text{ex}}(t_n, \mu)\|_2^2}$$



(d) Relative error for the different models using 961 nodes per subdomain

(d) Relative error for the different models using 961 nodes per subdomain

Role of system approximation



Conclusions and perspectives

- Domain coupling using the primal Schur-complement domain decomposition method.
- Local subproblems have been reduced by projection in low-dimensional subspaces obtained by the snapshot POD.
- This approach permits to flexibly reduce the computational cost associated with highly nonlinear problems. In particular:
 - the **local reduced spaces are generated independently**, and have independent dimensions, which allows us to focus the numerical effort where it is most needed.
 - subdomains that are close to highly damaged zones need a richer model to account for the effect of topological changes. The local **POD transforms automatically generate local reduced spaces of larger dimension in these zones**.
 - the domain decomposition framework enables us to **switch from reduced local solvers to full local solvers** in a transparent manner. This is particularly useful for the subdomains that contain process zones, as a solution obtained by projection would be more expensive than a direct solution for a desirable accuracy.
 - the transition between ``offline" and ``online" computations becomes flexible. The **reduced models can be used in the zones where the local reduced spaces converge quickly** when enriching the snapshot space, while still computing snapshots and refining the reduced models via a direct local solver in the remaining subdomains.

Perspectives (1/2)

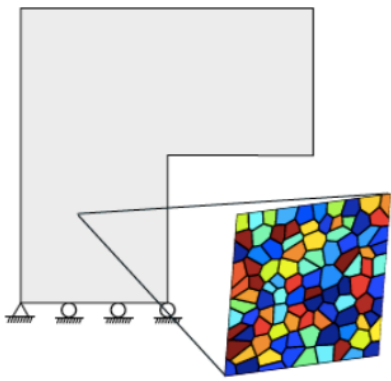
- Further work related to domain decomposition
 - **load balancing** mismatch would occur when using such a strategy in parallel. CPUs which support domains that are not reduced, or domains for which the corresponding subproblems need to be projected in a space of relatively high dimension, would require to perform more operations. The domain partitioning itself should be performed jointly with the model reduction in order to distribute the load evenly.
 - **the interface problem itself was not reduced** here, to guarantee the interface kinematic compatibility.
 - Suboptimal reduced order model. Would generate expensive communications in parallel
 - A reduction of the interface problem using the POD can be done but is neither elegant nor easy
 - Dual Schur-complement domain decomposition method would allow the kinematic approximation of the subproblems to include the interface. However, this would only deflect the difficulty to the necessary reduction of the interface Lagrange multiplier space. This issue is our current direction of research.

Perspectives (2)

- A Quarteroni, G Rozza, and A Manzoni. Certified reduced basis approximation for parametrized partial differential equations and applications. *Journal of Mathematics in Industry*, 1(3):1–44, 2011.

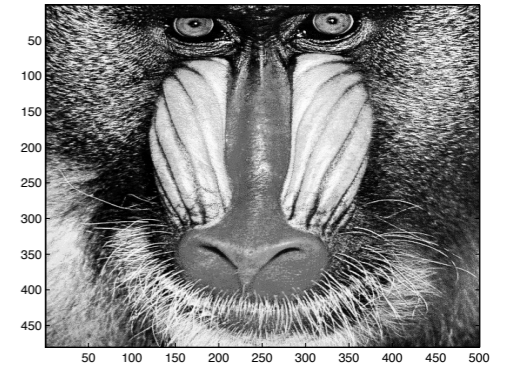
RESEARCH AREA

- We have used a cross validation technique. OK if sufficiently fine snapshot space.
- We cannot find zones of “non-smoothness” in the parameter space automatically.
- We used global Euclidian norms to evaluate the error. Needs refinement to tackle goals and quantities of interest.
- Use model reduction to identify “fracture zones” / localisation bands, etc.



Challenges

Reduce the problem size
Preserve essential features



Reduce computational expense - Control the error

**Physics based model reduction
a.k.a. Multiscale Methods**

**Algebraic based model
reduction a.k.a. Machine
Learning**

**Representative volume
elements do not exist after the
onset of fracture**

**The problem is not reducible in
the fracture process zone**

**Adaptive Multi-scale
Methods: hierarchical - semi-
concurrent - concurrent**

**Adaptive Domain
Decomposition Proper
Orthogonal Decomposition**

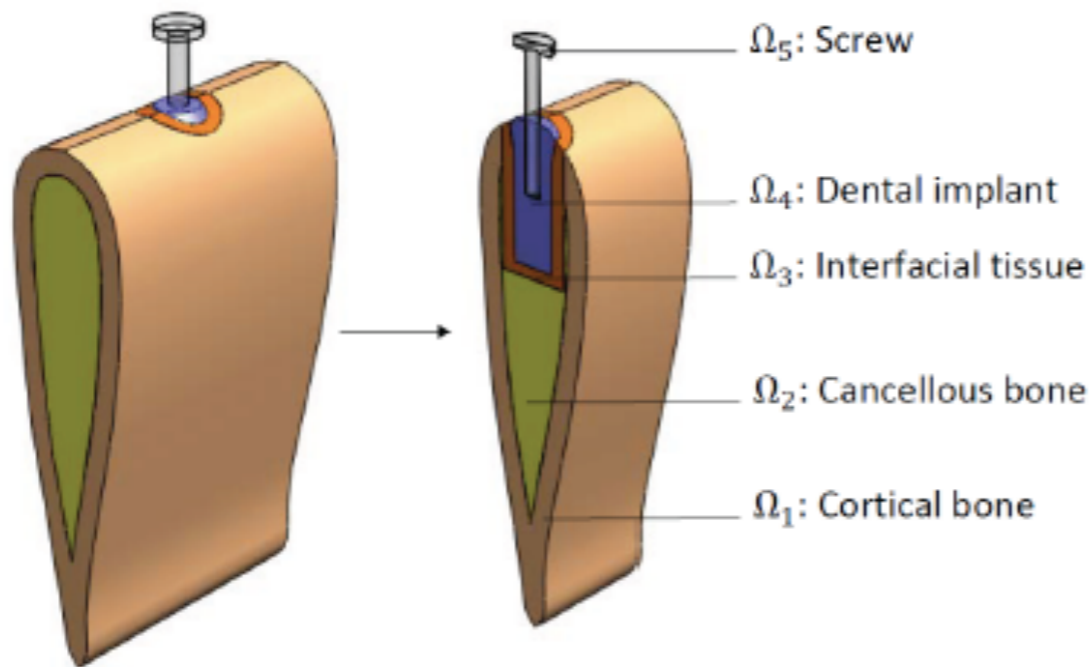
Open problems

- how to define the reduced area?
- precomputation time (offline)

Model reduction - algebraic

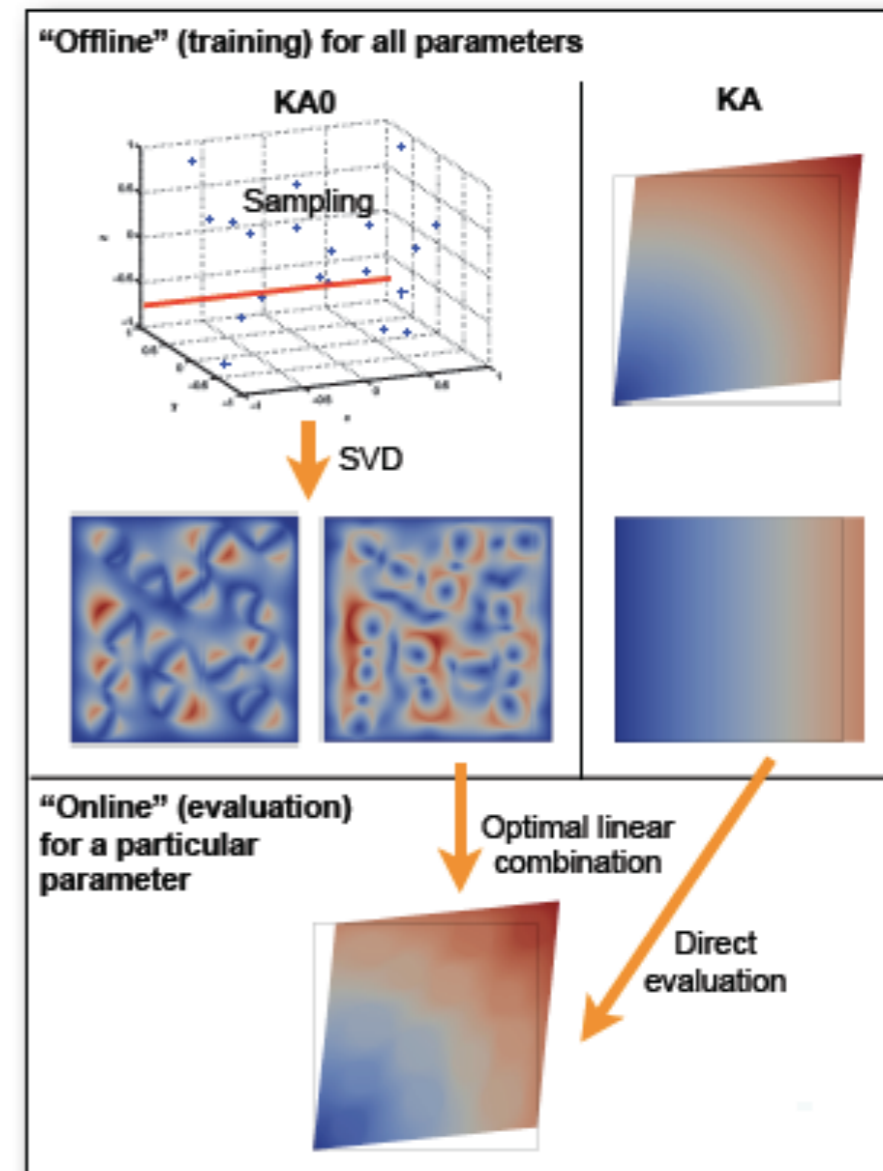
- Multilevel methods to reduce CPU time by orders of magnitude and devise robust, efficient code/model coupling

- Virtual chart with controlled accuracy via ROM for multiscale modelling and real-time optimisation



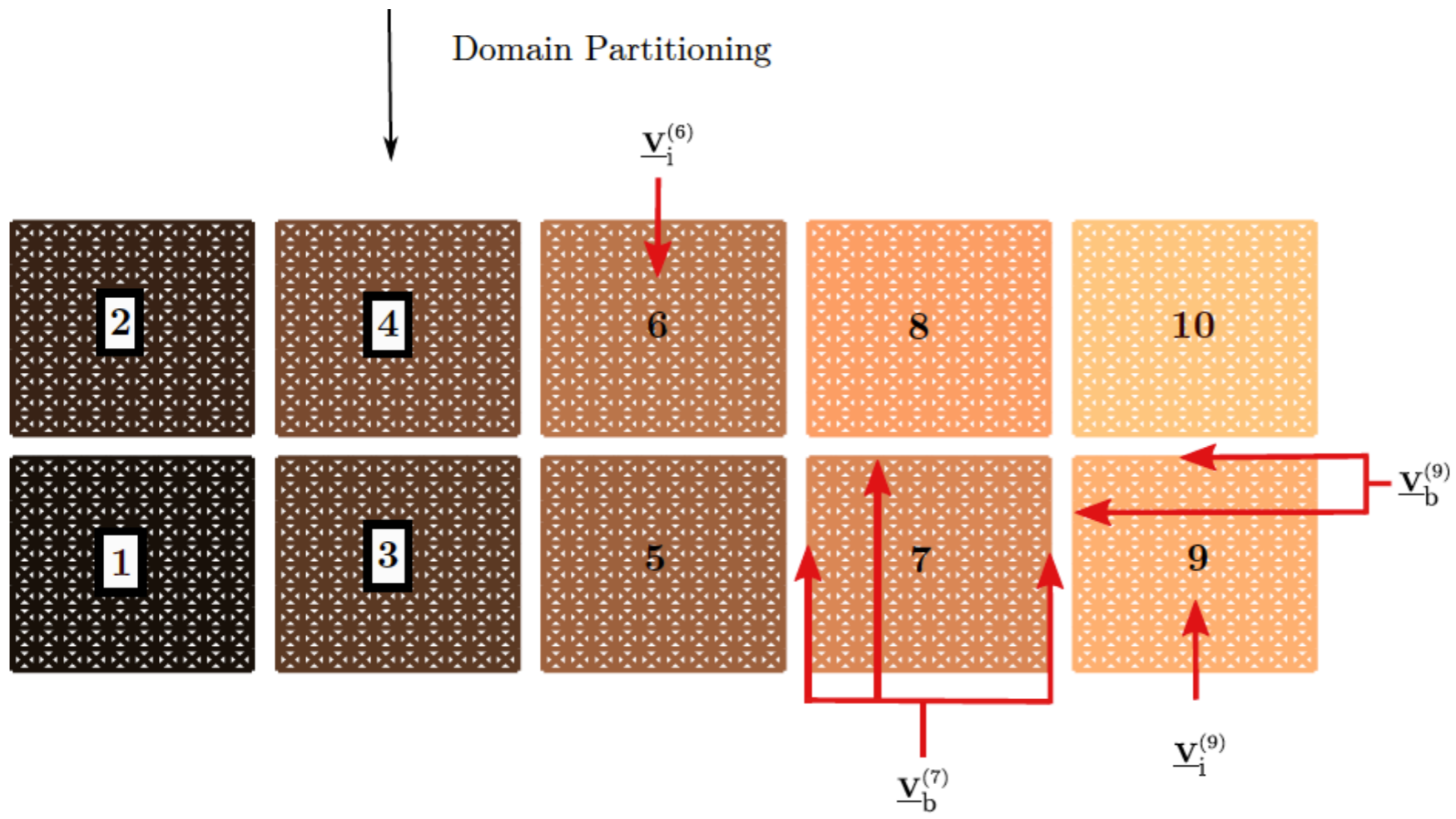
[Hoang et al., 2013]

“offline” / “online” strategy



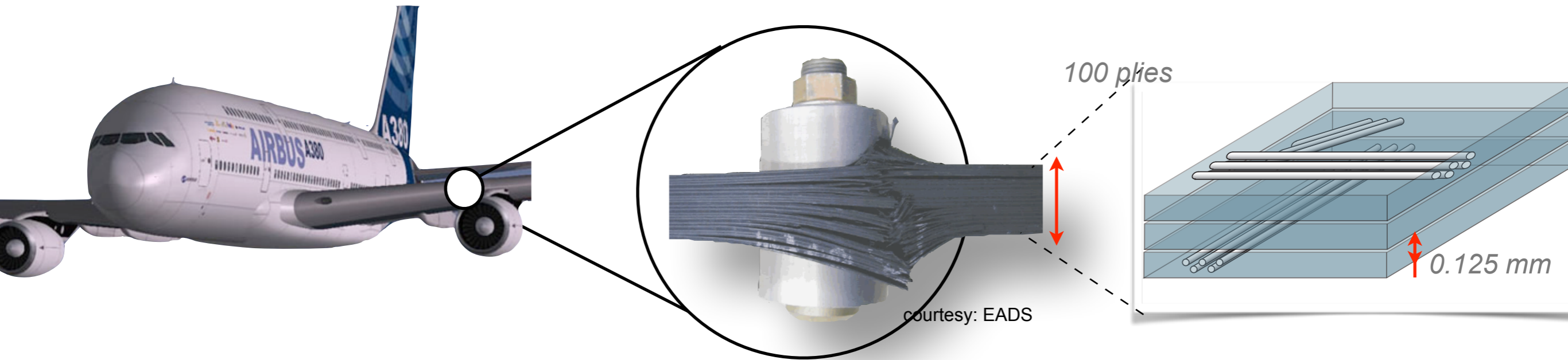
[Kerfriden et al., 2013]

Open problem: algebraic model reduction for non-linear problems with localisation - fracture, moving interfaces



Future?

Material complexity

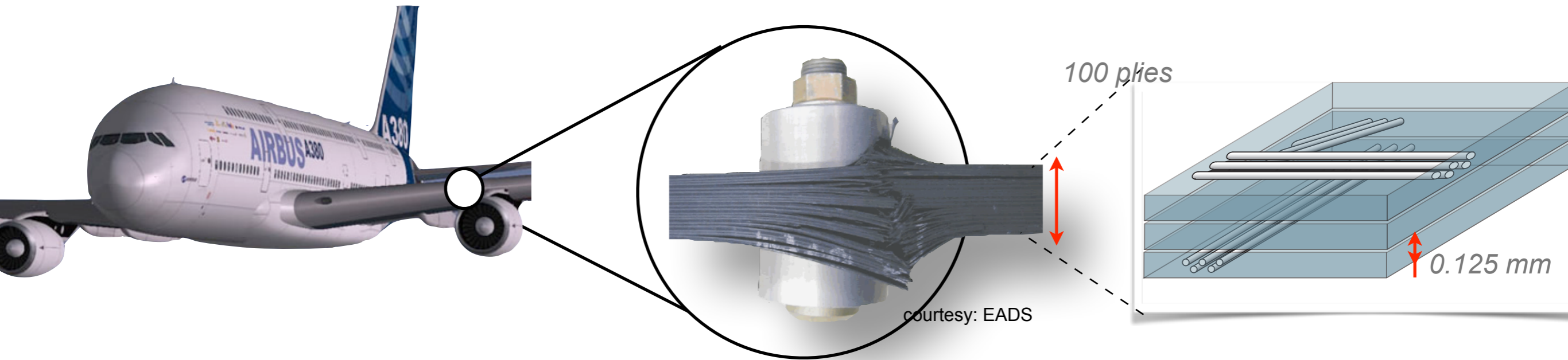


Heterogeneous & multi-functional materials

Can we optimise the material microstructure given macroscopic objective functions

Experiments required to attain sufficient confidence in their behavior are increasingly costly

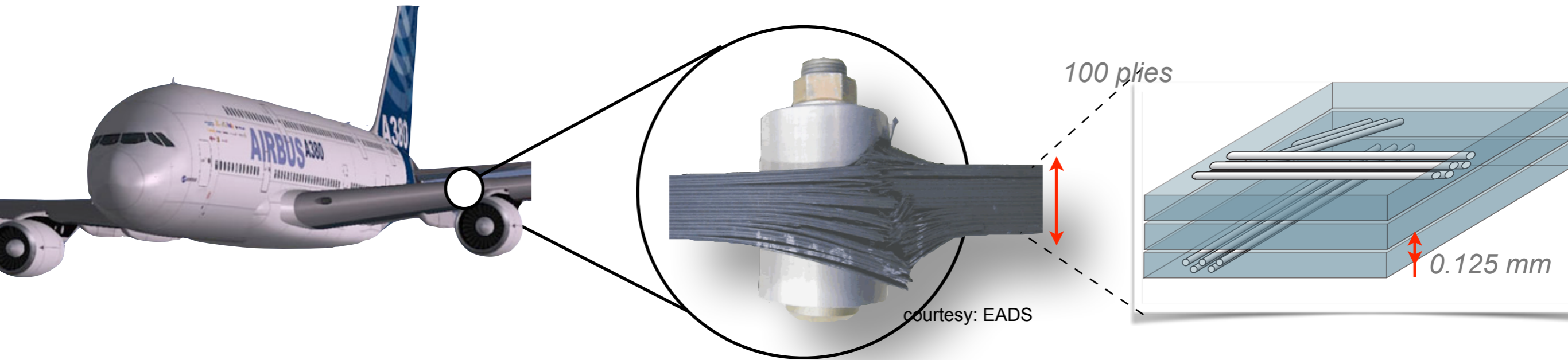
Material complexity



Factor-of-Safety or probabilistic based methods cannot handle unknown unknowns

Lack of similitude between testing (experimental) and operating conditions — also encountered in geophysics, medicine...

Challenges



- Move away from **heuristics** and experience-based engineering
- Develop **fundamental understanding** of physical processes (degradation, ...)

Digital twin concept

Actual aircraft

Digital aircraft model

Life prediction and extension

Situation awareness

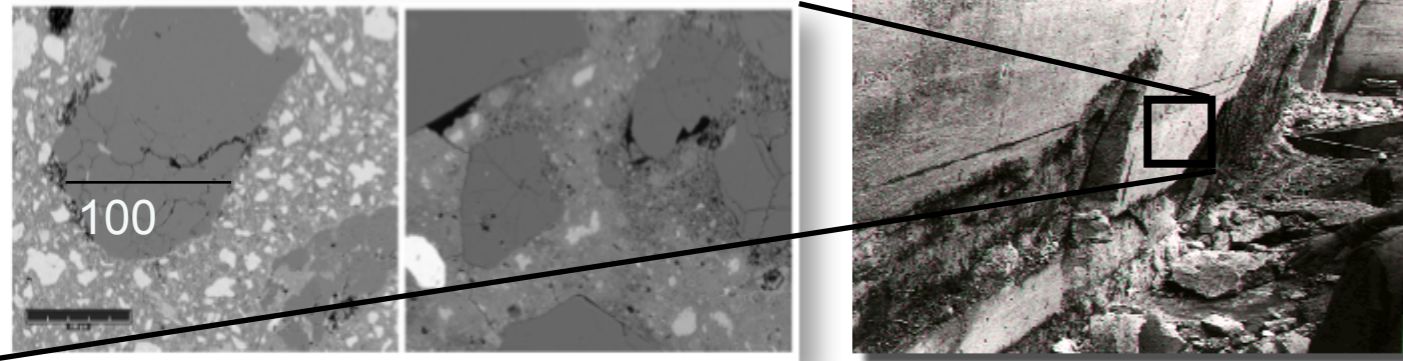
High fidelity modeling and simulation

Certification and design methods

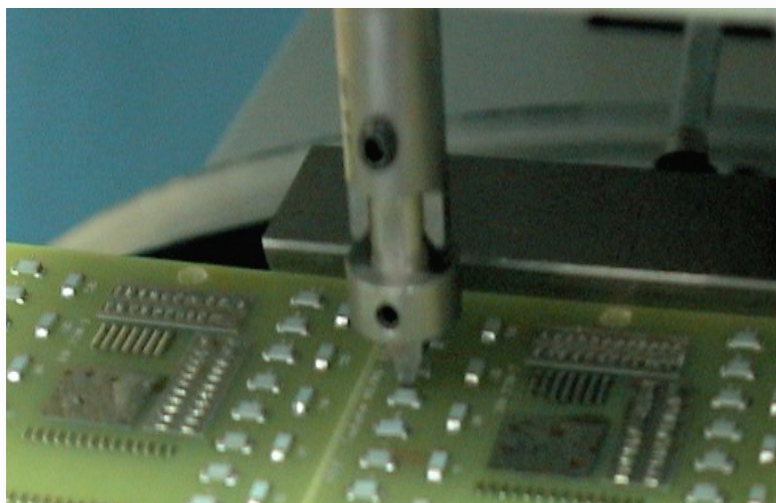
Requires real-time data assimilation, and model update...

Industrial and clinical applications

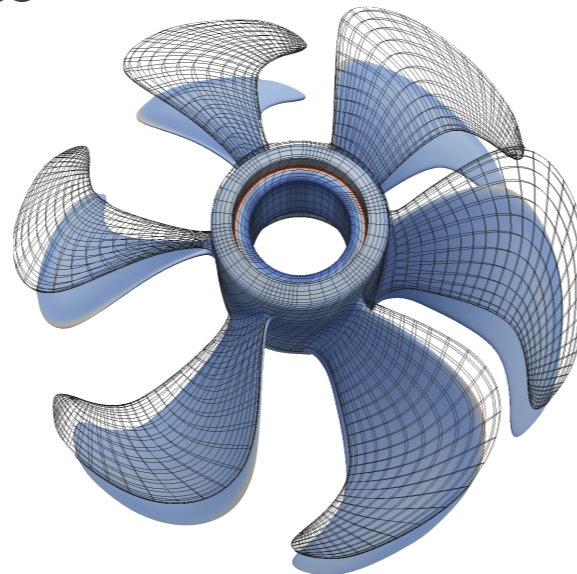
Industrial and clinical applications



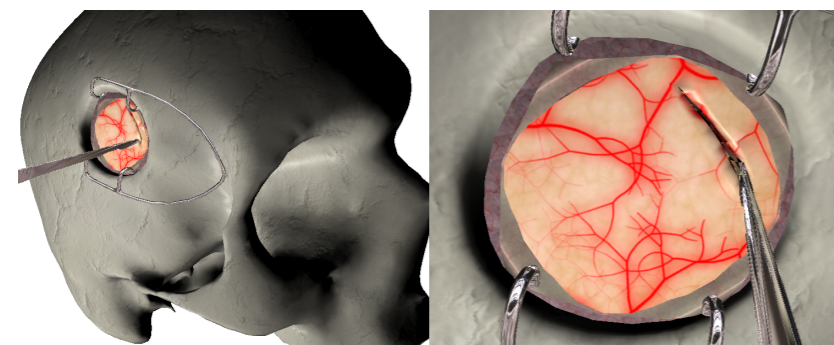
Alkali-silica reaction in concrete



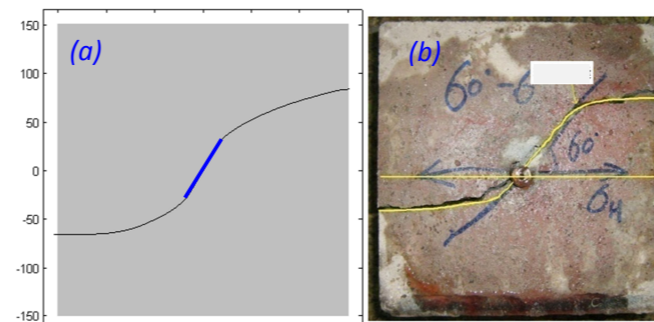
Solder joint durability in the car industry



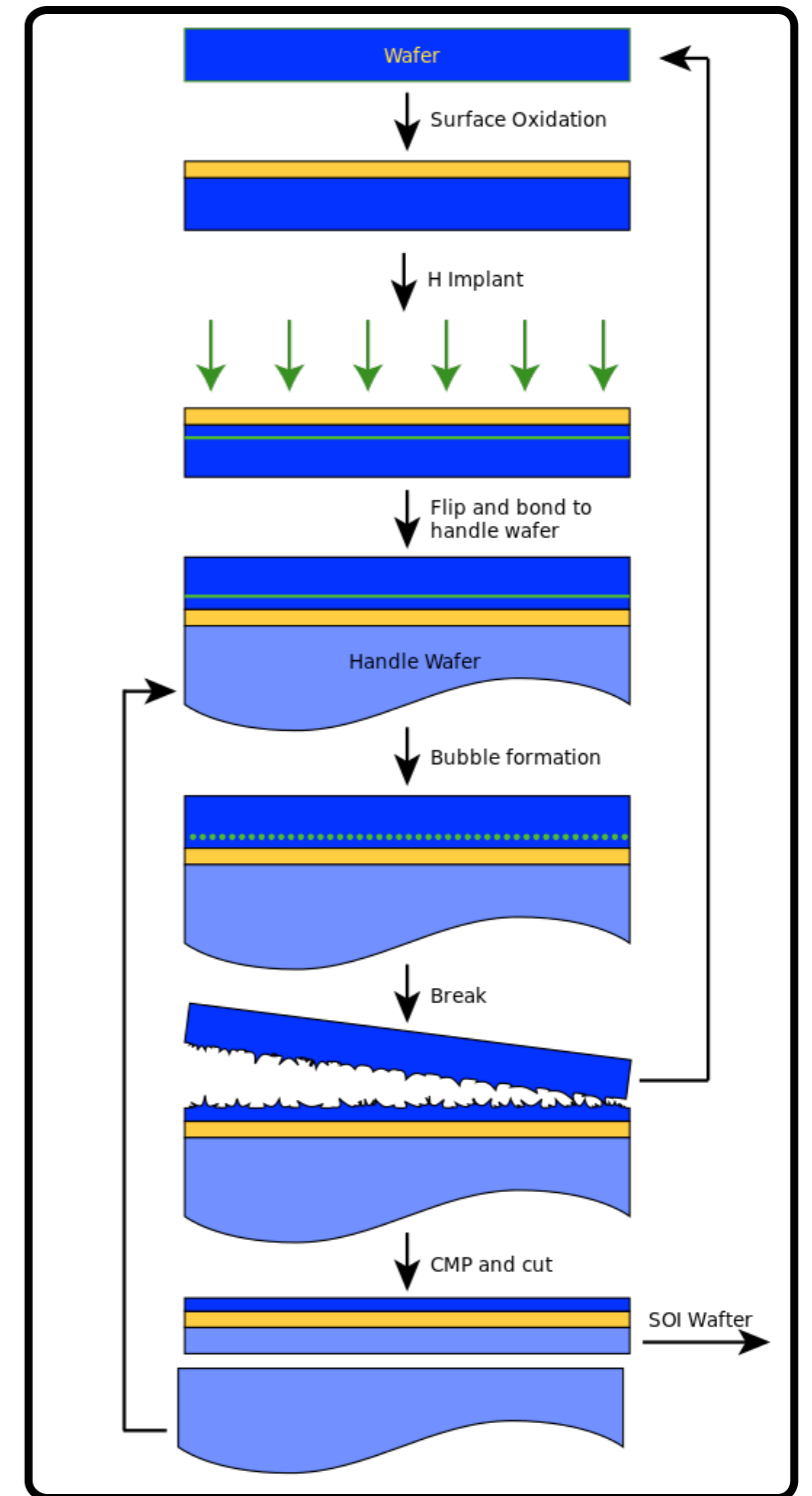
Turbine shape optimisation



Surgical simulation



Hydraulic fracture



Silicon wafer cutting

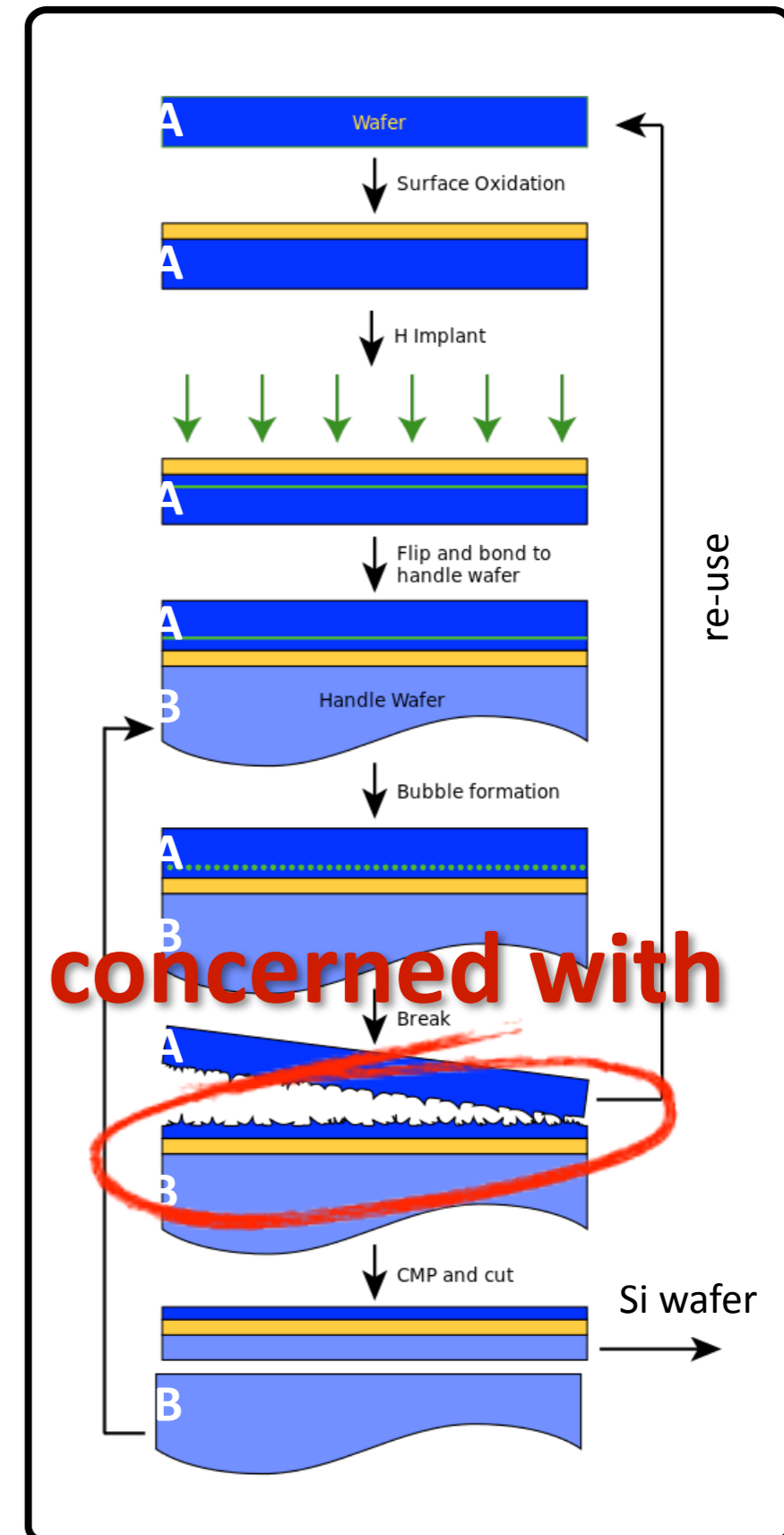
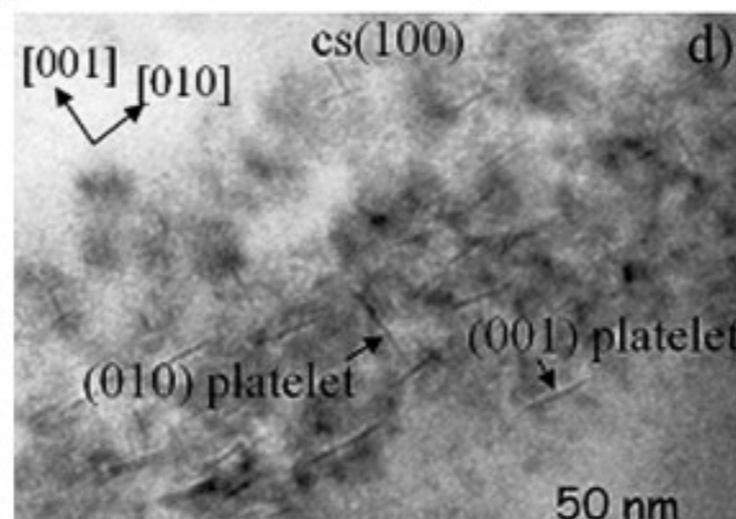
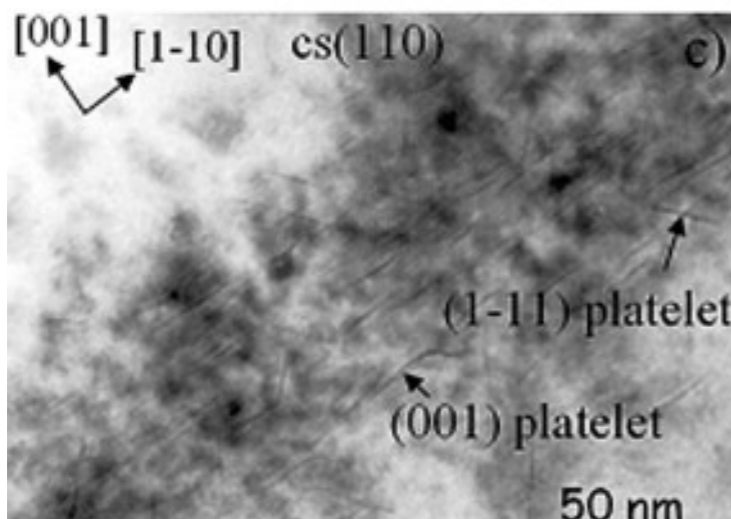


Numerical Modeling of SOI Wafer Splitting



Manufacturing process: *SmartCut*TM

- H⁺ ionization of a thin surface of Si
- Bonding to a handle-wafer (stiffener)
- High temperature thermal annealing
- Nucleation and growth of cavities filled with H₂
- Pressure driven micro crack growth
- Coalescence and post-split fracture roughness

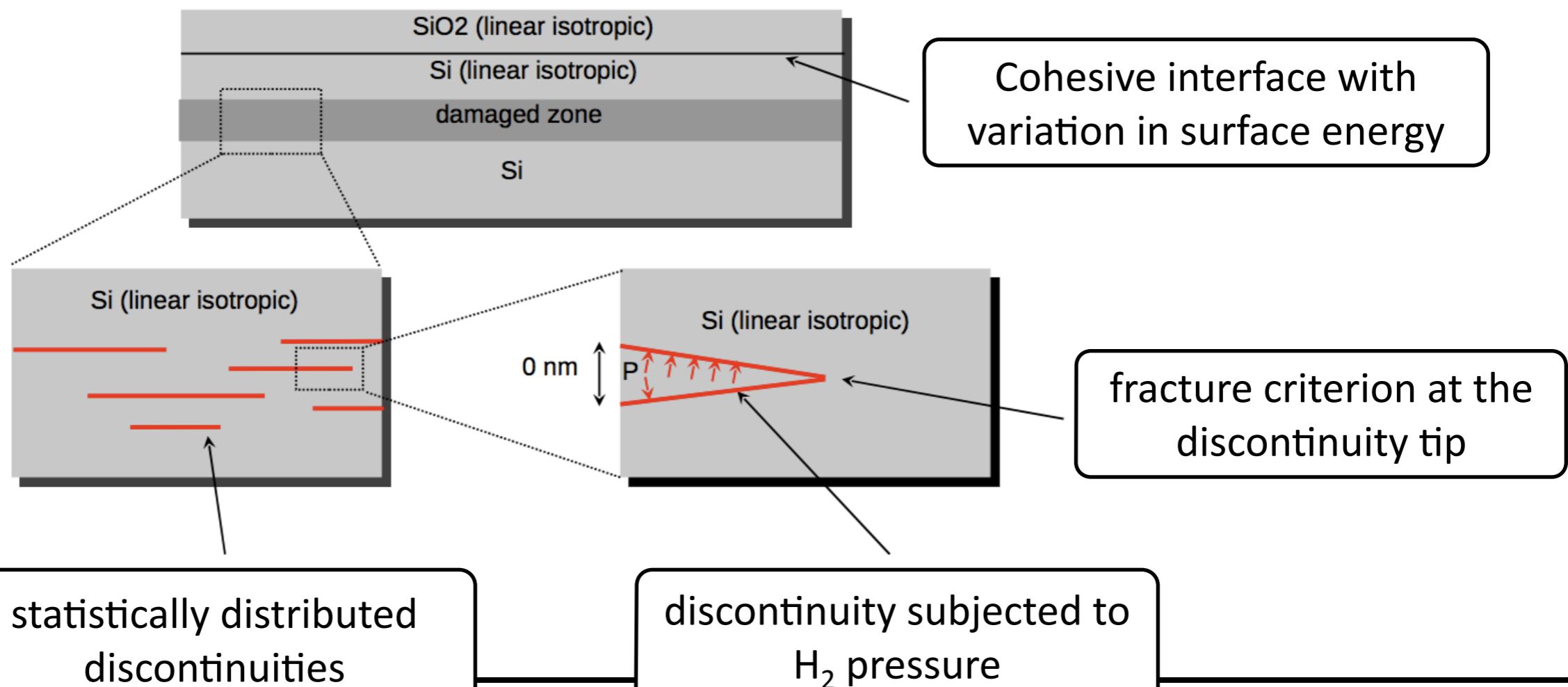


Modeling cavities by zero thickness surfaces

- discontinuities in the displacement field

Linear elastic fracture mechanics (LEFM)

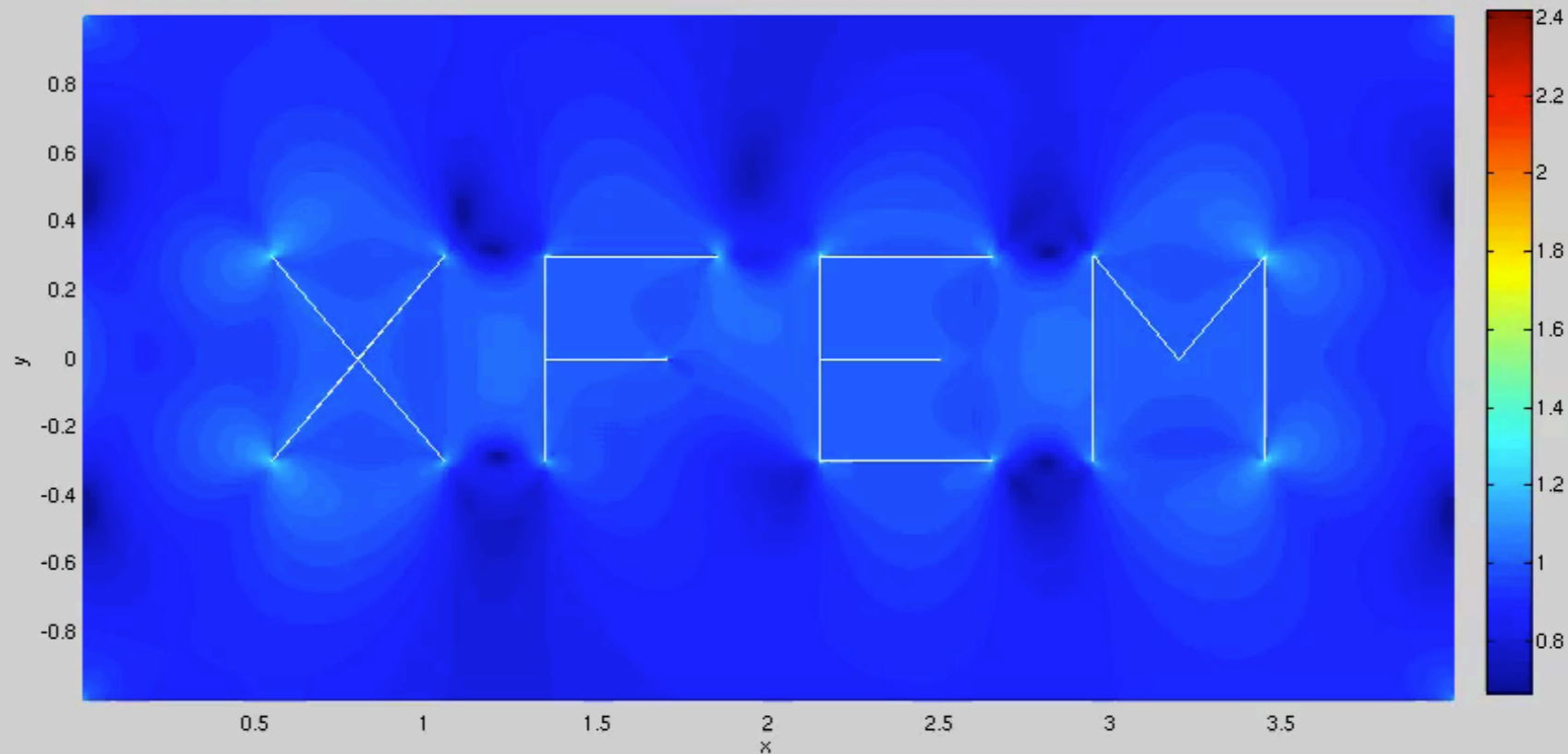
- infinite stress at crack tip, i.e. *singularity*

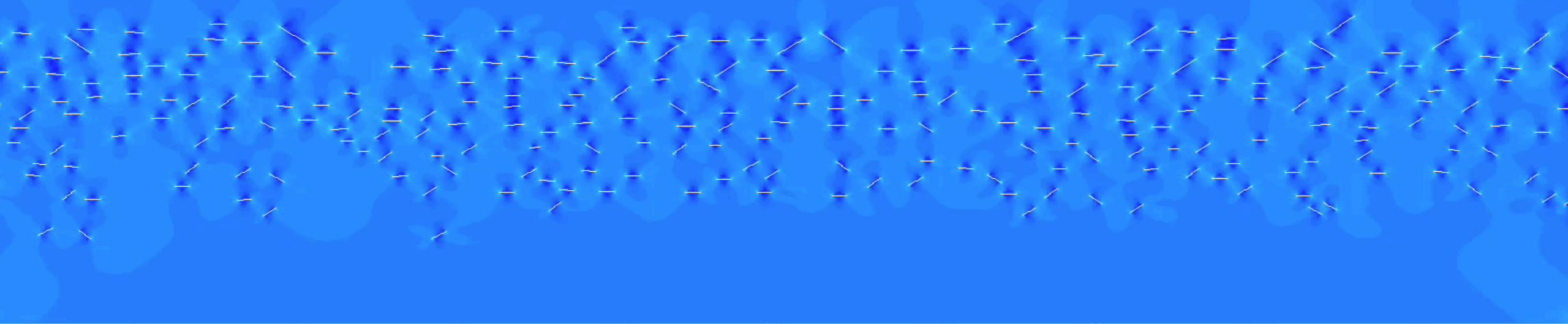


Extended Finite Element Method (XFEM)

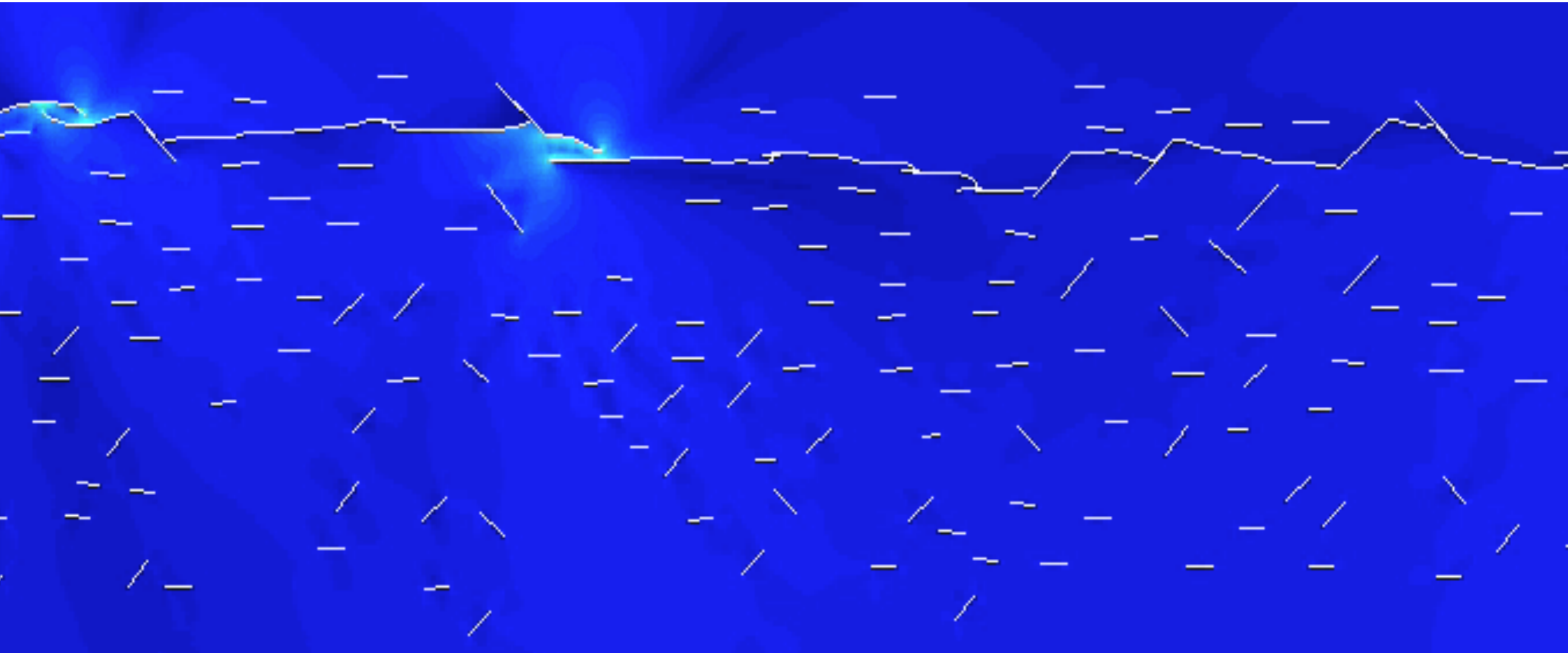
- Introduced by Ted Belytschko (1999) for elastic problems

Fracture of “XFEM” using XFEM





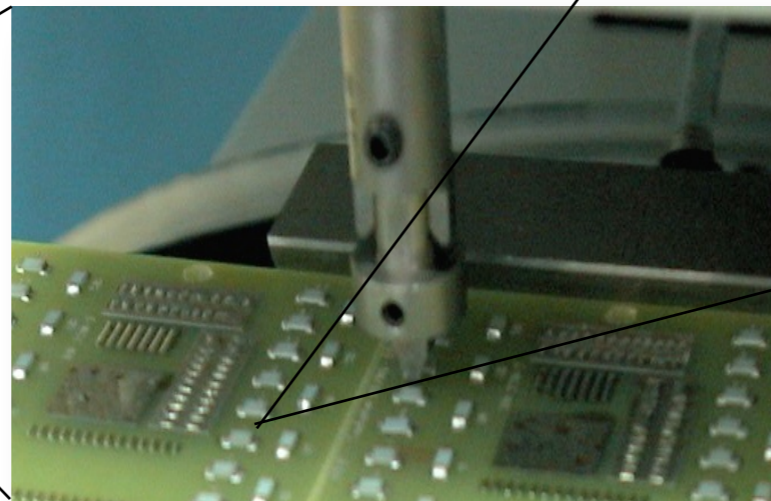
100 200 300 400 500 600 700 800 900 1000
x



Solder joint durability - role of Pb

Challenges

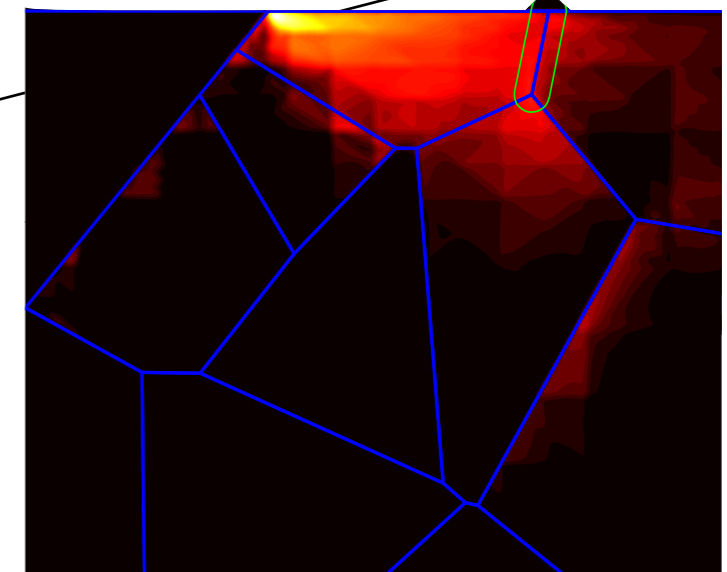
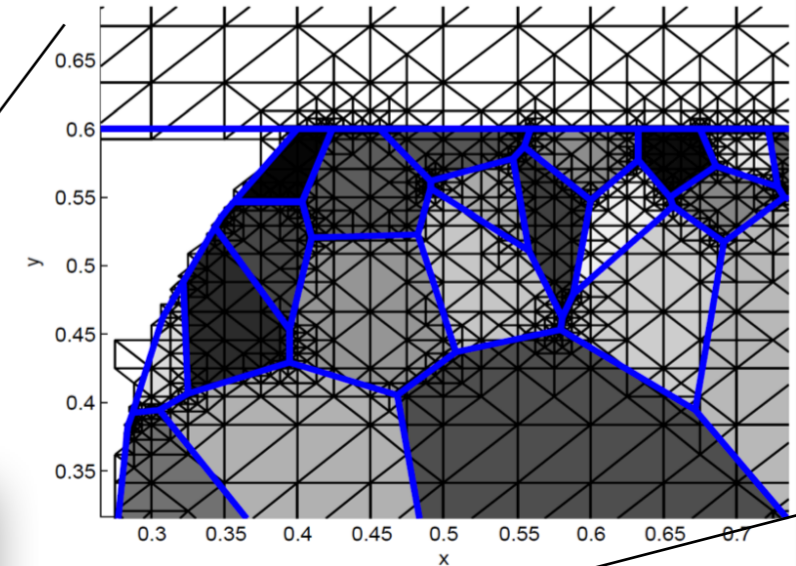
- microstructure/meshing - statistical variability
- robustness -> preconditioning
- maintain accuracy



Advanced
discretisation

Model
reduction

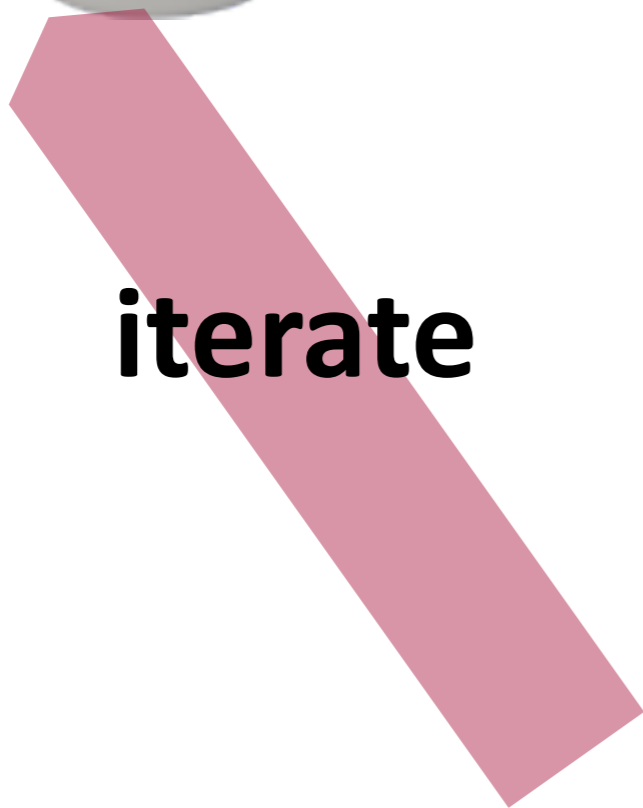
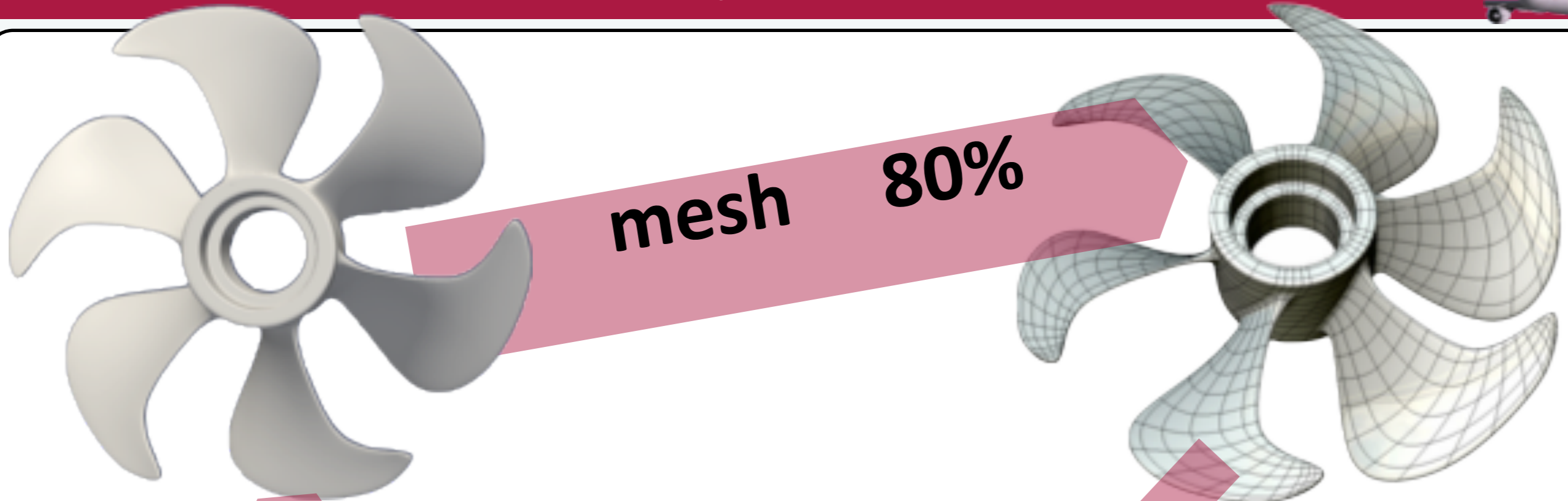
Computational
time?



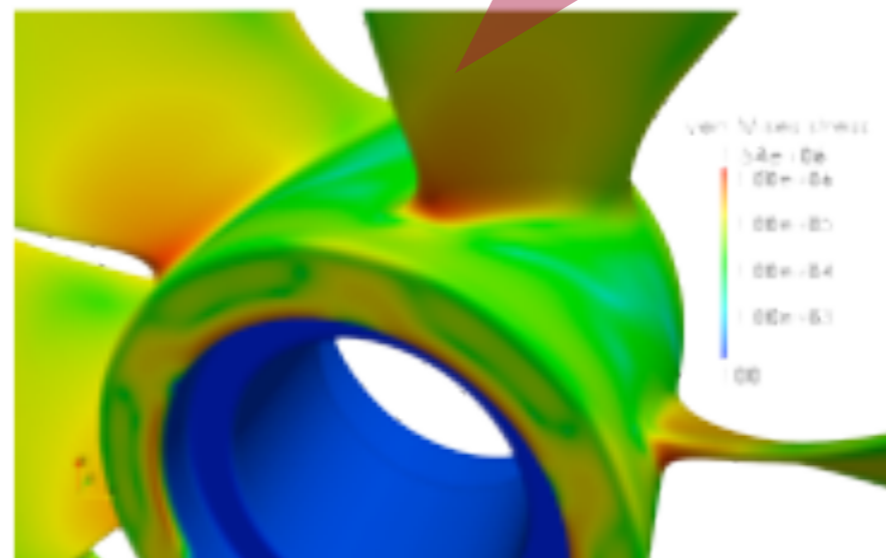
0.1mm

Conclusions : (1) microstructures play a determining role on thermo-mechanical fatigue life; (2) Pb increases the life span (of the solder)

Industrial applications of isogeometric analysis (IGA)



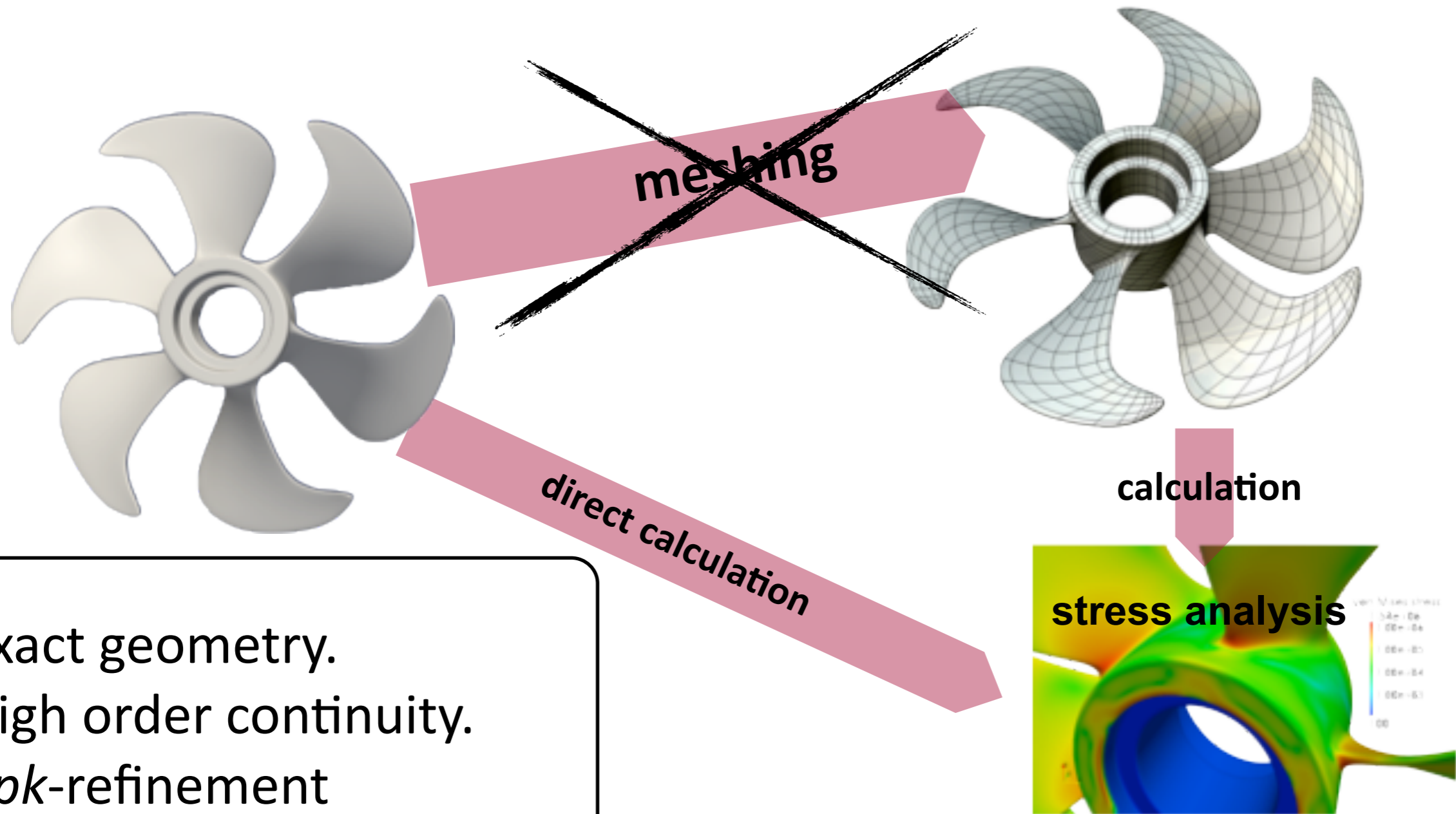
**calculate
20%**



vM stress distribution

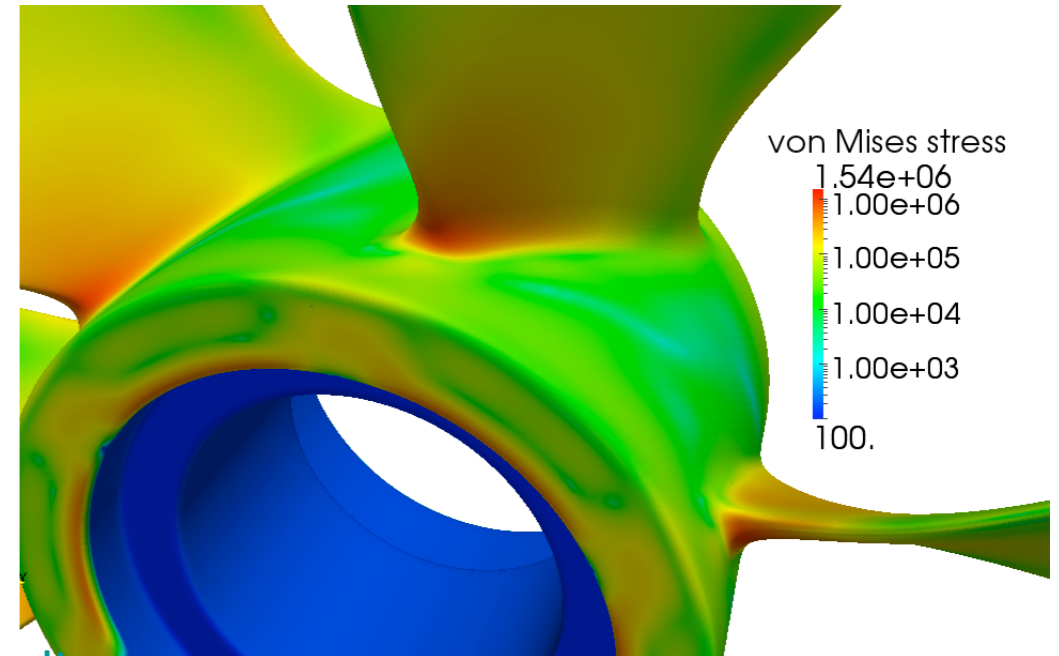
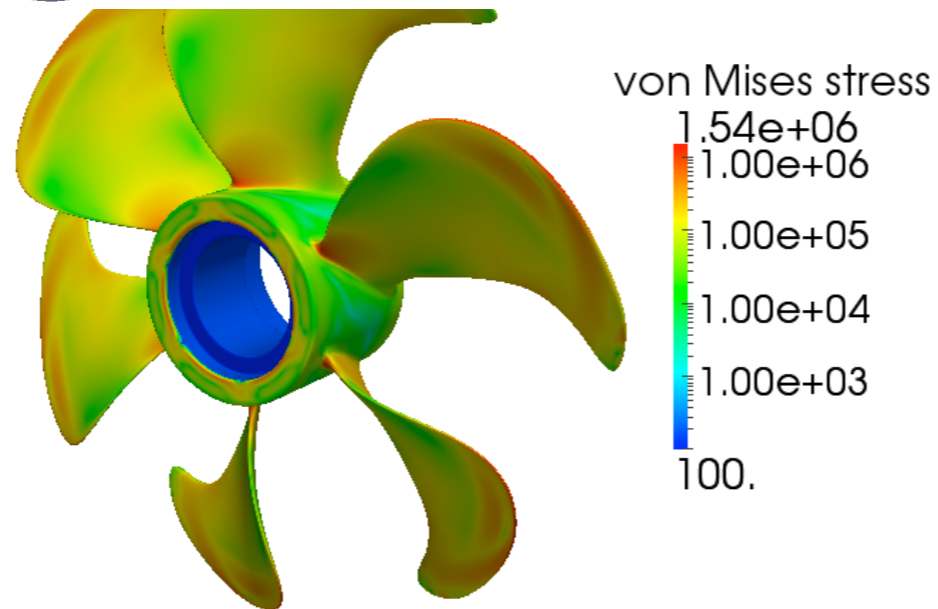
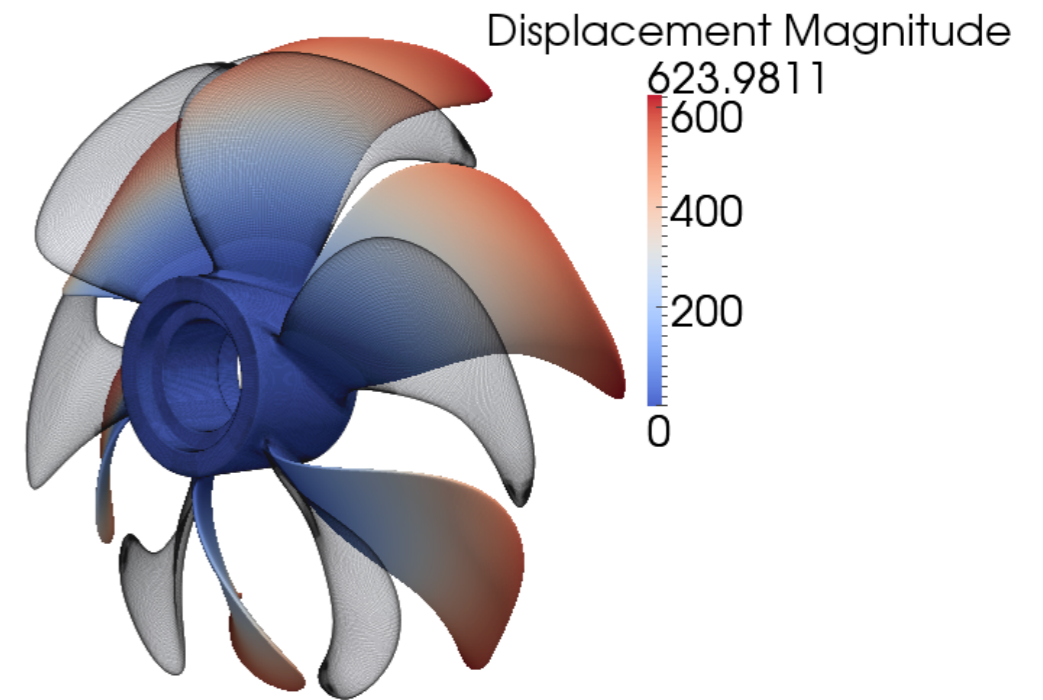
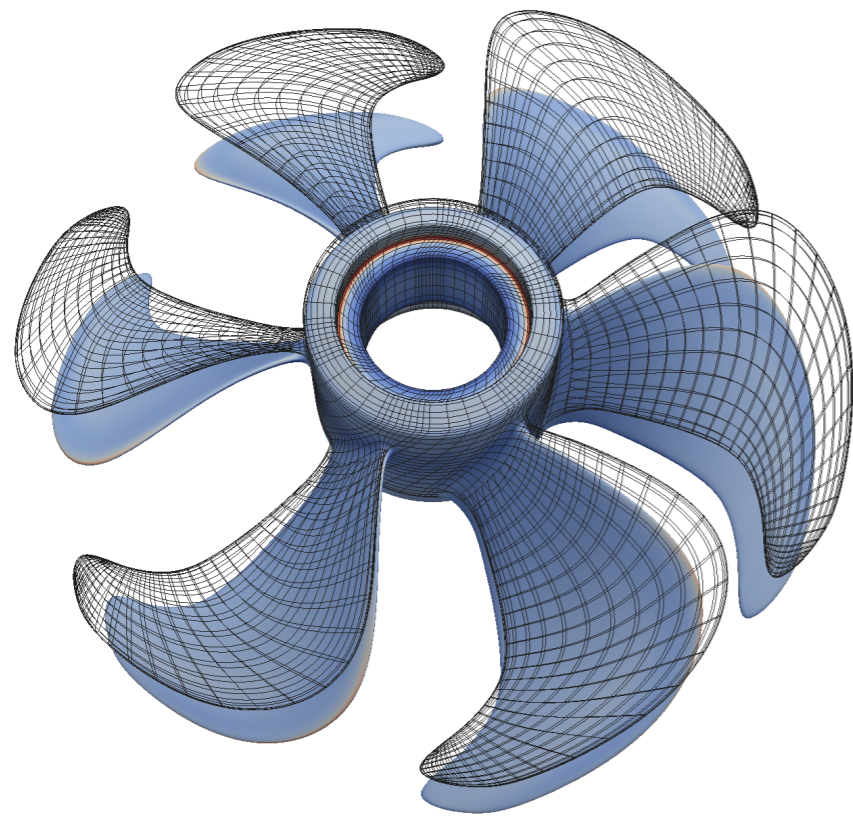


Approximate the unknown fields with the same basis functions (NURBS, T-splines ...) as that used to generate the CAD model



- Exact geometry.
- High order continuity.
- *hpk*-refinement

Propeller: NURBS would require several patches - single patch T-splines



Isogeometric boundary element analysis using unstructured T-splines

MA Scott, RN Simpson, JA Evans, S Lipton, SPA Bordas, TJR Hughes, TW Sederberg

CMAME, 2013. <http://orbilu.uni.lu/handle/10993/11850>

Shape and topology optimisation

Challenges for “conventional methods”

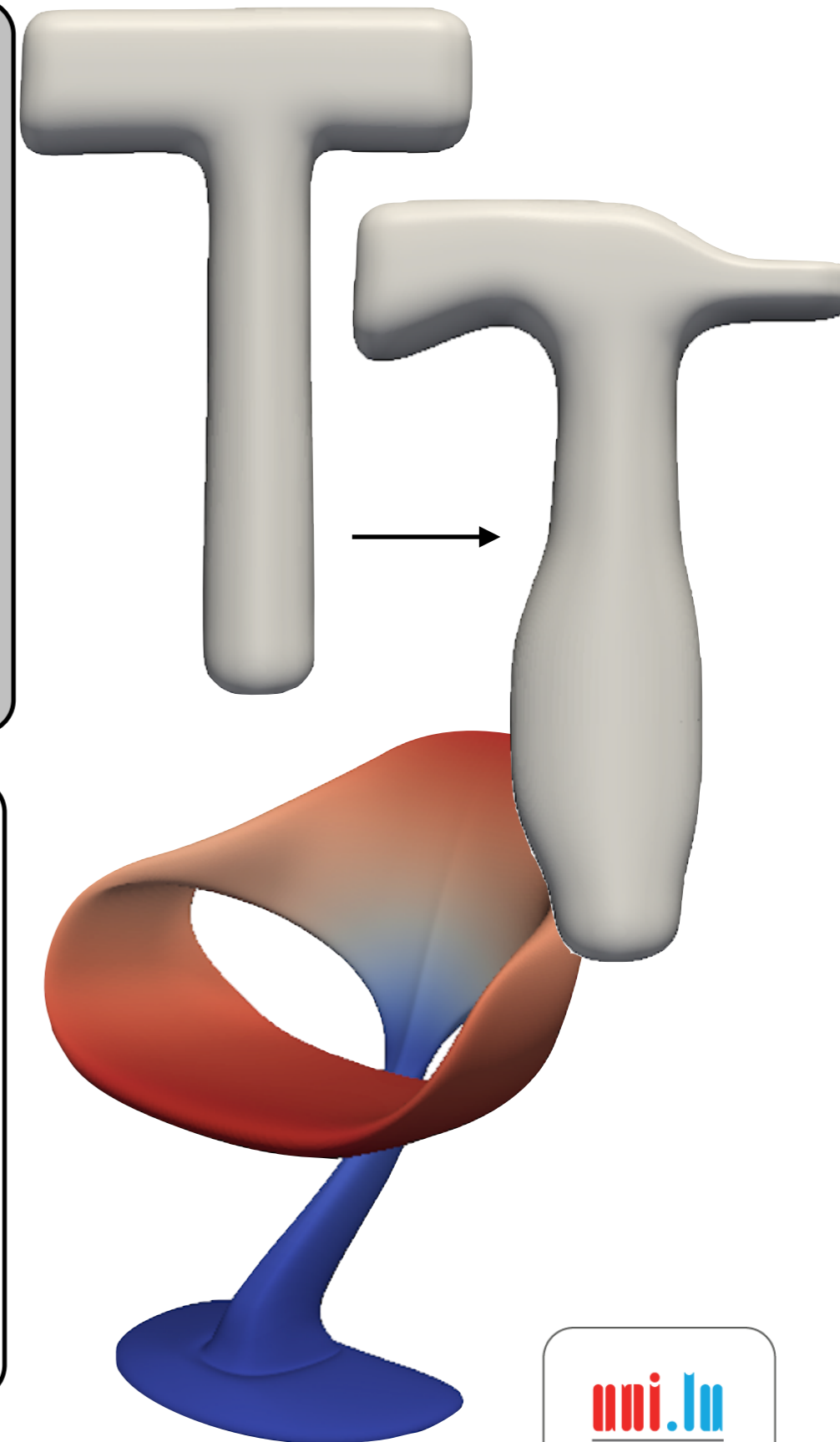
- Inverse problem - ill posed
- Choice of the approximation space for the boundary and the field approximation
- Evolving boundary (shape)
- Manual Redesign of the Topology: Smoothing of the “optimised” shape

Methods

- Isogeometric
- Boundary Elements
- Geometry-independent field approximation

Results

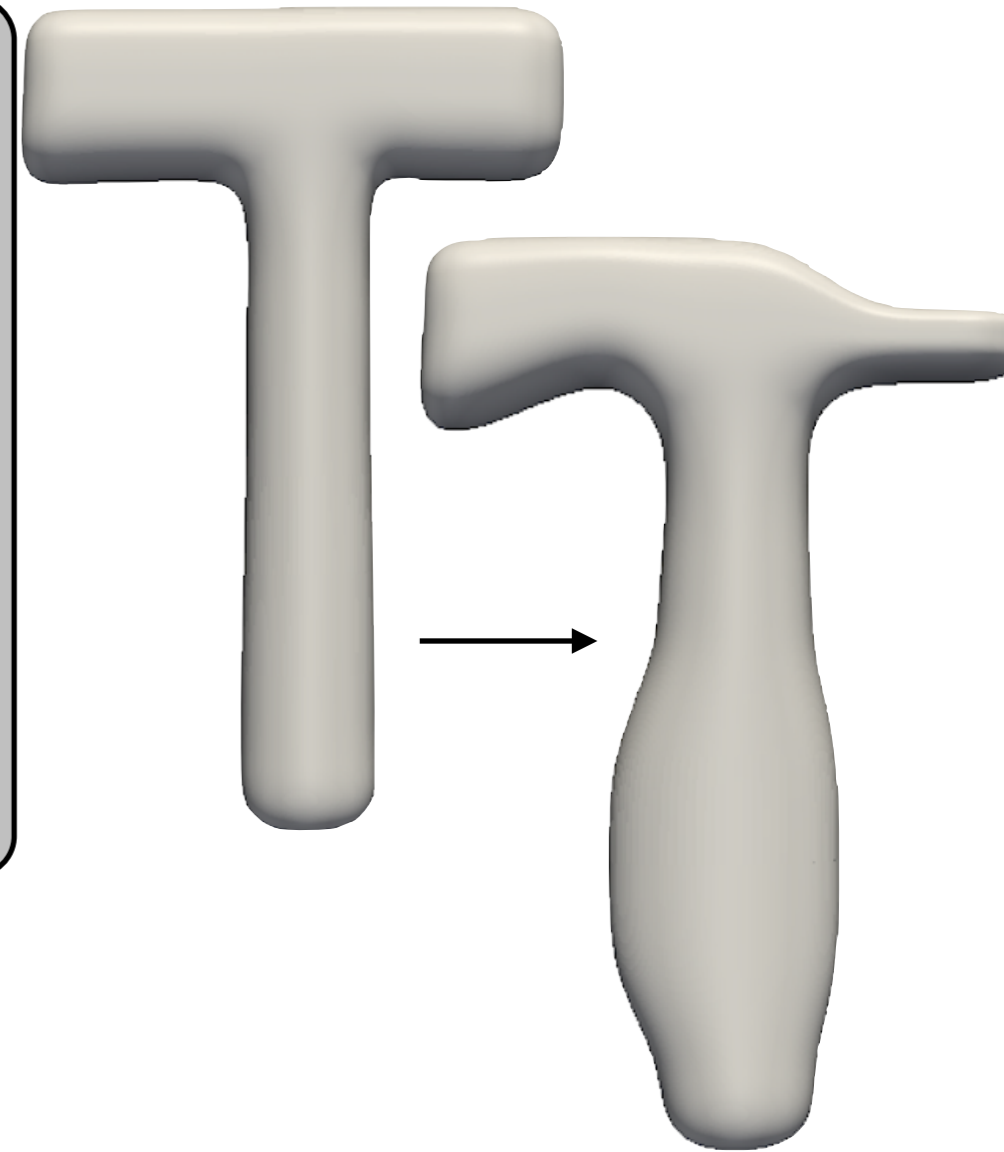
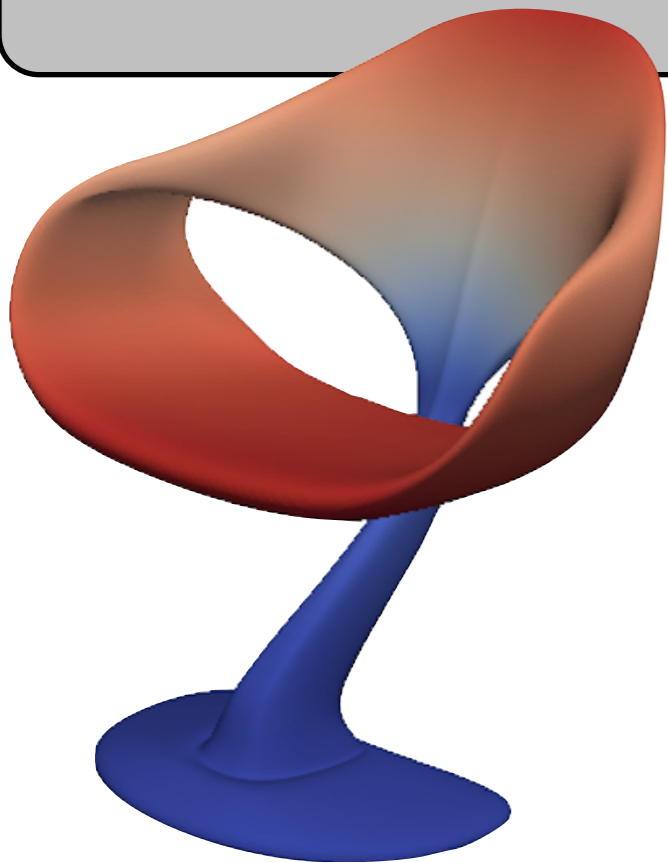
- Shape optimisation without meshing



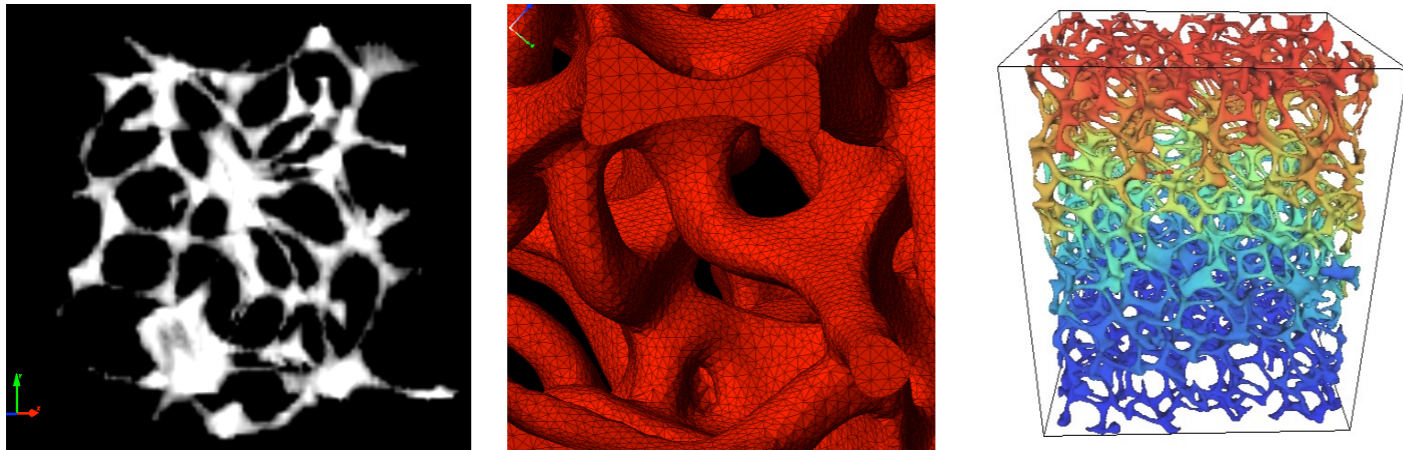
Shape and topology optimisation

Possible new approach

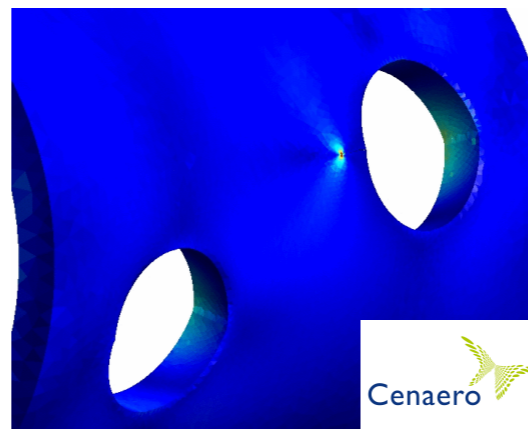
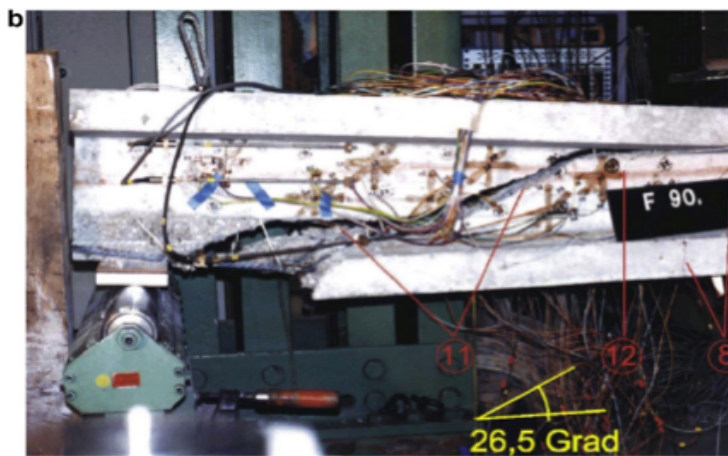
- start from an initial CAD
- use IGA to represent the surface
- optimise
- the CAD is still available and the piece can be displayed and reworked if necessary (no mesh).



Other applications

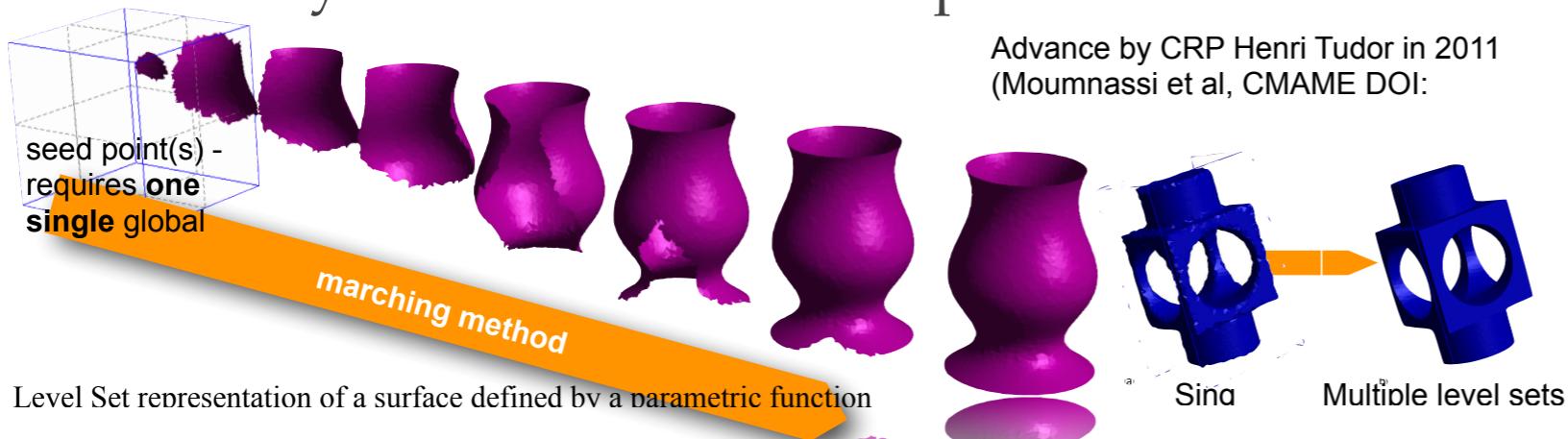


Microstructurally faithful material modeling

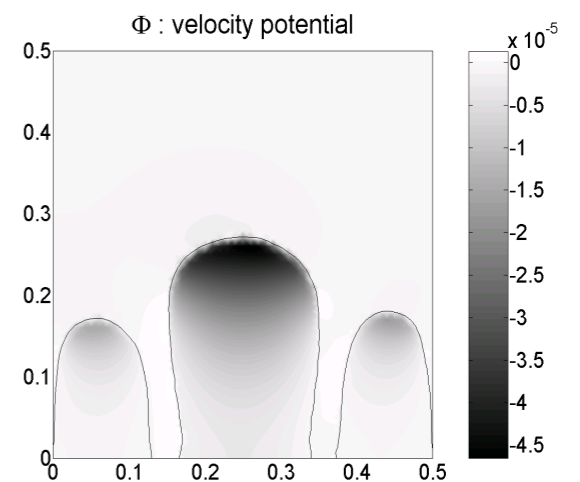
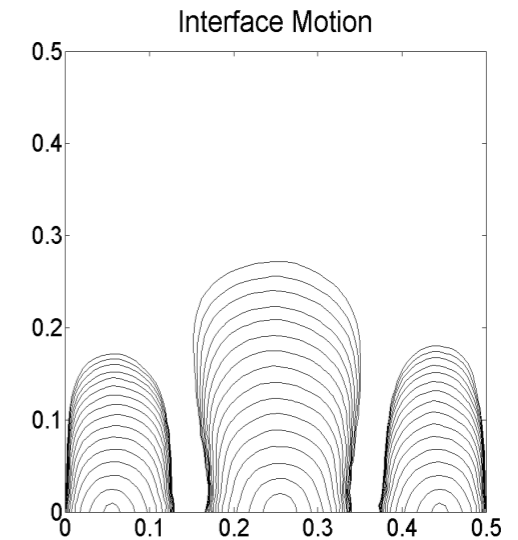


Durability of concrete and aerospace structures

Advance by CRP Henri Tudor in 2011
(Moumnassi et al, CMAME DOI:)



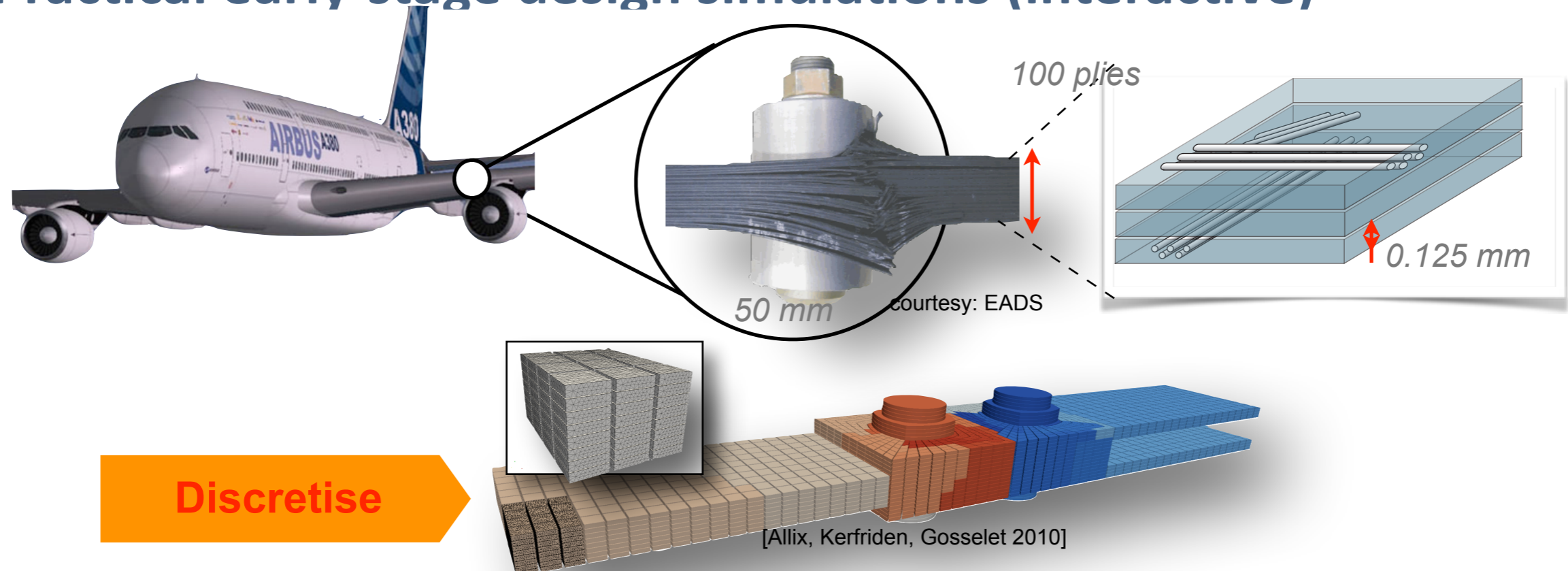
Implicit volume representations directly from CAD



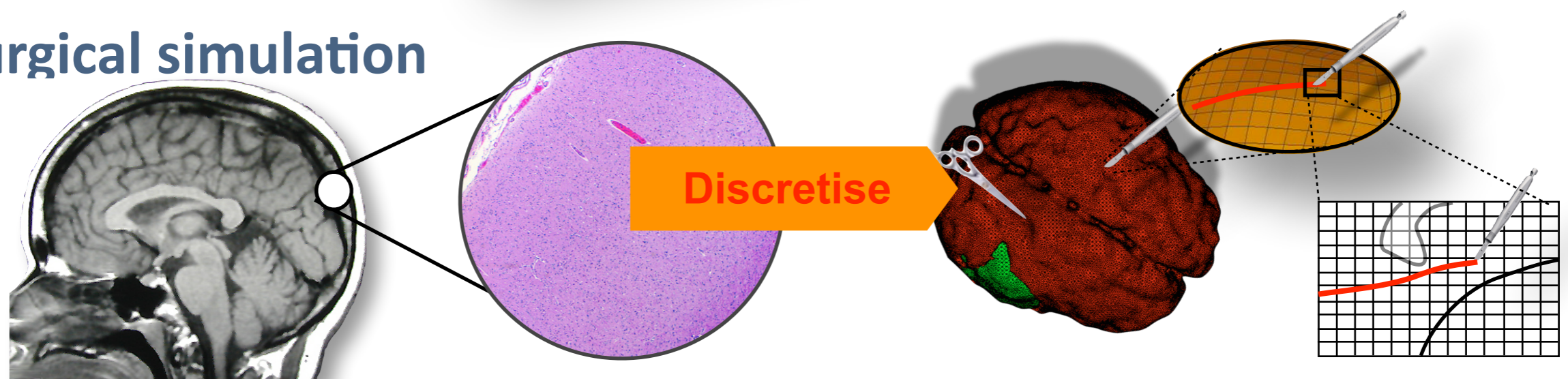
Biofilm growth

Patient/plane-specific simulation

Practical early-stage design simulations (interactive)

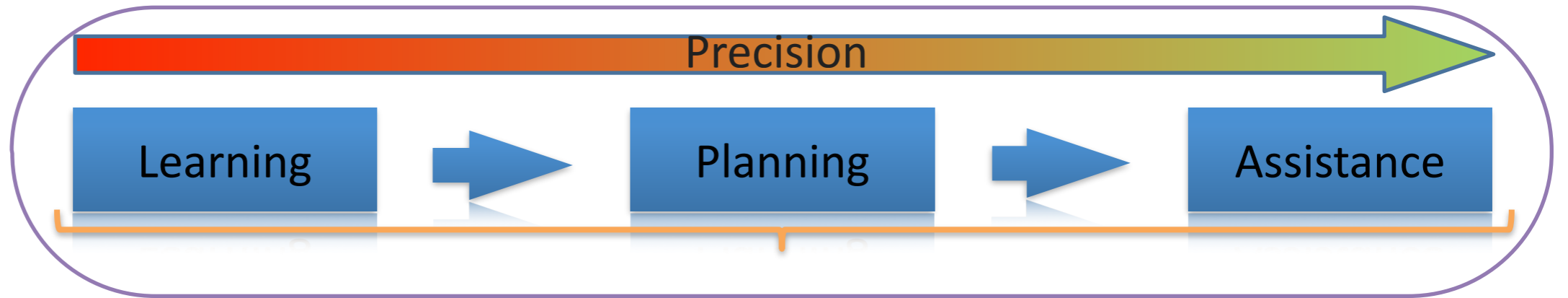


Surgical simulation

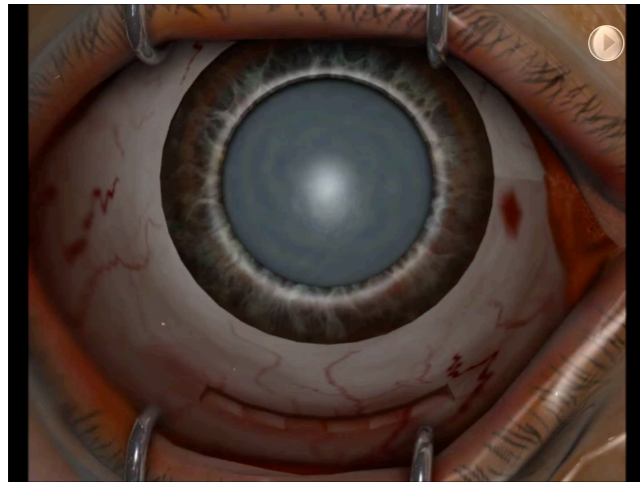


- ▶ Reduce the problem size while controlling the error (in QoI) when solving very large (multiscale) mechanics problems

Surgical simulation

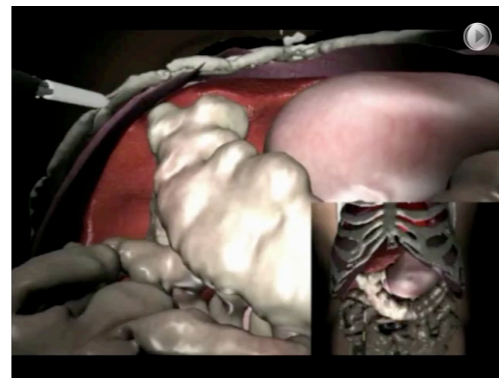


Cataract Surgery



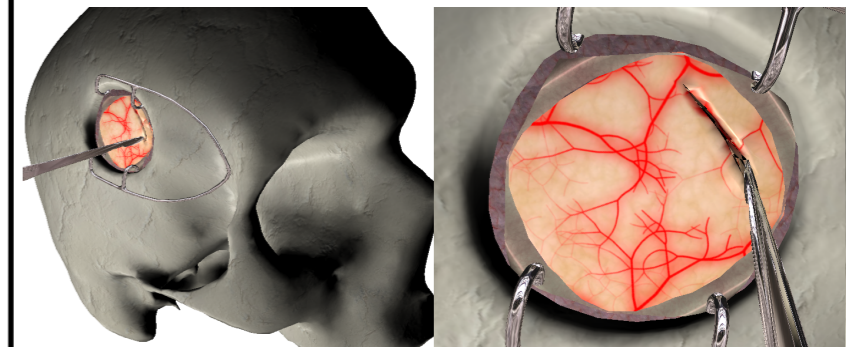
Inria

Abdominal minimally invasive surgery simulation (Inria, Shacra)



Inria

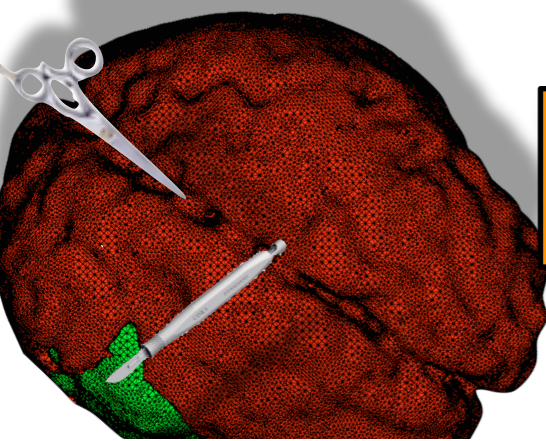
First implicit, interactive method for cutting with contact



[Courtecuisse et al., MICCAI, 2013 and Medical Image Analysis, 2014]

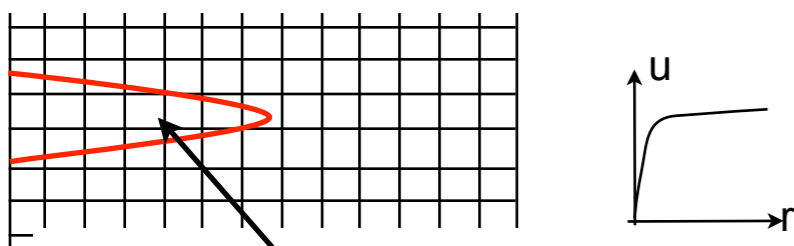
offline calculations

generate particular solutions



~10⁶ snapshots

compute asymptotic fields



instrument actions

sort the solutions (surgeon)

~10³ snapshots

patient-specific mapping

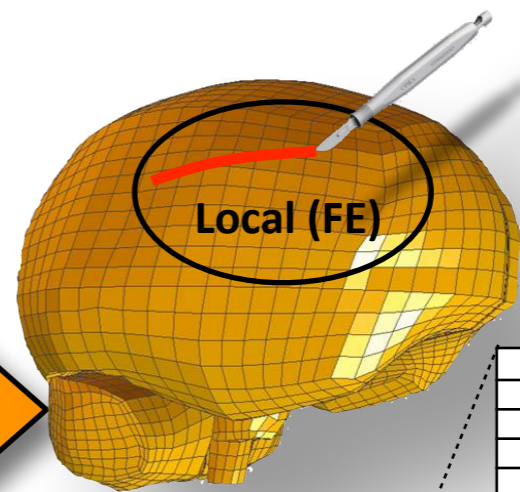
enrichment for tip of the cut

POD

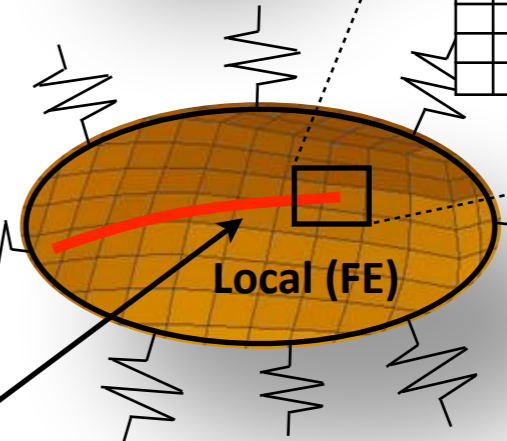
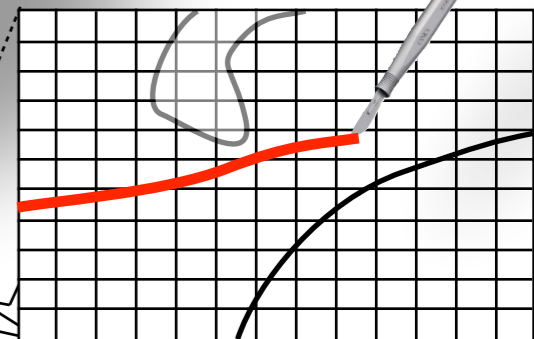
O(10) fonctions

small reduced order space

online calculations

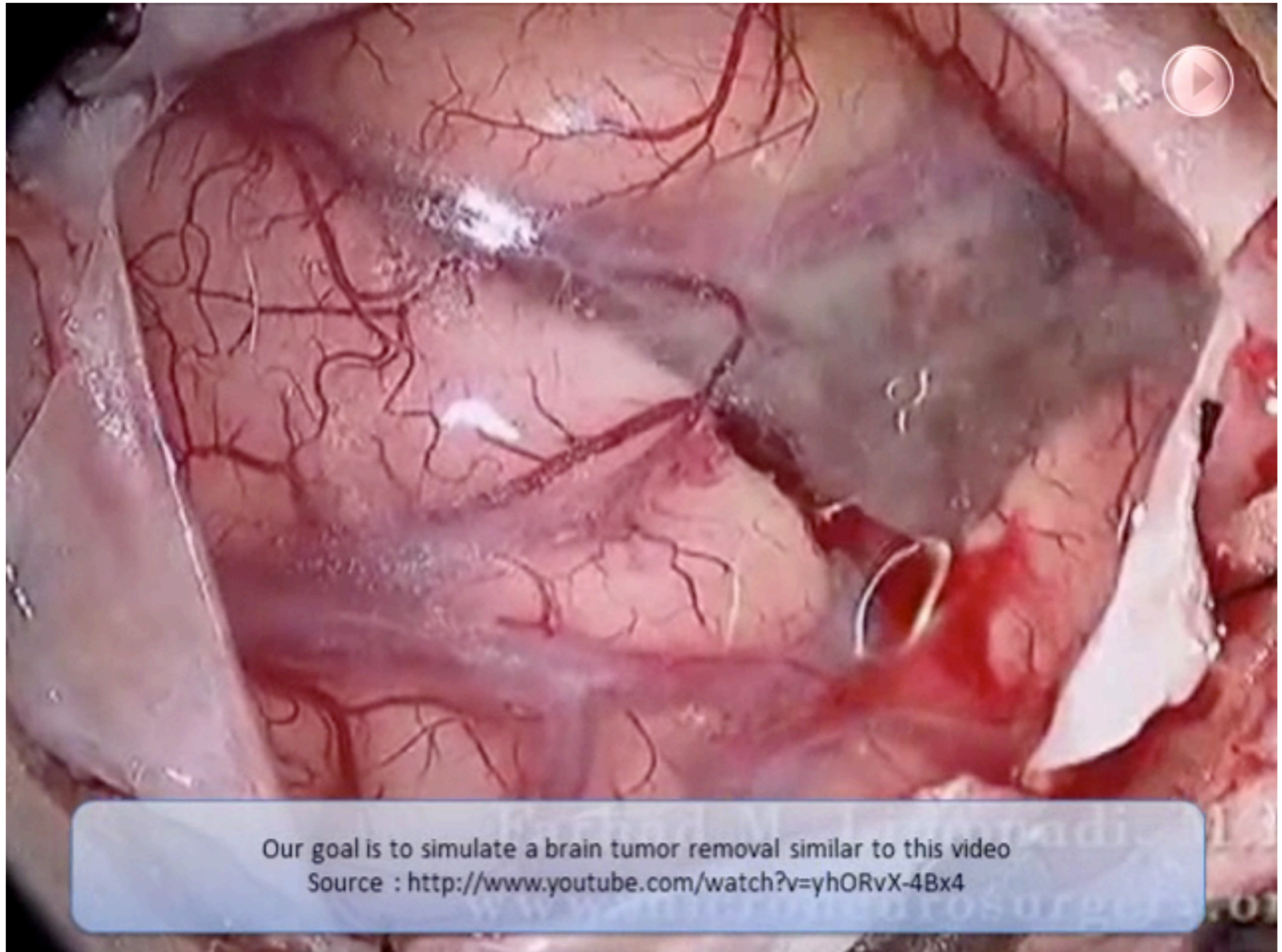


local representation



Global POD approximation

... not exactly brain surgery



- **Understanding and optimisation of fracture of heterogeneous materials - including human tissue :)**
 - multi-scale methods are being developed
 - these methods are expensive
 - model selection remains an open problem
 - variability of the material properties exacerbate these difficulties
 - taking into account realistic situations remains elusive
 - coupling with sensing systems may be the future

... twinning

real-time simulations could help engineers gain insight into complex non-intuitive phenomena by allowing to probe, quickly, the parameter space and design space



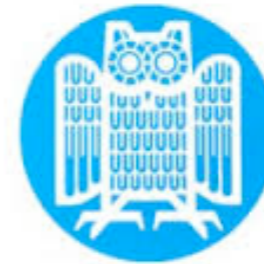
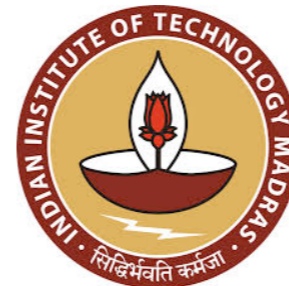
stephane.bordas@alum.northwestern.edu +352 621 131 048

merci de votre attention

Partners and Funding



UNIVERSIDAD DE CHILE



UNIVERSIDAD POLITÉCNICA DE VALENCIA



BOSCH
Technik fürs Leben



Rolls-Royce®

inuTech

Gracias por su atención
Merci de votre attention
Thank you for your attention
Danke für Ihre Aufmerksamkeit
Gracie per la vostra attenzione

product-specific

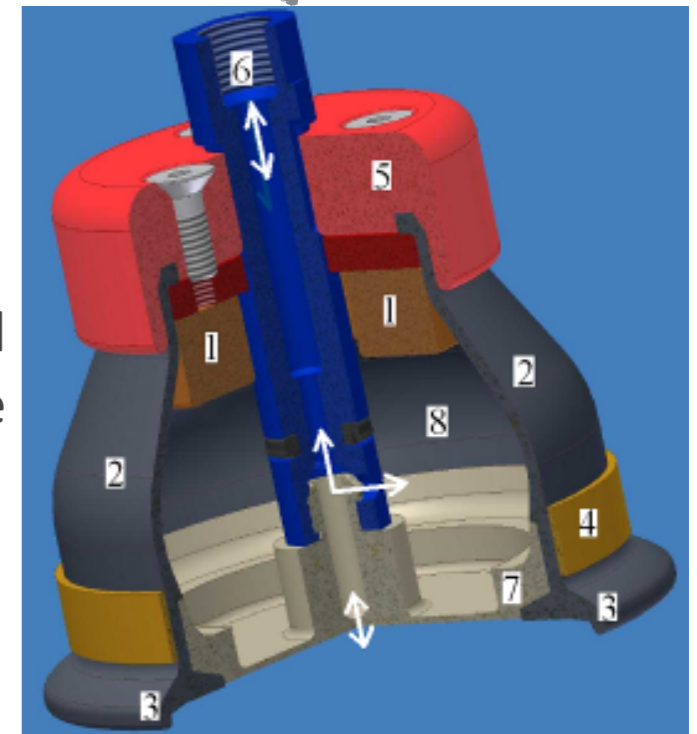


Increase product durability?

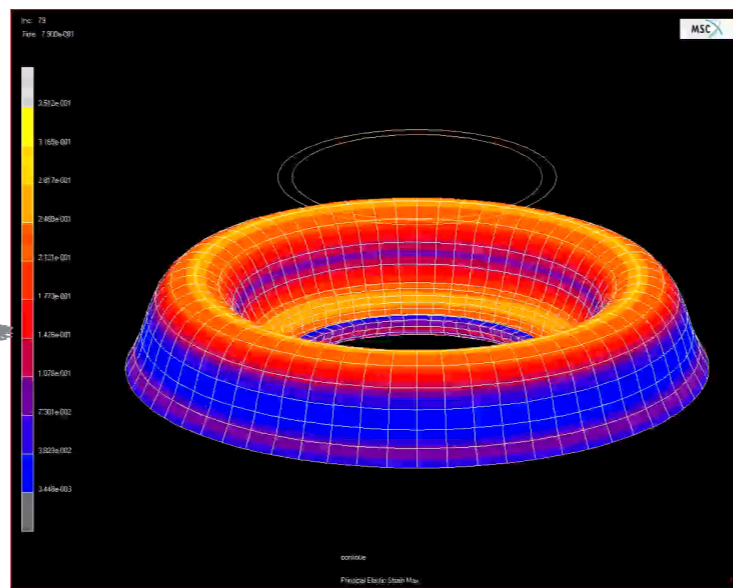


Analysis of the results

Virtual model of the device



Virtual testing & Simulation



market-specific



Buy or sell?

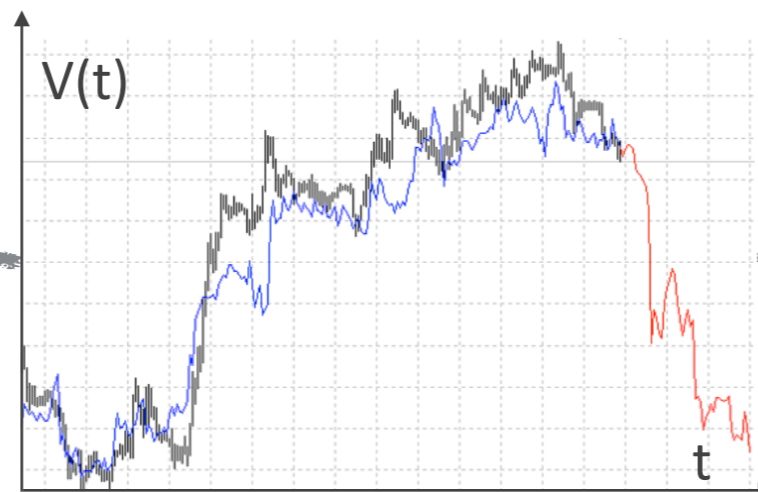


Identify behaviour

$$\frac{\partial V}{\partial t} + \frac{1}{2} \sigma^2 S^2 \frac{\partial^2 V}{\partial S^2} + rS \frac{\partial V}{\partial S} - rV = 0$$

Mathematical model + initial conditions

Real-time future option pricing



patient-specific



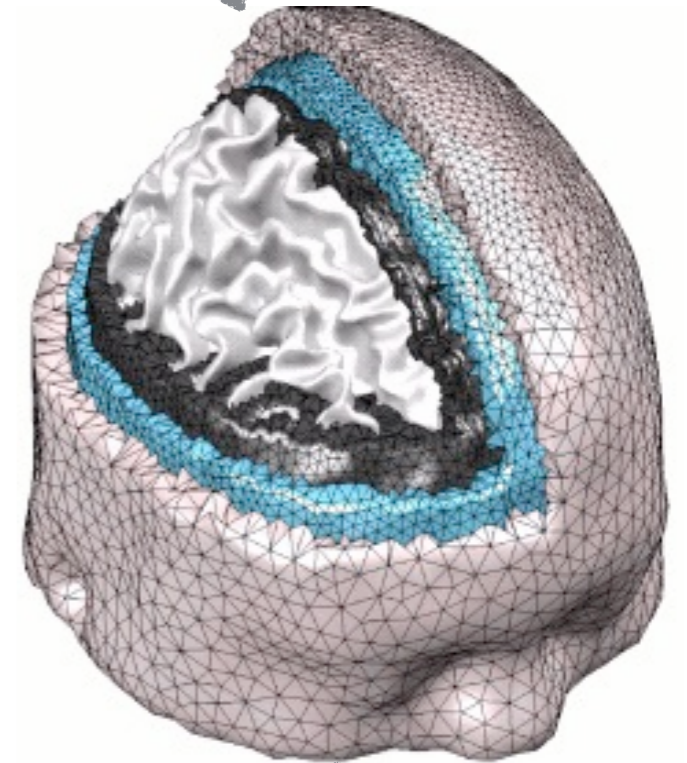
Devise effective deep brain stimulation

- reach the target area
- maintain contact with the electrode

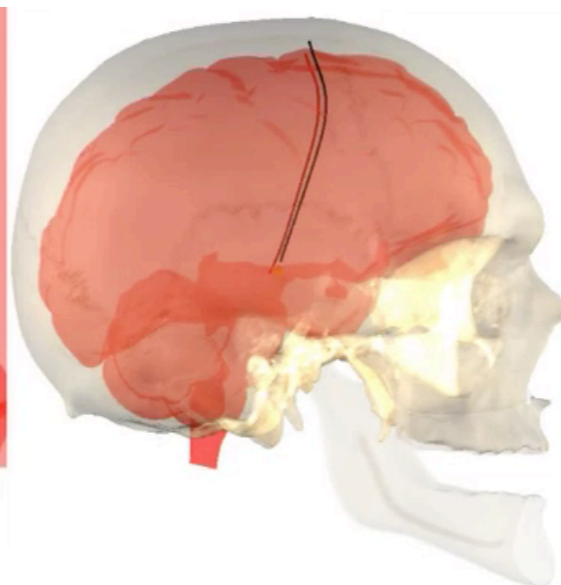
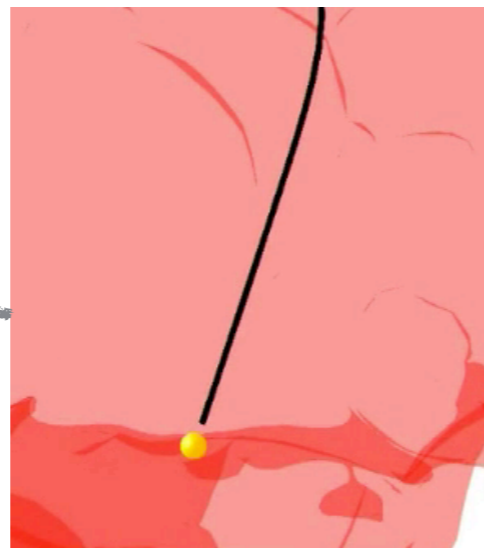


Electrode separates from target

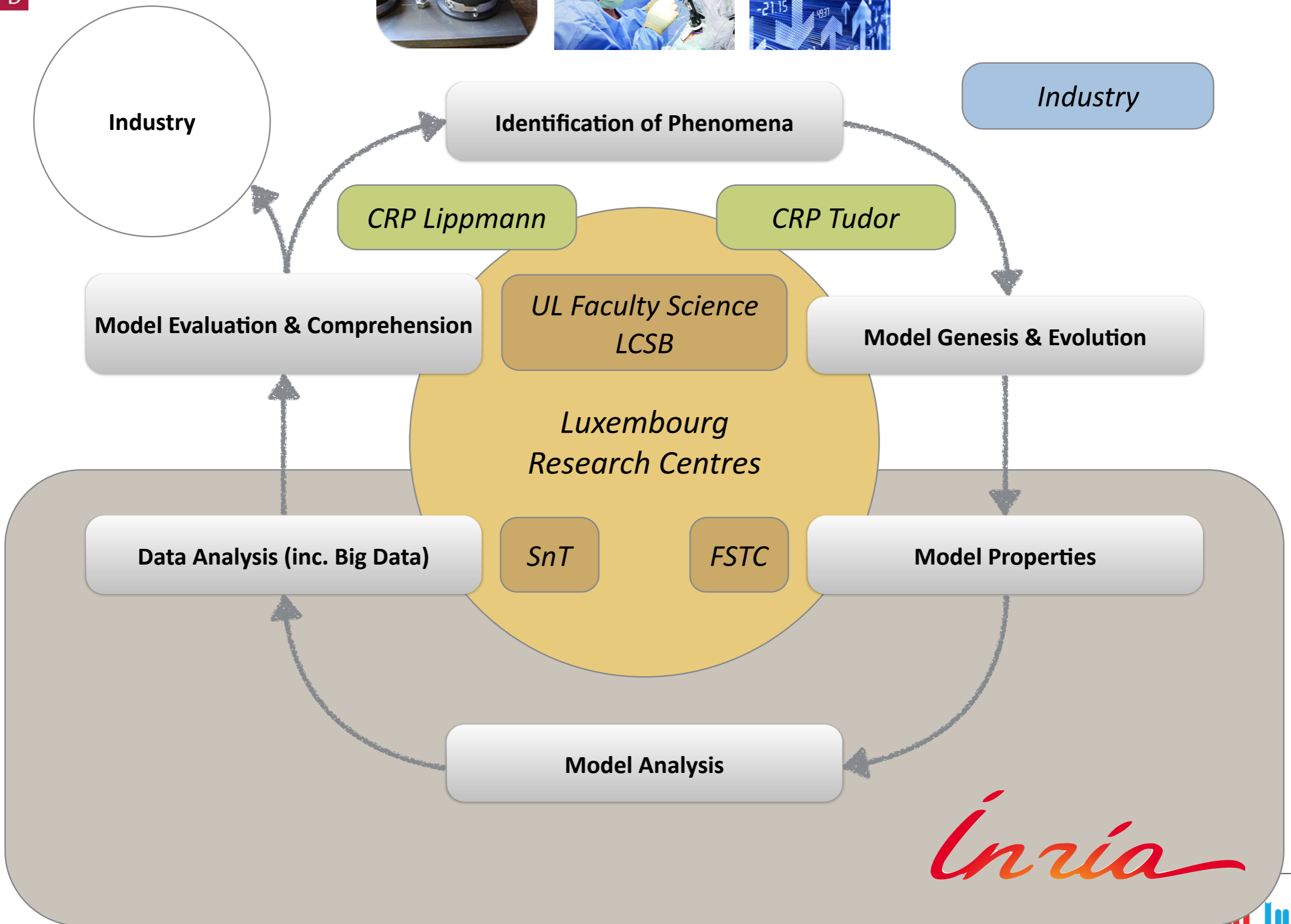
Model of the brain material



Predict electrode behaviour



Inria



Links to relevant publications

Acknowledgements

- The isogeometric BEM results were produced by Robert Simpson in collaboration with ICES in Texas, whose contribution is gratefully acknowledged.